UNIVERSITY OF PARMA
EARTH SCIENCE COURSE OF RESEARCH DOCTORATE

LATE QUATERNARY DEGLACIATION IN THE ARCTIC OCEAN: EVIDENCE FROM MICROFOSSILS

Photo of Longyearbyen, Svalbard, R/V Polarstern Cruise PS 99-1 (June 2016)

A DISSERTATION FOR THE DEGREE OF PHILOSOPHIAE DOCTOR

PH.D CANDIDATE
KATIA CARBONARA

SUPERVISORS
GIULIANA VILLA
RENATA GIULIA LUCCHI

XXIX PH.D CYCLE
2014-2016

UNIVERSITÀ DEGLI STUDI DI PARMA

Earth Science course of research doctorate

XXIX cycle

LATE QUATERNARY DEGLACIATION IN THE ARCTIC OCEAN: EVIDENCE FROM MICROFOSSILS

Coordinator:
Prof. Fulvio Celico

Ph.D. candidate:
Dr. Katia Carbonara

Tutor:
Prof. Giuliana Villa

Co-tutor:
Dr. Renata Giulia Lucchi

Thesis title:	Late Quaternary deglaciation in the Arctic Ocean: evidence from microfossils
Thesis submitted:	December, 2016
PhD Supervisor:	Prof. Giuliana Villa University of Parma
	Dr. Renata Giulia Lucchi Istituto Nazionale di Oceanografia e di Geofisica Sperimentale (OGS), Trieste

Table of contents

Chapter IV

Case study 2: Kveithola upper slope and trough, South of Svalbard (CORIBAR cores)

Chapter V

Case study 3: A new multi-proxy investigation of Late Quaternary palaeoenvironments along the southern Svalbard continental margin (northwestern Barents Sea) (EGLACOM project)

Chapter VI

Case study 4: Bellsund Drift, West of Svalbard (PREPARED project)

PREFACE

This thesis is the result of a three-year Ph.D investigation in the frame of three international research projects (1) OGS-EGLACOM (Evolution of a glacial Arctic continental margin: The Southern Svalbard ice stream-dominated sedimentary system), (2) PNRA-CORIBAR-IT (Ice dynamics and meltwater deposition in the NW Barents Sea: a 5-Nations effort for MeBo drilling the Arctic), and (3) Eurofleets2-PREPARED (Present and past flow regime on contourite drifts west of Spitsbergen).

The overall goal of the Ph.D project was to advance knowledge about the distributions patterns of microfossils, with particular attention to calcareous nannofossils, as proxy of past climate changes in the Arctic Ocean, south and west of Svalbard.

The micropaleontological approach used for palaeoclimate investigation is multi-proxy with the study of calcareous nannofossils compared with the results obtained from the analyses of other microfossil groups and sedimentological investigations, for a suited reconstruction of the late Quaternary palaeoenvironmental changes associated to climate.

This research was conducted within a PNRA project (CORIBAR-IT) and a Eurofleets-2 project (PREPARED), both coordinated by the Istituto Nazionale di Oceanografia e di Geofisica Sperimentale (OGS, Trieste) with the collaboration of several national and international universities and research institutes. The research group included: R. Melis (University of Trieste) working on benthic foraminifera; C. Morigi (University of Pisa and GEUS, Stratigraphy Department Geological Survey of Denmark and Greenland) and G. Varagona (University of Trieste) working on planktonic foraminifera; M. A. Bàrcena (University of Salamanca) and K. Mezgec (University of Trieste) working on diatoms; R.G. Lucchi (OGS, Trieste) coordinating the two projects and working on sediment facies, G. Giorgetti and M.E. Musco (University of Siena) working on clay minerals; A. Caburlotto (OGS, Trieste) working on multi-sensor core logger data; and M. Rebesco (OGS, Trieste) working on acoustic/seismic data, and coordination the OGS project EGLACOM.

The involvement on this kind of studies included the participation at the oceanographic expedition PS99-1 onboard the R/V Polarstern (Bremerhaven-Longyearbyen, 13-23 June, 2016), during a Eurofleets-2 project coordinated by OGS, and the presentation of the results during several national and international workshops. In addition, in the context of the Ph.D education, two summer schools, the EIOC (Elements, isotopes and organic matter in chemostratigraphy) and the 12th USSP (Urbino Summer School in Paleoclimatology) were attended in 2014 and 2015.

LIST OF ACRONYMS

AMS – Accelerator mass spectrometry

CEX' – % *Emiliania huxleyi* / (% *E. huxleyi* + % *Coccolithus pelagicus*) dissolution index

EG – EGLACOM core

ESC – Eastern Spitsbergen Current

GeoB – CORIBAR core

GS – PREPARED core

GZWs – Grounded Zone Wedge systems

H/P – *Emiliania huxleyi* and *Coccolithus pelagicus* ratio

HTM – Holocene Thermal Maximum

IRD – Ice rafted debris/detritus

LGM - Last Glacial Maximum

LIA – Little Ice Age

MIS – Marine Isotope Stage

MTD – Mass Transport Deposits

MWP – Melting Water Pulse event

NwAC – North Atlantic Current/Norwegian Atlantic Current

OX– oxidized layer

Suppl. – Supplementary material

TMF – Trough Mouth Fan

WSC – West Spitsbergen Current

WSG – Warm Species Group (diatoms)

YD - Younger Dryas

CHAPTER I

1 Introduction

Evidence from glacier ice, or left by glaciers in the landscape or within the geological record, provides one of the most important sources of information on environmental change (Nesje and Dahl, 2000).

1.1 Quaternary Ice Ages overview and Holocene climatic changes

The Earth's climate during the past hundreds of thousand years has naturally changed significantly with often swift changes between glacial and interglacial climatic mode, and *vice versa*. Periods with large ice-sheets extension are known as glacial periods (or ice ages) whereas shorter times with reduced ice-sheet extension are interglacial periods. The most recent glacial period occurred between about 120-11.7 ka, since then the Earth has been in an interglacial period named Holocene. The glacial-interglacial cycles are documented in many marine and terrestrial palaeoclimate records from around the world.

Marine Isotope Stages (MIS) refer to a sequence of periods defined and described by isotope analyses of drill cores from the seabed. Marine Isotope Stage periods are numbered so that even numbers refer to cold periods that is glaciations, while odd numbers refer to warm periods that is mainly interglacials. Scientists distinguish interglacials, with temperatures close to today's, from other warm periods with less high temperatures during glacial periods, which are interstadials.

The MIS 1 or Holocene is our present interglacial period. It started about 11.7 cal ka BP at the end of the Weichselian glaciation. Holocene is not yet completed and it is uncertain when a new glaciation will begin. The last interglacial MIS 3, between 60 and 27 cal ka BP, experienced several abrupt temperature variations (Van Meerbeeck et al., 2008), showing typical features of the last glacial cycle. Changes in the Arctic do not only affect local ecosystems, but act at global scale because the Arctic plays a key role in the global climate system.

At the beginning of the Pleistocene epoch at 2.58 Ma, large ice sheets, up to several kilometers thick, began to cover the northern hemisphere. These ice sheets advanced during cooler glacial periods and retreated during warmer interglacials. Some ice sheets were relatively stable and survived for thousands of years, as those of Greenland. Others were inherently unstable and underwent cyclical growth and shrink during the main phases of glacial and interglacial stages. No major ice sheets existed in the Arctic before 2.58 Ma, after which small ice sheets grew and melted mainly at a cycle of 41 kyr until about 0.9 Ma, after which oscillations centered in a period of ca. 100 kyr (Epica, 2004). Since the late 1800s only four glacial cycles were

traditionally recognized in North America and Europe and their names were chosen on the basis of the geographic area, but several of those are no longer accepted for stratigraphic use (Table 1).

Central U.S.A.	Northern Alps	Baltic lowlands	Approx. age (ka)
Wisconsin	Würm	Vistulian/ Weichselian	11.7-118
Sangamon	*R/W*	*Eemian*	118-125
Illinoian	Riss	Saalian	125-365
Yarmouthian	*M/R*	*Holsteinian*	365-405
Kansan	Mindelian	Elsterian	405-465
Aftonian	*G/M*	*Cromerian*	465-860
Nebraskan	Günz	Menapian	860-900

Table 1 Traditional glaciations (gray) and interglaciations (white) of North America and Western Europe.

The concept of four major glacial cycles during the Quaternary was accepted in the 20th century and became the basis for establishing Quaternary chronology and interpretation. The model of four Quaternary glaciations served well for more than half a century. Since the 1950s, however, new evidence indicates many more than four glaciations took place during the Quaternary. The exact number of major glacial cycles is not yet known, but it is at least ten or more during the last 1 Myr, each lasting about 41-100 kyr in duration. When the most recent glacial advance culminated 21.5 ka (Last Glacial Maximum, LGM), most of the Earth surface was very different from its current aspect. Ice sheets covered northern Europe, Canada, the northern United States and northern Asia. The permanent sea ice extent involved most of the Arctic Ocean (Mangerud et al., 2002) and global sea level was 110–125 m lower than today.

The three factors, beside of the orbital parameters, with the greatest potential to account for differences from modern climate conditions were the presence of larger ice sheets, atmospheric CO_2 levels and changes in seasonal contrast. Summer and winter insolation could not have been the major explanation of the differences in climate. The two factors left as probable explanation of the colder and drier glacial maximum climates involve increase in albedo and lower concentrations of greenhouse gases, leading to larger size of the ice sheets.

During the last 10 Myr, the Central America uplift gradually closed the deep ocean passage that previously separated the North from the South America in the region of Panama. The last stages of said uplift, created the Central American part of the Cordilleran mountain chain. The final closure of this ocean passage occurred just before 4 Ma with the formation of the Panama Isthmus. Indeed, several climate scientists (e.g. Maier-Reimer et al., 1990) have speculated that this episode is possibly linked to the first large-scale glaciation of North America at 2.58 Ma. They hypothesized that construction of the Panama Isthmus blocked the strong westward flow

of warm, salty tropical water, previously drove westward of the tropical Atlantic Ocean to flow into the eastern Pacific area by trade winds. The newly formed isthmus should have redirected this warm flow into the Gulf Stream to move toward the higher latitudes of the Atlantic. The scientists furthermore hypothesized that the northward-strengthened flow of warm and salty water would have suppressed the formation of sea ice in North polar regions because saltier waters resist freezing better than fresher water. According to their hypothesis, the reduced cover of sea ice would have made more moisture from the ocean available to nearby landmasses facilitating/triggering the growth of ice sheets: ice sheets formed in areas where winter snow did not melt entirely over the summer. Once formed, an ice sheet modifies significantly the local climate and likely have a strong impact on a regional scale. The glacial variations, evidenced by the oxygen isotope curve (the so-called *sawtooth* curve), show slow increasing glacial phase up to the maximum, followed by rapid deglaciation phases, in some cases called Termination (Broecker and van Donk, 1970). The coupling between ice sheet dynamics and oceanographic pattern is one of the climate forcing mechanism at global scale during the Quaternary (Broecker et al., 1985). The thermohaline circulation, transporting heat throughout the oceans, represents one of the major driving force of the present climate and the North Atlantic area plays a key role in that regard. The Atlantic Ocean transport heat through the Gulf Stream to the northern European margins (North Atlantic Current, NAC). In the Norwegian Sea , the NAC water salt excess is removed through freezing and brine rejection at the high latitudes during winter time (Geyer et al., 2009; Skogseth et al., 2005). The brine are very cold (≤ -2°C) and salty waters that form on the continental shelf area and cascade along the continental margins transporting oxygen and nutrients to the deeper oceanic environments. Continental shelf brine formation in polar areas represents the key process for deep-water ventilation and formation, representing the pump of the global thermohaline circulation system, together with the Antarctic regions. This system was weaker during the Pleistocene glaciations. Studies on the Greenland ice cores and deep-sea sediments suggest that the thermohaline Atlantic circulation pattern may have turned on and off abruptly in the past in relation to catastrophic events such as the massive flood, caused by the ice-dam brake of the Agassiz Lake (Laurentide Ice Sheet) pointed to have caused the Younger Dryas cold spell (YD, 12.9–11.7 cal ka BP, Broecker, 1999, 2010). It has been suggested that progressive anthropogenic accumulation of greenhouse gasses might lead to a new shutdown of the thermohaline circulation that would plunge the Earth into a new glacial phase similar to the Younger Dryas. However, this possibility remains remote and no climatic models have been able to reproduce large and abrupt changes in the Earth's atmosphere.

During peaks of glacial conditions, the sea ice was so extended and thick that little or no ice rafted debris (IRD) could be transported to the central Arctic basin from the surrounding continental margins, leaving a sediment-starved central Arctic Ocean. Although the thickness of glacial-age sea ice is not known precisely, multiyear sea ice may have dominated the glacial Arctic Ocean before the main phase of deglaciation began at approximately 20-15 ka. According to Winsborrow et al. (2010) the deglaciation of the SW Barents Sea (Bjørnøyrenna glacial trough system) initiated at ca. 15.5 cal ka BP, whereas Jessen et al. (2010) and Lucchi et al. (2013) indicated deglaciation on the NW Barents Sea occurred as early as ca. 20.5 cal ka BP.

Following the deglaciation, the Holocene (last 11.7 kyr), generally warm, shows climatic variability with numerous minor cold events as indicated by fossil associations, ice cores, dendrochronology and stable isotope records.

Three main climate phases characterize the Holocene:

- the early Holocene climatic oscillation (Preboreal period, 11.7-11.3 cal ka BP),
- the mid-Holocene Thermal Maximum (HTM) (Atlantic period, 11.3-8.2 cal ka BP),
- the late Holocene Neoglaciation (Sub-boreal and Sub-Atlantic periods, 8.2 cal ka BP-present).

The timing of these main phases differs somewhat around the globe, but the overall pattern is worldwide broadly similar. Holocene long-term warm trends were interrupted by "abrupt events" characterized by the sudden onset of cold climate conditions, namely the cooling 8.2 ka event (e.g. Nicolussi and Schlüchter, 2012; Seppä et al., 2010) and the Little Ice Age (LIA), from about 700 to 200 years BP (Matthes, 1939).

1.2 Microfossils as palaeonvironmental proxies in the Arctic Ocean

Instrumental records can refer about a too short time to fully evaluate the long-term effects of climate change on ecosystems, but the palaeoclimatology represents a remarkable discipline in climate change studies. In contrast to model simulations of climate, that focus on past and future scenarios, the palaeoclimatology reconstructs past climate conditions and permits to generate the parameters on which climate models are based.

Palaeoceanographic and palaeoclimatic proxies provide information for reconstructions of past environmental targets such as temperature, salinity, sea-ice cover, primary productivity, nutrient content and marine carbon dioxide concentrations.

The water masses are first characterized according to their specific physical and chemical properties, and then related to particular assemblages of certain organisms or to stable isotope variations. The most important and accurate information is provided by various microfossils,

either in the form of species assemblages or through their elemental and isotopic compositions. Surface and bottom-dwelling organisms are sensitive to environmental changes, with different sensitivity and reactions depending on individual species. These relationships are the subject of test-bearing organism investigations such as nannofossils, foraminifera and diatoms. The importance of microfossils as tool for palaeoclimate reconstructions was recognized early in the history of palaeoceanography.

The density of microfossils in sediments from Arctic Ocean is linked to interglacial and glacial climate regimes and changes in sea-ice cover, surface productivity, sedimentation and post-depositional processes. In addition to density, microfossil biodiversity is variable in the Arctic, where Shannon Wiener index varied several-fold. Microfossils are important also for biostratigraphic purposes, including relative dating of sediment cores.

The present research focuses on the marine ecosystem response to past climate changes using an integrated approach, based on Arctic sediment records of late Quaternary interval. The distribution of microfossils has been investigated in sediment cores recovered during recent cruises: the EGLACOM (Evolution of a glacial Arctic continental margin: The southern Svalbard ice stream-dominated sedimentary system) 2008 cruise on the Italian R/V OGS-Explora; the CORIBAR (Ice dynamics and meltwater deposits: coring in the Kveithola Trough, NW Barents Sea) 2013 cruise on the German R/V Maria S. Merian; and the Eurofleet2-PREPARED (Present and past flow regime on contourite drifts west of Spitsbergen expeditions in the Arctic Ocean) 2014 expedition on the Norwegian R/V G.O. Sars. All these research projects share objectives with the International Polar Year (IPY) Activity 367 NICESTREAMS (Neogene Ice Streams and Sedimentary Processes on High-Latitude Continental Margins). Micropalaeontological analyses were performed for palaeoenvironmental reconstructions and for the definition of a high latitude age model in support to radiocarbon dating.

The study of calcareous nannofossil assemblage represents the main investigation conducted for this doctoral thesis. The results from the study of nannofossils were combined with additional micropaleontological (foraminifera and diatoms) and sedimentological data in order to reconstruct the glacial-deglacial history of the studied areas.

1.3 Calcareous nannofossil ecological habits

Calcareous nannofossils are an exceptional microfossil group, with living counterparts, Coccolithophores, representing one of the major components of the present phytoplankton in the oceans. The abundant fossil record and the widespread distribution have permitted to consider them as one of the most important index-fossil groups and a significant palaeoenvironmental

and biostratigraphic tool also at high latitude (Baumann et al., 2000; Gard, 1988; Gard and Backman, 1990; Gard and Gard, 1993; Villa et al., 2005). Calcareous nannoplankton thrives in the photic zone and is influenced by temperature, nutrients and light. These conditions are not always met at very high latitudes, as water temperatures are low, light is scarce for part of the year and, in particular, the presence of sea-ice may additionally reduce the favorable condition for their growth.

A brief summary regarding the ecological preferences of the most common nannofossil species found in the studied samples is here reported:

Calcidiscus leptoporus (Murray and Blackman, 1898) Loeblich and Tappan, 1978; in the Norwegian–Greenland Sea, it is reported to have a lower temperature limit of about 11°C (Samtleben et al., 1995), while in the Southern Ocean Findlay and Giraudeau (2000) indicate for living species a temperature range between 5, 4 °C and 14, 2 °C.

Coccolithus pelagicus (Wallich, 1877) Schiller, 1930; generally considered a cold-water indicator in open ocean conditions (McIntyre and Bé, 1967; Roth and Coulbourn, 1982; Samtleben and Bickert, 1990). Cachão and Moita (2000) found a positive relationship with nutrient enrichment.

Emiliania huxleyi (Lohmann, 1902) Hay and Mohler in Hay et al., 1967; this is a euryhaline and eurythermal species (McIntyre and Bé, 1967; Okada and Mclntyre, 1979; Roth and Coulbourn, 1982), with no distinct seasonal abundance changes (Ziveri et al., 1995). For the Norwegian and Greenland Seas, Eide (1990) and Samtleben et al. (1995) reported this species ranging down to a minimum of 0°C to 8°C. On the basis of biometric subdivisions, the following morphotypes were distinguished within *E. huxleyi* group (Colmenero-Hidalgo et al., 2002):

- *E. huxleyi* ≤4 μm (warm-water adapted taxon)
- *E. huxleyi* >4 μm (cold-water adapted taxon).

Gephyrocapsa caribbeanica Boudreaux and Hay, 1967; though rare in the samples, confirms by its presence a cold-water preference, as suggested by Wells and Okada (1997).

Gephyrocapsa muellerae Bréhéret, 1978; associated with cold waters (Samtleben et al., 1995; Samtleben and Bickert, 1990; Wells and Okada, 1997), it is common to abundant in the oceanic temperate zones (Paasche, 1995).

Gephyrocapsa oceanica Kamptner, 1943; it prefers warm waters and marginal seas of normal to high salinity (Honjo and Okada, 1974). Typical of low-latitude upwelling areas (Ziveri et al., 1995), it is a warm-water species, replaced in cold water by *G. muellerae* (Weaver and Pujol, 1988).

1.4 Research objectives and thesis organization

The aim of this research is the reconstruction of the palaeoclimatic and palaeoenvironmental changes in the Arctic area, South of Svalbard, during the Late Pleistocene deglaciation and the Holocene (after LGM). New data, from an integrated micropalaeontological and sedimentological study on 8 sediment cores from the northwestern Barents Sea continental margin, are presented.

The thesis is organized as a series of scientific papers in the way they have been published, or they have been submitted, or currently in preparation.

A brief outline of the thesis is indicated in the following:

Chapter I

1. Introduction

Chapter II

2. Material and methods

Chapter III

Case study 1: Palaeoclimatic changes in Kveithola, Svalbard, during the Late Pleistocene deglaciation and Holocene: Evidences from microfossil and sedimentary records (CORIBAR project).

Chapter IV

Case study 2: Kveithola upper slope and trough, South of Svalbard (CORIBAR cores)

Chapter V

Case study 3: A new multi-proxy investigation of Late Quaternary palaeoenvironments along the southern Svalbard continental margin (northwestern Barents Sea) (EGLACOM project)

Chapter VI

Case study 4: Bellsund Drift, West of Svalbard (PREPARED project)

Chapter VII

Late Pleistocene and Holocene climate variability in the Barents Sea as revealed by coccolithophore assemblages

Supplementary material

Chapters III to VI contain results of the study areas, discussion and conclusion as individual papers.

Chapter VII binds the studied cases into a regional palaeoceanographic and palaeoenvironmental reconstruction and some consideration/conclusions will be presented.

This Ph.D contributed with a large dataset of nannofossil record made on 8 sediments cores for an overall of 499 analyzed samples.

References

Baumann, K.H., Andruleit, H., Samtleben, C., 2000. Coccolithophores in the Nordic Seas: Comparison of living communities with surface sediment assemblages. Deep. Res. Part II Top. Stud. Oceanogr. 47, 1743–1772. doi:10.1016/S0967-0645(00)00005-9

Broecker, W.S., 1999. What if the conveyor were to shut down? Reflections on a possible outcome of the great global experiment. GSA Today 9, 1–7.

Broecker, W.S., Denton, G.H., Edwards, R.L., Cheng, H., Alley, R.B., Putnam, A.E., 2010. Putting the Younger Dryas cold event into context. Quat. Sci. Rev. 29, 1078–1081. doi:10.1016/j.quascirev.2010.02.019

Broecker, W.S., Peteet, D.M., Rind, D., 1985. Does the ocean-atmosphere system have more than one stable mode of operation? Nature 315, 21–26. doi:10.1038/315021a0

Broecker, W.S., van Donk, J., 1970. Insolation Changes , Ice Volumes , and the O18 record in Deep-Sea Cores. Rev. Geophys. Sp. Phys. 8, 169–197. doi:10.1029/RG008i001p00169

Cachäo, M., Moita, M.T., 2000. Coccolithus pelagicus, a productivity proxy related to moderate fronts off Western Iberia. Mar. Micropaleontol. 39, 131–155. doi:10.1016/S0377-8398(00)00018-9

Colmenero-Hidalgo, E., Flores, J.A., Sierro, F.J., 2002. Biometry of Emiliania huxleyi and its biostratigraphic significance in the Eastern North Atlantic Ocean and Western Mediterranean Sea in the last 20 000 years. Mar. Micropaleontol. 46, 247–263.

Eide, L.K., 1990. Distribution of coccoliths in surface sediments in the Norwegian-Greenland Sea. Mar. Micropaleontol. 16, 65–75. doi:10.1016/0377-8398(90)90029-L

Epica, C.M., 2004. Eight glacial cycles from an Antarctic ice core. Nature 429, 623–628. doi:http://www.nature.com/nature/journal/v429/n6992/suppinfo/nature02599_S1.html

Findlay, C.S., Giraudeau, J., 2000. Extant calcareous nannoplankton in the Australian Sector of the Southern Ocean (austral summers 1994 and 1995). Mar. Micropaleontol. 40, 417–439. doi:10.1016/S0377-8398(00)00046-3

Gard, G., 1988. Late quaternary calcareous nannofossil biozonation, chronology and palaeo-oceanography in areas north of the faeroe-iceland ridge. Quat. Sci. Rev. 7, 65–78. doi:10.1016/0277-3791(88)90094-7

Gard, G., Backman, J., 1990. Synthesis of Arctic and sub-Arctic coccolith biochronology and history of North Atlantic drift water influx during the last 500 000 years, in: Geological History of the Polar Oceans: Arctic versus Antarctic. pp. 417–436.

Gard, G., Gard, G., 1993. Geology Late Quaternary coccoliths at the North Pole : Evidence of ice-free conditions and rapid sedimentation in the central Arctic Ocean Late Quaternary coccoliths at the North Pole : Evidence of ice-free conditions and rapid sedimentation in the centra 227–230. doi:10.1130/0091-7613(1993)021<0227

Geyer, F., Fer, I., Eldevik, T., 2009. Dense overflow from an Arctic fjord: Mean seasonal cycle, variability and wind influence. Cont. Shelf Res. 29, 2110–2121. doi:10.1016/j.csr.2009.08.003

Honjo, S., Okada, H., 1974. Community structure of coccolithophores in the photic layer of the mid-Pacific. Micropaleontology 20, 209–230.

Jessen, S.P., Rasmussen, T.L., Nielsen, T., Solheim, A., 2010. A new Late Weichselian and Holocene marine chronology for the western Svalbard slope 30,000-0 cal years BP. Quat. Sci. Rev. 29, 1301–1312. doi:10.1016/j.quascirev.2010.02.020

Lucchi, R.G., Camerlenghi, A., Rebesco, M., Colmenero-Hidalgo, E., Sierro, F.J., Sagnotti, L., Urgeles, R., Melis, R., Morigi, C., Bàrcena, M.A., Giorgetti, G., Villa, G., Persico, D., Flores, J.A., Rigual-Hernandez, A.S., Pedrosa, M.T., Macri, P., Caburlotto, A., 2013. Postglacial sedimentary processes on the Storfjorden and Kveithola trough mouth fans: Significance of extreme glacimarine sedimentation. Glob. Planet. Change 111, 309–326. doi:10.1016/j.gloplacha.2013.10.008

Maier Reimer, E., Mikolajewicz, U., Crowley, T., 1990. Ocean General Circulation Model Sensitivity Experiment with an open Central American Isthmus. Paleoceanography 5, 349–366. doi:10.1029/PA005i003p00349

Mangerud, J., Astakhov, V., Svendsen, J.I., 2002. The extent of the Barents-Kara ice sheet during the Last Glacial Maximum. Quat. Sci. Rev. 21, 111–119. doi:10.1016/S0277-3791(01)00088-9

Matthes, F.E., 1939. Report of Committee on Glaciers, April 1939. Trans. Am. Geophys. Union 20, 518. doi:10.1029/TR020i004p00518

McIntyre, A., Bé, A.W.H., 1967. Modern coccolithophoridae of the atlantic ocean—I. Placoliths and cyrtoliths. Deep Sea Res. Oceanogr. Abstr. 14, 561–597. doi:10.1016/0011-7471(67)90065-4

Nesje, A., Dahl, S.O., 2000. Glaciers and environmental change. Arnold 203.

Nicolussi, K., Schlüchter, C., 2012. The 8.2 ka event-Calendar-dated glacier response in the Alps. Geology 40, 819–822. doi:10.1130/G32406.1

Okada, H., Mclntyre, A., 1979. Seasonal Distribution of Modern Coccolithophores in the Western North Atlantic Ocean. Mar. Biol. 54, 319–328. doi:10.1007/BF00395438

Paasche, E., 1995. Coccolithophores (A. Winter and W. G. Siesser [eds.]). Limnol. Oceanogr. 40, 645–646. doi:10.4319/LO.1995.40.3.0645

Roth, P.H., Coulbourn, W.T., 1982. Floral and solution patterns of coccoliths in surface sediments of the North Pacific. Mar. Micropaleontol. 7, 1–52. doi:10.1016/0377-8398(82)90014-7

Samtleben, C., Bickert, T., 1990. Coccoliths in sediment traps from the Norwegian Sea. Mar. Micropaleontol. 16, 39–64. doi:10.1016/0377-8398(90)90028-K

Samtleben, C., Schofer, P., Andruleit, H., Baumann, A., Baumann, K.H., Kohly, A., Matthiessen, J., Schrder-Ritzrau, A., 1995. Plankton in the Norwegian-Greenland Sea: from living communities to sediment assemblages -an actualistic approach. Geol. Rundschau 84, 108–136. doi:10.1007/BF00192245

Seppä, H., Birks, H.J.B., Bjune, A.E., Nesje, A., 2010. Current continental palaeoclimatic research in the Nordic region (100 years since Gunnar Andersson 1909) - Introduction. Boreas 39, 649–654. doi:10.1111/j.1502-3885.2010.00170.x

Skogseth, R., Haugan, P.M., Jakobsson, M., 2005. Watermass transformations in Storfjorden. Cont. Shelf Res. 25, 667–695. doi:10.1016/j.csr.2004.10.005

Van Meerbeeck, C.J., Renssen, H., Roche, D.M., 2008. How did Marine Isotope Stage 3 and Last Glacial Maximum climates differ? Perspectives from equilibrium simulations. Clim. Past Discuss. 4, 1115–1158. doi:10.5194/cpd-4-1115-2008

Villa, G., Palandri, S., Wise, S.W., 2005. Quaternary calcareous nannofossils from Periantarctic basins: Paleoecological and paleoclimatic implications. Mar. Micropaleontol. 56, 103–121. doi:10.1016/j.marmicro.2005.03.006

Weaver, P.P.E., Pujol, C., 1988. History of the last deglaciation in the alboran sea (western Mediterranean) and adjacent north Atlantic as revealed by coccolith floras. Palaeogeogr. Palaeoclimatol. Palaeoecol. 64, 35–42. doi:10.1016/0031-0182(88)90140-X

Wells, P., Okada, H., 1997. Response of nannoplankton to major changes in sea-surface temperature and movements of hydrological fronts over Site DSDP 594 (south Chatham Rise, southeastern New Zealand), during the last 130 kyr. Mar. Micropaleontol. 32, 341–363. doi:10.1016/S0377-8398(97)00025-X

Winsborrow, M.C.M., Andreassen, K., Corner, G.D., Laberg, J.S., 2010. Deglaciation of a marine-based ice sheet: Late Weichselian palaeo-ice dynamics and retreat in the southern Barents Sea reconstructed from onshore and offshore glacial geomorphology. Quat. Sci. Rev. 29, 424–442. doi:10.1016/j.quascirev.2009.10.001

Ziveri, P., Thunell, R.C., Rio, D., 1995. Export production of coccolithophores in an upwelling region: Results from San Pedro Basin, Southern California Borderlands. Mar. Micropaleontol. 24, 335–358. doi:10.1016/0377-8398(94)00017-H

CHAPTER II

2 Material and methods

This chapter contains a description of the material and methods applied for the present study. The Ph.D research is based on the investigation of 7 sediment gravity cores (EG-01, EG-02, EG-03; GeoB17601-5, GeoB17603-3, GeoB17605-3, GeoB17623-2) and a Calypso piston core (GS191-01PC). EG prefix indicates *EGLACOM* cores, GeoB176 designates *CORIBAR* cores, in the following indicated as 176xx-x for brevity, and GS specifies for *PREPARED* core (Table 2).

Core ID	Lat. N	Long. E	Water depth (m)	Total recovery (cm)	N. of nannofossil samples	AMS ^{14}C
EG-01	76°06,201'	13°37,625'	1069	220	23	4
EG-02	75°12,907'	13°04,587'	1722	305	30	3
EG-03	75°50,615'	12°58,353'	1432	285	39	3
17601-5	74° 51,53'	16° 5,82'	369,1	537	51	/
17603-3	74° 51,00'	14° 48,09'	1430	974	98	23
17605-3	74° 47,09'	15° 31,27	768,1	405	41	/
17623-2	75° 0,46'	17° 58,85	150,2	442	21	5
GS191-01PC	76°31,30'	12°44,30'	1647	1967	196	8

Table 2 Core details. EG= *EGLACOM*; 176xx-x= *CORIBAR*; GS= *PREPARED*

2.1 Slide preparation for nannofossil analyses

A total of 499 samples were analyzed for calcareous nannofossil content with a sampling interval of approximately 10 cm in each core. All *CORIBAR* and *PREPARED* samples were prepared from unprocessed material as smear slides, following standard techniques (Bown and Young, 1998). The nannofossils were counted in 200 fields of view, corresponding to a smear slide area of 6.28 mm^2 following the method described by Backman and Shackleton (1983) and Rio et al. (1990). Sample preparation for *EGLACOM* analyses follows the settling methodology described by de Kaenel and Villa (1996). Counting of specimens was performed on a 50 fields of view, equivalent to 1.57 mm^2. All the samples were examined using a Zeiss Axioskop polarized-light microscope at 1250× magnification. Relative abundance, expressed in percentage, and absolute abundance, expressed as number of specimens per 10 mm^2 in the slides for *CORIBAR* and *PREPARED* samples and as numbers of observed specimens for *EGLACOM* samples, were calculated.

2.2 Palaeoecological indices

A number of palaeoecological indices, based on nannofossil data, were calculated and considered for environmental reconstruction, such as:

- The ratio between the two dominant species *Emiliania huxleyi* and *Coccolithus pelagicus* (H/P ratio). According to recent oceanographic settings, in the Nordic seas an H/P > 1 is indicative of Atlantic influenced conditions while an H/P < 1 indicates Arctic to Polar influenced conditions (Andruleit and Baumann, 1998). Here this ratio was measured in logarithmic scale and, thus, the considered threshold is 0;
- The dissolution index (CEX'), adapted from Dittert et al. (1999), was calculated as ratio between the delicate *E. huxleyi* and the dissolution-resistant *C. pelagicus*. The calculated index is based on the differential dissolution behavior of coccoliths, as used to estimate the effect of carbonate dissolution on the nannofossil assemblages; it differs from Dittert et al. (1999) CEX that, instead, considered the dissolution-resistant *Calcidiscus leptoporus* nannofossil species which is extremely rare in the studied cores and, therefore, is not statistically reliable.

The CEX' index was calculated as:

$$CEX' = \%\ E.\ huxleyi\ /\ (\%\ E.\ huxleyi + \%\ C.\ pelagicus)$$

having lower values with increasing carbonate dissolution.

- Dominance and Shannon Wiener diversity indices were calculated from species relative abundance, using the software PAST (Hammer et al., 2001).

2.3 Sedimentary analyses

This study focuses on 8 sediment cores, collected from the Storfjorden and Kveithola continental slopes and the Bellsund Drift during, respectively, the R/V OGS Explora cruise (Kristiansund, July 7–August 04, 2008) within the *OGS-EGLACOM* project, the R/V Maria S. Merian cruise (Tromsø, July 16–August 15, 2013) during the *CORIBAR* project, and the R/V G.O. Sars cruise (Tromsø, June 5–June 15, 2014) during the Eurofleets2-*PREPARED* project. All cores were initially radiographed and analyzed using a GEOTEK Multi-sensor Core Logger for wet bulk density and magnetic susceptibility (*k*). The cores were then opened, visually logged and sampled at 5-10 cm space for water content and grain size characteristics, using a coulter counter laser Beckman LS-230 to measure the 0.04–2000 μm fraction at 0.004 μm resolution. The results were classified according to Friedman and Sanders (1978) grain-size scale. X-ray fluorescence (XRF) core-scan analyses were performed at 1 cm resolution using an Avaatech instrument at 10 and 50 kV setting and the Ca, Fe and Ti contents were obtained. Clay mineral analyses were performed by X-ray diffraction (XRD) on sediments collected at 30–40

cm sampling interval. For these analyses, the clay samples were mounted on smear slides, and analyzed with a Philips PW1710 powder diffraction system, using CuKα radiation (40 kV, 40 mA). Semi-quantitatively estimation of the main clay mineral abundance (smectite, chlorite, kaolinite and illite) was determined using the MacDiff software, relative percentages of each clay mineral were computed using weighting factors (Biscaye, 1965).

The studied cores usually contain Mass Transport Deposits (MTD), emplaced during LGM and consisting of glacigenic sediments, locally incorporating older stratigraphic intervals. Above this lithofacies, the deposition of massive IRD and laminated sediments corresponds to the transition from fully glacial to interglacial conditions with high terrigenous input associated to the main Svalbard ice-sheet retreating phase. Sedimentological characteristics suggest that laminated deposition occurred under the effects of extensive subglacial melting water pulse (plumites). The Holocene interval is characterized by crudely layered and bioturbated sediments, indicating the presence of bottom currents and palaeoenvironmental conditions favorable to bioactivity (Lucchi et al., 2013).

Each study case chapter will report detailed core descriptions.

2.4 Chronology

A total of 46 Accelerator Mass Spectrometry (AMS) ^{14}C age determinations, at selected stratigraphic intervals (Table 3), were performed mainly on planktonic foraminifera, although some dating was performed on benthic foraminifera owing to the scarcity of planktonic specimens. All samples were analyzed at NOSAM Woods Hole Oceanographic Laboratory (Massachusetts). The values of radiocarbon dating obtained need to be adjusted (calibrated) considering the local marine reservoir effect that derives from the age differences between surface water dissolved carbon and atmospheric carbon. The differences are due to a prolonged residence time of ^{14}C in the ocean; the reservoir effect varies in different geographic areas. Therefore, the radiocarbon ages were calibrated with the softwares Calib 6.0 (*EGLACOM*) and Calib 7.1 (*CORIBAR* and *PREPARED*) (Stuiver and Reimer, 1993), using the Marine09 and Marine13 calibration curve (Reimer, 2013) and applying an average marine regional reservoir effect $\Delta R = 84 \pm 23$ (*EGLACOM*) and $\Delta R = 67 \pm 34$ years (*CORIBAR* and *PREPARED*), obtained from the Marine Reservoir Correction Database of Calib softwares for the northwestern Barents Sea area (Mangerud et al., 2006; Mangerud and Gulliksen, 1975). All cited ages in this thesis were recalibrated following the same procedure in order to make ages comparable. Calibrated ages at $\pm 1\sigma$ and $\pm 2\sigma$ are delivered by the program, normalized to

calendar year and reported in the following as cal a BP or as cal ka BP, where the present is defined as AD 1950 by convention.

	Lab. code	Depth (cm)	Material	^{14}C Age	Age error	1 σ cal age (cal a BP)	2 σ cal age (cal a BP)	Median probability (cal a BP)
EG-01	OS-78409	2.5	Sediment (C org)	4830	35			4968 ± 78
	OS-98259	60.5	Foraminifera	12500	110			13874
	OS-78452	101.5	Sediment (C org)	28900	190			32792 ± 364
	OS-78453	191.5	Sediment (C org)	36700	310			41357 ± 273
EG-02	OS-78387	30	Foraminifera	4570	130			4665 ± 164
	OS-78389	90	Foraminifera	9460	180			10235 ± 234
	OS-78383	181.5	Foram. and Pteropods	12100	180			13481 ± 181
EG-03	OS-78385	90	Foraminifera	4910	120			5118 ± 161
	OS-78382	160	Foraminifera	8590	130			9147 ±167
	OS-78324	230	Foraminifera	9740	80			10508 ± 87
17603-3	OS-123791	0	Nps	720	20	257-336/ 344-356	151-159/ 227-424	302
	OS-123794	10	Nps	1260	30	680-775	653-854	736
	OS-123803	10B	mix benthonic foraminifera	1430	25	859-960	787-1006	909
	OS-123804	20	Nps	2280	35	1745-1873	1686-1938	1813
	OS-123422	30	Nps	2580	45	2118-2274	2028-2317	2183
	OS-123805	50	Nps	3560	35	3323-3440	3236-3502	3377
	OS-123796	80	Nps	4590	35	4654-4663/ 4673-4807	4569-4832	4723
	OS-123408	140	Nps	6520	50	6851-7027	6787-7129	6946
	OS-123536	160	Nps	6840	35	7250-7357	7201-7408	7303

	OS-123786	210	mix planktonic foraminifera	7750	40	8054-8200	8010-8281	8143
	OS-123795	210B	*C. wuellerstorfi*	8030	55	8360-8492	8306-8566	8426
	OS-123404	240	Nps	8240	65	8544-8777	8479-8933	8676
	OS-123406	270	Nps	8440	60	8848-9069	8706-9171	8954
	OS-123409	360	mix planktonic foraminifera	8770	60	9299-9450	9199-9509	9370
	OS-123657	660	Nps	10900	40	12221-12476	12085-12539	12335
	OS-123405	680	Nps	11650	80	12951-13169	12834-13263	13059
	OS-123420	680B	mix benthonic foraminifera	11650	160	12886-13229	12718-13354	13051
	OS-123782	720	mix benthonic foraminifera	11700	65	13031-13220	12915-13289	13119
	OS-123421	790	mix benthonic foraminifera	12450	190	13619-14089	13382-14489	13869
	OS-123411	820	mix planktonic foraminifera	12400	120	13652-13957	13495-14083	13800
	OS-123413	820B	mix benthonic foraminifera	12750	110	14024-14508	13899-14837	14286
	OS-123424	860B	mix benthonic foraminifera	13300	160	15077-15620	14663-15875	15305
	OS-123425	970	mix benthonic foraminifera	12850	170	14126-14802	13957-15125	14505
17623-2	OS-123537	30	Foraminifera	1810	15	1259-1327	1224-1274	1294
	OS-123538	90	Foraminifera	3590	20	3356-3451	3318-3528	3409
	OS-123539	170	Foraminifera	5550	20	5808-5916	5737-5949	5864

	OS-123577	310	Foraminifera	8480	25	8967-9074	8886-9144	9017
	OS-123578	320	Foraminifera	8840	30	9408-9488	9341-9524	9446
GS191-01PC	OS-123414	45	Foraminifera	1740	40	1166-1271	1074-1305	1212
	OS-123438	231	Foraminifera	4850	30	4912-5087/ 5093-5114	4859-5209	5017
	OS-123439	322	Foraminifera	7030	30	7408-7494	7360-7551	7450
	OS-123440	915	Foraminifera	15150	55	17758-17944	17636-18027	17841
	OS-123412	934	Foraminifera	15900	150	18516-18827	18322-18967	18666
	OS-123527	1053	Foraminifera	20200	100	23587-23888	23436-24032	23736
	OS-123526	1137	Foraminifera	21500	120	25209-25524	25030-25664	25359
	OS-123407	1713	Foraminifera	34900	1500	36966-40388	35522-41726	38722

Table 3 Radiocarbon dates and calendar year calibrations for the studied cores. EG= *EGLACOM*; 176xx-x= *CORIBAR*; GS= *PREPARED*; Nps= *N. pachyderma* (s)

The age model for core 17603-3 is based on magnetic susceptibility correlations with two *EGLACOM* studied sediment cores, located in the neighboring area, following the procedure described in Sagnotti et al. (2011), in which the radiometric ages from EG-02 and EG-03 cores were transferred to a common stratigraphic depth on core 17603-3. Refining of the age model of core 17603-3 was assisted by the 23 new radiocarbon dates. Downcore ages were obtained by linear interpolation between dated/correlated levels.

The age model for core GS191-01PC was developed by linear interpolation between the calibrated radiocarbon dated levels.

The late glacial–Holocene chronostratigraphic intervals are based on the most recent divisions defined on the basis of Greenland ice cores (Rasmussen et al., 2007; Steffensen et al., 2008;

Walker et al., 2012): Bølling–Allerød interstadial 14.5 to 12.9 cal ka BP, Younger Dryas 12.9 to 11.7 cal ka BP and Holocene 11.7 cal ka BP to Present.

References

Andruleit, H.A., Baumann, K.H., 1998. History of the last deglaciation and holocene in the Nordic seas as revealed by coccolithophore assemblages. Mar. Micropaleontol. 35, 179–201. doi:10.1016/S0377-8398(98)00021-8

Backman, J., Shackleton, N.J., 1983. Quantitative biochronology of Pliocene and early Pleistocene calcareous nannofossils from the Atlantic, Indian and Pacific oceans. Mar. Micropaleontol. 8, 141–170. doi:10.1016/0377-8398(83)90009-9

Biscaye, P.E., 1965. Mineralogy and Sedimentation of Recent Deep-Sea Clay in the Atlantic Ocean and Adjacent Seas and Oceans. Geol. Soc. Am. Bull. 76, 803–832. doi:10.1130/0016-7606(1965)76[803:masord]2.0.co;2

Bown, P.R., Young, J.R., 1998. Calcareous Nannofossil Biostratigraphy.

de Kaenel, E., Villa, G., 1996. Oligocene–Miocene calcareous nannofossils biostratigraphy and paleoecology from the Iberia Abyssal Plain, in: Proceedings of the Ocean Drilling Program, 149 Scientific Results. Ocean Drilling Program. doi:10.2973/odp.proc.sr.149.208.1996

Dittert, N., Baumann, K.H., Bickert, T., Henrich, R., Kinkel, H., Meggers, H., 1999. Carbonate dissolution in the Deep-Sea: Methods, Quantification and Paleoceanographic Application. Proxies Paleoceanogr. Examples from South Atl. 255–284.

Friedman, G.M., Sanders, J.E., 1978. Principles of Sedimentology, John Wiley. ed. New York.

Hammer, Ø., Harper, D.A.T., Ryan, P.D., 2001. PAST: Palaeontological statistics software package for education and data analysis. Palaeontol. Electron. 4, 1–9. doi:10.1163/001121611X566785

Lucchi, R.G., Camerlenghi, A., Rebesco, M., Colmenero-Hidalgo, E., Sierro, F.J., Sagnotti, L., Urgeles, R., Melis, R., Morigi, C., Bàrcena, M.A., Giorgetti, G., Villa, G., Persico, D., Flores, J.A., Rigual-Hernandez, A.S., Pedrosa, M.T., Macri, P., Caburlotto, A., 2013. Postglacial sedimentary processes on the Storfjorden and Kveithola trough mouth fans: Significance of extreme glacimarine sedimentation. Glob. Planet. Change 111, 309–326. doi:10.1016/j.gloplacha.2013.10.008

Mangerud, J., Bondevik, S., Gulliksen, S., Karin Hufthammer, A., Høisæter, T., 2006. Marine 14C reservoir ages for 19th century whales and molluscs from the North Atlantic. Quat. Sci. Rev.

25, 3228–3245. doi:10.1016/j.quascirev.2006.03.010

Mangerud, J., Gulliksen, S., 1975. Apparent radiocarbon ages of recent marine shells from Norway, Spitsbergen, and Arctic Canada. Quat. Res. 5, 263–273. doi:10.1016/0033-5894(75)90028-9

Rasmussen, T.L., Thomsen, E., Ślubowska, M.A., Jessen, S., Solheim, A., Koç, N., 2007. Paleoceanographic evolution of the SW Svalbard margin (76°N) since 20,000 14C yr BP. Quat. Res. 67, 100–114. doi:10.1016/j.yqres.2006.07.002

Reimer, P., 2013. IntCal13 and Marine13 Radiocarbon Age Calibration Curves 0–50,000 Years cal BP. Radiocarbon 55, 1869–1887. doi:10.2458/azu_js_rc.55.16947

Rio, D., Raffi, I., Villa, G., 1990. Pliocene-Pleistocene calcareous nannofossil distribution patterns in the western Mediterranean. Proc., Sci. results, ODP, Leg 107, Tyrrhenian Sea 107, 513–533.

Sagnotti, L., MacRì, P., Lucchi, R., Rebesco, M., Camerlenghi, A., 2011. A Holocene paleosecular variation record from the northwestern Barents Sea continental margin. Geochemistry, Geophys. Geosystems 12, 1–24. doi:10.1029/2011GC003810

Steffensen, J.P., Andersen, K.K., Bigler, M., Clausen, H.B., Dahl-Jensen, D., Fischer, H., Goto-Azuma, K., Hansson, M., Johnsen, S.J., Jouzel, J., Masson-Delmotte, V., Popp, T., Rasmussen, S.O., Röthlisberger, R., Ruth, U., Stauffer, B., Siggaard-Andersen, M.-L., Sveinbjörnsdóttir, A.E., Svensson, A., White, J.W.C., 2008. High-resolution Greenland ice core data show abrupt climate change happens in few years. Science 321, 680–684. doi:10.1126/science.1157707

Stuiver, M., Reimer, P.J., 1993. Extended 14C data base and revised CALIB 3.0 ^{14}C age calibration program. Radiocarbon 35, 215–230.

Walker, M.J.C., Berkelhammer, M., Björck, S., Cwynar, L.C., Fisher, D.A., Long, A.J., Lowe, J.J., Newnham, R.M., Rasmussen, S.O., Weiss, H., 2012. Formal subdivision of the Holocene Series/Epoch: A Discussion Paper by a Working Group of INTIMATE (Integration of ice-core, marine and terrestrial records) and the Subcommission on Quaternary Stratigraphy (International Commission on Stratigraphy). J. Quat. Sci. 27, 649–659. doi:10.1002/jqs.2565

CHAPTER III

Case study 1: Palaeoclimatic changes in Kveithola, Svalbard, during the Late Pleistocene deglaciation and Holocene: Evidences from microfossil and sedimentary records (CORIBAR project)

This paper has been published as Carbonara K., Mezgec K., Varagona G., Musco M.E., Lucchi R.G., Villa G., Morigi C., Melis R., Caffau M., on the Journal Palaeogeography Palaeoclimatology Palaeoecology, 463: 136-149. doi.org/10.1016/j.palaeo.2016.10.003, October 2016.

Palaeogeography, Palaeoclimatology, Palaeoecology 463 (2016) 136–149

Contents lists available at ScienceDirect

Palaeogeography, Palaeoclimatology, Palaeoecology

journal homepage: www.elsevier.com/locate/palaeo

Palaeoclimatic changes in Kveithola, Svalbard, during the Late Pleistocene deglaciation and Holocene: Evidences from microfossil and sedimentary records

Katia Carbonara [a,*], Karin Mezgec [b], Gabriella Varagona [c], Maria Elena Musco [b], Renata Giulia Lucchi [d], Giuliana Villa [a], Caterina Morigi [e,f], Romana Melis [c], Mauro Caffau [d]

[a] Department of Physics and Earth Sciences, Università di Parma, 43124 Parma, Italy
[b] Department of Physical Sciences, Earth and Environment, Università di Siena, 53100 Siena, Italy
[c] Department of Mathematics and Geosciences, Università di Trieste, 34128 Trieste, Italy
[d] OGS (Istituto Nazionale di Oceanografia e di Geofisica Sperimentale), 34010 Sgonico, TS, Italy
[e] GEUS (Stratigraphy Department Geological Survey of Denmark and Greenland), 1350 Copenhagen, Denmark
[f] Department of Earth Sciences, Università di Pisa, 56126 Pisa, Italy

ARTICLE INFO

Article history:
Received 9 June 2016
Received in revised form 29 September 2016
Accepted 5 October 2016
Available online 6 October 2016

Keywords:
Palaeoclimate
Arctic sediment core
Microfossils
Holocene
Late Pleistocene
Clay minerals

ABSTRACT

Climate changes are reflected in the Arctic ecosystem history over different timescales. We use a multi proxy-based approach for palaeoenvironmental and palaeoclimatic reconstructions, conducted on sediment cores, compared with summer insolation and Greenland ice core $\delta^{18}O$ data in order to establish a framework for climate changes from Late Pleistocene to late Holocene. Our dataset includes the results compiled from a sediment core, collected on the middle slope of the Kveithola Trough Mouth Fan (South of Svalbard) during the CORIBAR cruise (2013). The studied core presents remarkable lithological and magnetic susceptibility similarities with cores recovered in the same area during the SVAIS (2007) and the OGS-EGLACOM cruise (2008), allowing the construction of the age model. The results indicate that during the last 14.5 cal ky BP advances and retreats of the Svalbard Barents Sea Ice Sheet were strictly linked to the interplay of Atlantic and Arctic water inflows to the study area. During the deglaciation, from the Last Glacial Maximum to the onset of the Holocene, the climate underwent a series of abrupt changes including the Bølling-Allerød warm interstadial and the Younger Dryas cold event. During the early Holocene, the investigated area was dominated by enhanced warm Atlantic water inflow, which was concomitant with summer insolation increase, characterizing the Holocene Thermal Maximum. Conversely, the late Holocene was governed by deteriorating climatic conditions, with predominant Arctic/Polar water inflow on the surface water masses off Western Svalbard, possibly associated with summer insolation decline due to orbital forcing.

1. Introduction

The polar oceans are sites of deep-water formation driving the thermohaline circulation and affecting climate on a global scale. Palaeoclimatic reconstructions can be achieved through proxies, such as microfossil assemblages and clay mineral distribution, that provide key information for water masses provenance and environmental targets such as sea surface temperature (SST), salinity, sea-ice cover and marine biological productivity.

Here we focus on the marine biotic response to Late Pleistocene and Holocene climate changes, using an integrated approach on a sediment core. The aim of the present research is the reconstruction of the palaeoclimatic and palaeoenvironmental changes in the Kveithola glacial trough system (South of Svalbard) during the Late Pleistocene deglaciation and the Holocene on the basis of the microfossil phyto and zooplankton assemblages and clay mineral distribution. The Late Pleistocene deglaciation was an unsteady process; ice sheets, at various times, temporarily arrested, advanced and/or retreated affecting the climate of the surrounding areas. According to Winsborrow et al. (2010) the deglaciation of the SW Barents Sea (Bjørnøyrenna glacial trough system) initiated at ca. 15.5 cal ka BP, while Jessen et al. (2010) and Lucchi et al. (2013) indicated deglaciation on the NW Barents Sea started at ca. 20.5 cal ka BP. The subsequent Holocene is the youngest phase of the Earth climate history that began when the last glaciation ended. During the Quaternary, commonly preserved microfossil groups in polar areas include calcareous nannofossils (Backman et al., 2009), diatoms (Koç and Schrader, 1990) and planktonic foraminifera (Wollenburg and

* Corresponding author.
E-mail address: katia.carbonara@studenti.unipr.it (K. Carbonara).

http://dx.doi.org/10.1016/j.palaeo.2016.10.003
0031-0182/

Kuhnt, 2000). The distribution of these microfossils has been investigated in a sediment core, collected from the Kveithola Trough Mouth Fan (TMF) middle slope in the framework of the international project CORIBAR, sharing objectives with the International Polar Year (IPY) Activity 367 NICESTREAMS (Neogene Ice Streams and Sedimentary Processes on High-Latitude Continental Margins). The results from the studied core were compared with the dataset obtained from neighbouring sediment cores recovered during IPY 2007–2009: the SVAIS project (Development of an Arctic ice stream-dominated sedimentary system: The Southern Svalbard continental margin), funded as Spanish IPY research program, and the EGLACOM project (Evolution of a glacial Arctic continental margin: The Southern Svalbard ice stream-dominated sedimentary system), funded by the Istituto Nazionale di Oceanografia e di Geofisica Sperimentale (OGS), as contribution to IPY Italian activity.

The study of the Kveithola represents an excellent opportunity to improve the understanding of palaeoclimate variations over the approximately last 14.5 cal ky BP, because of the presence of an expanded and continuous sedimentary sequence from the last deglaciation to the Holocene. Past climatic reversals had major impacts on Arctic regions over timescales much shorter than orbital cycles and they provide a unique framework for today's climatic changes.

2. Study area

The Kveithola Trough Mouth Fan (TMF) is situated North-West of the Bjørnøya island and South of the Spitsbergenbanken, the shallowest bank in the Barents Sea having a water depth of 30–80 mbsl (Rüther et al., 2012) (Fig. 1a). The Kveithola is a glacial U-shaped trough with an East-West orientation and it is about 90 km long, 15 km wide, with a water depth that ranges between 200 and 400 mbsl (Rebesco et al., 2011; Rüther et al., 2012). The Kveithola, part of the Storfjorden glacial system, was carved by ice streams that during the last glacial period drained ice from both Svalbard, located in the Northern area, and Bjørnøya, located in the Southern area (Andreassen et al., 2008; Rebesco et al., 2011). The Storfjorden-Kveithola palaeo-ice stream is a small system compared to the major drainage systems of the Barents Sea (Svendsen et al., 2004); however, it contains a valuable high-resolution sedimentary and climate archive for its location close to the Fram Strait that represents the only deep-sea gateway for water masses exchange between the Arctic Ocean and the Greenland-Norwegian Sea. Two main currents interact in the study area: the West Spitsbergen Current (WSC) and the Eastern Spitsbergen Current (ESC) (Fig. 1b). At about 70°N the Norwegian Atlantic Current (NwAC) splits into the North Cape Current (NCaC), that flows into the Southern part of the Barents Sea, and the West Spitsbergen Current (WSC), that carries on Northward along the Western slope of Svalbard into the Arctic Ocean (Blindheim and Rey, 2004; Groot et al., 2014). The WSC transports relatively warm (6 to 8 °C) and salty (35.1 to 35.3‰) Atlantic water, keeping this area free of ice year-round (Aagaard et al., 1987). A branch of the WSC mixes with Polar water moving North of Svalbard and enters again the Barents Sea East of Spitsbergen. This current, the Eastern Spitsbergen Current (ESC), is characterized by lower temperature (0 °C) and salinity (34.3–34.8‰) with respect to the WSC being covered by seasonal sea-ice during winter that causes dense deep water formation by brine rejection (Loeng, 1991). The extent of the sea-ice cover is controlled by the Polar and Atlantic surface water boundaries, that constrain the location of the two oceanic fronts, the Polar front (PF) and the Arctic front (AF) (Fig. 1b). The PF corresponds to the average summer sea-ice margin and the AF is associated with the maximum extension of sea-ice during winter (Zamelczyk et al., 2012).

3. Material and methods

This study is based on the investigation of a 974 cm long gravity core (GeoB17603-3, in the following indicated as 17603-3) recovered on the

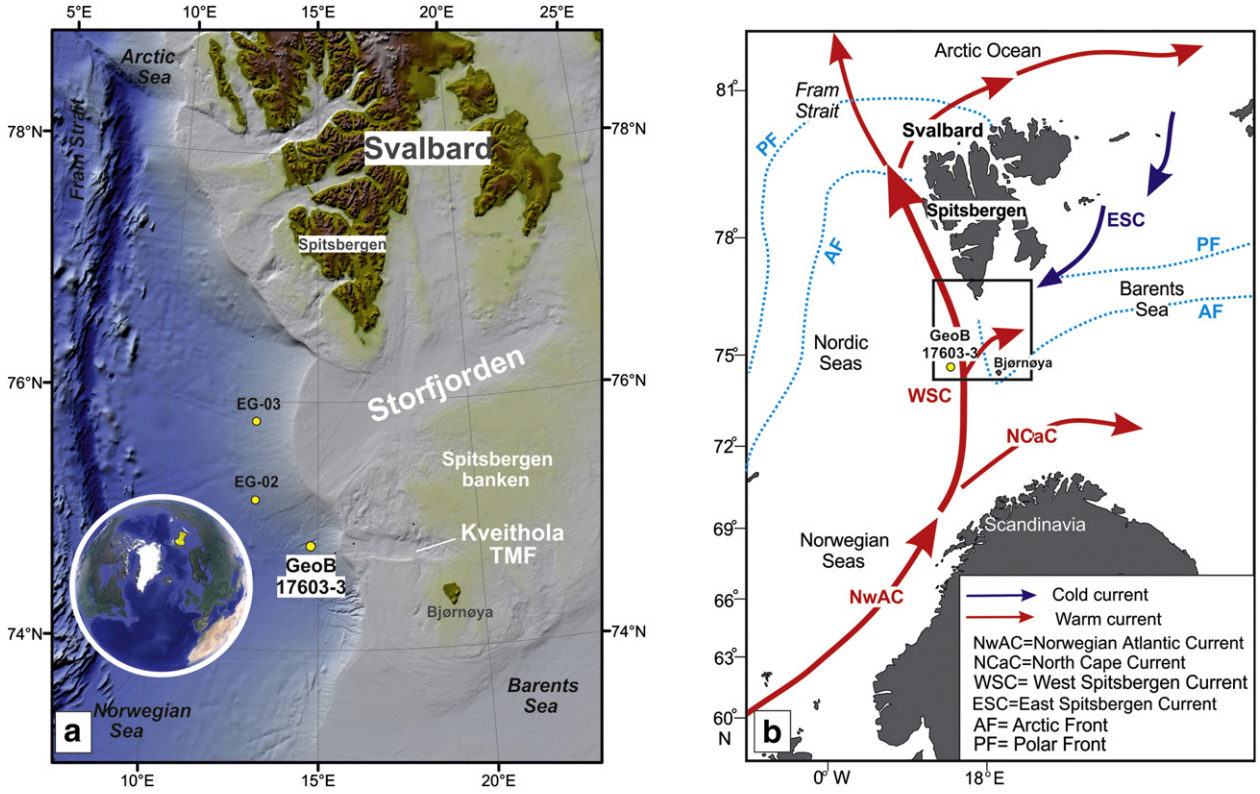

Fig. 1. a – Location of the study area. Yellow dots indicate the studied core CORIBAR 17603-3 and other cores also discussed in the text (EGLACOM cores); TMF = Trough Mouth Fan; b – oceanographic circulation in the NW Barents Sea. The black box indicates location of the study area.

Table 1
Core location, water depth and total sediment recovery for core 17603-3. TMF = Trough Mouth Fan.

Core ID	Lat. N	Long. E	Water depth (m)	Location	Total recovery (cm)
GeoB17603-3	74° 51,00′	14° 48,09′	1430	Middle slope of Kveithola TMF	974

Kveithola TMF middle slope during the CORIBAR cruise on board the R/V Maria S. Merian (summer 2013) (Table 1, Fig. 1a). The core was initially analysed using a GEOTEK Multi-sensor Core Logger for Magnetic Susceptibility (k), opened and visually logged. Sediment samples were collected regularly at 10 cm intervals and analysed for sedimentological characteristics and microfossil content, including calcareous nannofossils, diatoms and planktonic foraminifera.

3.1. Sedimentary analyses

A total of 29 samples were analysed for water content and grain size characteristics using a coulter counter laser Beckman LS-230 to measure the 0.04–2000 μm fraction at 0.004 μm resolution. The samples were initially treated with diluted peroxide and the disaggregated sediments were re-suspended into a 0.1% sodium-hexametaphosphate solution and left for 3 min in ultrasonic bath prior to measurement. The results were classified according to Friedman and Sanders (1978) grain-size scale.

Clay mineral analyses were performed on 29 samples at 30–40 cm sampling interval. Separation of the clay fraction was obtained by centrifugation during 1 min at 1050 rounds/min to settle the particles 2–63 μm (silt), and 10 min at 3980 rounds/min to settle the clay fraction leaving the pore water salt in suspension within distilled water.

X-ray diffraction (XRD) was performed on the clay samples mounted on smear slides, using a Philips PW1710 powder diffraction system, using CuKα radiation (40 kV, 40 mA). Each sample was analysed between 2° and 40° 2θ, with a step size of 0.02° 2θ in the air-dry state and after ethylene glycol solvation that permits the expansion of smectite peak to a basal spacing of about 17 Å. A slower scan, between 23° and 25.5° 2θ, with a step size of 0.005° 2θ was performed on the glycolated samples, in order to obtain a better resolution of the chlorite-kaolinite twin peak. Semi-quantitatively estimation of the main clay mineral abundance (smectite, chlorite, kaolinite and illite) was determined using the MacDiff software, relative percentages of each clay mineral were computed using weighting factors (Biscaye, 1965). Clay mineral percentage standard deviations were calculated using illite ±1%, smectite ±1%, chlorite ±2.5%, kaolinite ±2% according to Damiani et al. (2006).

X-ray fluorescence (XRF) core-scan analyses were performed at 1 cm resolution using an Avaatech instrument at 10 and 50 kV setting and the Ca, Fe and Ti contents were determined.

3.2. Chronology

Ten Accelerator Mass Spectrometry (AMS) ^{14}C ages were performed on planktonic foraminifera at NOSAM Laboratory (Table 2). The radiocarbon ages were calibrated with the software Calib 7.1 (Stuiver and Reimer, 1993) using the Marine13 calibration curve (Reimer, 2013) and applying an average marine regional reservoir effect $\Delta R = 67 \pm 34$ years, obtained from the Marine Reservoir Correction Database of Calib 7.1 for the North-Western Barents Sea area (Mangerud and Gulliksen, 1975; Mangerud et al., 2006). Calibrated ages at $\pm 1\sigma$ and $\pm 2\sigma$ are delivered by the program normalized to calendar year and are indicated in the following as cal a BP or as cal ka BP.

The age model for core 17603-3 is based on magnetic susceptibility correlations with two previously studied sediment cores (Fig. 2), located in the surrounding area, following the procedure described in Sagnotti et al. (2011), in which the radiometric ages from the EGLACOM cores EG-02 and EG-03 were transferred to a common stratigraphic depth on core 17603-3. Refining of the age model of core 17603-3 was assisted by the new radiocarbon dates. The lithological sequence and the magnetic susceptibility are consistent between the CORIBAR and EGLACOM cores and, for this reason, the upper part of the core 17603-3 was correlated to the Holocene sequence of core EG-03, whereas the lower part of the core was correlated to the post LGM sequence recovered in core EG-02. Down core ages were obtained by linear interpolation between dated/correlated levels (Fig. 2). Sediment accumulation rate was also determined (Fig. 3).

3.3. Micropalaeontological analyses

3.3.1. Calcareous nannofossils

A total of 98 samples were analysed for calcareous nannofossil content with a sampling interval of 10 cm. All samples were prepared from unprocessed material as smear slides, following standard techniques (Bown and Young, 1998) and examined using a Zeiss Axioskop light microscope at 1250× magnification. The coccoliths were counted in 200 fields of view, corresponding to a smear slide area of 6.28 mm^2 following the method described by Backman and Shackleton (1983) and Rio et al. (1990). Relative abundance, expressed in percentage, and absolute abundance, expressed as number of specimens per 10 mm^2 in the slides, were calculated. Only one sample is completely barren and few samples in the lower part of the core, mainly corresponding to the ice-rafted debris (IRD) deposits, contain very rare nannofossils. The state of coccolith preservation varies from poor to good. A number of ecological indices were calculated and considered for environmental reconstruction, such as:

- the ratio between *Emiliania huxleyi* and *Coccolithus pelagicus* s.l. (H/P ratio) that in the Nordic Seas fossil assemblages gives indication on the location of the Arctic Front (Andruleit and Baumann, 1998) separating the seasonally sea ice covered Polar and Arctic water from the warmer and saltier Atlantic-derived water. This ratio was expressed in logarithmic scale;

Table 2
Radiocarbon dates and calendar year calibrations for core 17603-3 record.

Lab. code	Depth (cm)	Material	^{14}C age	Age error	1 σ cal age (cal a BP)	2 σ cal age (cal a BP)	Median probability (cal a BP)
OS-123791	0	*N. pachyderma* sin	720	20	257–336 and 344–356	151–159 and 227–424	302
OS-123804	20	*N. pachyderma* sin	2280	35	1745–1873	1686–1938	1813
OS-123796	80	*N. pachyderma* sin	4590	35	4654–4663 and 4673–4807	4569–4832	4723
OS-123408	140	*N. pachyderma* sin	6520	50	6851–7027	6787–7129	6946
OS-123536	160	*N. pachyderma* sin	6840	35	7250–7357	7201–7408	7303
OS-123786	210	Mix planktonic foraminifera	7750	40	8054–8200	8010–8281	8143
OS-123409	360	Mix planktonic foraminifera	8770	60	9299–9450	9199–9509	9370
OS-123657	660	*N. pachyderma* sin	10,900	40	12,221–12,476	12,085–12,539	12,335
OS-123411	820	Mix planktonic foraminifera	12,400	120	13,652–13,957	13,495–14,083	13,800
OS-123425	970	Mix planktonic foraminifera	12,850	170	14,126–14,802	13,957–15,125	14,505

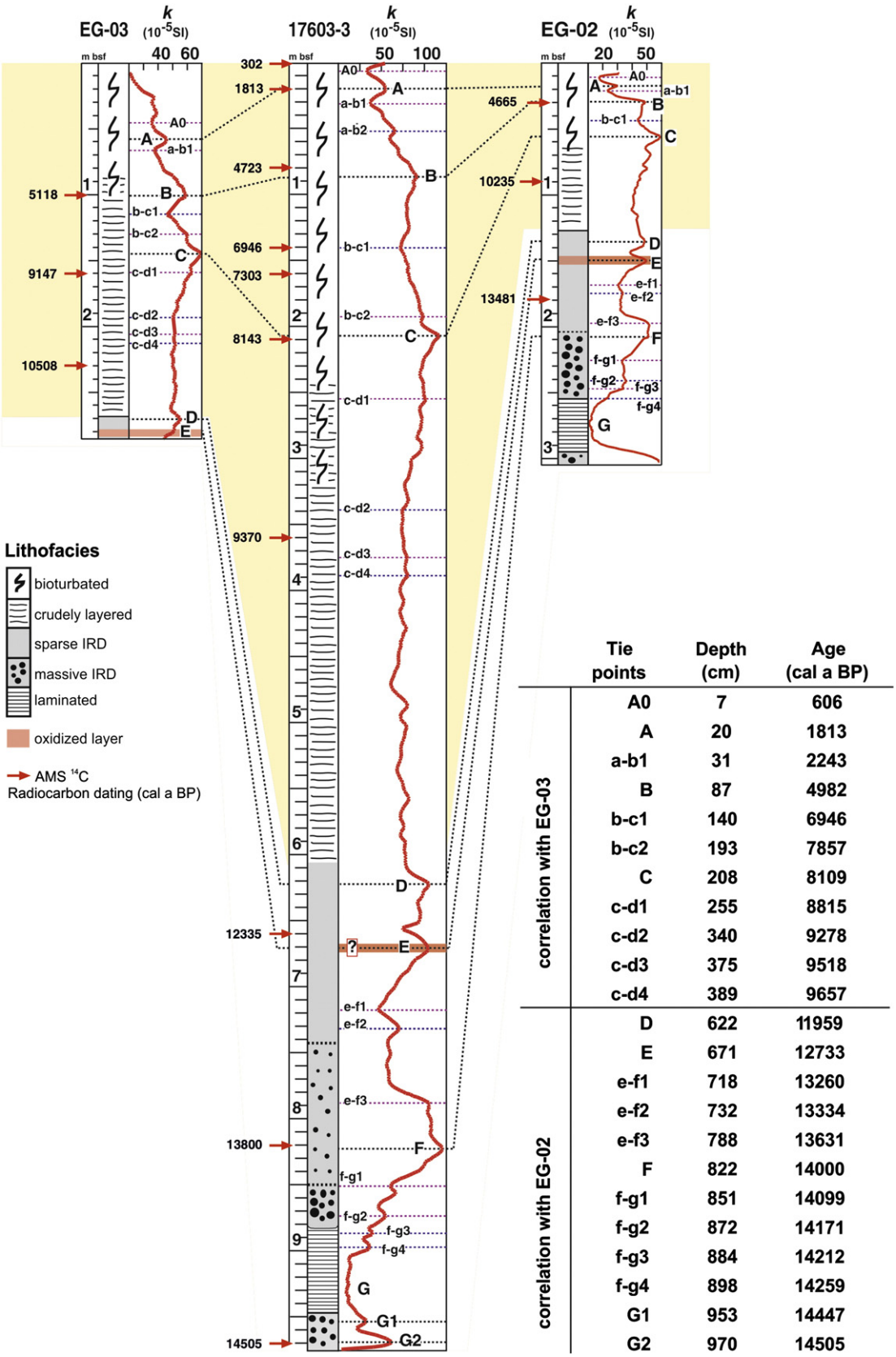

	Tie points	Depth (cm)	Age (cal a BP)
correlation with EG-03	A0	7	606
	A	20	1813
	a-b1	31	2243
	B	87	4982
	b-c1	140	6946
	b-c2	193	7857
	C	208	8109
	c-d1	255	8815
	c-d2	340	9278
	c-d3	375	9518
	c-d4	389	9657
correlation with EG-02	D	622	11959
	E	671	12733
	e-f1	718	13260
	e-f2	732	13334
	e-f3	788	13631
	F	822	14000
	f-g1	851	14099
	f-g2	872	14171
	f-g3	884	14212
	f-g4	898	14259
	G1	953	14447
	G2	970	14505

Fig. 2. Correlation between 17603-3, EG-02 and EG-03 cores, based on the proposed age model (see text for details). Calibrated calendar ages are indicated with red arrows.

- the dominance and Shannon Wiener diversity indices were calculated from species relative abundance, using the software PAST (Hammer et al., 2001).

Additionally, the cold-water taxa, obtained by the sum of the *C. pelagicus* s.l., *E. huxleyi* (>4 μm) and *Gephyrocapsa muellerae*, were plotted against warm-water taxa that includes *E. huxleyi* (<4 μm), *Gephyrocapsa oceanica* and small *Gephyrocapsa* spp.

3.3.2. Diatoms

A total of 48 samples were analysed for diatom content at a variable spacing distance of 10–20 cm. Slides for diatoms were prepared following the technique described by Rathburn et al. (1997). At least 300 diatom valves were identified in each sample and counted at 1000× magnification using an Ortholux light microscope following the method described by Crosta and Koç (2007). In the samples containing rare diatoms, in terms of numbers, the counting was extended to 1000 fields of view. Relative abundance, expressed in percentage, and total absolute diatom abundance (ADA), expressed as number of frustules per gram of dry weight (v/gdw), were calculated for each sample using the methodology described by Armand (1997). The dominance and Shannon Wiener diversity indices were calculated from species relative abundance, using the software PAST (Hammer et al., 2001).

3.3.3. Planktonic foraminifera

The 51 samples analysed for planktonic foraminifera were dry weighed and wet sieved at 63 μm, keeping the silt-clay fraction for mineralogical analysis. The sandy residues were dried at 50 °C, weighed and dry-sieved at 150 μm. Only the latter fraction (>150 μm) was analysed, for comparison with the results obtained from the sediment cores recovered in the area surrounding site 17603-3 (i.e. Lucchi et al., 2013). About 250 specimens were counted for each sample and identified at species level; subsequently relative abundance of each species was expressed as relative percentage. The taxonomy follows that of Hemleben et al. (1989) and Darling et al. (2006). The flux of planktonic foraminiferal assemblage (planktonic foraminiferal accumulation rate - PFAR) (number/cm^2/kyr) was determined together with the flux of the three dominant species *Neogloboquadrina pachyderma* (s), *Turborotalita quinqueloba* and *Neogloboquadrina incompta* as:

$$\text{Species AR} = \text{Abundance of planktonic foraminifera per g of dry sediment } (\text{n}\cdot\text{g}^{-1}) \cdot \text{dry bulk density } (\text{g}\cdot\text{cm}^{-3}) \cdot \text{sedimentation rate } \left(\text{cm}\cdot\text{ka}^{-1}\right).$$

In addition, the number of planktonic foraminiferal fragments was counted and expressed as the relative percentage of the total planktonic foraminiferal abundance to quantify the degree of dissolution according to Thunell (1976) and Conan et al. (2002). The dominance and Shannon diversity indices were calculated from species relative abundance, using the software PAST (Hammer et al., 2001).

4. Results

The age model for the studied core and the comparison with the sedimentary sequence of the neighbouring core EG-02, indicate the presence of an expanded sequence spanning last 14.5 cal ky BP (974 cm-thick, instead of 305 cm of core EG-02, Fig. 2). In particular, the Holocene sequence appears exceptionally expanded with over 600 cm with respect to the 250 cm of core EG-03 and many other cores collected in this area (e.g. Jessen et al., 2010 and references therein).

4.1. Lithology and sediment characteristics

The sedimentary sequence (Fig. 3) from the bottom to the top of the core consists of ice-rafted debris (IRD)-rich sediments and finely laminated sediments, containing cm/mm-thick sandy or silty layers (974–880 cm). The interval 880–605 cm contains sparse IRD that are abundant between 835 and 880 cm. Sandy/silty mottles and crudely layered sediments (605–240 cm) contain abundant black patches composed of organic matter rich sediments (vigorous reaction to peroxide water). The interval 240–0 cm consists of bioturbated sediments.

The grain size distribution (Fig. 3) is characterized by predominant silt, often over 60% with an almost constant clay content (ca. 22% on average), and little sand content (10% on average). Peaks of sand correspond to the sandy layers of the laminated facies (e.g. at 940 cm), whereas slightly higher contents characterize the crudely layered lithofacies.

The water content increases progressively from bottom to the top of the core with minimum values corresponding to sandy layers.

The predominant clay mineral is illite (43–66%), followed by kaolinite (12–31%), chlorite (14–23%) and smectite (4–18%) (Fig. 3). Illite, chlorite and kaolinite have an almost stable percentage down core, except within the laminated sediments, where illite decreases having an opposite trend with respect to chlorite and kaolinite (slight increase of percentages). Smectite has an up-core general increasing trend, with low–trace values at the base of the core where laminated and IRD-rich sediments occur and consistently higher values in the crudely layered and heavily bioturbated sediments.

The Ca/Ti and Fe/Ti ratios (Fig. 3) were used to distinguish between biogenic and terrigenous input respectively. The two trends are almost opposite with biogenic-Ca barren sediments in the laminated and massive IRD lithofacies at the base of the core. The biogenic-Ca content increases progressively from 835 cm (14 cal ka BP) to the top of the core. At about 660 cm (12.3 cal ka BP) there is a distinct relative increase of the Fe content (minimum of Ca content), corresponding to a peak of the magnetic susceptibility that, in other cores, has been related to the presence of an oxidized layer (OX1, Lucchi et al., 2013), not observed in the studied core.

4.2. Micropalaeontological content

4.2.1. Calcareous nannofossils

The following taxa are discussed: *Calcidiscus leptoporus*, *Coccolithus pelagicus* s.l., *Emiliania huxleyi, Gephyrocapsa muellerae*, *Gephyrocapsa oceanica*; *Gephyrocapsa* <3 μm are indicated as small *Gephyrocapsa* spp. The assemblage is well represented by Holocene species together with some Palaeogene and Cretaceous reworked taxa (*Discoaster binodosus*, *Arkhangelskiella maastrichtiana*, *Biscutum* spp., *Staurolithites* spp., *Eiffellithus* spp., *Microrhabdulus* spp., *Tranolithus* spp., *Watznaueria* spp., *Zeugrhabdotus* spp.). For most micropalaeontological studies, the presence of reworked specimens is usually considered as a disturbing factor where palaeoenvironmental and biostratigraphic interpretations are to be made. However, reworking of microfossils, such as calcareous nannofossils, can be used providing useful information on erosion-transport processes acting in the area (Ferreira et al., 2008). Chiefly on the basis of biometric subdivisions, the following *E. huxleyi* morphotypes were distinguished: *E. huxleyi* <4 μm and *E. huxleyi* > 4 μm, following Colmenero-Hidalgo et al. (2002). The *E. huxleyi* <4 μm variety shows warm-water preferences, whereas the *E. huxleyi* > 4 μm variety is considered to represent a cold-water form (Colmenero-Hidalgo et al., 2002; Flores et al., 2010). The nannofossil total abundance (without reworking), calculated on number of specimens per fixed area, spans from 0 to 11,476 coccoliths/10 mm^2 through the core (Fig. 4). The interval from 974 to 596 cm is characterized by low total abundance of nannofossils (up to 1331 coccoliths/10 mm^2), with predominant *E. huxleyi* (up to 1293 coccoliths/10 mm^2 or 100%) (Fig. 4). The increase of the relatively cold-water species *G. muellerae* (up

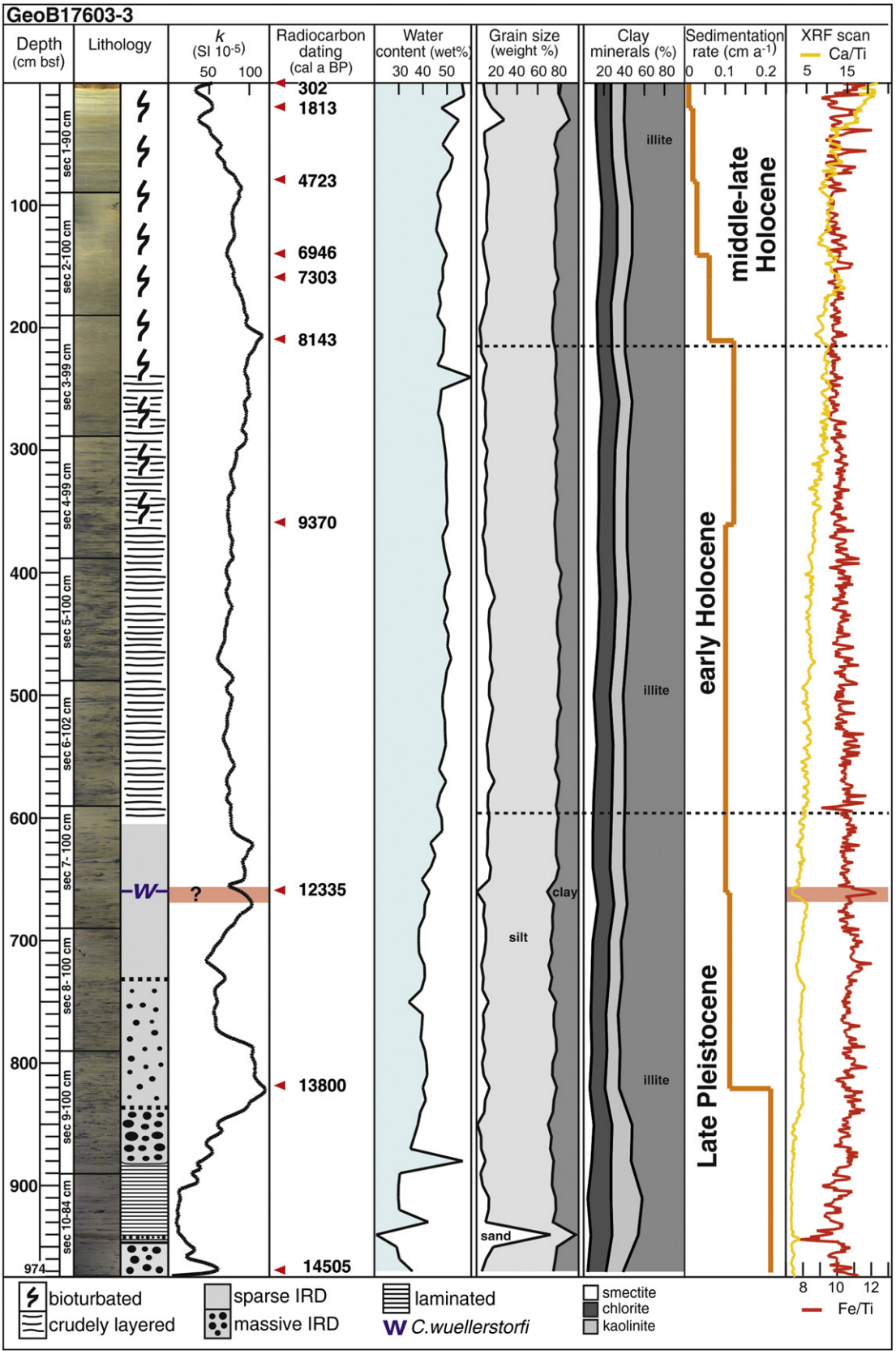

Fig. 3. Lithological log of core 17603-3 showing magnetic susceptibility (κ), water content, grain sizes, clay mineral content, sedimentation rate, Ca/Fe and Ca/Ti plots against core depth. The radiocarbon dated levels are also indicated. W = *Cibicides wuellerstorfi* first occurrence. The horizontal dotted lines correspond to time interval limits, commented in the discussions.

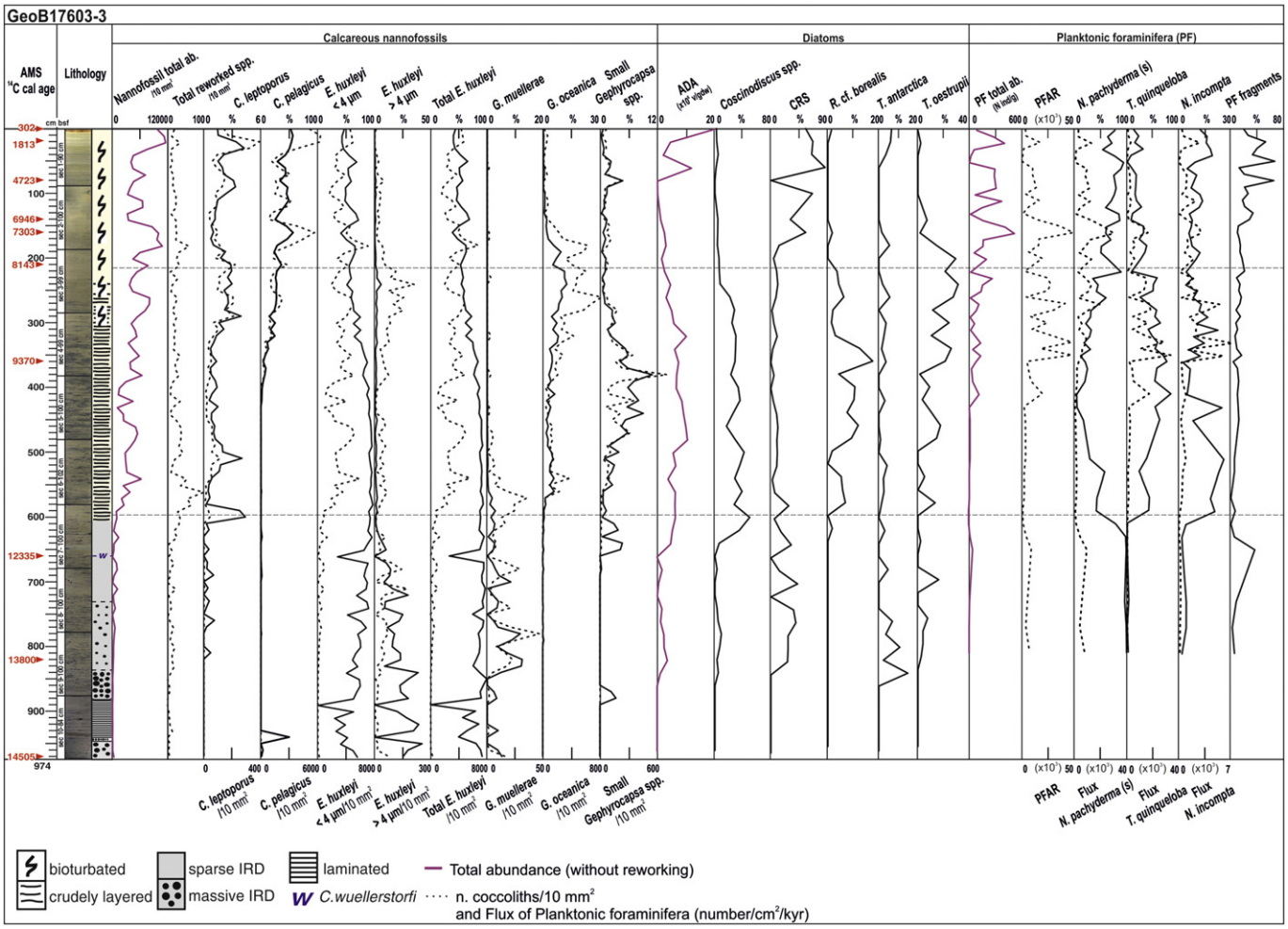

Fig. 4. Abundances of calcareous nannofossil, diatom and planktonic foraminiferal species for the investigated core plotted versus depth. ADA = absolute diatom abundance; CRS = *Chaetoceros* resting spore; W = *Cibicides wuellerstorfi* first occurrence; PF = planktonic foraminifera; PFAR = planktonic foraminiferal accumulation rate; microfossil total abundances are shown in purple. Red arrows indicate calibrated calendar ages dated by AMS ^{14}C (see Table 2 for details). Dotted lines indicate nannofossil absolute abundance, expressed as n. of coccoliths/10 mm^2 in the slide, and flux of planktonic foraminifera, expressed as number/cm^2/kyr.

to 12.39%) characterizes this interval along with a slight increase of total reworking (Fig. 4). A distinct crossover in abundance between *E. huxleyi* (>4 μm) and *E. huxleyi* (<4 μm) occurs between 650 and 630 cm (Fig. 4). The interval from 596 to 215 cm is characterized by increase of the total abundance of nannofossils (up to 8014 coccoliths/10 mm^2). The total reworking reaches values up to 97 coccoliths/10 mm^2 at 560 cm and it decreases towards the top of the core (Fig. 4). The interval between 596 and 215 cm is dominated by *E. huxleyi* (up to 94%) together with *C. leptoporus* (up to 4%), *G. oceanica* (up to 13%) and small *Gephyrocapsa* spp. (up to 11%) (Fig. 4). A drop of cold-water species *G. muellerae* (up to 0.5%) and a rise of relatively warm-water taxa *G. oceanica* (up to 6%) and small *Gephyrocapsa* spp. (up to 3%) occur at 560 cm (Fig. 4). A main crossover between dominance and diversity indices occurs at 410 cm (Fig. 5). An abrupt increase of relatively cold-water species *C. pelagicus* s.l. up to 36.04% and a concomitant slight decrease of *E. huxleyi* up to 53.49% occur between 390 and 215 cm (Fig. 4). The highest *G. oceanica* percentage is recorded at 240 cm with values up to 12.54% (Fig. 4). The interval between 215 and 0 cm is characterized by high values of *C. pelagicus* s.l. (up to 56.63%) and *E. huxleyi* (up to 69.11%). *Gephyrocapsa oceanica* records an abrupt decrease together with a general nannofossil total abundance drop (up to 3210 coccoliths/10 mm^2); although small *Gephyrocapsa* spp. relative abundance is generally low, its abundance trend shows a peak above 4% at 80 cm. The nannofossil total abundance increases to its highest value (11,476 coccoliths/10 mm^2) and it is persistently high up to the top of the core (Fig. 4).

Since the nannofossil assemblage is of low diversity through the core (Shannon Wiener diversity index up to 1.56), important changes in the assemblage structure can be described by ratio variations of the two dominant species *E. huxleyi* and *C. pelagicus* s.l. (H/P ratio), following Andruleit and Baumann (1998) (Fig. 5). According to recent oceanographic settings in the Nordic Seas an H/P ratio of >0 is indicative of Atlantic influenced conditions, while an H/P ratio of <0 indicates Arctic to Polar influenced conditions. The H/P ratio spans from −0.16 to 3.14 through the core (Fig. 5). An abrupt H/P ratio decrease is shown within the interlaminated lithofacies at 940 cm (up to 0); the highest H/P ratio is recorded between 460 and 450 cm with values up to 3.14. The H/P ratio presents a descending trend towards the top of the core (Fig. 5).

4.2.2. Diatoms

Seventeen diatom genera and 33 species were recognized. The absolute diatom abundance (ADA) spans from 0 to 23.3 × 10^6 v/gdw. The interval from 974 to 840 cm is characterized by the total absence of diatoms. The first diatom appearance occurs at 840 cm. The ADA shows values between 0 and 7.4 × 10^6 v/gdw from 840 to 596 cm. *Chaetoceros* (subgenus *Hyalochaete*) resting spore (CRS) dominates the assemblage reaching relative abundances up to 42.9%; the slight

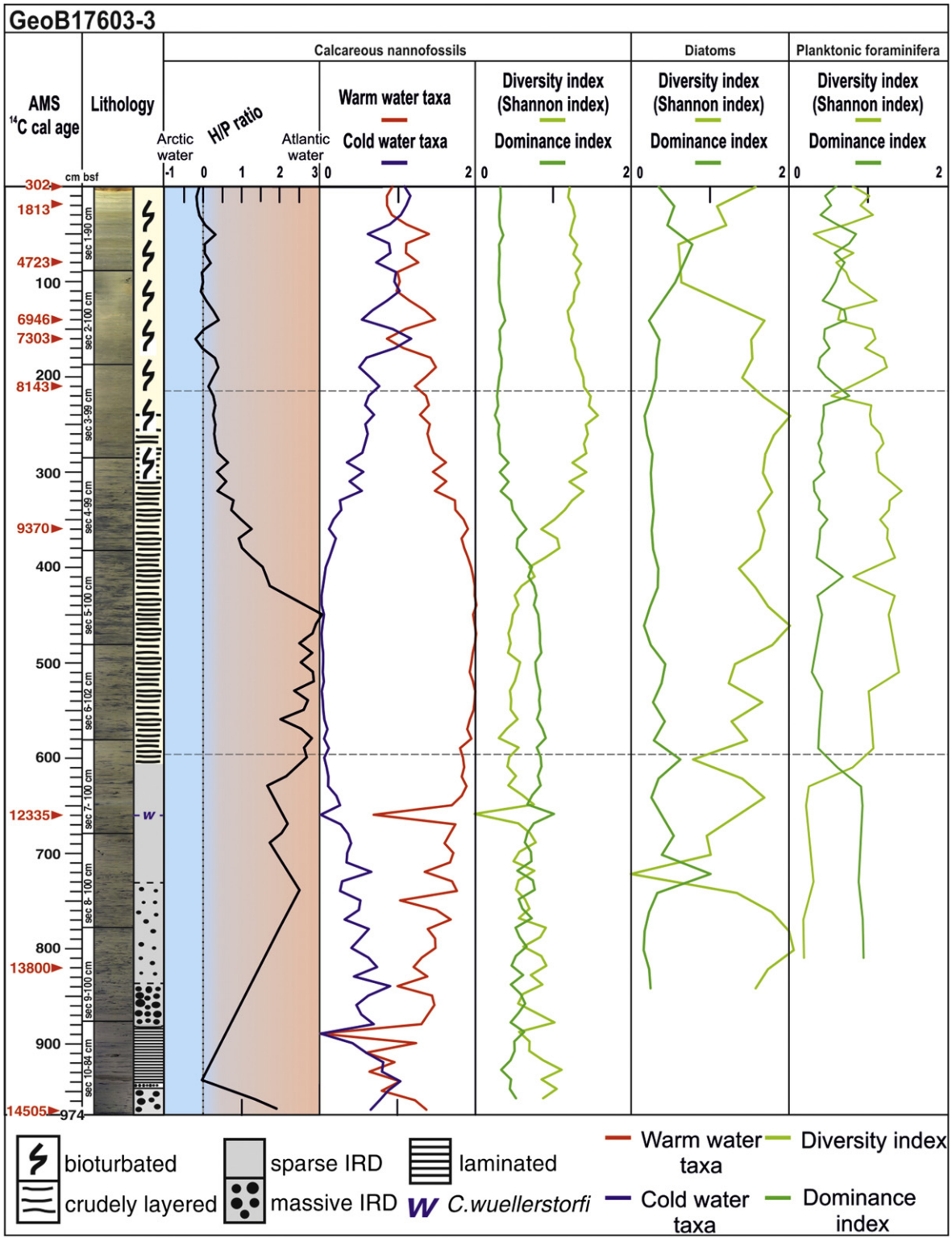

Fig. 5. Various ecological indices plotted against depth. The ratio of the two nannofossil dominant species *Emiliania huxleyi* and *Coccolithus pelagicus* (H/P ratio) equal to 0, approximately, marks the transition from Atlantic to Arctic influenced conditions. The cold-water taxa group (*C. pelagicus*, *E. huxleyi* (>4 μm) and *Gephyrocapsa muellerae*) are plotted against warm-water taxa (*E. huxleyi* (<4 μm), *Gephyrocapsa oceanica* and small *Gephyrocapsa* spp.). Dominance and Shannon Wiener diversity indices for all microfossil groups are shown. W = *Cibicides wuellerstorfi* first occurrence. Calibrated calendar ages are indicated with red arrows.

increase of relatively warm-water taxa *Coscinodiscus* spp. (up to 75%) and *Thalassiosira oestrupii* (up to 14%) characterizes the interval between 840 and 596 cm along with three peaks of the cold-water species *Thalassiosira antarctica*. The latter presents a descending trend towards the top of this interval with the highest peak at 840 cm (14%) (Fig. 4). The interval from 596 to 215 cm is characterized by the decrease of CRS and the abrupt increase of ADA, associated to high relative abundance of warm-water species *Coscinodiscus* spp. (mainly *C. marginatus* and *C. radiatus*). This genus reaches values up to 63% between 596 and 215 cm and slightly decreases towards the top of this interval.

Rhizosolenia cf. *borealis*, proxy for mixing water, derived from warmer (Norwegian) and colder (Arctic) waters, occurs between 596 and 215 cm. A peak of *T. oestrupii* abundance (28%) is recorded at 240 cm. Although *T. antarctica* relative abundance is generally very low, its abundance trend shows a peak above 5% at 260 cm. The ADA presents two main peaks at 480 cm (12.4×10^6 v/gdw) and at 320 cm (11.9×10^6 v/gdw). The interval from 215 to 0 cm is characterized by an abrupt increase of CRS (up to 87.1%). *Coscinodiscus* spp. and *T. oestrupii* show values up to ~6% until 140 cm, then they abruptly decrease to 0%. Generally low ADA ($0.2–3.6 \times 10^6$ v/gdw) is recorded until 80 cm. Diatoms disappear abruptly around 80 cm (Fig. 4). *Coscinodiscus* spp. is the only warm-water taxa in the upper part of the core having relative abundance above 2%. The cold-water related species *T. antarctica* increases in the topmost 40 cm of the core showing values up to 6%. The ADA abruptly increases in the uppermost 80 cm reaching the highest value (23.3×10^6 v/gdw) at the top of the core (Fig. 4). Shannon Wiener diversity index spans from 0 to 2.04 and it is generally higher than dominance (0.16–1) (Fig. 5).

4.2.3. Planktonic foraminifera

The dominant planktonic foraminiferal species are *Neogloboquadrina pachyderma* (s), followed by *Turborotalita quinqueloba* and *Neogloboquadrina incompta*. *Globigerina bulloides*, *Globigerina falconensis*, *Globigerinita glutinata*, *Globigerinita uvula* and *Orcadia riedeli* are present in low percentages (<19%). In this paper, we considered only the dominant species as they represent >80% of the entire association and they are the most significant taxa for palaeoenvironmental interpretations. Planktonic foraminifera are rare or absent from the base of the core up to 410 cm and the total abundance shows an increasing trend towards the top of the core, reaching values higher than 500 ind/g of dry sediment (Fig. 4). The PFAR shows a slight decrease between 410 and 215 cm, it rises between 215 and 160 cm, reaching its highest value (about 50,000 ind/cm^2/ky) at 160 cm; in the upper part of the core, between 160 and 0 cm it drops to value lower than 20,000 ind/cm^2/ky. In the interval from 974 to 596 cm, *Neogloboquadrina pachyderma* (s) is the dominant species, but always with low abundance; its flux reaches the value of 8765 ind/cm^2/ky at the 650 cm (Fig. 4). A drastic reduction of *N. pachyderma* (s) both as percentage and as flux occurs between 596 and 410 cm and following, until 215 cm, again a rise with percentages exceeding 86% (Fig. 4). *Turborotalita quinqueloba* is the second most common species. In the lower part of the core it is virtually absent up to 596 cm. It is present with high percentages (22–81%) between 596 and 215 cm, and then it decreases in the upper part of the core (215–0 cm) up to 7%. The flux of *T. quinqueloba* shows low values until 420 cm (0–2064 ind/cm^2/ky) and it reaches its highest value (32,520 ind/cm^2/ky) at 350 cm. *Neogloboquadrina incompta* is found in very low percentages between 974 and 596 cm. It follows an increase up to 430 cm reaching percentages of 20–25%, with a decrease up to 8% at 450 cm. From 410 to 215 cm it increases with a maximum of 22% at 310 cm. In the upper part of the core (215–0 cm) *N. incompta* occurs with low percentages (up to 19%) (Fig. 4). The percentages of fragmented tests are high (up to 35%) between 974 and 596 cm and they span from 0 to 20% between 596 and 215 cm. In the upper part of the core (215–0 cm), the percentages of fragments show an increasing trend, reaching values of 32% at 130 cm (Fig. 4). Two main crossovers between dominance and Shannon diversity indices occur at 610 cm and 220 cm; other minor fluctuations are recorded towards the top of the core (Fig. 5).

5. Discussions

The recovered core contains an expanded sedimentary sequence that includes continuous Upper Pleistocene and Holocene sediments. The climatic fluctuations within the studied intervals are well depicted by the microfossil assemblages and distribution of smectite that, in the studied area, is mainly transported by the North Atlantic Current (Junttila et al., 2010). On the basis of the age model and variations in microfossil assemblages, three intervals of significant climate changes during the last 14.5 cal ky BP are identified: Late Pleistocene (14.5–11.7 cal ka BP; 974–596 cm), early Holocene (11.7–8.2 cal ka BP; 596–215 cm) and middle-late Holocene (8.2–0.3 cal ka BP; 215–0 cm).

5.1. Late Pleistocene: 14.5–11.7 cal ka BP (974–596 cm)

The oldest recognized sediments, at the base of the core, deposited between 14.5 and 11.7 cal ka BP. It includes the Bølling-Allerød interstadial (B-A, 14.5–12.9 cal ka BP; Kienast and McKay, 2001) and the Younger Dryas stadial (YD, 12.9–11.7 cal ka BP; Broecker et al., 2010), correlated with δ^{18}O record of the Greenland GRIP ice core (Johnsen et al., 1997) (Fig. 6). During the Late Pleistocene, the Svalbard/Barents Sea Ice Sheet (SBSIS) melting and retreat, forced by the seasonal contrast in insolation, influenced climate changes (Anderson et al., 1988), contributing to trigger the deglacial two-step dynamic (Alley et al., 1997; Broecker et al., 1985). The rare occurrence of nannofossils, diatoms and planktonic foraminifera in the lowermost part of core 17603-3 (Fig. 6) is related to low productivity as a result of sea-ice cover (Villa et al., 2005; Zamelczyk et al., 2012). In particular, the scarcity of calcareous nannofossils was primarily related to low sea surface temperature (SST) as well as the presence of large volume of dense sediment-laden meltwater, affecting light penetration during the initial phase of the deglaciation, dampening the primary productivity.

The laminated lithofacies, dating 14.4–14.2 cal ka BP, was interpreted as deriving from sediment-laden meltwater associated to the Meltwater Pulse 1A (MWP-1A) (Lucchi et al., 2013, 2015) (Fig. 6). The MWP-1A was responsible for massive input of terrigenous sediments in the depositional system as indicated also by the high sedimentation rate recorded during this interval (Fig. 3). According to Kienast et al. (2003) this event coincides with the Bølling warm interstadial. Lucchi et al. (2013) argued that this warm event was possibly characterized by multi-year sea ice on the basis of the scarcity of IRD content in the laminated sediments. In this scenario, the absence of diatoms between 14.5 and 14.1 cal ka BP could be related to the presence of turbid meltwaters and/or by dissolution due to the presence of aggressive stratified water masses.

The generally warming trend is depicted during the B-A through the increase of the *Emiliania huxleyi* and *Coccolithus pelagicus* s.l. ratio (H/P ratio) and progressive increase of smectite content, indicating enhanced advection of Atlantic water to the study area. Although low temperature water affinity (Braarud, 1979; Samtleben et al., 1995), the nannoplankton *C. pelagicus* s.l. preference for fronts of moderate salinity gradients (Cachão and Moita, 2000) is tentatively used to explain its rare occurrence during the Late Pleistocene deglaciation, responsible for freshwater release. Above the laminated sediments, the massive IRD interval (Fig. 3), dated between 14.2 and 14.0 cal ka BP according to our age model, indicates a sudden, massive increase of iceberg calving offshore the Kveithola Trough. According to Lucchi et al. (2013) this interval records one of the main SBSIS collapses that cleared the outer shelf area from permanent ice cover.

Following this ice-sheet collapse, the sedimentary sequence dated between 14.0 and 12.9 cal ka BP is characterized by the presence of cold-water taxa such as *Emiliania huxleyi* (>4 μm), *Gephyrocapsa muellerae* and *Thalassiosira antarctica* that suggest development of seasonal sea-ice. Freshwater released by iceberg melting, following the outer ice-sheet collapse, would result in increased sea-ice formation. As a matter of fact, present day observations from Southern high latitudes indicate that, while subsurface warm ocean current causes basal ice-shelf melting, freshwater around Antarctica, having a higher freezing point, caused the extension of the seasonal sea-ice over the past few years, despite increased temperatures (Collins et al., 2013; Turner and Overland, 2009). As confirmation of the analogy, a concurrent occurrence of the nannofossil *E. huxleyi* (<4 μm), and the diatoms *Coscinodiscus* spp. and *Thalassiosira oestrupii* suggests intrusion of

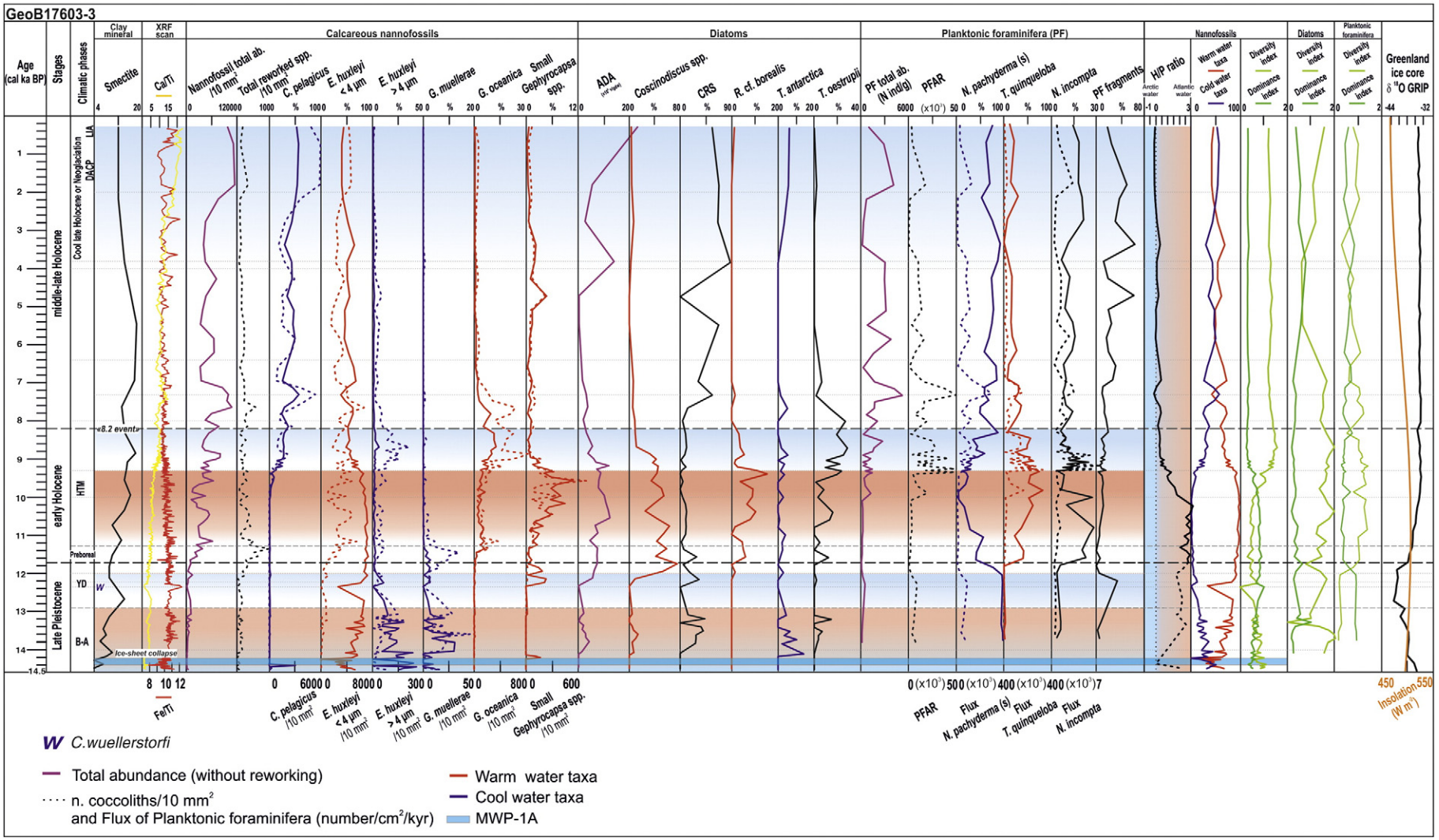

Fig. 6. Abundances of calcareous nannofossil, diatom and planktonic foraminiferal species for the investigated core plotted versus calendar age. Smectite and Ca/Fe, Ca/Ti ratio plots are shown. H/P ratio, warm and cold-water taxa curve, dominance and Shannon Wiener diversity are plotted versus calendar age. The lower part of the H/P ratio curve is dotted due to the absence of *C. pelagicus*, commented in the text. The summer insolation curve at 65° N for the studied interval, following Laskar et al. (2004), is shown in orange on the right of the figure. The Greenland ice core δ^{18}O GRIP and the summer insolation were selected and downloaded from official data repositories (e.g., International Research Institute for Climate and Society database, https://iridl.ldeo.columbia.edu/SOURCES/.ICE/.CORE/.GRIP/.o18/ and Virtual Observatory Paris Data Centre, http://vo.imcce.fr/insola/earth/online/earth/earth.html). ADA = absolute diatom abundance; CRS = *Chaetoceros* resting spore; W = *Cibicides wuellerstorfi* first occurrence; PF = planktonic foraminifera; PFAR = planktonic foraminiferal accumulation rate; MWP-1A = Meltwater Pulse 1A; B-A = Bølling-Allerød; YD = Younger Dryas; HTM = Holocene Thermal Maximum; DACP = Dark Ages Cold Period; LIA = Little Ice Age. Microfossil total abundances are shown in purple. Dotted lines indicate nannofossil absolute abundance, expressed as n. of coccoliths/10 mm^2 in the slide, and flux of planktonic foraminifera, expressed as number/cm^2/kyr.

relatively warm Atlantic water in the studied area. The absence of *Coccolithus pelagicus* s.l. and the decrease of *E. huxleyi* (>4 μm), *G. muellerae* and *T. antarctica* from 14.0 to 12.9 cal ka BP confirm the general climatic amelioration (B-A). Notably, the sharp decrease of *E. huxleyi* (>4 μm) confirms that this larger variety is a cold-water form (Colmenero-Hidalgo et al., 2002) whose abundance was reduced as a consequence of the progressive warming due to North Atlantic water during the B-A, supported also by the nannofossil cold-water and warm-water taxa curves, which indicate the climatic amelioration (Fig. 6). In addition, the presence of diatom *Chaetoceros* resting spores (CRS), between 14.1 and 12.9 cal ka BP, further indicates highly stratified and low salinity surface waters (Armand et al., 2005; Crosta et al., 1997), typical of intense melting during deglaciation conditions.

Between 12.9 and 11.7 cal ka BP the nannofossil, diatom and planktonic foraminiferal total abundances were generally low. In particular, between 12.9 and 12.2 cal ka BP, the neat decrease of the warm-water taxa *E. huxleyi* (<4 μm), the low abundance of *Coscinodiscus* spp. and the high planktonic foraminiferal fragmentation may indicate low SST. The concomitant presence of the cold-water taxa *Neogloboquadrina pachyderma* (s), *E. huxleyi* (>4 μm), *G. muellerae* and *T. antarctica* suggests evidences of a cold period that could correspond to the YD cold event, in agreement with Barron et al. (2009) who affirmed that microfossil proxies declined during the YD. The deterioration of the climate, during the interval 12.9–12.2 cal ka BP, is confirmed by the slight decrease of H/P ratio, indicating a Southern displacement of the Polar front (Andruleit and Baumann, 1998). Such conditions suggest an enhanced East Spitsbergen Current, which might have contributed to the inflow of polar waters in the Storfjorden-Kveithola. A possible re-advance of the ice sheet in the area is testified by a relative increase of Fe content in the sediments, representing the terrigenous component input with consequent reduction of the Ca content (Fig. 6).

The transition to warmer conditions, towards the end of the YD, was accompanied by enhanced biological productivity as reflected by the increase in the microfossil abundances at ca. 12 cal ka BP, the increase of Ca content and the regional first occurrence of the benthic foraminifer *Cibicidoides wuellerstorfi* (12.3 cal ka BP), defined as the first warming signal of bottom waters after the YD by T.L. Rasmussen et al. (2007) and Sarnthein et al. (2003).

5.2. Early Holocene: 11.7–8.2 cal ka BP (596–215 cm)

The interval between 11.7 and 8.2 cal ka BP includes the *Pre-Boreal Oscillation* (11.7–11.3 cal ka BP, Björck et al., 1997; T.L. Rasmussen et al., 2007; S.O. Rasmussen et al., 2007)) and the *Holocene Thermal Maximum* (HTM), also indicated as *Altithermal* or *Hypsithermal* (Wanner et al., 2008). The *Pre-Boreal Oscillation* represents the transition from Late Pleistocene to early Holocene milder climatic conditions. This early interval of the Holocene is characterized by the deposition of crudely layered sediments (Fig. 3), having sedimentological characteristics that indicate deposition under the effect of bottom currents (Lucchi et al., 2013). During this climatic transition, the biological productivity recovered and determined a rapid increase of the foraminiferal biodiversity, with high percentages of subpolar taxa as *Turborotalita quinqueloba* and *Neogloboquadrina incompta* that are indicative of productive surface water masses found in the vicinity of the Arctic and Polar fronts (Fig. 6). The increase of Ca content, during this period, is correlated to calcareous nannofossil increasing trend. This rise indicates seasonal ice-free condition, as also supported by higher H/P ratio that marks the beginning of the interglacial conditions.

The peak of Cretaceous reworked coccoliths at 11.4 cal ka BP (Fig. 6) can be explained by resedimentation of Cretaceous sediments (Hjelle, 1993) eroded by ice streams during the previous deglaciation phase (Andreassen et al., 2008; Ottesen et al., 2008).

Following the *Pre-Boreal Oscillation*, a relatively warm stable climatic phase occurred (11.3–9.3 cal ka BP), characterized by a sharp increased abundance of calcareous nannofossils, dominated by *Emiliania huxleyi* (<4 μm), *Gephyrocapsa oceanica*, small *Gephyrocapsa* spp., along with the diatoms *Coscinodiscus* spp., *Thalassiosira oestrupii*, *Rhizosolenia* cf. *borealis*, that are warm-water taxa indicating a pronounced inflow of warm Atlantic water into the study area. The increase of smectite supports this interpretation. The presence of *Coscinodiscus* spp. and *R.* cf. *borealis* among diatoms reflects shallowing of the mixed layer (Koç and Schrader, 1990) as a consequence of stronger summer insolation. The high flux of the planktonic foraminifer *N. incompta* confirms the climatic amelioration with strongly stratified water column, characterized by a reduced mixed layer and high chlorophyll-a concentrations (King and Howard, 2003). This climatic interval is defined as the HTM because the subsurface waters along the Western margin of Svalbard were dominated by Atlantic water reaching their maximum temperature (Jansen et al., 2009; Jessen et al., 2010; Kaufman et al., 2004; Rasmussen and Thomsen, 2014; Wanner et al., 2008). Our data are comparable with the diatom results observed in cores EG-02, EG-03 and SV-04, collected in the neighbouring Storfjorden TMF (Lucchi et al., 2013). The coccolith and diatom concentration peak, registered at ca. 10 cal ka BP, might reflect the response of the phytoplankton to the orbitally-forced maximum summer insolation (Laskar et al., 2004; Wanner et al., 2008), responsible for the HTM (Kaufman et al., 2004; Renssen et al., 2009, 2012). The H/P ratio supports the SST increase at around 10 cal ka BP, in agreement with the insolation curve (Laskar et al., 2004) (Fig. 6). Warm conditions are sustained also by the crossover between dominance and diversity indices of the nannofossil and planktonic foraminiferal assemblages (Fig. 6). Cronin and Cronin (2015) and Moran et al. (2006) asserted that the strengthening of warm inflowing Atlantic water in the Arctic is one of the mechanisms driving the species increasing diversity. According to Baumann et al. (2000) this warm environment determined the Northern displacement of the Arctic front.

A cooling trend, starting at approximately 9.3 cal ka BP, is marked by a relative increase of cold-water taxa, such as *Coccolithus pelagicus* s.l., *Thalassiosira antarctica* and *N. pachyderma* (s) (Fig. 6). The decrease of smectite values confirms a decline of Atlantic water inflow in the area, in agreement with a decrease of the H/P ratio. Evidence of climatic deterioration towards the top of the early Holocene is supported by reduction of warm-water taxa, as *E. huxleyi* (<4 μm), small *Gephyrocapsa* spp., *Coscinodiscus* spp., *R.* cf. *borealis, T. quinqueloba* and *N. incompta*, culminating in the so-called “8.2 event” (Alley et al., 1997). The latter event was hypothetically generated by a catastrophic release of freshwater from the glacial lakes Agassiz and Ojibway that drained cold-waters through the Hudson Strait after the Laurentide Ice Sheet collapse, affecting the North Atlantic Deep Water formation (Barber et al., 1999). According to Alley et al. (1997) this is considered to be the most noticeable climatic event of the Holocene recorded in the Greenland ice cores.

5.3. Middle-late Holocene: post 8.2–0.3 cal ka BP (215–0 cm)

The stratigraphic interval between 8.2 and 0.3 cal ka BP is characterized by bioturbated sediments (Fig. 3) that were deposited by contour currents under progressively ameliorated environmental conditions favourable to the biological productivity.

Starting from ca. 8 cal ka BP the calcareous microfossil abundances experienced a new increasing trend (Fig. 6). The peaks of *Coccolithus pelagicus* s.l. and CRS at 7.3 cal ka BP are not to be ascribed to high primary productivity, but rather to higher dissolution resistance of these species (Fig. 6).

The calcareous microfossil concentration increases during the interval 6.4–4 cal ka BP corresponding to a short period of reintensification of Atlantic Water advection, which maximum clearly occurred during the previous HTM. During this interval, the calcareous nannofossil association is characterized by shared relative abundances between cold and warm water-taxa.

A gradual cooling during the late Holocene, since ca. 4 cal ka BP, is recorded by nannofossil total abundance decrease together with the

increase of cold-water taxa as *Coccolithus pelagicus* s.l., *Neogloboquadrina pachyderma* (s) and *Thalassiosira antarctica*. This change indicates sea surface cooling with seasonal sea ice presence, in agreement with Ślubowska-Woldengen et al. (2008) who indicated that an atmospheric cooling and a reduction of the Atlantic water inflow occurred between 4 and 2 cal ka BP. The preference of *Gephyrocapsa muellerae*, a well-known cold-water adapted taxon (Bollmann, 1997), in this interval is not supported by our data. The highest CRS peak recorded at 3.8 cal ka BP indicates spring sea ice melting coinciding with the ADA peak (14×10^6 v/gdw). The cooling trend corresponds to the so-called Cool Late Holocene (Andersen et al., 2004) known also as Neoglacial cold event that was described by Koç et al. (1993) and attributed to the decline of summer insolation in the Northern high latitude by Imbrie et al. (1992) and Wanner et al. (2011).

According to our age model, the interval dating 2.5–2 cal ka BP is characterized by a crossover between warm and cold-water nannofossil taxa. However, the sampling resolution in the upper part of the core is too low to provide detailed information on very short climatic variation. A clear increase of the cold-water nannofossil taxa *C. pelagicus* s.l. marks a climatic deterioration since ca. 2 cal ka BP that we related to the Dark Ages Cold Period (DACP; Ljungqvist, 2010). The latter and the following Little Ice Age (LIA) are thought to have been triggered by a combination of a reduction in solar irradiance and explosive volcanism (Wanner et al., 2011). The very last sample, dated at 0.3 cal ka BP, falls within the LIA time; the only micropalaeontological evidences that could suggest harsh LIA conditions are the high *C. pelagicus* s.l., *N. pachyderma* (s) and *T. antarctica* abundances. The increasing trend of the nannofossil cold-water taxa curve supports the Neoglaciation evidences towards the top of the core (Fig. 6).

6. Conclusions

The 974 cm long sediment core collected from the Kveithola TMF middle slope (GeoB17603-3) contains an expanded sedimentary record dating 14.5–0.3 cal ka BP; over 600 cm deposited during the Holocene. Quantitative microfossil assemblage analyses (calcareous nannofossils, diatoms and planktonic foraminifera) and clay minerals gave promising results outlining their close relation to the climatically induced changes in the characteristics of surface water on the NW Barents Sea over last 14.5 cal ky BP. Accordingly with previous studies in the region, we assigned the microfossil species to different palaeoecological groups, and in particular with respect to Sea Surface Temperature (SST). Nannofossil indices such as *E. huxleyi* and *C. pelagicus* s.l. (H/P) ratio, poorly used in the Arctic environment, is considered in support of major climatic variations. The reconstructions of surface water conditions highlight the strong coupling between the advances and retreats of the Svalbard-Barents Sea Ice Sheet (SBSIS), the interplay of Atlantic/Arctic water masses flows over the study area, and insolation orbital forcing.

Three intervals of significant climate change were identified: Late Pleistocene (14.5–11.7 cal ka BP; 974–596 cm), early Holocene (11.7–8.2 cal ka BP; 596–215 cm) and middle-late Holocene (8.2–0.3 cal ka BP; 215–0 cm):

- Late Pleistocene sediments (14.5–11.7 cal ka BP) record a) the Bølling-Allerød interstadial, consisting of laminated lithofacies, indicating intense ice-melting, and massive IRD deposition that accompanied the SBSIS collapse; and b) the Younger Dryas stadial, characterized by a general decrease of microfossils abundance with presence of cold taxa and often fragmented/reworked species.
- The transition to warmer conditions, during the late YD is indicated by the increase in microfossil abundances and the first occurrence of the benthic foraminifer *Cibicidoides wuellerstorfi* as proxy for Atlantic influx and climatic amelioration. According to calibrated radiocarbon ages the first occurrence of *C. wuellerstorfi* dates as early as 12.3 cal ka BP.
- The early Holocene interval (11.7–8.2 cal ka BP) records a) the Pre-Boreal Oscillation, characterized by a progressive increase of microfossils biodiversity and abundance, with high H/P ratio marking the onset of interglacial condition; and b) the Holocene Thermal Maximum (HTM) characterized by a sharp increase of microfossil abundance (warm-water taxa), Ca and smectite contents. The high concentration of coccoliths and diatoms observed at ca. 10 cal ka BP has been related to the phytoplankton response to the orbitally-forced maximum summer insolation, responsible for the HTM. From approximately 9.3 cal ka BP, an environmental cooling trend is depicted on the microfossils assemblage and the H/P ratio, culminating at around 8.2 cal ka BP;
- The middle-late Holocene is characterized by an initial (8.2–4.0 cal ka BP) environmental amelioration, characterized by a slight dominance of warm taxa, after which another gradual cooling is recorded by the increase of cold-water adapted taxa that we associated to the decline of summer insolation in the Northern high latitude, responsible for the onset of the Neoglacial cold event.

Acknowledgements

The authors acknowledge the Captain, crew, and scientific party of the CORIBAR cruise onboard the German R/V Maria S. Merian (Tromsø, 15 July–Tromsø, 15 August 2013). In particular, we acknowledge T.J.J. Hanebuth as chief scientist during the cruise and H. Landzik for organizing the sampling party and the preliminary analyses (Radiographs, and Multi sensor core logger) at MARUM laboratories. We thank S. Miserocchi of the CNR-ISMAR Bologna (Italy) for the help given during the XRF core-scan analysis. Special thanks are also addressed to M. Rebesco and D. Accettella that kindly contributed with bathymetric data and G.A. Prista for scientific discussion and suggestions that greatly improved the manuscript. We would like to acknowledge B. Trummel of Polar Educators International for critically reading the manuscript and for valuable comments. We thank the Editor and the reviewers for their worthy comments on the manuscript. This study was supported by the PNRA project CORIBAR-IT (PNRA PdR C2/2013), the Italian project Premiale ARCA, and the Spanish project DEGLABAR (CTM2010-17386).

References

Aagaard, K., Foldvik, A., Hillman, S., 1987. The West Spitsbergen Current: disposition and water mass transformation. J. Geophys. 92, 3778. http://dx.doi.org/10.1029/JC092iC04p03778.

Alley, R.B., Mayewski, P.A., Sowers, T., Stuiver, M., Taylor, K.C., Clark, P.A., 1997. Holocene climate variability: a prominent widespread event 8200 years ago. Geology 25, 483–486. http://dx.doi.org/10.1130/0091-7613(1997)025<0483:HCIAPW>2.3.CO;2.

Andersen, C., Koç, N., Jennings, A., Andrews, J.T., 2004. Nonuniform response of the major surface currents in the Nordic Seas to insolation forcing: implications for the Holocene climate variability. Paleoceanography 19, 1–16. http://dx.doi.org/10.1029/2002PA000873.

Anderson, C.W., Barnosky, P.J., Bardein, P.J., Behling, L., Brubaker, E.J., Cushing, J., Dodson, B., Dworetsky, P.J., Guetter, S.P., Harrison, B., Huntley, J.E., Kutzbach, V., Markgraf, R., Marvel, M.S., McGlone, A., Mix, N.T., Moar, J., Morley, R.A., Perrottn, G.M., Peterson, W.L., Prell, I.C., Prentice, J.C., Ritchie, N., Roberts, W., Ruddiman, F., Salinger, M.J., Spaulding, W.G., Street-Perrott, F.A., Thompson, R.S., Wang, P.K., Webb III, T., Winer, M.G., Wright, H.E., 1988. Climatic changes of the last 18,000 years: observations and model simulations. Science 241 (4869), 1043–1052.

Andreassen, K., Laberg, J.S., Vorren, T.O., 2008. Seafloor geomorphology of the SW Barents Sea and its glacidynamic implications. Geomorphology 97, 157–177.

Andruleit, H.A., Baumann, K.H., 1998. History of the Last Deglaciation and Holocene in the Nordic seas as revealed by coccolithophore assemblages. Mar. Micropaleontol. 35, 179–201. http://dx.doi.org/10.1016/S0377-8398(98)00021-8.

Armand, L., 1997. The Use of Diatom Transfer Functions in Estimating Sea-surface Temperature and Sea-ice in Cores from the Southeast Indian Ocean (Ph.D. Thesis) Australian National University, Canberra.

Armand, L.K., Crosta, X., Romero, O., Pichon, J.J., 2005. The biogeography of major diatom taxa in Southern Ocean sediments: 1. Sea ice related species. Palaeogeogr. Palaeoclimatol. Palaeoecol. 223, 93–126. http://dx.doi.org/10.1016/j.palaeo.2005.02.015.

Backman, J., Shackleton, N.J., 1983. Quantitative biochronology of Pliocene and early Pleistocene calcareous nannofossils from the Atlantic, Indian and Pacific oceans. Mar. Micropaleontol. 8, 141–170. http://dx.doi.org/10.1016/0377-8398(83)90009-9.

Backman, J., Fornaciari, E., Rio, D., 2009. Biochronology and paleoceanography of late Pleistocene and Holocene calcareous nannofossil abundances across the Arctic Basin. Mar. Micropaleontol. 72, 86–98. http://dx.doi.org/10.1016/j.marmicro.2009.04.001.

Barber, D.C., Dyke, A., Hillaire-Marcel, C., Jennings, A.E., Andrews, J.T., Kerwin, M.W., Bilodeau, B., McNeely, R., Southon, J., Morehead, M.D., Gagnon, J.-M., 1999. Forcing of the cold event of 8,200 years ago by catastrophic drainage of Laurentide lakes. Nature 400, 344–348. http://dx.doi.org/10.1038/22504.

Barron, J.A., Bukry, D., Dean, W.E., Addison, J.A., Finney, B., 2009. Paleoceanography of the Gulf of Alaska during the past 15,000 years: results from diatoms, silicoflagellates, and geochemistry. Mar. Micropaleontol. 72, 176–195. http://dx.doi.org/10.1016/j.marmicro.2009.04.006.

Baumann, K.H., Andruleit, H., Samtleben, C., 2000. Coccolithophores in the Nordic Seas: comparison of living communities with surface sediment assemblages. Deep. Res. Part II Top. Stud. Oceanogr. 47, 1743–1772. http://dx.doi.org/10.1016/S0967-0645(00)00005-9.

Biscaye, P.E., 1965. Mineralogy and sedimentation of recent deep-sea clay in the Atlantic Ocean and adjacent seas and oceans. Geol. Soc. Am. Bull. 76, 803–832. http://dx.doi.org/10.1130/0016-7606(1965)76[803:masord]2.0.co;2.

Björck, S., Rundgren, M., Ingólfsson, Ó., Funder, S., 1997. The Preboreal oscillation around the Nordic Seas: terrestrial and lacustrine responses. J. Quat. Sci. 12, 455–465. http://dx.doi.org/10.1002/(SICI)1099-1417(199711/12)12:6<455::AID-JQS316>3.0.CO;2-S.

Blindheim, J., Rey, F., 2004. Water-mass formation and distribution in the Nordic Seas during the 1990s. ICES J. Mar. Sci. 61, 846–863. http://dx.doi.org/10.1016/j.icesjms.2004.05.003.

Bollmann, J., 1997. Morphology and biogeography of *Gephyrocapsa* coccoliths in Holocene sediments. Science 29 (80-.), 319–350. http://dx.doi.org/10.1016/S0377-8398(96)00028-X.

Bown, P.R., Young, J.R., 1998. Calcareous Nannofossil Biostratigraphy. Chapman-Hall, Dordrecht, The Netherlands.

Braarud, T., 1979. The temperature range of the non-motile stage of *Coccolithus pelagicus* in the North Atlantic region. Br. Phycol. J. 14, 349–352.

Broecker, W.S., Peteet, D.M., Rind, D., 1985. Does the ocean-atmosphere system have more than one stable mode of operation? Nature 315, 21–26. http://dx.doi.org/10.1038/315021a0.

Broecker, W.S., Denton, G.H., Edwards, R.L., Cheng, H., Alley, R.B., Putnam, A.E., 2010. Putting the Younger Dryas cold event into context. Quat. Sci. Rev. 29, 1078–1081. http://dx.doi.org/10.1016/j.quascirev.2010.02.019.

Cachão, M., Moita, M.T., 2000. *Coccolithus pelagicus*, a productivity proxy related to moderate fronts off Western Iberia. Mar. Micropaleontol. 39, 131–155. http://dx.doi.org/10.1016/S0377-8398(00)00018-9.

Collins, M., Knutti, R., Arblaster, J., Dufresne, J.-L., Fichefet, T., Friedlingstein, P., Gao, X., Gutowski, W.J., Johns, T., Krinner, G., Shongwe, M., Tebaldi, C., Weaver, A.J., Wehner, M., 2013. Long-term climate change: projections, commitments and irreversibility. Clim. Chang. 2013 Phys. Sci. Basis. Contrib. Work. Gr. I to Fifth Assess. Rep. Intergov. Panel Clim. Chang., pp. 1029–1136. http://dx.doi.org/10.1017/CBO9781107415324.024.

Colmenero-Hidalgo, E., Flores, J.A., Sierro, F.J., 2002. Biometry of *Emiliania huxleyi* and its biostratigraphic significance in the Eastern North Atlantic Ocean and Western Mediterranean Sea in the last 20 000 years. Mar. Micropaleontol. 46, 247–263.

Conan, S.M.H., Ivanova, E.M., Brummer, G.J.A., 2002. Quantifying carbonate dissolution and calibration of foraminiferal dissolution indices in the Somali Basin. Mar. Geol. 182, 325–349. http://dx.doi.org/10.1016/S0025-3227(01)00238-9.

Cronin, T.M., Cronin, M.A., 2015. Biological response to climate change in the Arctic Ocean: the view from the past. Arktos 1, 4. http://dx.doi.org/10.1007/s41063-015-0019-3.

Crosta, X., Koç, N., 2007. Chapter eight diatoms: from micropaleontology to isotope geochemistry. Dev. Mar. Geol. http://dx.doi.org/10.1016/S1572-5480(07)01013-5.

Crosta, X., Pichon, J.J., Labracherie, M., 1997. Distribution of Chaetoceros resting spores in modern peri-Antarctic sediments. Mar. Micropaleontol. 29, 283–299. http://dx.doi.org/10.1016/S0377-8398(96)00033-3.

Damiani, D., Giorgetti, G., Turbanti, I.M., 2006. Clay mineral fluctuations and surface textural analysis of quartz grains in Pliocene-Quaternary marine sediments from Wilkes Land continental rise (East-Antarctica): paleoenvironmental significance. Mar. Geol. 226, 281–295. http://dx.doi.org/10.1016/j.margeo.2005.11.002.

Darling, K.F., Kucera, M., Kroon, D., Wade, C.M., 2006. A resolution for the coiling direction paradox in *Neogloboquadrina pachyderma*. Paleoceanography 21. http://dx.doi.org/10.1029/2005PA001189.

Ferreira, J., Cachão, M., González, R., 2008. Reworked calcareous nannofossils as ocean dynamic tracers: the Guadiana shelf case study (SW Iberia). Estuar. Coast. Shelf Sci. 79, 59–70. http://dx.doi.org/10.1016/j.ecss.2008.03.012.

Flores, J.A., Colmenero-Hidalgo, E., Mejía-Molina, A.E., Baumann, K.H., Henderiks, J., Larsson, C., Prabhu, C., Sierro, F.J., Rodrigues, T., 2010. Distribution of large *Emiliania huxleyi* in the Central and Northeast Atlantic as a tracer of surface ocean dynamics during the last 25,000 years. Mar. Micropaleontol. 76, 53–66.

Friedman, G.M., Sanders, J.E., 1978. Principles of Sedimentology. John Wiley, New York.

Groot, D.E., Aagaard-Sørensen, S., Husum, K., 2014. Reconstruction of Atlantic water variability during the Holocene in the western Barents Sea. Clim. Past 10, 51–62. http://dx.doi.org/10.5194/cp-10-51-2014.

Hammer, Ø., Harper, D.A.T., Ryan, P.D., 2001. PAST: palaeontological statistics software package for education and data analysis. Palaeontol. Electron. 4, 1–9. http://dx.doi.org/10.1163/001121611X566785.

Hemleben, C., Spindler, M., Anderson, O.R., 1989. Modern Planktonic Foraminifera. Springer.

Hjelle, A., 1993. The Geology of Svalbard: Oslo. Norsk Polarinstitutt (163 pp.).

Imbrie, J., Boyle, E.A., Clemens, S.C., Duffy, A., Howard, W.R., Kukla, G., Kutzbach, J., Martinson, D.G., McIntyre, A., Mix, A.C., Molfino, B., Morley, J.J., Peterson, L.C., Pisias, N.G., Prell, W.L., Raymo, M.E., Shackleton, N.J., Toggweiler, J.R., 1992. On the structure and origin of major glaciation cycles 1. Linear responses to Milankovitch forcing. Paleoceanography 7, 701–738. http://dx.doi.org/10.1029/92pa02253.

Jansen, E., Andersson, C., Moros, M., Nisancioglu, K.H., Nyland, B.F., Telford, R.J., 2009. The early to mid-Holocene thermal optimum in the North Atlantic. Nat. Clim. Var. Glob. Warm. A Holocene Perspect. 123–137 http://dx.doi.org/10.1002/9781444300932.ch5.

Jessen, S.P., Rasmussen, T.L., Nielsen, T., Solheim, A., 2010. A new Late Weichselian and Holocene marine chronology for the western Svalbard slope 30,000–0 cal years BP. Quat. Sci. Rev. 29, 1301–1312. http://dx.doi.org/10.1016/j.quascirev.2010.02.020.

Johnsen, S.J., Clausen, H.B., Dansgaard, W., Gundestrup, N.S., Hammer, C.U., Andersen, U., Andersen, K.K., Hvidberg, C.S., Dahl-Jensen, D., Steffensen, J.P., Shoji, H., Sveinbjörnsdóttir, Á.E., White, J., Jouzel, J., Fisher, D., 1997. A record along the Greenland Ice Core Project deep ice core and the problem of possible Eemian climatic instability. J. Geophys. Res. 102, 26397. http://dx.doi.org/10.1029/97JC00167.

Junttila, J., Aagaard-Sørensen, S., Husum, K., Hald, M., 2010. Late Glacial-Holocene clay minerals elucidating glacial history in the SW Barents Sea. Mar. Geol. 276, 71–85. http://dx.doi.org/10.1016/j.margeo.2010.07.009.

Kaufman, D.S., Ager, T.A., Anderson, N.J., Anderson, P.M., Andrews, J.T., Bartlein, P.J., Brubaker, L.B., Coats, L.L., Cwynar, L.C., Duvall, M.L., Dyke, A.S., Edwards, M.E., Eisner, W.R., Gajewski, K., Geirsdottir, A., Hu, F.S., Jennings, A.E., Kaplan, M.R., Kerwin, M.W., Lozhkin, A.V., MacDonald, G.M., Miller, G.H., Mock, C.J., Oswald, W.W., Otto-Bliesner, B.L., Porinchu, D.F., Rhland, K., Smol, J.P., Steig, E.J., Wolfe, B.B., 2004. Holocene thermal maximum in the western Arctic (0–180°W). Quat. Sci. Rev. 23, 529–560. http://dx.doi.org/10.1016/j.quascirev.2003.09.007.

Kienast, S.S., McKay, J.L., 2001. Sea-surface Temperature Reconstruction of Sediment Core JT96-09PC. http://dx.doi.org/10.1594/PANGAEA.738484.

Kienast, M., Hanebuth, T.J.J., Pelejero, C., Steinke, S., 2003. Synchroneity of meltwater pulse 1a and the Bølling warming: new evidence from the South China Sea. Geology 31, 67–70. http://dx.doi.org/10.1130/0091-7613(2003)031<0067:SOMPAT>2.0.CO;2.

King, A., Howard, W.L., 2003. Planktonic foraminiferal flux seasonality in Subantarctic sediment traps: a test for paleoclimate reconstructions. Paleoceanography 18, 1–17. http://dx.doi.org/10.1029/2002PA000839.

Koç, N., Schrader, H., 1990. Surface sediment diatom distribution and Holocene paleotemperature variations in the Greenland, Iceland and Norwegian Sea. Paleoceanography 5, 557–580. http://dx.doi.org/10.1029/PA005i004p00557.

Koç, N., Jansen, E., Haflidason, H., 1993. Paleoceanographic reconstructions of surface ocean conditions in the Greenland, Iceland and Norwegian seas through the last 14 ka based on diatoms. Quat. Sci. Rev. 12, 115–140. http://dx.doi.org/10.1016/0277-3791(93)90012-B.

Laskar, J., Robutel, P., Joutel, F., Gastineau, M., Correia, C.M., Levrard, B., 2004. Astrophysics a long-term numerical solution for the insolation. Astronomy 285, 261–285. http://dx.doi.org/10.1051/0004-6361.

Ljungqvist, F.C., 2010. A new reconstruction of temperature variability in the extra-tropical northern hemisphere during the last two millennia. Geogr. Ann. Ser. A Phys. Geogr. 92, 339–351. http://dx.doi.org/10.1111/j.1468-0459.2010.00399.x.

Loeng, H., 1991. Features of the physical oceanographic conditions of the Barents Sea. Polar Res. 10, 5–18. http://dx.doi.org/10.1111/j.1751-8369.1991.tb00630.x.

Lucchi, R.G., Camerlenghi, A., Rebesco, M., Colmenero-Hidalgo, E., Sierro, F.J., Sagnotti, L., Urgeles, R., Melis, R., Morigi, C., Bàrcena, M.A., Giorgetti, G., Villa, G., Persico, D., Flores, J.A., Rigual-Hernandez, A.S., Pedrosa, M.T., Macri, P., Caburlotto, A., 2013. Post-glacial sedimentary processes on the Storfjorden and Kveithola trough mouth fans: significance of extreme glacimarine sedimentation. Glob. Planet. Chang. 111, 309–326. http://dx.doi.org/10.1016/j.gloplacha.2013.10.008.

Lucchi, R.G., Sagnotti, L., Camerlenghi, A., Macrì, P., Rebesco, M., Pedrosa, M.T., Giorgetti, G., 2015. Marine sedimentary record of Meltwater Pulse 1a along the NW Barents Sea continental margin. Arktos 1, 7. http://dx.doi.org/10.1007/s41063-015-0008-6.

Mangerud, J., Gulliksen, S., 1975. Apparent radiocarbon ages of recent marine shells from Norway, Spitsbergen, and Arctic Canada. Quat. Res. 5, 263–273. http://dx.doi.org/10.1016/0033-5894(75)90028-9.

Mangerud, J., Bondevik, S., Gulliksen, S., Karin Hufthammer, A., Høisæter, T., 2006. Marine ^{14}C reservoir ages for 19th century whales and molluscs from the North Atlantic. Quat. Sci. Rev. 25, 3228–3245. http://dx.doi.org/10.1016/j.quascirev.2006.03.010.

Moran, K., Backman, J., Brinkhuis, H., Clemens, S.C., Cronin, T., Dickens, G.R., Eynaud, F., Gattacceca, J., Jakobsson, M., Jordan, R.W., Kaminski, M., King, J., Koc, N., Krylov, A., Martinez, N., Matthiessen, J., McInroy, D., Moore, T.C., Onodera, J., O'Regan, M., Pälike, H., Rea, B., Rio, D., Sakamoto, T., Smith, D.C., Stein, R., St John, K., Suto, I., Suzuki, N., Takahashi, K., Watanabe, M., Yamamoto, M., Farrell, J., Frank, M., Kubik, P., Jokat, W., Kristoffersen, Y., 2006. The Cenozoic palaeoenvironment of the Arctic Ocean. Nature 441, 601–605. http://dx.doi.org/10.1038/nature04800.

Ottesen, D., Stokes, C.R., Rise, L., Olsen, L., 2008. Ice-sheet dynamics and ice streaming along the coastal parts of northern Norway. Quat. Sci. Rev. 27, 922–940. http://dx.doi.org/10.1016/j.quascirev.2008.01.014.

Rasmussen, T.L., Thomsen, E., 2014. Brine formation in relation to climate changes and ice retreat during the last 15,000 years in Storfjorden, Svalbard, 76–78 N. Paleoceanography 29, 911–929. http://dx.doi.org/10.1002/2014PA002643.

Rasmussen, T.L., Thomsen, E., Ślubowska, M.A., Jessen, S., Solheim, A., Koç, N., 2007a. Paleoceanographic evolution of the SW Svalbard margin (76°N) since 20,000 ^{14}C yr BP. Quat. Res. 67, 100–114. http://dx.doi.org/10.1016/j.yqres.2006.07.002.

Rasmussen, S.O., Vinther, B.M., Clausen, H.B., Andersen, K.K., 2007b. Early Holocene climate oscillations recorded in three Greenland ice cores. Quat. Sci. Rev. 26, 1907–1914. http://dx.doi.org/10.1016/j.quascirev.2007.06.015.

Rathburn, A.E., Pichon, J.J., Ayress, M.A., De Deckker, P., 1997. Microfossil and stable-isotope evidence for changes in Late Holocene palaeoproductivity and palaeoceanographic

conditions in the Prydz Bay region of Antarctica. Palaeogeogr. Palaeoclimatol. Palaeoecol. 131, 485–510. http://dx.doi.org/10.1016/S0031-0182(97)00017-5.

Rebesco, M., Liu, Y., Camerlenghi, A., Winsborrow, M., Laberg, J.S., Caburlotto, A., Diviacco, P., Accettella, D., Sauli, C., Wardell, N., Tomini, I., 2011. Deglaciation of the western margin of the Barents Sea Ice Sheet - a swath bathymetric and sub-bottom seismic study from the Kveithola Trough. Mar. Geol. 279, 141–147. http://dx.doi.org/10.1016/j.margeo.2010.10.018.

Reimer, P., 2013. IntCal13 and Marine13 radiocarbon age calibration curves 0–50,000 years cal BP. Radiocarbon 55, 1869–1887. http://dx.doi.org/10.2458/azu_js_rc.55.16947.

Renssen, H., Seppä, H., Heiri, O., Roche, D.M., Goosse, H., Fichefet, T., 2009. The spatial and temporal complexity of the Holocene thermal maximum. Nat. Geosci. 2, 411–414. http://dx.doi.org/10.1038/ngeo513.

Renssen, H., Seppä, H., Crosta, X., Goosse, H., Roche, D.M., 2012. Global characterization of the Holocene Thermal Maximum. Quat. Sci. Rev. 48, 7–19. http://dx.doi.org/10.1016/j.quascirev.2012.05.022.

Rio, D., Raffi, I., Villa, G., 1990. Pliocene-Pleistocene calcareous nannofossil distribution patterns in the western Mediterranean. Proc., Sci. results, ODP, Leg 107. Tyrrhenian Sea 107, 513–533.

Rüther, D.C., Bjarnadóttir, L.R., Junttila, J., Husum, K., Rasmussen, T.L., Lucchi, R.G., Andreassen, K., 2012. Pattern and timing of the northwestern Barents Sea Ice Sheet deglaciation and indications of episodic Holocene deposition. Boreas 41, 494–512. http://dx.doi.org/10.1111/j.1502-3885.2011.00244.x.

Sagnotti, L., Macrì, P., Lucchi, R., Rebesco, M., Camerlenghi, A., 2011. A Holocene paleosecular variation record from the northwestern Barents Sea continental margin. Geochem. Geophys. Geosyst. 12, 1–24. http://dx.doi.org/10.1029/2011GC003810.

Samtleben, C., Schäfer, P., Andruleit, H., Baumann, A., Baumann, K.-H., Kohly, A., Matthiessen, J., Schro¨der-Ritzrau, A., Synpal Working Group, 1995. Plankton in the Norwegian– Greenland Sea: from living communities to sediment assemblages — an actualistic approach. Geol. Rundsch. 84, 108–136.

Sarnthein, M., Van Kreveld, S., Erlenkeuser, H., Grootes, P.M., Kucera, M., Pflauman, U., Schulz, M., 2003. Centennial-to-millennial-scale periodicities of Holocene climate and sediment injections off the western Barents shelf, 75°N. Boreas 32, 447–461. http://dx.doi.org/10.1111/j.1502-3885.2003.tb01227.x.

Ślubowska-Woldengen, M., Koç, N., Rasmussen, T.L., Klitgaard-Kristensen, D., Hald, M., Jennings, A.E., 2008. Time-slice reconstructions of ocean circulation changes on the continental shelf in the Nordic and Barents Seas during the last 16,000 cal yr B.P. Quat. Sci. Rev. 27, 1476–1492. http://dx.doi.org/10.1016/j.quascirev.2008.04.015.

Stuiver, M., Reimer, P.J., 1993. Extended ^{14}C data base and revised CALIB 3.0 ^{14}C age calibration program. Radiocarbon 35, 215–230.

Svendsen, J.I., Alexanderson, H., Astakhov, V.I., Demidov, I., Dowdeswell, J.A., Funder, S., Gataullin, V., Henriksen, M., Hjort, C., Houmark-Nielsen, M., Hubberten, H.W., Inglfsson, I., Jakobsson, M., Kjr, K.H., Larsen, E., Lokrantz, H., Lunkka, J.P., Lysa, A., Mangerud, J., Matiouchkov, A., Murray, A., Moller, P., Niessen, F., Nikolskaya, O., Polyak, L., Saarnisto, M., Siegert, C., Siegert, M.J., Spielhagen, R.F., Stein, R., 2004. Late Quaternary ice sheet history of northern Eurasia. Quat. Sci. Rev. 1229–1271 http://dx.doi.org/10.1016/j.quascirev.2003.12.008.

Thunell, R.C., 1976. Optimum indices of calcium carbonate dissolution, in deep-sea sediments. Geology 4, 525–528. http://dx.doi.org/10.1130/0091-7613(1976)4<525:OIOCCD>2.0.CO;2.

Turner, J., Overland, J., 2009. Contrasting climate change in the two polar regions. Polar Res. 28, 146–164. http://dx.doi.org/10.1111/j.1751-8369.2009.00128.x.

Villa, G., Palandri, S., Wise, S.W., 2005. Quaternary calcareous nannofossils from Periantarctic basins: paleoecological and paleoclimatic implications. Mar. Micropaleontol. 56, 103–121. http://dx.doi.org/10.1016/j.marmicro.2005.03.006.

Wanner, H., Beer, J., Bütikofer, J., Crowley, T.J., Cubasch, U., Flückiger, J., Goosse, H., Grosjean, M., Joos, F., Kaplan, J.O., Küttel, M., Müller, S.A., Prentice, I.C., Solomina, O., Stocker, T.F., Tarasov, P., Wagner, M., Widmann, M., 2008. Mid- to Late Holocene climate change: an overview. Quat. Sci. Rev. 27, 1791–1828. http://dx.doi.org/10.1016/j.quascirev.2008.06.013.

Wanner, H., Solomina, O., Grosjean, M., Ritz, S.P., Jetel, M., 2011. Structure and origin of Holocene cold events. Quat. Sci. Rev. 30, 3109–3123. http://dx.doi.org/10.1016/j.quascirev.2011.07.010.

Winsborrow, M.C.M., Andreassen, K., Corner, G.D., Laberg, J.S., 2010. Deglaciation of a marine-based ice sheet: Late Weichselian palaeo-ice dynamics and retreat in the southern Barents Sea reconstructed from onshore and offshore glacial geomorphology. Quat. Sci. Rev. 29, 424–442. http://dx.doi.org/10.1016/j.quascirev.2009.10.001.

Wollenburg, J.E., Kuhnt, W., 2000. The response of benthic foraminifers to carbon flux and primary production in the Arctic Ocean. Mar. Micropaleontol. 40 (3), 189–231. http://dx.doi.org/10.1016/S0377-8398(00)00039-6.

Zamelczyk, K., Rasmussen, T.L., Husum, K., Haflidason, H., de Vernal, A., Ravna, E.K., Hald, M., Hillaire-Marcel, C., 2012. Paleoceanographic changes and calcium carbonate dissolution in the central Fram Strait during the last 20 ka. Quat. Res. 78, 405–416. http://dx.doi.org/10.1016/j.yqres.2012.07.006.

CHAPTER IV

Case study 2: Kveithola upper slope and trough, South of Svalbard (CORIBAR cores)

4.1 Introduction

The need for a better understanding of the Arctic Ocean system and its impact on the climate has been recognized by the international palaeoceanographic community since long time. The progress of knowledge has been troubled by a limited availability of good quality sediment core material due to the general inaccessibility of the Arctic Ocean in terms of logistic operations or limited availability of suitable age control in existing cores. In 2013, the CORIBAR expedition acquired new gravity core material from the Kveithola, in the southwestern Svalbard continental margin, surveyed for the first time during the previous EGLACOM cruise in 2008. The study area is under the influence of both Atlantic and Arctic waters, and therefore, it is a highly sensitive area to global climate changes. These characteristics make Kveithola an ideal setting for studying the interactions between ice sheet dynamics and climate.

In the following, a new calcareous nannofossil dataset obtained from the study of 3 CORIBAR cores are presented. The key purposes of this study are (i) to determine occurrences of calcareous nannofossils in sediments across the Kveithola depositional system in the Arctic area during late Pleistocene deglaciation and Holocene epoch and (ii) to discuss the affinity of the observed calcareous nannofossil assemblages with respect to Atlantic and/or Arctic oceanographic influences.

During the last glaciation, the Kveithola glacial system hosted large ice streams, draining ice from the southern Svalbard and Bear Island (Andreassen et al., 2008; Pedrosa et al., 2011). The CORIBAR cruise, on board R/V Maria S. Merian (Tromsø 16/7 - Tromsø 15/8/2013), addressed the investigation of ice dynamics and meltwater deposits by coring the Kveithola Trough and Trough Mouth Fan (TMF). The studied cores usually consist of laminated/ layered sediments, locally incorporating slump and/or older stratigraphic intervals and shell debris. Laminated deposition occurred under the effects of extensive subglacial melting water pulse (plumites). The Holocene interval is characterized by bioturbated sediments, indicating palaeoenvironmental conditions favourable to bioactivity (Lucchi et al., 2013).

4.2 Material and methods

4.2.1 Core location and lithological description

The late glacial and Holocene intervals from 3 sediment cores were studied for this investigation (Table 1). The core sites are located along the narrow (13 km-wide) 100 km-long, east–west trending Kveithola trough, located in the northwestern Barents Sea, South of Svalbard (Bjarnadóttir et al., 2013; Rebesco et al., 2011; Rüther et al., 2012) (Fig. 1).

Core ID	Lat. N	Long. E	Water depth (m)	Total recovery (cm)	Location
GeoB17601-5	74° 51.53'	16° 5.82'	369.1	537	GZW (outer shelf)
GeoB17605-3	74° 47.09'	15° 31.27	768.1	405	Active gully (upper slope)
GeoB17623-2	75° 0.46'	17° 58.85	150.2	442	N-S oriented channel (inner shelf)

Table 1 Core site locations and total length of sediment cores investigated in this study.

GZW= Grounding Zone Wedge

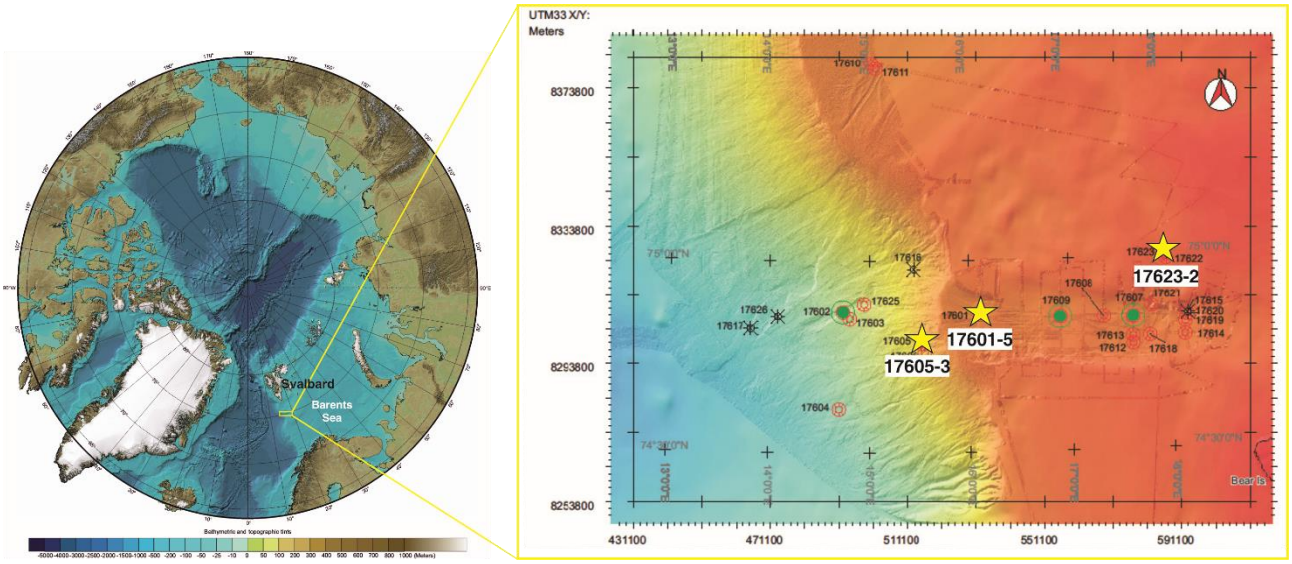

Fig. 1 Studied area in the Arctic Basin, shown on the IBCAO map (on the left), and close-up of the Kveithola Trough depositional system (on the right) with studied core locations (yellow stars).

The 405-cm-long gravity core 17605-3 was collected from 768.1 m water depth in an upper-slope active gully. The uppermost 75 cm contain mud with sparse shell fragments; the base of this interval appears sharply oblique. Slumped/reworked sediments are identified in the interval 75-310 cm bsf, suggesting slope instability that should occur at the beginning of the deglaciation, after the LGM. A scoured boundary between laminated and slumped facies

occurred at 310 cm. The bottom of the core (310-405 cm bsf) consists of finely laminated mud (Fig. 2).

The 537-cm-long gravity core 17601-5 was retrieved from ice-margin deposits (Grounded Zone Wedge system, GZW) on the outer part of the Kveithola trough, from a water depth of 369.1 m. Grounded Zone Wedges formed by deposition of subglacial till during episodic ice stream retreat. The sedimentary sequence deposited on the top of the GZW is suggested to have accumulated at a very high rate (on average in the order of 1–1.5 m ka^{-1}, Rebesco et al., 2011) and, consequently, may preserve a high-resolution palaeoclimatic record of deglaciation and post-glacial conditions in this sector of the Barents Sea. The upper 30 cm consist of bioturbated sediments with sparse broken shells, lacking IRD content; at 25 cm, an erosive base is observed. The lower 209 cm (30-239 cm bsf) comprise rare, sparse IRD facies, whereas the lowest 298 cm (239-537 cm bsf) contain laminated sediments, including sandy layers (plumites) (Fig. 2). The presence of a red oxidized level at 125 cm was taken into account as it consistently occurs within neighbour EGLACOM cores.

The 442-cm-long gravity core 17623-2 was recovered from a North-South oriented channel/fault area from a water depth of 150.2 m. The upper 150 cm, consisting in silty sediments with shell debris (0-140 cm bsf) and crudely layered deposits (140-150 cm bsf), were analyzed for nannofossil content (Fig. 2).

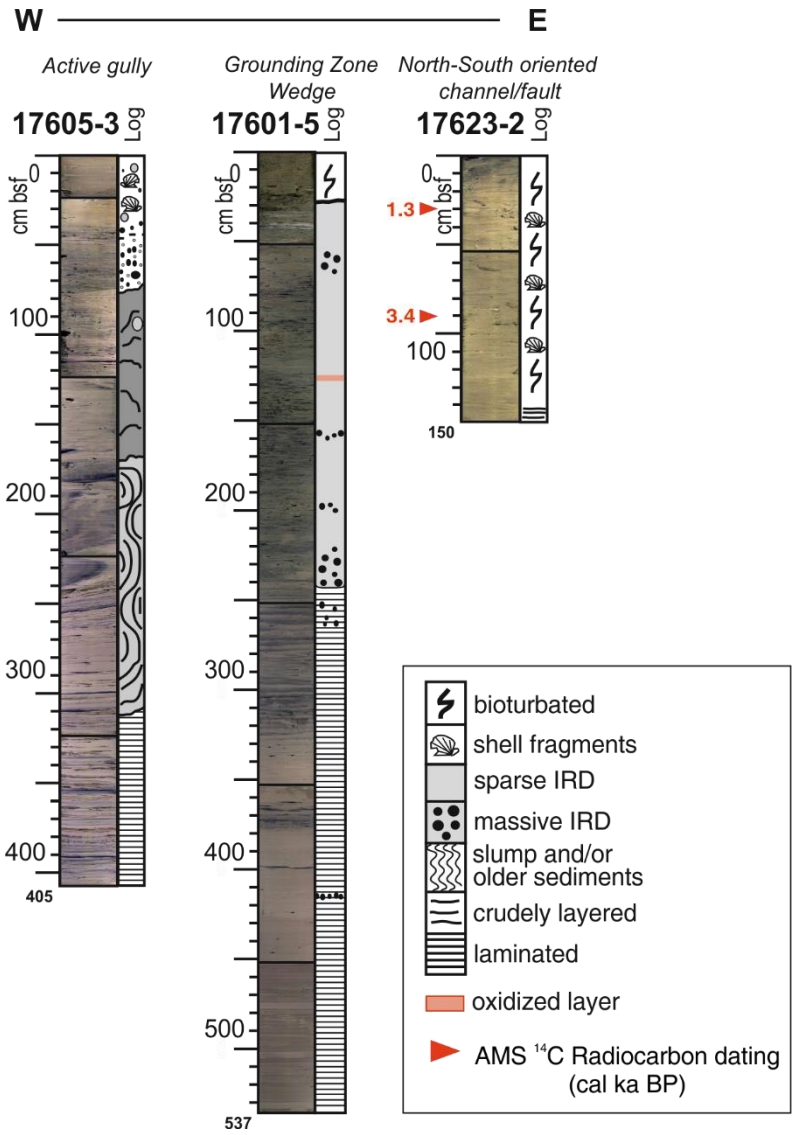

Fig. 2 Lithological logs of the three investigated cores with ^{14}C dates indicated. For core location see Fig. 1.

4.2.2 Preparation and counting of nannofossils

In all the site cores, samples for nannofossil counts were prepared and examined as indicated in Chapter II. Changes in the assemblage structure was described by ratio variations of the two dominant species *Emiliania huxleyi* and *Coccolithus pelagicus* (H/P ratio), following Andruleit and Baumann (1998). The dissolution index (CEX') was measured as ratio between the fragile *E. huxleyi* and the dissolution-resistant *C. pelagicus*, following the conceptual idea indicated by Dittert et al. (1999), as shown in Chapter II.

Shannon diversity and dominance indices were calculated directly from relative species abundance data.

4.2.3 Chronology of studied cores

Two Accelerator mass spectrometry (AMS) ^{14}C dating on benthic foraminifera of core 17623-2 supports the chronostratigraphy of this study that was built by the integration of magnetic susceptibility curves and lithofacies analyses. The radiometric ages have been corrected for the ocean-reservoir effect and calibrated with the software Calib 7.1 (Stuiver and Reimer, 1993), using the Marine13 calibration curve (Reimer, 2013), applying an average marine regional reservoir effect $\Delta R = 67 \pm 34$ years, obtained from the Marine Reservoir Correction Database of Calib 7.1 for the northwestern Barents Sea area (Mangerud et al., 2006; Mangerud and Gulliksen, 1975). Ages are given in calendar years and are reported in the following as cal a BP or as cal ka BP.

4.3 Results

4.3.1 Core 17605-3 – active gully (upper slope)

At the base of the core, laminated sediments contain scarce nannofossils (14.33-156.05 coccoliths/10 mm^2), indicating dilution due to abundant input of terrigenous sediments delivered by meltwaters (main phase of deglaciation). Slumped/reworked sediments were emplaced during the main phase of deglaciation and possibly contributed to the gully formation. The gully excavation suggests high efficiency of erosive processes on the upper slope (Pedrosa et al., 2011). Mass gravity deposits contain rare and often broken/reworked nannofossils, whereas the shell fragment-rich deposits show a reworking drop (Fig. 4). Peaks of absolute total abundance are recorded in correspondence of the lithofacies boundary (at 320 cm and 70 cm). Core 17605-3 has a relatively uniform flora with constantly more than 55.27% of *E. huxleyi* (up to 88.78%). Other species recorded in the samples are *Gephyrocapsa muellerae* (up to 10%) and *C. pelagicus* (up to 6.67%). Species which are only present in minor amounts and which have rarely been seen in the cores are not discussed. The H/P ratio spans from 0.60 to 1.86 through the core showing a peak at 320 cm (Fig. 3). The scarcity of *C. pelagicus* undermines this ratio and the CEX' index. Shannon Wiener diversity index spans from 0.20 to 0.92 and it is generally lower than dominance through the core (Fig. 3).

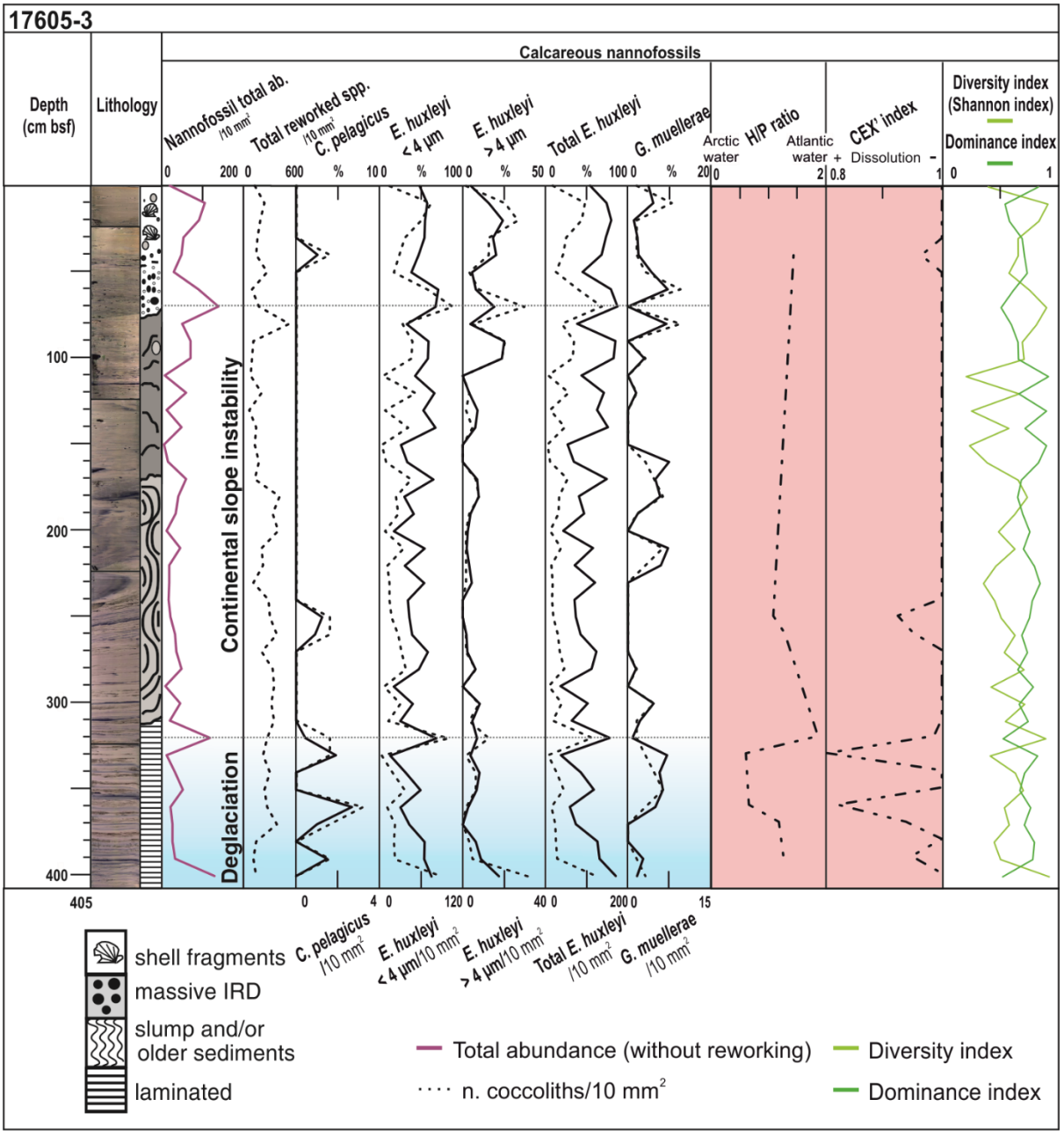

Fig. 3 Coccolith absolute abundances (dotted curve), expressed as n. of coccoliths/10 mm^2 in the slide, and relative abundances (solid curve), expressed in percentage, of single species in core 17605-3. H/P ratio, CEX', Shannon Wiener diversity and dominance indices are plotted versus depth. The H/P ratio and the CEX' curves are dash-dotted due to the scarcity of *C. pelagicus*.

4.3.2 Core 17601-5 – GZW (outer shelf)

The laminated and massive/sparse IRD sediments, observed at the base of the sequence between 537-30 cm, are characterized by rare occurrence of coccoliths (0-242.04 coccoliths/10 mm^2). The presence of a meter-thick sequence of laminated sediments deposited by subglacial release of turbid meltwater (plumites) indicates rapid ice melting and retreat. In this interval, the presence of pre-Quaternary reworked specimens such as *Watznaueria barnesae*, *Eiffelithus turriseiffelii*, *Arkhangelskiella* spp., and *Tranolithus* spp.,

Micula spp., suggests the input of allochthonous, reworked sediments supporting the idea of a sedimentation associated to the deglaciation phase with environmental conditions influenced by meltwaters. The overlaying sequence of massive and sparse IRD sediments records the progressive retreat inland of the ice sheet with seasonal delivery of coarser sediments. This interval is mainly barren of nannofossils, but some *E. huxleyi* and *G. muellerae* are occasionally present. The transition from the sparse-IRD sediment facies and the overlaying bioturbated sediments is characterized by a significant absolute abundance increase in all species records (Fig. 4), suggesting Holocene deposition above the erosional base at 25 cm, as Rüther et al. (2012) documented in the same area. The erosional contact could have been possibly caused by the Storegga tsunami at 8.1 cal ka BP (Dawson et al., 2011; Haflidason et al., 2005) and it includes sandy patches. The bioturbated sediment facies is marked by a distinct increase in nannofossil absolute total abundance, reaching a maximum at the top of the core. The assemblage in the topmost 30 cm is dominated by *E. huxleyi* and *C. pelagicus*, which together comprise more than 93% of the association. Other species recorded in this interval are *G. muellerae* (0.14-4.19%), small *Gephyrocapsa* spp. (2.99-4.82%) and *Gephyrocapsa caribbeanica* (0-0.36%).

The H/P ratio varies from 0 to 0.87 through the core (Fig. 4). An abrupt H/P ratio increase is shown from 510 to 30 cm, associated to *E. huxleyi* dominance. Shannon Wiener diversity index spans from 0 to 1.09 and it is higher than dominance index in the bioturbated lithofacies (Fig. 4). CEX' index, in good agreement with the H/P ratio, spans from 0.5 to 1 through the core and abruptly decreases within the bioturbated lithofacies. The CEX' presents a descending trend in the topmost 30 cm in agreement with the *C. pelagicus* increase (Fig. 4).

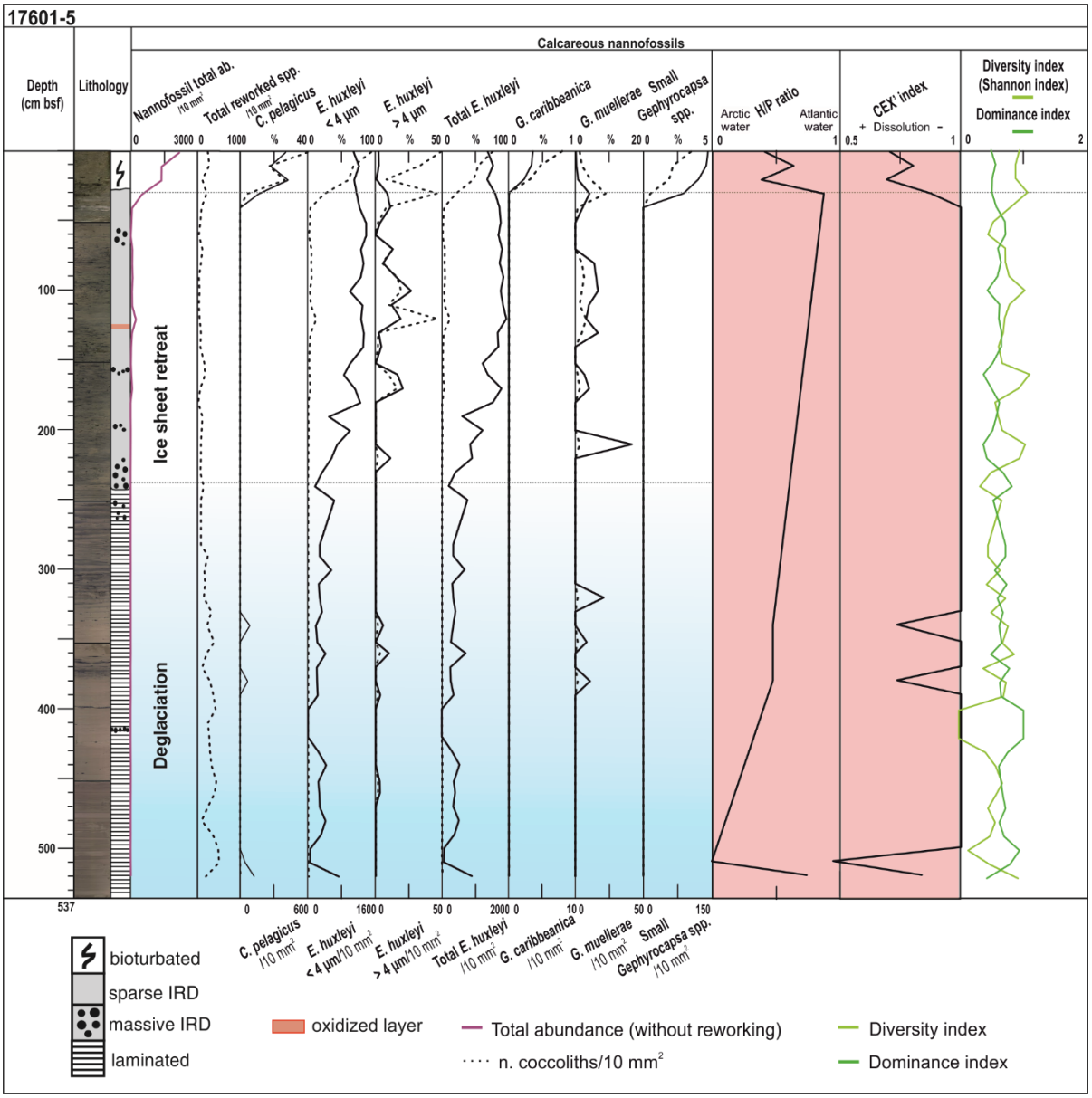

Fig. 4 Coccolith absolute abundances (dotted curve), expressed as n. of coccoliths/10 mm^2 in the slide, and relative abundances (solid curve), expressed in percentage, of single species in core 17601-5. H/P ratio, CEX', Shannon Wiener diversity and dominance indices are plotted versus depth.

4.3.3 Core 17623-2 – North-South oriented channel/fault area (inner shelf area)

The crudely layered sediments, located at the base of the core, are characterized by rare occurrence of coccoliths (84.39 coccoliths/10 mm^2). *Coccolithus pelagicus* dominates the association in this interval. The overlaying bioturbated sediments are characterized by nannofossil absolute total abundance increase (up to 479.30 coccoliths/10 mm^2) with predominant *C. pelagicus* (up to 80%) along with *E. huxleyi* (up to 48.10%) and rare *C. leptoporus* (up to 3.77%), small *Gephyrocapsa* spp. (up to 1.30%), *G. muellerae* (up to 0.93%) and *G. oceanica* (up to 0.93%) (Fig. 5). The nannofossil assemblage does not show significant evidence of reworking. The H/P ratio spans from -0.92 to -0.02, while CEX'

index ranges between 0.11-0.49 through the core. Shannon Wiener diversity and dominance indices span, respectively, from 0.62-0.94 and 0.45-0.66 (Fig. 5).

The sharp contact between laminated and bioturbated deposits suggests the evidence of a hiatus corresponding to the absence of the IRD-rich sediment facies.

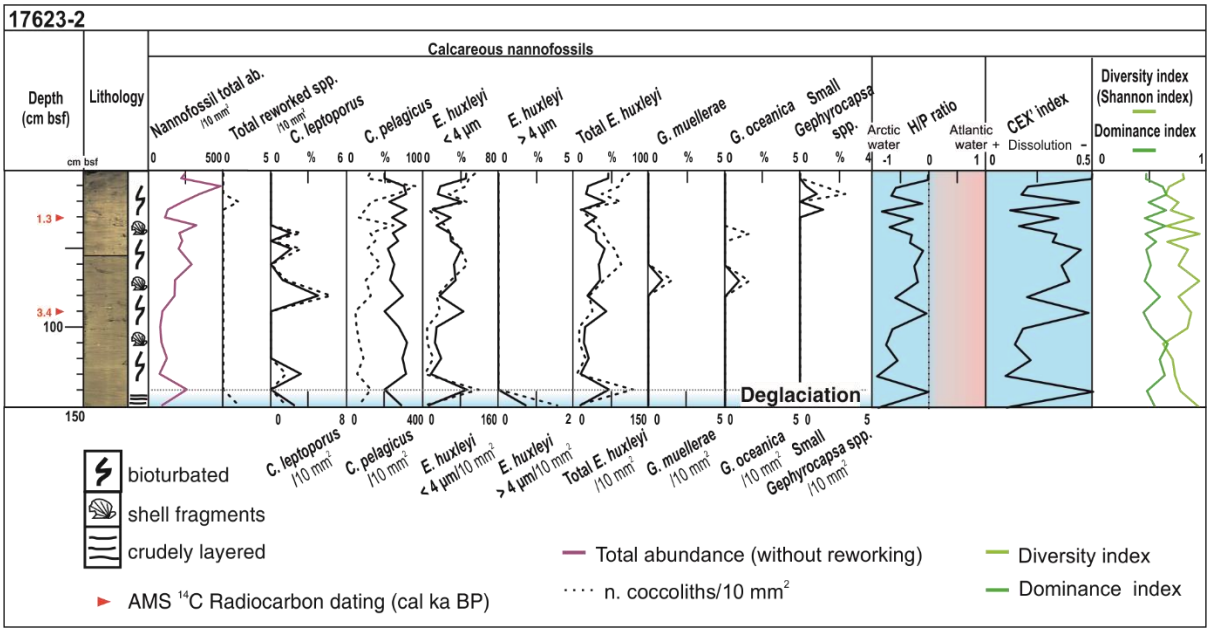

Fig. 3 Coccolith absolute abundances (dotted curve), expressed as n. of coccoliths/10 mm2 in the slide, and relative abundances (solid curve), expressed in percentage, of single species in core 17623-2. H/P ratio, CEX', Shannon Wiener diversity and dominance indices are plotted versus depth.

4.4 Discussion

Although only two radiometric ages are available, the micropalaeontological analyses and lithological characteristics of the Kveithola trough cores indicate the recovery of the late Pleistocene deglaciation and Holocene record.

4.4.1 Deglaciation

The timing and rate of ice-sheet retreat across polar continental shelves and ice-stream collapses during the deglaciation are still a matter of debate (Alley et al., 2007; Clark et al., 2001; Clark and Mix, 2002). However, if the ice-stream associated catchment area is locally restricted, the deposits, which typically form in such environment, should sensitively record these ice advance and retreat dynamics. The Kveithola trough was selected because the sea floor contains depositional ridges (GZW) that typically form during ice stream standstills during retreat testifying an episodic-mode of the ice sheet decay; moreover, the Kveithola

former ice stream had a limited extent and, thus, is expected to have sensitively responded to even small climate changes.

The laminated/layered sediments, recovered at the base of the three investigated cores (Fig. 6), deposited by settling from meltwater sediment-laden plumes (plumites), generated during the main phase of glacial retreat similarly to the deglacial sequence described by Lucchi et al. (2013) in neighbouring cores. Rare occurrences of coccoliths are recorded during this phase, due to the massive terrigenous/detrital input and adverse environmental conditions with reduced salinities for ice melting and increased water turbidity that probably hampered coccolithophore productivity, as also reported for this lithofacies in Lucchi et al. (2013) (Anderson et al., 1988). Numerous records based on stable isotopes from sediment cores collected throughout the Nordic seas demonstrated that the late glacial interval was punctuated by several melt-water events due to the decay of the surrounding ice-sheets (e.g. Jones and Keigwin, 1988; Sarnthein and Altenbach, 1995), confirming our observations.
Reworked calcareous nannofossils provide useful information on the erosion and transport of sediments deriving from adjacent areas. The nearby shallow continental shelf and surrounding flanks of the Kveithola trough, must have acted as the local detrital source of the sediments released through the ice-stream melting during deglaciation. Cretaceous taxa, in particular, most probably originated from southern areas, were, therefore, interpreted as indicative of a northward drift of the released icebergs (Baumann and Matthiessen, 1992). The reworked species abundances are thought to represent a relatively good proxy to a first Atlantic water intrusion to the Arctic, this interpretation could be confirmed by expected radiocarbon dates in cores 17601-5 and 17605-3, when available. Instead, the most intensive reworking, observed in core 17605-3, located in the active gully (upper slope of the TMF), is interpreted as funnelled from the shelf sediments moving along the slope towards the deeper environment. This core is characterized by the occurrence of slumped sediments, originated by gravitational instability of the slope during the deglaciation (Llopart et al., 2015).

The IRD-rich sediment facies observed in cores 17601-5 and 17605-3 is associated with break-up and retreat of the ice sheet (Fig. 6). The overlaying massive-IRD sediment facies, associated to increased calving rates in a warming environment (Dowdeswell et al., 2000), confirms the transition from late glacial to interglacial conditions with terrigenous input related to the main Svalbard ice-sheet retreating phase. The scarce occurrence of nannofossils could be due to large volumes of suspended materials in the surface waters during this period. Slightly increased abundances of *E. huxleyi*, *C. pelagicus* and *G.*

muellerae in cores 17601-5 and 17605-3 during this deglacial sequence may be interpreted as allochthonous species, indicating that material transported from the South influenced the local Arctic assemblage.

4.4.2 Holocene

Following the deglaciation phase, the sedimentation changed to bioturbated deposits with abundant shells (Fig. 6), indicating environmental conditions favourable to the productivity (Marchal et al., 2002; Martrat et al., 2003). The increase of nannofossils in the uppermost part of the sedimentary sequence of the 3 investigated cores, indicates that open-water conditions must have existed in the Arctic Ocean during Holocene since nannofossils were photosynthetic algae that could not live under permanent sea ice cover (Gard, 1993). In the present Nordic seas, intervals in which coccolithophores occur in high amount reflect warmer periods (interglacials) with influences of North Atlantic surface waters, whereas barren intervals or intervals with only reworked species represent colder conditions (Gard, 1988; Gard and Backman, 1990), confirming our interpretations. The increased occurrence of nannofossil species that, in turn, produces high Shannon Wiener diversity values, is interpreted as an indication of intensified inflow of Atlantic surface water to the Arctic Ocean. This explanation is supported by H/P and CEX' values, except for core 17623-2 that shows lower numbers for these indices, probably reflecting the cool late Holocene conditions or Neoglaciation, in agreement with the available calibrated ages.

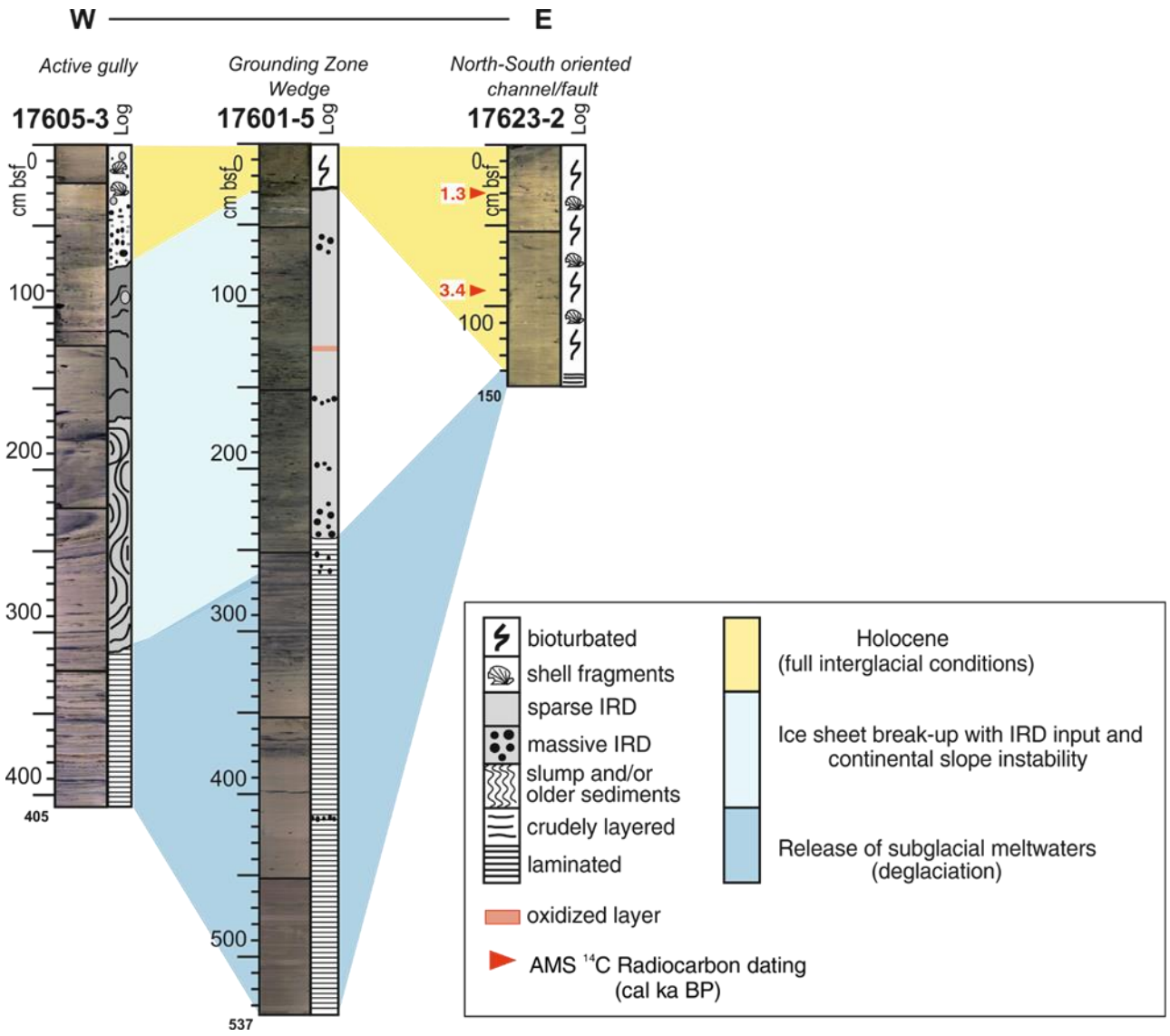

Fig. 4 Core correlation and environmental interpretation. ^{14}C dates (cal ka BP) are shown for core 17623-2.

4.5 Conclusions

Three sediment cores from the northwestern Barents Sea provided a basis to study the development of the coccolithophore assemblages and their relation to the climatically induced changes in surface waters of the Arctic sea. Based on our data, two climatic intervals are recognized, the last Pleistocene deglaciation and the Holocene. The following conclusions can be drawn:

- according to sedimentological characteristics, the laminated/layered sequence represents a depositional event associated with a meltwater release (deglaciation); sparse occurrences of nannofossils were generally observed in this interval, confirming environmental conditions with a dominant influence of meltwater;

- the deglacial interval is characterized by poor micropalaeontological content, whereas numerous records based on stable isotopes from throughout the Nordic seas demonstrate that the late glacial interval was punctuated by several melt-water events due to the decay of the surrounding ice-sheets. Therefore, reduced salinities due to ice melting and increased water turbidity probably have hindered coccolithophore growth;

- reworking reflect changes in the ocean circulation, being a good proxy to a first Atlantic water intrusion to the Arctic from the South or representing remobilization of sediments from the shelf to deeper environments;

- delivery of IRD-rich sediments was associated with initial climatic warming with enhanced calving rate and it records the progressive retreat inland of the ice sheet; nannofossils are scarce, but *E. huxleyi* and *G. muellerae* are occasionally present;

- significant increase in coccolithophores can be observed during Holocene, when ameliorated climatic/environmental conditions seem favourable to the biological productivity clearly influenced by a stronger influx of North Atlantic surface waters;

- the investigated coccolithophore assemblages were of low diversity and consisted almost entirely of *E. huxleyi* and *C. pelagicus*. Other species, such as *G. muellerae*, small *Gephyrocapsa* spp., *G. caribbeanica* and *C. leptoporus* contribute to a lesser extent to the assemblages.

- the sharp contact between laminated sediments and bioturbated deposits in core 17623-2, suggests the evidence of a hiatus corresponding to the absence of the IRD-rich sediment facies.

References

Alley, R.B., Anandakrishnan, S., Dupont, T.K., Parizek, B.R., Pollard, D., 2007. Effect of sedimentation on ice-sheet grounding-line stability. Science (80-.). 315, 1838–1841. doi:10.1126/science.1138396

Anderson, P. M., Barnosky, C. W., Bartlein, P. J., Behling, P. J., Brubaker, L., Cushing, E. J., Dodson, J., Dworetsky, B., Guetter, P. J., Harrison, S. P., Huntley, B., Kutzbach, J. E., Markgraf, V., Marvel, R., McGlone, M. S., Mix, A., Moar, N. T., Morley, J., Perrott, R. A., Peterson, G. M., Prell, W. L., Prentice, I. C., Ritchie, J. C., Roberts, N., Ruddiman, W. F., Salinger, M. J., Spaulding, W. G., Street-Perrott, F. A., Thompson, R. S., Wang, P. K., Webb, T., III, Winkler, M. G., Wright, H. E., Jr., 1988. Climatic changes of the last 18,000 years: observations and model simulations. Science. 241.

Andreassen, Karin, Laberg, J.S., Vorren, T.O., 2008. Andreassen K., Leberg J.S., Vorren T.O. -- Seafloor geomorphology of the SW Barents Sea and its glacidynamic implications. Geomorphology 97, 157–177.

Andruleit, H.A., Baumann, K.H., 1998. History of the last deglaciation and holocene in the Nordic seas as revealed by coccolithophore assemblages. Mar. Micropaleontol. 35, 179–201. doi:10.1016/S0377-8398(98)00021-8

Backman, J., Shackleton, N.J., 1983. Quantitative biochronology of Pliocene and early Pleistocene calcareous nannofossils from the Atlantic, Indian and Pacific oceans. Mar. Micropaleontol. 8, 141–170. doi:10.1016/0377-8398(83)90009-9

Baumann, K.H., Matthiessen, J., 1992. Variations in surface water mass conditions in the Norwegian Sea: Evidence from Holocene coccolith and dinoflagellate cyst assemblages. Mar. Micropaleontol. 20, 129–146. doi:10.1016/0377-8398(92)90003-3

Bjarnadóttir, L.R., Rüther, D.C., Winsborrow, M.C.M., Andreassen, K., 2013. Grounding-line dynamics during the last deglaciation of Kveithola, W Barents Sea, as revealed by seabed geomorphology and shallow seismic stratigraphy. Boreas 42, 84–107. doi:10.1111/j.1502-3885.2012.00273.x

Bown, P.R., Young, J.R., 1998. Calcareous Nannofossil Biostratigraphy.

Clark, P.U., Marshall, S.J., Clarke, G.K.C., Hostetler, S.W., Licciardi, J.M., Teller, J.T., 2001. Freshwater forcing of abrupt climate change during the last glaciation. Science. 293, 283–287. doi:10.1126/science.1062517

Clark, P.U., Mix, a. C., 2002. Ice sheets and sea level of the Last Glacial Maximum. Quat. Sci. Rev. 21, 1–7. doi:10.1016/S0277-3791(01)00118-4

Dawson, A., Bondevik, S., Teller, J.T., 2011. Relative timing of the Storegga submarine slide, methane release, and climate change during the 8.2 ka cold event. The Holocene 21, 1167–1171. doi:10.1177/0959683611400467

Dittert, N., Baumann, K.H., Bickert, T., Henrich, R., Kinkel, H., Meggers, H., 1999. Carbonate dissolution in the Deep-Sea: Methods, Quantification and Paleoceanographic Application. Proxies Paleoceanogr. Examples from South Atl. 255–284.

Dowdeswell, J.A., Whittington, R.J., Jennings, A.E., Andrews, J.T., Mackensen, A., Marienfeld, P., 2000. An origin for laminated glacimarine sediments through sea-ice build-up and suppressed iceberg rafting. Sedimentology 47, 557–576. doi:10.1046/j.1365-3091.2000.00306.x

Gard, G., 1988. Late quaternary calcareous nannofossil biozonation, chronology and palaeo-oceanography in areas north of the faeroe-iceland ridge. Quat. Sci. Rev. 7, 65–78. doi:10.1016/0277-3791(88)90094-7

Gard, G., Backman, J., 1990. Synthesis of Arctic and sub-Arctic coccolith biochronology and history of North Atlantic drift water influx during the last 500 000 years, in: Geological History of the Polar Oceans: Arctic versus Antarctic. pp. 417–436.

Gard, G., Gard, G., 1993. Geology Late Quaternary coccoliths at the North Pole : Evidence of ice-free conditions and rapid sedimentation in the central Arctic Ocean Late Quaternary coccoliths at the North Pole : Evidence of ice-free conditions and rapid sedimentation in the centra 227–230. doi:10.1130/0091-7613(1993)021<0227

Haflidason, H., Lien, R., Sejrup, H.P., Forsberg, C.F., Bryn, P., 2005. The dating and morphometry of the Storegga Slide. Mar. Pet. Geol. 22, 123–136. doi:10.1016/j.marpetgeo.2004.10.008

Jones, G.A., Keigwin, L.D., 1988. Evidence from Fram Strait (78° N) for early deglaciation. Nature 336, 56–59. doi:10.1038/336056a0

Llopart, J., Urgeles, R., Camerlenghi, A., Lucchi, R.G., Rebesco, M., De Mol, B., 2015. Late Quaternary development of the Storfjorden and Kveithola Trough Mouth Fans, northwestern Barents Sea. Quat. Sci. Rev. 129, 68–84. doi:10.1016/j.quascirev.2015.10.002

Lucchi, R.G., Camerlenghi, A., Rebesco, M., Colmenero-Hidalgo, E., Sierro, F.J., Sagnotti, L., Urgeles, R., Melis, R., Morigi, C., Bàrcena, M.A., Giorgetti, G., Villa, G., Persico, D., Flores, J.A., Rigual-Hernandez, A.S., Pedrosa, M.T., Macri, P., Caburlotto, A., 2013. Postglacial sedimentary processes on the Storfjorden and Kveithola trough mouth fans: Significance of extreme glacimarine sedimentation. Glob. Planet. Change 111, 309–326. doi:10.1016/j.gloplacha.2013.10.008

Mangerud, J., Bondevik, S., Gulliksen, S., Karin Hufthammer, A., Høisæter, T., 2006. Marine 14C reservoir ages for 19th century whales and molluscs from the North Atlantic. Quat. Sci. Rev. 25, 3228–3245. doi:10.1016/j.quascirev.2006.03.010

Mangerud, J., Gulliksen, S., 1975. Apparent radiocarbon ages of recent marine shells from Norway, Spitsbergen, and Arctic Canada. Quat. Res. 5, 263–273. doi:10.1016/0033-5894(75)90028-9

Marchal Cacho, I., Stocker, T.F., Grimalt, J.O., Calvo, E., Martrat, B., Shackleton, N., Vautravers, M., Cortijo, E., van Kreveld, S., Andersson, C., Koç, N., Chapman, M., Sbaffi, L., Duplessy, J.-C., Sarnthein, M., Turon, J.-L., Duprat, J., Jansen , E., O., 2002. Apparent long-termcooling of the sea surface in the northeast\rAtlantic and Mediterranean during the Holocene. Quat. Sci.

Rev. 21, 455–483.

Martrat, B., Grimalt, J.O., Villanueva, J., Van Kreveld, S., Sarnthein, M., 2003. Climatic dependence of the organic matter contributions in the north eastern Norwegian Sea over the last 15,000 years. Org. Geochem. 34, 1057–1070. doi:10.1016/S0146-6380(03)00084-6

Pedrosa, M.T., Camerlenghi, A., De Mol, B., Urgeles, R., Rebesco, M., Lucchi, R.G., 2011. Seabed morphology and shallow sedimentary structure of the storfjorden and kveithola trough-mouth fans (north west barents sea). Mar. Geol. 286, 65–81. doi:10.1016/j.margeo.2011.05.009

Rebesco, M., Liu, Y., Camerlenghi, A., Winsborrow, M., Laberg, J.S., Caburlotto, A., Diviacco, P., Accettella, D., Sauli, C., Wardell, N., Tomini, I., 2011. Deglaciation of the western margin of the Barents Sea Ice Sheet - A swath bathymetric and sub-bottom seismic study from the Kveithola Trough. Mar. Geol. 279, 141–147. doi:10.1016/j.margeo.2010.10.018

Reimer, P., 2013. IntCal13 and Marine13 Radiocarbon Age Calibration Curves 0–50,000 Years cal BP. Radiocarbon 55, 1869–1887. doi:10.2458/azu_js_rc.55.16947

Rio, D., Raffi, I., Villa, G., 1990. Pliocene-Pleistocene calcareous nannofossil distribution patterns in the western Mediterranean. Proc., Sci. results, ODP, Leg 107, Tyrrhenian Sea 107, 513–533.

Rüther, D.C., Bjarnadóttir, L.R., Junttila, J., Husum, K., Rasmussen, T.L., Lucchi, R.G., Andreassen, K., 2012. Pattern and timing of the northwestern Barents Sea Ice Sheet deglaciation and indications of episodic Holocene deposition. Boreas 41, 494–512. doi:10.1111/j.1502-3885.2011.00244.x

Sarnthein, M., Altenbach, A., 1995. Late Quaternary changes in surface water and deep water masses of the Nordic Seas and north-eastern North Atlantic: a review. Geol. Rundschau 84, 89–107. doi:10.1007/BF00192244

Stuiver, M., Reimer, P.J., 1993. Extended ^{14}C data base and revised CALIB 3.0 ^{14}C age calibration program. Radiocarbon 35, 215–230.

CHAPTER V

Case study 3: A new multi-proxy investigation of Late Quaternary palaeoenvironments along the southern Svalbard continental margin (northwestern Barents Sea) (EGLACOM project)

This paper has been submitted on Journal of Quaternary Science as Melis R., Carbonara K., Villa G., Morigi C., Lucchi R.G., Bàrcena M.A., Giorgetti G., Caburlotto A., Rebesco M., November 2016.

The layout has been revised.

Abstract

An integrated micropalaeontological and sedimentological study on planktonic and benthic foraminifera, calcareous nannofossils and diatoms was performed on three sediment cores on the Storfjorden Trough Mouth Fan to reconstruct the Late Quaternary palaeoenvironmental and climatic history. Sediments pertaining to Marine Isotope Stage 3 have been recovered only in core EG-01, the other two cores contain post Last Glacial Maximum and Recent sediments, in particular, core EG-03 contains an expanded Holocene succession.

The age model relies on palaeomagnetic parameters together with 10 radiocarbon dates. Late Weichselian and deglacial sediments largely diluted the biogenic record that was scarce and badly preserved. The first occurrence of Cibicidoides wuellerstorfi, together with Turborotalita quinqueloba and Coscinodiscus spp. at 11.3k cal a BP follows the end of the Younger Dryas cold event and marks the early Holocene warm period that culminates in the Holocene Thermal Maximum during 10.4-9.5k cal a BP. Smectite content variation supports this evidence. Cooling events were identified during the Holocene e.g. at around 8.2 and 3.2-2k cal a BP, as shown by the presence of cold-water taxa such as Gephyrocapsa muellerae and Neogloboquadrina pachyderma (s). These variations were influenced by sea ice extension, cold or relatively warm current influxes.

Introduction

The continental margin of the Barents Sea around the Svalbard archipelago (76-80 °N) has been studied over the last two decades in order to reconstruct the palaeoceanographic variations which occurred during the last 10-30 ka (Ślubowska et al., 2005; Rasmussen et al., 2007;

Ślubowska-Woldengen et al., 2007, 2008; Risebrobakken et al., 2011; Werner et al., 2013; Groot et al., 2014; Chauhan et al., 2016). This time span witnessed the most recent global climatic changes, including the Last Glacial Maximum (LGM), the following deglaciation, characterized by several climatic inversions (e.g. the Heinrich event H1, the Bølling-Allerød, the Younger Dryas, etc.) and the climatically dynamic Holocene.

The northwestern continental margin of the Barents Sea, located on the eastern side of the Fram Strait (Fig. 1A), represents the only gateway for the flux of warm water from middle latitudes to the Arctic Ocean. Two main oceanographic currents affect the Storfjorden area (Fig. 1B): the shallow, warm, moderately saline Western Spitsbergen Current (WSC), flowing northwards along the continental slope, and the cold, deeper, low salinity Eastern Spitsbergen Current (ESC). The former derives from the North Atlantic Current/Norwegian Atlantic Current (NwAC) (Ślubowska-Woldengen et al., 2008), whereas the latter is a modified WSC that splits in the northern Spitsbergen margin, in the Arctic Ocean (Ślubowska et al., 2005), to flow back to the Storfjorden Trough along the eastern and southern margins of the Spitsbergen archipelago. A branch of the ESC enters the Storfjorden Trough where it meets the WSC. The thermal and saline gradients between these two water masses cause the development of the Polar Front (PF) to the North, and the Arctic Front (AF) to the South, both variably located on the continental shelf of the Storfjorden Trough (Saloranta and Svendsen, 2001). The reconstruction of these water front shifts over time is very important as it influences the position of seasonal sea-ice coverage and, therefore, the primary productivity in the area (Stabell, 1986; Wollenburg et al., 2004; Zamelczyk et al., 2012).

The strength of the warm WSC influx into the Arctic Seas varied considerably over time (Rahmstorf, 2002; Rasmussen et al., 2007; 2014; Ślubowska-Woldengen et al., 2007, 2008; Risebrobakken et al., 2011; Klitgaard Kristensen et al., 2013; Werner et al., 2013). In this respect, the Svalbard western margin represents a key area for the study of the palaeoceanographic and palaeoenvironmental conditions occurred during the LGM and the following deglaciation.

The potential for microfossils as palaeoenvironmental proxies in the Nordic Seas has been outlined by several authors (e.g. Gard and Backman, 1990; Baumann and Matthiessen, 1992; Giraudeau et al., 2004; Rasmussen et al., 2007; Ślubowska-Woldengen et al., 2007, 2008; Groot et al., 2014; Rasmussen et al., 2014; Rasmussen and Thomsen, 2015). The majority of these studies were focused on the continental shelf area and the northern and western slope of Svalbard. In this contribution we present new data from an integrated micropalaeontological study on three sediment cores collected on the middle slope of the western Barents Sea

continental margin, South of Svalbard (Fig. 1A), aiming to investigate the palaeoenvironmental and palaeoclimatic conditions of the study area after the LGM. The results from planktonic foraminifera, calcareous nannofossils and diatoms, as proxies for surface water conditions, were compared with the results from benthic foraminifera as indicators of bottom water conditions. The palaeontological investigation was also integrated with the results from previously published sedimentological and palaeomagnetic studies (Sagnotti et al., 2011; Lucchi et al., 2013).

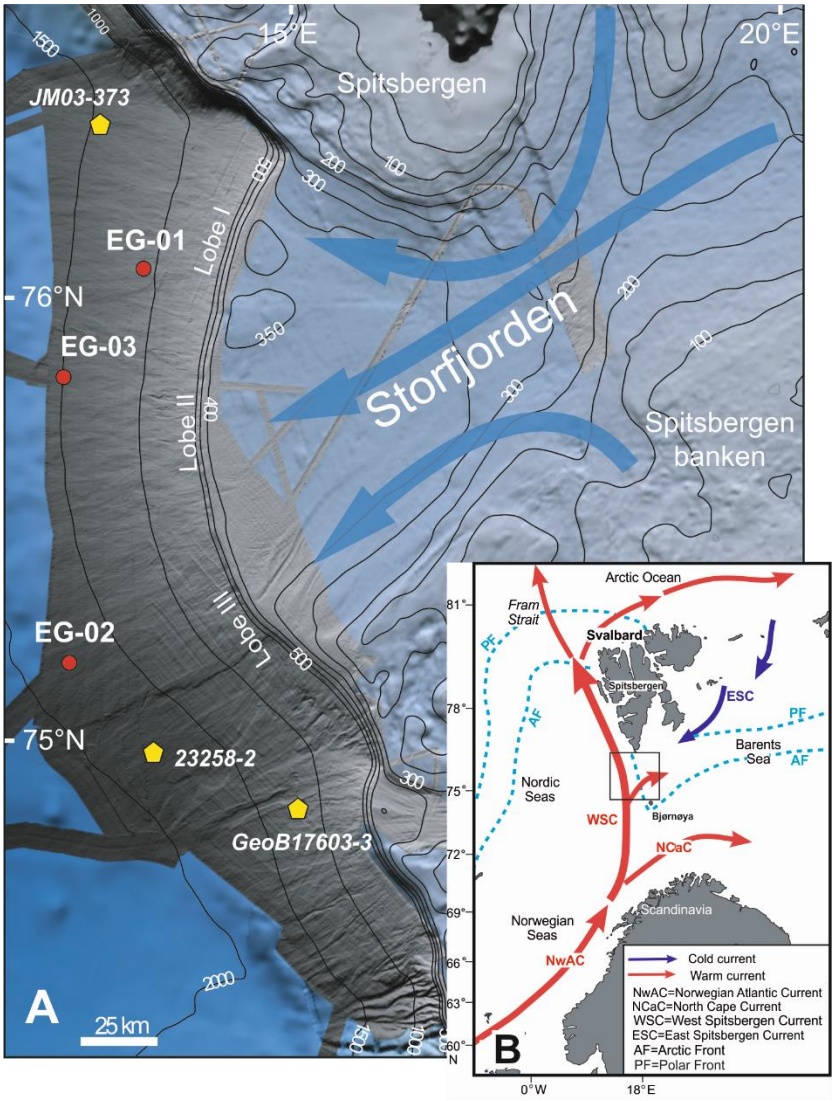

Fig. 1 Figure 1 - A) Location of the study area and oceanographic circulation in the NW Barents Sea (Arctic) (from Ślubowska-Woldengen et al., 2008, modified). The black box indicates the location of the study area. B) Bathymetric map of the studied area. The grey-scale shaded relief bathymetry derives from the merged high-resolution surveys carried out during the SVAIS and EGLACOM cruises (modified after Pedrosa et al., 2011). Red dots indicate the EGLACOM (EG-) core location. Yellow symbols indicate the location of the cores JM03-373 (Rasmussen et al., 2007), 23258-2 (Sarnthein et al., 2003) and GeoB17603-3 (Carbonara et al., 2016) discussed in the text. Blue arrows represent the direction of the main palaeoice-streams of Storfjorden trough during the LGM (from Lucchi et al., 2013).

Sedimentary sequence and age model

The Storfjorden Trough Mouth Fan (TMF) depositional system is a NE-SW oriented glacigenic complex located south of Spitsbergen Island in the NW Barents Sea (Hjelstuen et al., 1996; Laberg and Vorren, 1996). Seismo-stratigraphic data indicate that the onset of glacially influenced sedimentation in the area occurred at about 1.8 Ma, when the Barents Sea Ice Sheet reached the continental shelf edge starting the build-up of the TMF systems (Knies et al., 2009). They are composed of amalgamated alternations of glacigenic debris flows and interglacial sediments (Laberg and Vorren, 1996; Pedrosa et al., 2011).

The multi-beam bathymetry and the seismic reflection data on the Storfjorden TMF indicate the presence of three depositional lobes, referred as Lobe I, II, and III from North to South (Pedrosa et al., 2011) (Fig. 1A). The three lobes differ from each other in stratigraphic architecture with thicker and laterally continuous glacigenic debris flow in Lobe I and II with respect to Lobe III, and thicker post-glacial deposits on Lobe III with respect to the northern Lobes I and II (Pedrosa et al., 2011).

The age model used for this study follows Sagnotti et al. (2011) and Lucchi et al. (2013); it was based on palaeomagnetic rock parameters and radiocarbon dates calibrated using Calib 6.0 software (Stuiver and Reimer, 1993), using the marine09 calibration curve (Reimer et al., 2009), and applying an average marine regional reservoir effect $\Delta R = 84 \pm 23$ years (Mangerud and Gulliksen, 1975). The mean values of the calibrated age range of $\pm 1\sigma$ were normalized to the calendar year (Table S1). The palaeomagnetic curves obtained for the Holocene interval were correlated to the closed palaeosecular variation (PSV) and relative palaeointensity (RPI) variation reference curves of regional palaeomagnetic data or from global geo-magnetic models (Sagnotti et al., 2011), whereas in the older part of the sequences, tie points were obtained by correlation of the core magnetic susceptibility with the stacked record proposed by Jessen et al. (2010), assisted by radiocarbon dates, considering a linear sedimentation rate between tie points (Lucchi et al., 2013).

Slight differences between the radiocarbon ages and the reconstructed age model, which is mainly based on palaeomagnetic rock parameters (Sagnotti et al., 2011), are related to the underestimation of the local regional reservoir correction applied during calibration of mixed benthic and planktonic foraminifera radiocarbon samples. Indeed, Sarnthein (2011), Rae et al. (2014) and Thornalley et al. (2015) indicated that deep ocean waters after the LGM and during deglaciation were up to 1-2 ka older than they are today resulting in a higher local reservoir age.

Sample ID	depth bsf (cm)	Lab ref.	Sample type	Description	Process	Raw AMS ^{14}C	Age err.	∂13C	Cal. yr BP
EG1-1-2.5/3.5	2.5-3.5	OS-78409	Sediment (Corg)	powdered sediment	OC	4830	35	-22.38	4968 ± 78
EG1-2-23/24	60.5-61.5	OS-98259	Foraminifera	benthic foraminifera	HY	12500	110	-0.81	13874 ± 132
EG1-2-64/65	101.5-102.5	OS-78452	Sediment (Corg)	powdered sediment	OC	28900	190	-24.47	32792 ± 364
EG1-3-62/63	191.5-192.5	OS-78453	Sediment (Corg)	powdered sediment	OC	36700	310	-24.76	41357 ± 273
EG2-1-30/31	30-31	OS-78387	Foraminifera	bethic+planktonic	HY	4570	130	-25	4665 ± 164
EG2-1-90/91	90-91	OS-78389	Foraminifera	bethic+planktonic	HY	9460	180	0	10235 ± 234
EG2-2-60/61	181.5-182.5	OS-78383	Forams & Pteropods	benthic+plankt.+pterop.	HY	12100	180	1.41	13481 ± 181
EG3-1-90/91	90-91	OS-78385	Foraminifera	bethic+planktonic	HY	4910	120	-25	5118 ± 161
EG3-2-56/57	160-161	OS-78382	Foraminifera	bethic+planktonic	HY	8590	130	0.01	9147 ± 167
EG3-3-38/39	230-231	OS-78324	Foraminifera	bethic+planktonic	HY	9740	80	0.73	10508 ± 87

Table S1 Radiocarbon dates and ages used to create the age model of the studied cores, from Sagnotti et al. (2011) and Lucchi et al. (2013, see Fig. 7 pag. 319). These data are indicative of the age model created using a combination of rock palaeomagnetic parameters and radiocarbon dates as reported in the chapter 2 in detail.

The stratigraphic sequence was subdivided into units following the acoustic and depositional units described by Pedrosa et al. (2011) and Lucchi et al. (2013).

Core EG-01, collected from a minor gully located in the upper slope off Lobe I (water depth 1069 m below sea level, bsl), contains a major stratigraphic discontinuity between the IRD-rich sediments of the upper part of the core dating ca. 16k cal a BP to present, and older deposits dating interglacial MIS 3 (>32k cal a BP) (Fig. 2A). Core EG-02, located on the southern middle slope offshore Lobe III (water depth 1722 m bsl), contains a sequence spanning the last 16k cal a BP. The deeper part of the sequence is formed by silty clay with abundant IRD related to ice-sheet collapse (massive presence of IRD) and by extensive subglacial meltwater input (interlaminated sediments), which occurred during the transition from fully glacial to interglacial conditions (deglaciation) (Unit A2). The Holocene sedimentary sequence is composed of fine-grained, crudely layered and heavily bioturbated sediments that were deposited under the transport of persistent bottom currents (contourites) (Unit A1, Fig. 2B). Core EG-03, located on the middle slope off Lobe II (water depth 1432 m bsl), contains the last 12k cal a BP depositional record with a relatively expanded interglacial MIS 1 sequence with respect to core EG-02 (Unit A1, Fig. 2C).

Materials and methods

The three analysed sediment cores were collected in the Storfjorden glacial sedimentary system, during the EGLACOM cruise on board the R/V OGS-Explora (July-August 2008). The gravity cores EG-01, EG-02, EG-03, having respective lengths of 220 cm, 305 cm and 285 cm, were collected from the continental slope of the North Barents Sea (Fig. 1A, Table 1).

Core ID	Lat N	Lon E	Water depth (m)	Location	Total recovery (cm)
EG-01	76°06.201'	13°37.625'	1069	Gully upper slope lobe II	220
EG-02	75°12.907'	13°04.587'	1722	Middle-slope lobe III	305
EG-03	75°50.615'	12°58.353'	1432	Middle-slope lobe II	291

Table 1 Core locations, water depth and total sediment recovery for the three cores. EG= EGLACOM

One-cm thick samples were collected at an average spacing of 10 cm in the three cores (Fig. 2A-C). Benthic and planktonic foraminifera were analysed in 83 samples, calcareous nannofossils in 92 samples, and diatoms in 60 samples.

For the study of foraminifera, each sample was initially dried at 50°C, weighed and wet-sieved at 63 µm. The sandy residues were dry-sieved at 150 µm and about 250 specimens in the >150 µm fraction were counted for each sample and identified at species level. We followed the taxonomy of Hemleben et al. (1989) and Darling et al. (2006) for the identification of *Neogloboquadrina* genus. The planktonic total abundance was reported as the number of planktonic foraminifera per gram of dry sediment (ind/g) (Fig. 2A-C). For the purposes of this study, we focused on the pattern of the three most abundant species (*Neogloboquadrina pachyderma* (s), *N. incompta* and *Turborotalita quinqueloba*). The count of the other species is reported in Suppl. E-G.

The whole fraction >63 µm was investigated for the benthic foraminiferal assemblage. Quantitative analyses reported in Suppl. E-G were obtained counting about 300 tests when possible. In foraminifera-rich sediments, the samples were subdivided by dry splitting to obtain a sub-sample aliquot containing approximately 300 specimens. Specimen counting were performed on well-preserved tests and recorded as relative abundance (percentage). Test fragmentation index was calculated as the rate of benthic foraminiferal broken tests over the sum of benthic foraminiferal broken and intact counted tests. The benthic total abundance was reported as the number of benthic foraminifera per gram of dry sediment (ind/g). All benthic foraminifera were identified at species level, except unilocular forms (*Fissurina*, *Lagena* and *Oolina*) and small Discorbidae, which were identified at generic level. The generic taxonomy of benthic foraminifera was assessed in line with Loeblich and Tappan (1987) and species classification mainly followed the Arctic systematic studies of Feyling-Hanssen et al. (1971), Ishman and Foley (1996), Lagoe (1979), Scott and Vilks (1991) and Wollenburg and Mackensen (1998). The Ellis and Messina online catalogue of foraminifera (http://www.micropress.org/) was used for taxa description. Selected specimens were photographed by a scanning electron microscope (Leica Stereoscan 430i) at the University of Trieste and reported in Figure S1.

Sample preparation for calcareous nannofossil analyses followed the methodology described by de Kaenel and Villa (1996). Counting of specimens was performed on a fixed area of the slide equivalent to 1.57 mm^2, using a polarized-light microscope at a magnification of 1250x. The abundances were reported as number of coccoliths per 1.57 mm^2 in the slides.

Cleaning of the sediment samples and preparation of permanent mounts for diatoms studies were accomplished according to the standard randomly distributed microfossils method. Absolute diatom numbers (n. valve/gram of dry sediment) were determined using a Leica DMLB microscope at 1000-x magnification. A count of at least 100 valves of non-dominant taxa per sample was performed using the method of Schrader and Gersonde (1978). In general, more than 300 valves per sample were measured. Sediment samples were considered barren if no valves were found along at least five transects. Species identification follows that of Tomas (1997).

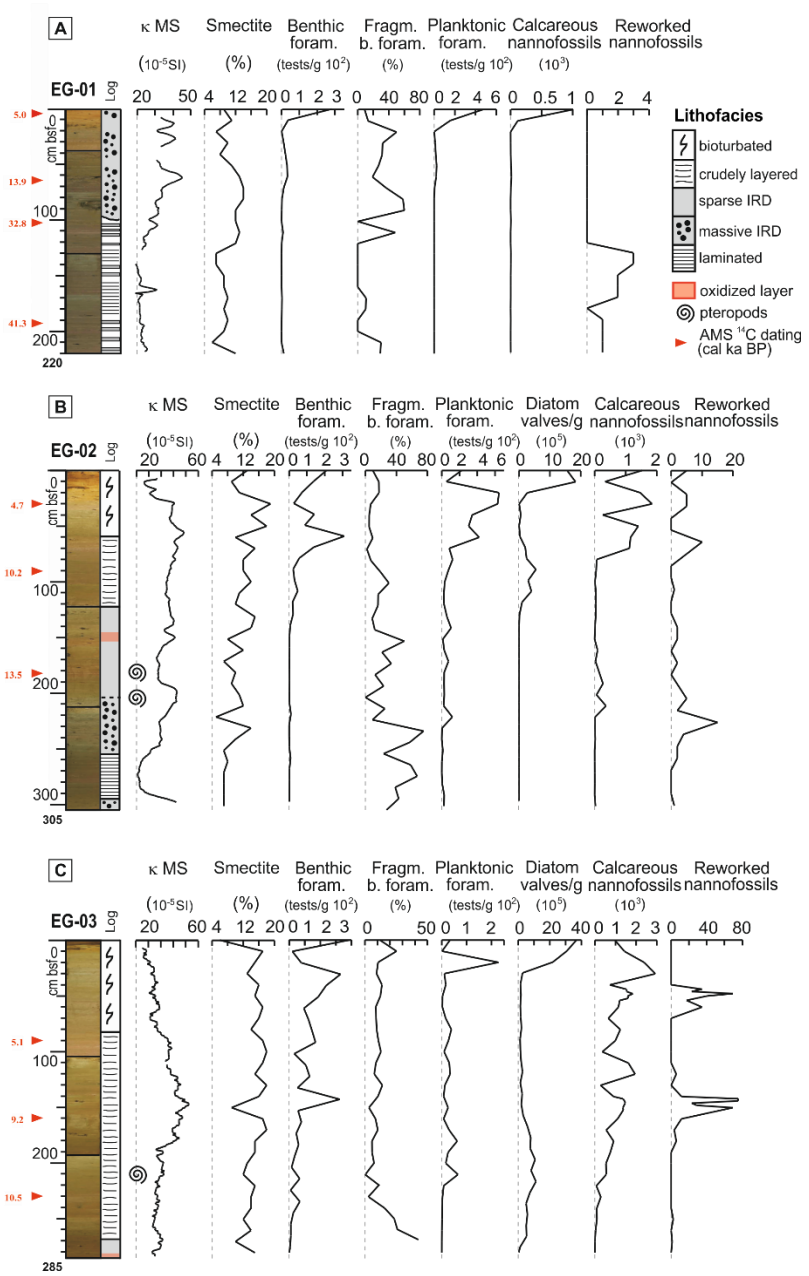

Fig. 2 Lithological logs and down-core compositional characteristics of the three studied cores. Unit A1 and A2 refer to seismic facies (Lucchi et al., 2013; Pedrosa et al., 2011). Calcareous nannofossil abundance is expressed as n. of coccoliths/10 mm2 in the slide. Calibrated calendar ages are indicated in red.

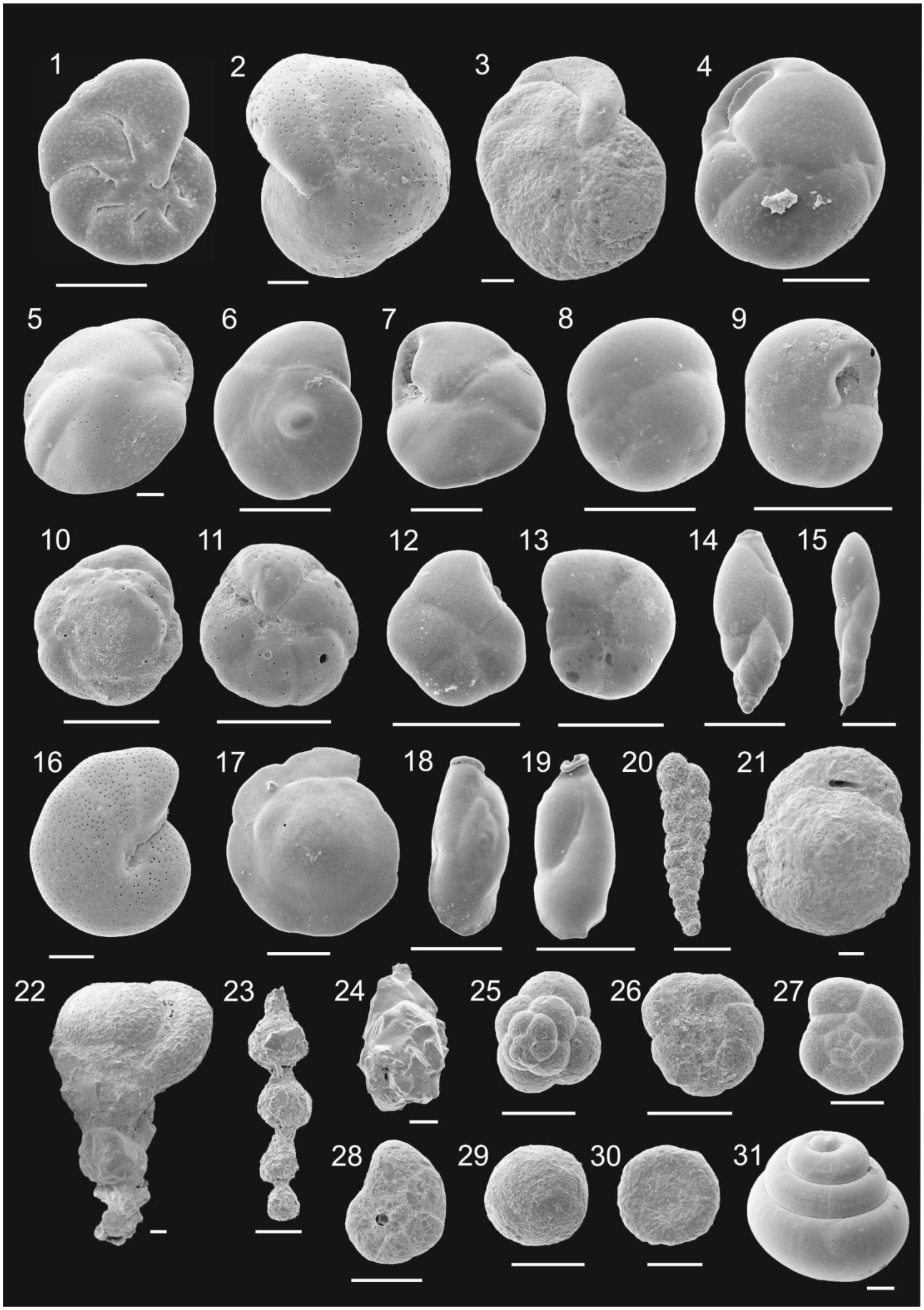
1
2
3
4
5
6
7
8
9
10
11
12
13
14
15
16
17
18
19
20
21
22
23
24
25
26
27
28
29
30
31

Fig. S1 Scanning electron photomicrographs of some foraminifer species representative of the palaeoenvironments recorded in the EGLACOM cores (magnification: bar = 30 µm): 1 - *Astrononion gallowayi*, side view; 2 - *Cibicides lobatulus*, umbilical side view; 3 - *Cibicidoides wuellerstorfi*, umbilical side view; 4 - *Cassidulina reniforme*, side view; 5 - *Cassidulina neoteretis*, side view; 6 - *Epistominella exigua*, spiral side view; 7 - *E. exigua*, umbilical side view; 8 - *Epistominella arctica*, spiral side view; 9 - *E. arctica*, umbilical side view; 10 - *Eilohedra nipponica* spiral side view; 11 - *E. nipponica*, umbilical side view; 12 - *Stetsonia horvathi*, umbilical side view; 13 – *S. horvathi*, spiral side view; 14 - *Stainforthia fusiformis*, side view; 15 - *Stainforthia loeblichi*, side view; 16 - *Melonis barleeanus*, side view; 17- *Oridorsalis tener*, spiral side view; 18 - *Seabrookia earlandi*, side view; 19 - *S. earlandi*, opposite side view; 20 - *Textularia earlandi*, side view; 21 - *Recurvoides turbinatus*, apertural view; 22 - *Reophax scorpiurus*, side view; 23 - *Hormosinella guttifera*, side view; 24 - *Lagenammina difflugiformis*, side view; 25 - *Trochammina globigerineformis*, spiral side view; 26 - *Trochammina ochracea* spiral side view; 27 - *Portatrochammina karica*, spiral side view; 28 - *Deuterammina grahami*, spiral side view; 29, 30 - Calcispherae, side view; 31 - *Limacina helicina*, pteropod, side view.

Results

Planktonic foraminifera

Planktonic foraminiferal assemblages in the three cores are constituted by 11 species, with a high dominance of *Neogloboquadrina pachyderma* (s) (see Suppl. E-F). Other species such as *Turborotalita quinqueloba* and *Neogloboquadrina incompta* occurred with high percentages mainly in the upper part of the three cores, whereas *Globigerina bulloides* and *Globigerinita glutinata* were present only in a few levels with low percentages (see Suppl. E-F).

The lower part of core EG-01 was barren of planktonic foraminifera from 220 cm to 90 cm, scarce abundances were recorded from 80.5 cm to 30 cm. In the upper part of the core (Unit A) *N. pachyderma* (s) dominated and only in the uppermost 10 cm *N. incompta* was seen albeit with relatively low percentages (about 5%). *Turborotalita quinqueloba* was present only at the top of the core (Fig. 3A).

Core EG-02 was divided into two different zones based on the overall planktonic foraminiferal abundance and species changes (Fig. 3B). In the lower part (305-150 cm), the biogenic fraction was scarce and generally badly preserved (Fig. 2B). Few levels were barren (270, 260 and 230 cm) and, in two levels (253 and 223 cm) Cretaceous calcispheres were present (Fig. S1, photos 29, 30). In this interval, the planktonic foraminiferal assemblage was dominated by *N. pachyderma* (s); *T. quinqueloba* and *N. incompta* were virtually absent (Fig. 3B). Well-preserved pteropod tests were recorded in levels 181 and 201 cm (Fig. S1, photo 31). In the

upper part of the core, from 150 cm to the top, *N. pachyderma* (s) still dominated the assemblage, but demonstrated a negative peak between 110-80 cm while *T. quinqueloba* reached percentages of about 50-70% and *N. incompta* attained a maximum relative abundance (Fig. 3B).

In core EG-03, *N. pachyderma* (s) showed a fluctuation in relative abundance, with a minimum located between 210-170 cm; in this interval *T. quinqueloba* occurred with high percentages (Fig. 3C). In the upper part of the core, from 140 cm to the top, *T. quinqueloba* occurred with very low percentages. *Neogloboquadrina incompta* occurred with low percentages along the entire core and demonstrated fluctuating abundances with peaks of more than 7% between 170-140 cm and between 40-0 cm (Fig. 3C). Well-preserved pteropod tests were recorded at 220 cm.

Benthic foraminifera

The total abundance and species richness of benthic foraminifera are variable along the cores but they are commonly more abundant and diversified in the uppermost sediments where several agglutinated taxa were recorded (Suppl. E-F).

In core EG-01, the total abundance of benthic foraminifera reached the maximum value of 282 ind/g at the top; several levels at the base of the core are scarce or barren of these microfossils. The abundance and richness increase considerably in the uppermost 20 cm (Suppl. E-F; Fig. 2A). The fragmentation of the benthic tests varies from 9% to 60% of the total assemblage and reaches higher values at the base of Unit A (around 90-70 cm), showing other peaks from the base to the top of the core (Fig. 2A). The glacigenic diamicton ("old sediments", Fig. 2A), which was present at the base of the core EG-01 (220-90 cm), contained badly preserved specimens of *Cassidulina reniforme*, *Cassidulina neoteretis*, *Elphidium excavatum clavatum*, *Rhabdammina abyssorum* and *Stainforthia loeblichi*, whereas *Melonis barleeanus*, *C. neoteretis* and *Islandiella* spp. (mainly *I. helenae* and *I. norcrossi*) dominated the upper IRD-rich sediment assemblage of the core (Unit A). A significant occurrence of *C. neoteretis*, together with agglutinated taxa, mainly represented by *Reophax scorpiurus* and *Hormosinella guttifera*, were recorded in the uppermost 10 cm of the core (Suppl. E-F; Fig. 3A).

In core EG-02, the total abundance reached the maximum value of 310 ind/g at 60 cm and demonstrated very low values in the interlaminated sediments (Unit A2) and in the IRD-rich lithofacies (Fig. 2B). The benthic foraminifera were poorly preserved at the base of core EG-

02 (Unit A2) (fragmentation up to 75% at 232.5 cm), mainly characterized by *C. reniforme* and *C. neoteretis*, and well preserved in the sediments of the Unit A1 (Fig. 2B). *Oridorsalis tener* increased towards the top of Unit A2, since 161.5 cm (Fig. 3B). In the upper sequence (Unit A1), diversity, total abundance and preservation state of the benthic foraminifera increased (Fig. 2B). The first occurrence of *Cibicidoides wuellerstorfi* was recorded at 131.5 cm. This taxon, along with other important species such as *O. tener*, *Seabrookia earlandi* and *Stetsonia horvathi*, characterizes the crudely-layered lithofacies (70-120 cm), which represents the beginning of the contour currents (Lucchi *et al.*, 2013) (Fig. 3B). From 150 cm upward, a decrease in *C. reniforme* and *C. neoteretis* was evidenced. The upper 60 cm of bioturbated sediments, indicative of recent hemiplegic sedimentation, recorded a decrease in benthic foraminiferal total abundance up to 30 cm, followed by an increase in species richness and total abundance toward the top of the core (Fig. 2B). The assemblage in the topmost 60 cm was characterized by the low abundances in *C. wuellerstorfi*, *C. reniforme*, *S. horvathi*, *S. earlandi*, *C. neoteretis*, *O. tener* and high relative abundances of *Epistominella arctica*, *E. exigua* and *Ioanella tumidula* (Suppl. E-F). The occurrence of *S. horvathi* and *S. earlandi* was evidenced in a straddle position between the crudely-stratified and the bioturbated lithofacies (Fig. 3B). The topmost levels were characterized by the significant occurrence of several agglutinated species, especially represented by *Recurvoides turbinatus*, *H. guttifera* and *R. scorpiurus* (Suppl. E-F).

In core EG-03, the total abundance gradually increased from the bottom to the top, where it reached the maximum value of 382 ind/g (Fig. 2C). The benthic foraminifera were not as well preserved at the base of the core (fragmentation until 41% at 270 cm) and commonly well preserved in all the sediments of Unit A1 (Fig. 2C). This core contained an expanded sequence (260 cm instead of 120 cm of core EG-02) of fine-grained, crudely laminated and heavily bioturbated sediments pertaining to the acoustically transparent unit (Unit A1), already described in core EG-02 (Fig. 2B). A part from the very basal level of the core, which was barren of foraminifera, the crudely laminated interval was characterized by the occurrence of *C. wuellerstorfi* and *C. reniforme,* with other significant species such as *C. neoteretis*, *O. tener*, *S. earlandi*, *S. horvathi* (Fig. 3C) and *Stainforthia* spp. (Suppl. E-F). As in core EG-02, the occurrence of *S. horvathi* was evidenced in a straddle position between the crudely-stratified and the bioturbated lithofacies, from 160-60 cm; on the contrary, *S. earlandi* was more abundant in the interval 150-200 cm (Fig. 3C).

The upper 80 cm of bioturbated sediments, indicative of recent hemiplegic sedimentation, recorded an increase in the benthic foraminiferal total abundance up to 30 cm, followed by a

decrease up to 10 cm and yet another definitive increase toward the top of the core, as already observed in core EG-02 (Fig. 2B). The assemblage was characterized by a low abundance of *C. wuellerstorfi* and *O. tener* and the relative increase of *C. neoteretis*, a peak of *E. arctica* at 70 cm and, subordinately, *E. exigua* and *I. tumidula* (Suppl. E-F). The interval 10-0 cm was characterized by the significant occurrence of several agglutinated species, represented by the same taxa recovered in core EG-02 (Suppl. E-F).

Calcareous nannofossils

In cores EG-02 and EG-03 nannofossils were well represented by Holocene species together with some Palaeogene and Cretaceous reworked taxa. The total abundance, calculated as observed coccoliths on a fixed area, shows variations through the cores (Fig. 2B, C). Quantitative data are reported in Suppl. E-F.

Core EG-01 is almost barren in nannofossils, with the exception of the topmost samples, containing few specimens of *Calcidiscus leptoporus*, *Coccolithus pelagicus* s.l. (*C. pel. pelagicus* and *C. pel. braarudi*), *Emiliania huxleyi* and *Gephyrocapsa* spp.

The lower part of core EG-02 (from the bottom to 220 cm) was almost barren of nannofossils. Reworked taxa showed the highest abundance at around 230 cm, in correspondence of the IRD-rich lithofacies. The highest nannofossil abundance was recorded in the upper sediments, from 80 cm upward; here the assemblage was characterized by the occurrence of *C. leptoporus, C. pel. pelagicus, C. pel. braarudi, E. huxleyi* and *Gephyrocapsa muellerae* (Fig. 3B). Abrupt decreases in abundance were evidenced at 40 cm and 10 cm (Fig. 2B).

The lower part of core EG-03 (from the bottom to 250 cm) was almost barren of nannofossils. Reworked taxa were present in two intervals, peaking at 150 cm and 50 cm (Fig. 2C). The highest nannofossil abundance was recorded in the upper sediments, from 160 cm upward. The association was dominated by *E. huxleyi* and *C. pel. pelagicus*; other species recorded consistently in the samples are *G. muellerae*, *C. leptoporus* and *C. pel. braarudi* (Fig. 3C). An abrupt decrease in abundance was recorded at 130 cm. The distribution of *G. muellerae* showed a peak in abundance at 148 cm and 50 cm (Fig. 3C).

Diatoms

In the IRD-rich lithofacies of Unit A2 of cores EG-02 and EG-03 diatoms were absent. In core EG-02, diatoms appeared at 131.5 cm. Their overall abundance was characterized by two

distinct maxima centred approximately in the middle part of the crudely-layered interval (at 110 and 90 cm), with a maximum abundance of 5.4 x 10^5 valves/g at the depth of 90 cm, and in the uppermost part of the heavily-bioturbated sediments, with an abundance of 1.8 x 10^6 valves/g at 10 cm (Fig. 2B). An abrupt decrease in abundance from 50 to 30 cm was evidenced, with values two orders of magnitude below the maximum. The former peak was mainly characterized by warm-water adapted taxa with species belonging to the *shade-flora*, able to grow under low light conditions: *Coscinodiscus* spp. (up to 90%) associated with *Paralia sulcata* and, subordinately, with *Thalassiosira* spp. and *Chaetoceros* RS (resting spores) (Fig. 3B). The latter peak was characterized by a decreasing abundance of *Coscinodiscus* spp. and *P. sulcata* and a relative increase in *Chaetoceros* RS (up to 70% of the assemblage) with *Thalassiosira* spp., *Thalassionema nitszchioides*, and *Rhizosolenia* spp. (Suppl. E-F). At the same time, a group of species including *Azpeitia* spp., *Hemidiscus cuneformis*, *Rhizololenia bergonii*, *Roperia tessellata*, *Thalassiosira oestrupii*, was considered in this paper to be a Warm Species Group (WSG).

In core EG-03, diatoms appeared at 270 cm, at the base of the crudely layered interval (Units A1). Similar to the previous core, their overall abundance was characterized by three maxima, centred approximately in the middle part of the crudely-layered interval at 220 cm and 200 cm, and in the uppermost part of the heavily-bioturbated sediments, with an abundance of 3.6 x 10^6 valves/g at the top of the core (Fig. 2C). *Coscinodiscus* spp., *Rhizosolenia* spp. associated with *P. sulcata* define the assemblage at the base of the core EG-03. At the same time, the group of species included in the Warm Species Group (WSG), reaches their higher abundance. *Paralia sulcata* was very abundant in the interval 140-60 cm. The uppermost peak was characterized by a decreasing abundance of *Coscinodiscus* spp. and *P. sulcata* and a relative increase in *Chaetoceros* RS (up to 80% of the assemblage) with *Thalassiosira* spp., *T. nitszchioides* and *Rhizosolenia* spp. (Suppl. E-F; Fig. 3C). Quantitative analyses of these cores are reported in Suppl. E-F.

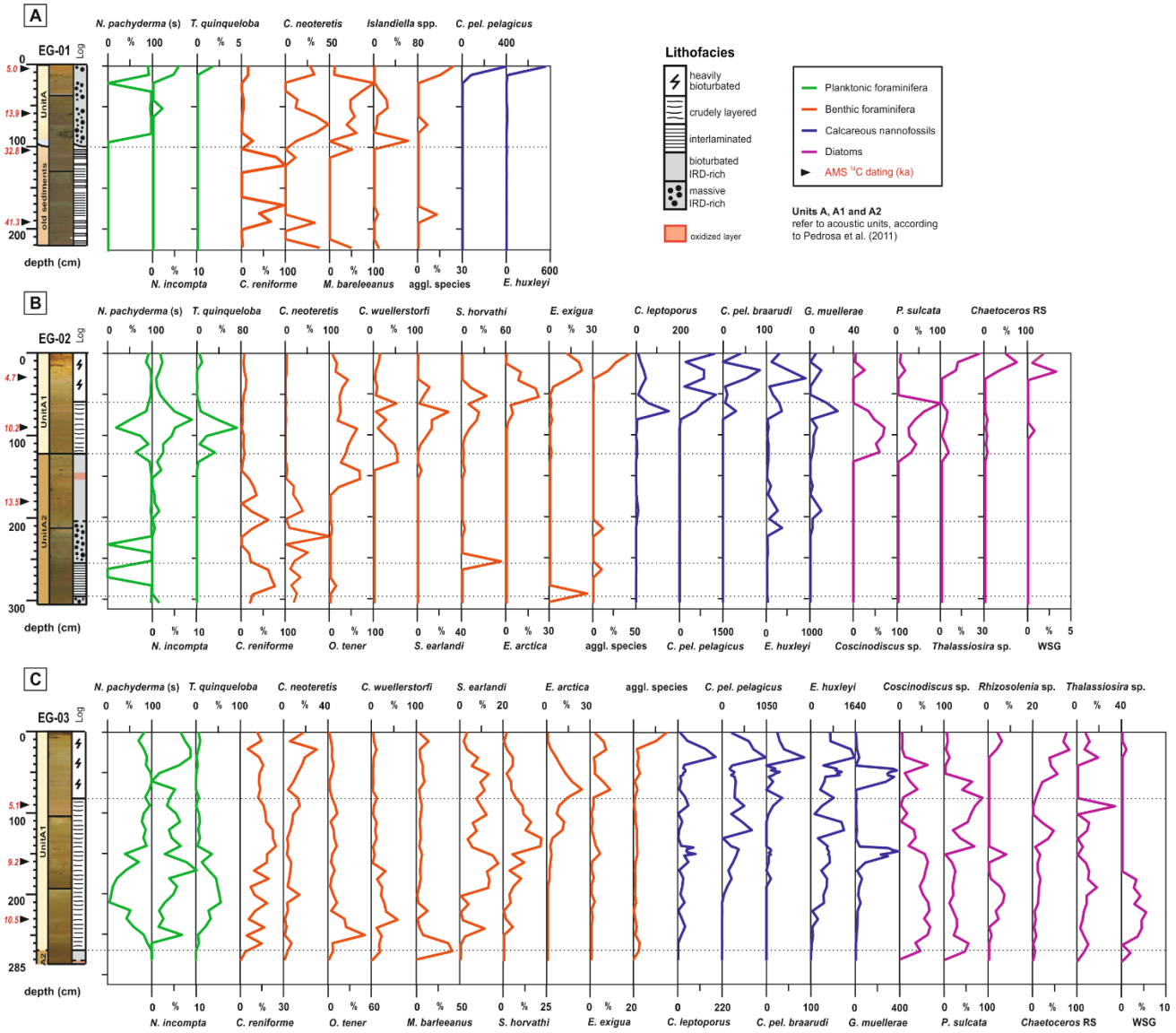

Fig. 3 Microfossil abundances plotted versus depth for core EG-01 (A), EG-02 (B) and EG-03 (C). Calibrated calendar ages are indicated in red. Dotted lines indicate lithofacies boundary. WSG = warm species group.

Discussion

The studied cores contain sedimentary sequences that include Upper Pleistocene and Holocene sediments. According to our age model, microfossil assemblage distributions and lithostratigraphy, the studied records were subdivided into three main intervals: Late Weichselian (44-32k cal a BP), post LGM deglaciation (16.2-11.7k cal a BP) and Holocene Interglacial (11.7k cal a BP-Recent).

Late Weichselian: 44-32k cal a BP

The consolidated diamicton recovered at the base of core EG-01 corresponds to a glacigenic diamicton (*sensu* Dowdeswell *et al*., 2000). In agreement with Laberg and Vorren (1996) and Pedrosa *et al.* (2011) the presence of this type of deposit on the upper slope implies that the ice sheet was grounded at the shelf edge. The sequence, dated 44-32k cal a BP, was deposited during the Middle-Weichselian interglacial MIS 3 from the down-slope transport of glacigenic sediments (Lucchi *et al*., 2013) (Fig. 4). The MIS 3 sequence is characterised by scattered occurrences of microfossils, mainly benthic foraminifera. This paucity may be caused by a variable glacigenic sediment accumulation resulting in a dilution of microfossil abundance and the generally poor preservation of the specimens. A direct comparison of microfossil groups appears to be somewhat difficult and has not yet been attempted during this interval.

The presence of *Cassidulina neoteretis* during this interval, together with *Melonis barleeanus* in the very bottom level could be related to relatively warm bottom water conditions (Chauhan *et al*., 2016) since the former species is an infaunal taxon confined to areas influenced by transformed subsurface Atlantic Water (AW) (Table 2). Badly preserved specimens of *Cassidulina reniforme* show high abundances during this interval. These benthic species presently live in the Arctic-Polar areas under the influence of both Arctic and AW (Ishman and Foley, 1996; Wollenburg and Mackensen, 1998; Scott *et al*., 2008), confirming the interglacial conditions.

Foraminifera species	Ecological chatacters	References
Neogloboquadrina pachyderma (s) (Ehrenberg, 1861)	Polar species related to Arctic and Polar waters, living at or just below the depth of the maximum chlorophyll concentration, which it exploits as a food source zone. It ingests either phytoplankton or detrital chlorophyll.	Hemleben et al., 1989; Kohfeld et al., 1996;
Neogloboquadrina incompta (Cifelli, 1961)	Sub-polar species associated to warm Atlantic water. It occupies the upper 60 m of the water column and its seasonal peak abundance is in late summer.	Hemleben et al., 1989; Schiebel et al., 2001; Schiebel and Hemleben, 2000
Turborotalita quinqueloba (Natland, 1938)	Near surface dweller sub-polar species associated to Arctic waters and Arctic/Polar fronts	Hemleben et al., 1989
Cibicidoides wuellerstorfi (Schwager, 1866)	Epibenthic suspension feeder taxon which requires strong current activity	Lutze and Thiel, 1989; Wollenburg and Mackensen, 1998
Cassidulina neoteretis Seidenkrantz, 1995	Infaunal species confined to areas influenced by cool, slightly transformed subsurface Atlantic Water (AW) with stable salinity	Ishman & Foley, 1996; Jennings et al., 2004; Lagoe, 1979; Lubinski et al., 2001; Osterman et al.,

		1999; Wollenburg et al., 2004
Cassidulina reniforme (Nørvang, 1945)	Arctic-Polar species linked to cold and salty AW, and locally related to distal glaciomarine environments especially if associated to E. excavatum. Occasionally indicates establishment of dysoxic or periodic anoxic conditions at the bottom	Hald and Korsun, 1997; Korsun and Hald, 2000; Polyak et al., 2002; Steinsund, 1994
Cibicides lobatulus (Walker & Jacob, 1798)	Epifaunal species correlated with coarse sediments and high hydrodynamism	Hald and Korsun, 1997; Murray, 2006; Schröder-Adams et al., 1990
Epistominella arctica Green, 1959	Arctic areas with low to no bottom current activity and characterized by seasonally ice-free areas; affinity with both low-productivity evnvironments and phytoplancton blooms	Gooday, 1993; Wollenburg and Mackensen, 1998; Wollenburg and Kuhnt, 2000
Episominella exigua (Brady, 1884)	Opportunistic species able to feeding on fresh phytodetritus	Gooday, 1993; Thomas et al., 1995; Wollenburg and Mackensen, 1998
Ioanella tumidula (Brady, 1884)	Seasonally ice-free areas between 1500-3000 m; opportunistic phytodetritus feeders, unpredictable food productivity	Thomas et al., 1995; Wollenburg and Mackensen, 1998

Islandiella helenae Feyling-Hanssen & Buzas, 1976 /*I. norcrossi* (Cushman, 1933)	"Low arctic conditions" characterised by high seasonal productivity; also in distal glacio-marine sediments	Korsun et al., 1995; Korsun and Hald, 1998; Pogodina, 1999; Stenisund, 1994
Melonis barleeanus (Williamson, 1958)	Arctic–Boreal infaunal species related to Atlantic-derived water with supply of degraded organic matter; high salinities	Caralp, 1989; Jennings et al., 2004; Polyak et al., 2002
Oridorsalis tenerus (Brady, 1884)	Low productivity area in water depth of 2000-3000 m	Osterman et al., 1999; Wollenburg and Mackensen, 1998
Seabrookia earlandi (Wright, 1891)	Rarely recovered, it represents oxic surface sediments and in presence of symbiotic methane-and sulfur-oxidizing bacteria	Wollenburg and Mackensen, 2009
Stetsonia horvathi Green, 1959	Presently restricted to permanently ice-covered areas at water depth >2200 m, or in areas with seasonal sea ice with low or instable phytodetritus accumulation values	Husum et al., 2015; Lagoe, 1977; Wollenburg and Mackensen, 1998

Table 2 Taxonomy and ecology and of the most abundant planktonic and benthic foraminiferal species recorded in the three studied cores.

Calcareous nannofossils are only represented by some reworked taxa from Paleogene and upper Cretaceous. Calcareous nannoplankton thrives in marine water influenced by temperature, nutrients and light. At very high latitudes, these conditions are not always reached as water temperatures are low, light is scarce for part of the year and in particular, the presence of sea-ice may additionally reduce the favourable conditions necessary for growth (Villa *et al*., 2005). These environmental conditions could be responsible for the absence of nannofossil, planktonic foraminiferal and diatom during the Late Weichselian.

In core EG-01 the acoustic Unit A overlies older sediments aged >32.8k cal a BP. According to our age model, the base of Unit A dates ca. 16k cal a BP indicating the presence of a prominent stratigraphic gap (Fig. 4). According to the multibeam bathymetry and the sub-bottom record, core EG-01 was collected from a minor gully in which the older sediments represent a debrites deposited during LGM. The scoured contact boundary with the overlaying sediments of Unit A derives from meltwater erosion and/or non-deposition occurred during the early phase of deglaciation preventing deposition of the sediments associated with the main deglaciation phase (interlaminated facies) (Lucchi *et al*., 2013).

Post LGM deglaciation: 16.2 - 11.7k cal a BP

The post LGM deglaciation phase is represented by Unit A2 in core EG-02 and EG-03, whereas in core EG-01 there is not a clear separation between acoustic Units A2 and A1 (Fig. 3A-C). Core EG-02 recorded an expanded deglacial sequence and does not contain evidence of the erosion tied to the early deglaciation (Lucchi *et al*., 2013), whereas core EG-03 contains only the later stage of deglaciation recorded only in the 10 cm at the bottom of the core.

The deglaciation is characterised in core EG-02 (305-295 cm, Fig. 2B) by coarse-massive IRD-rich sediments and by a peak of magnetic susceptibility that was already recognised in sediment cores collected in the same area (Rasmussen *et al*., 2007; Jessen *et al*., 2010). Lucchi *et al.* (2013) correlated this magnetic peak to the Heinrich Event H1, dated 16.8k cal a BP. Benthic calcareous foraminifera are extremely poor and represented by few individuals of *Cassidulina* spp., whereas the monospecific planktonic foraminifera assemblage is constituted by *Neogloboquadrina pachyderma* (s), indicating polar surface water (Fig. 3B). The interlaminated sediments above the IRD-massive deposits (core EG-02, 15.0-14.6k cal a BP, Fig. 5) were interpreted as plumites derived from the meltwater discharge from the Storfjorden-Kveithola glacial system and represented the polar marine record of Meltwater Pulse 1a (MWP-1a) (Lucchi *et al.* 2015, 2013).

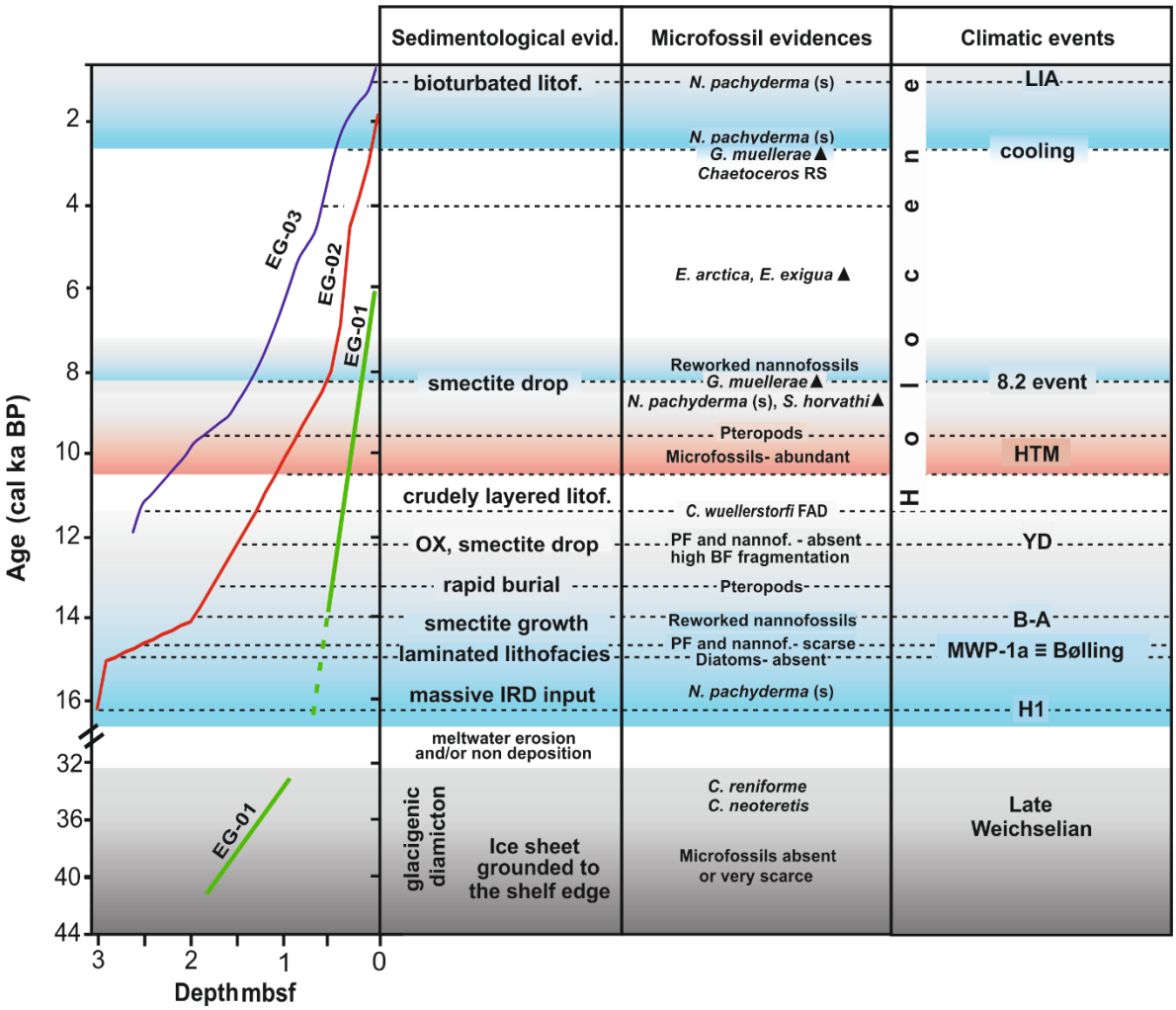

Fig. 4 Age-depth plot for the three investigated cores. The main climatic and palaeoenvironmental events are illustrated, supported by sedimentological and micropalaeontological evidences. At the base, the grey area represents the deglaciation with terrigenous input through meltwaters and IRD, the blue areas represent colder periods and the red area represents warmer period. Horizontal dotted lines limited the recognized events with related ages on the left axis. H1 = Heinrich event, MWP-1A = Meltwater Pulse 1A, B-A = Bølling-Allerød, YD = Younger Dryas, OX = oxidized level, HTM = Holocene Thermal Maximum, LIA = Little Ice Age. BF = benthic foraminifera; PF = planktonic foraminifera. Black triangle indicates increasing occurrence of the relative species.

In this level the very scarce presence, or absence, of planktonic foraminifera and nannoplankton, and the absence of diatoms indicate deteriorated surface water conditions, likely having been affected by a more extensive sea-ice cover in winter and meltwater layer during spring, as also suggested by Rasmussen *et al.* (2007) in the surrounding area. *Jessen et al.* (2010) described a similar interlaminated sequence in the western Svalbard slope, dated

14.7-14.3k cal a BP, corresponding to the early Bølling interstadial, according to Kienast *et al.* (2003). Carbonara *et al.* (2016) identify another similar laminated sequence, dated 14.4-14.2k cal a BP, from neighbouring sediment on the middle slope of the Kveithola Trough Mouth Fan (South of Svalbard).

Even if statistically non-representative, the presence of *Cassidulina reniforme* and *C. neoteretis* during this interval may indicate the influence of cold and salty AW at the bottom of the middle slope (Table 2). The preservation of the foraminiferal tests is very poor (fragmentation up to 60%) suggesting both mechanical damage and water corrosion. Along the Storfjorden continental shelf, the influence of aggressive bottom water was evidenced by the increased occurrence of agglutinated benthic foraminifera by Rasmussen and Thomsen (2015); however these forms are rarely present during this phase (Figs 3A-B and 5) in the studied cores.

The overlaying massive IRD-rich sediments (Fig. 3A-B) (core EG-02: 14.6-14.0k cal a BP; core EG-01: 14.0-5k cal a BP) indicate the progressively stronger influence of AW over the area, shown by the occurrence of rare *Neogloboquadrina incompta* and *Emiliania huxleyi*, among the planktonic taxa (Fig. 5), and *Melonis barleeanus* among the benthonic taxa (core EG-01 only, Fig. 3A). The increasing influence of AW is also indicated by the gradual increase in the percentages of smectite in the clay mineral assemblage (Fig. 2A-B), as suggested by Junttila *et al.* (2010), hence supporting the correlation with the Bølling-Allerød warm phase. The study by Fagel *et al.* (2001) indicates that sources for smectite of basaltic origin can be identified in the Greenland Faroe Ridge including Iceland and Vøring Plateau; AW is then responsible for the enrichment of smectite in the SW Barents Sea sediments (Vogt and Knies, 2009). The presence of reworked Palaeogene and Cretaceous nannofossil taxa, together with Cretaceous calcispheres in the massive IRD-rich sediments (EG-02, 250–210 cm, Fig. 2B), confirms sediment release by the ice front during the final phase of deglaciation.

The abundant occurrence of pteropods (*Limacina helicina*, Fig. S1, photo 31) in the stratigraphic record of core EG-02 at 201 and 181 cm, corresponding to ca. 14.0 and 13.3k cal a BP, confirms the favourable environmental conditions with massive input of sediments that allowed the rapid burial of the pteropod specimens after deposition, resulting in the preservation of the aragonite tests (Fig. 4). The presence of pteropods during the same interval in Arctic sediment cores has also been reported by Ślubowska-Woldengen *et al.* (2007).

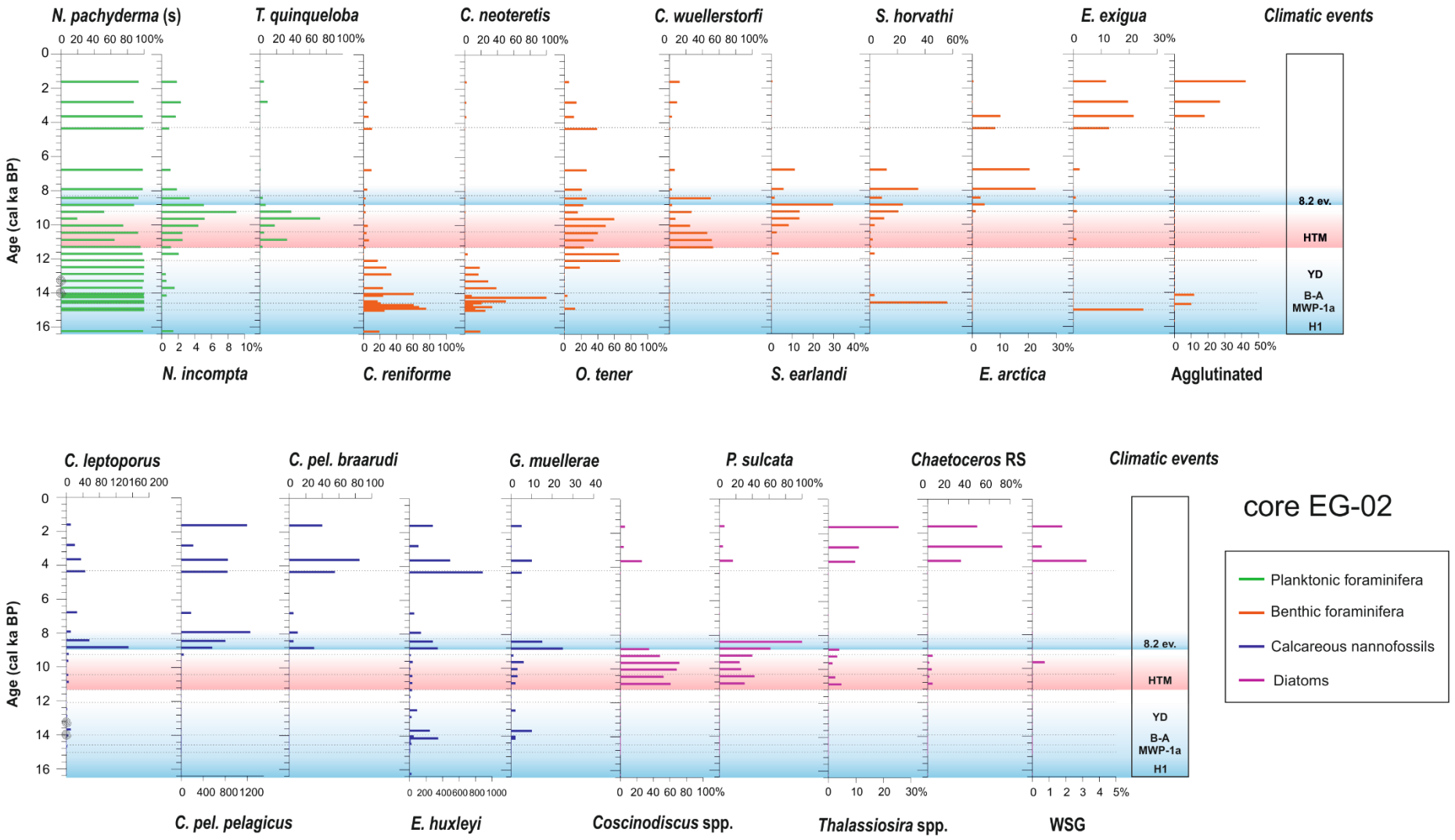

Fig. 5 Down-core micropaleontological composition of core EG-02 plotted versus age. Dotted lines indicate the main events discussed in the text. Blue areas represent colder periods, red areas represent warmer periods. WSG = warm species group. The spiral on the left identifies the pteropods presence. The top level of this core dates 1.6k cal a BP.

In core EG-01 a relative increase of *Islandiella* spp. at about 50 cm (12.3k cal a BP) together with the significant presence of *Melonis barleeanus* (Fig. 3A), suggest the persistence of the AW influence, characterised by high seasonal productivity as indicated by these taxa preferences (Table 2). The still abundant presence of IRD in this interval is related to the proximity of the location of core EG-01 to the shelf break.

The percentage of benthic foraminifer fragmentation increases considerably in the interval between 190-150 cm of core EG-02 (Fig. 2B), reaching a maximum at a depth of 150 cm (12.1k cal a BP) where the oxidized layer (OX-1) was identified (Fig. 2B). This layer has been interpreted by Lucchi *et al.* (2013) as the Younger Dryas cold event (YD) or its termination (Broecker *et al.*, 2010). The scarce presence of benthic foraminifera, together with high percentage of fragmentation suggests the dissolution of calcium carbonate probably related to this cold period. The absence of nannofossils and *N. incompta* in the oxidized layer supports the cold condition of the superficial water column, suggested also by a drop of smectite concentration transported by AW (Junttila *et al.*, 2010).

Holocene Interglacial: 11.7k cal a BP-Recent

The upper acoustic Unit A1 records the onset of the Holocene and appears more expanded and continuous in core EG-03 with respect to the other cores (Fig. 2A-C). The percentage of fragmentation of benthic foraminifera in this unit is definitely lower than those recorded in Unit A2, indicating a reduced influence of the sedimentary glacial processes (Fig. 2A-C).

The boundary between Unit A2 and Unit A1 in cores EG-02 and EG-03 is delineated by the passage to the crudely layered facies suggesting a deposition influenced by strong bottom currents (Lucchi *et al*., 2013). Just above this boundary at about 11.3k cal a BP (EG-02, 131.5 cm and EG-03, 270 cm), the first appearance of the benthic foraminifer *Cibicidoides wuellerstorfi* was noticed (Figs 4-6). *Cibicidoides wuellerstorfi* is an epibenthic suspension-feeder taxon that requires permanent lateral advective currents (Table 2). The sudden occurrence of *C. wuellerstorfi* follows the end of the YD which can be considered nearly synchronous in the Storfjorden area as well as the southwestern margin of Svalbard (Sarnthein *et al.*, 2003). This species is absent in core EG-01, located in a shallower area. This bioevent was recorded by Rasmussen *et al.* (2007) in the north-western part of the Svalbard slope at about 10k ^{14}C cal a BP (AMS dating corrected by reservoir effect only) and it is considered the first warming indication of bottom water after the YD. In addition, the benthic assemblage at the onset of the Holocene includes *Cassidulina reniforme, Oridorsalis tener* and *Melonis*

barleeanus (mainly in core EG-01) (Figs 3A, 5, 6). The significant occurrence of both *C. wuellerstorfi* and *O. tener* is indicative of conditions similar to the modern deep-sea slopes of the Nordic seas (Sejrup *et al.*, 1981; Mackensen *et al.*, 1985); *M. barleeanus* suggests the influence of relatively warm AW with a supply of degraded organic matter (Table 2). It is noteworthy that in the same time interval the presence of *Cassidulina neoteretis* is mostly less than 10% in core EG-03, and it is almost absent in core EG-02, in agreement with observations on the Holocene of the northwestern part of the Svalbard slope (Rasmussen *et al.*, 2007) (Figs 5, 6). *Cassidulina neoteretis* is common in the Arctic Ocean and it indicates subsurface AW masses and not permanently ice-covered conditions (Table 2), however the exact nature of the relationship with this water is still subject to debate (Osterman *et al.*, 1999; Wollenburg *et al.*, 2004). Its reduced presence could suggest a reduced influence of subsurface AW masses during the onset of the Holocene but it could also indicate that the AW was strongly mixed with shelf waters, as suggested by Lubinski *et al.* (2001) in a study carried out in the Kara and Barents Seas. The contemporary presence of the diatom *Paralia sulcata* could support this indication.

Starting from about 11.3k cal a BP, a significant occurrence of diatoms dominated by *Coscinodiscus* spp., together with *P. sulcata*, *Thalassiosira* spp., *Rhizosolenia* spp., WSG species (especially for core EG-03), and subordinate *Chaetoceros* RS is recorded in cores EG-02 and EG-03 (Figs 5, 6). High abundance of *Coscinodiscus* spp. is related to warm AW masses and was suggested as a chronostratigraphic marker for the early Holocene in the western Svalbard slope area (Jessen *et al.*, 2010). Furthermore, the coexistence of this genus together with *Rhizosolenia* spp. (Fig. 6) could also indicate a deepening of the nutricline (Kemp *et al.*, 2000; Kemp and Villareal, 2013). The relatively high abundance of the WSG species recorded in core EG-03 would be in agreement with the entrance of warm AW. *Paralia sulcata* is a bottom species sometimes found in neritic plankton and very common along the south-eastern shores of the North Sea (McQuoid and Nordberg, 2003). On the other hand, the relatively high content of *P. sulcata* has been used as an indicator of high primary productivity as it is a neritic species characteristic of coastal upwelling conditions (Abrantes, 1988). This species is usually associated with Norwegian-Atlantic current with relatively warm-water temperatures in the Nordic Seas (Koç and Schrader, 1990). Nevertheless, and according to Bárcena and Abrantes (1998), the abundant presence of *P. sulcata* should be related with silica preservation more than coastal productivity, since their frustules are highly silicified and would reflect a differential dissolution of less silicified taxa.

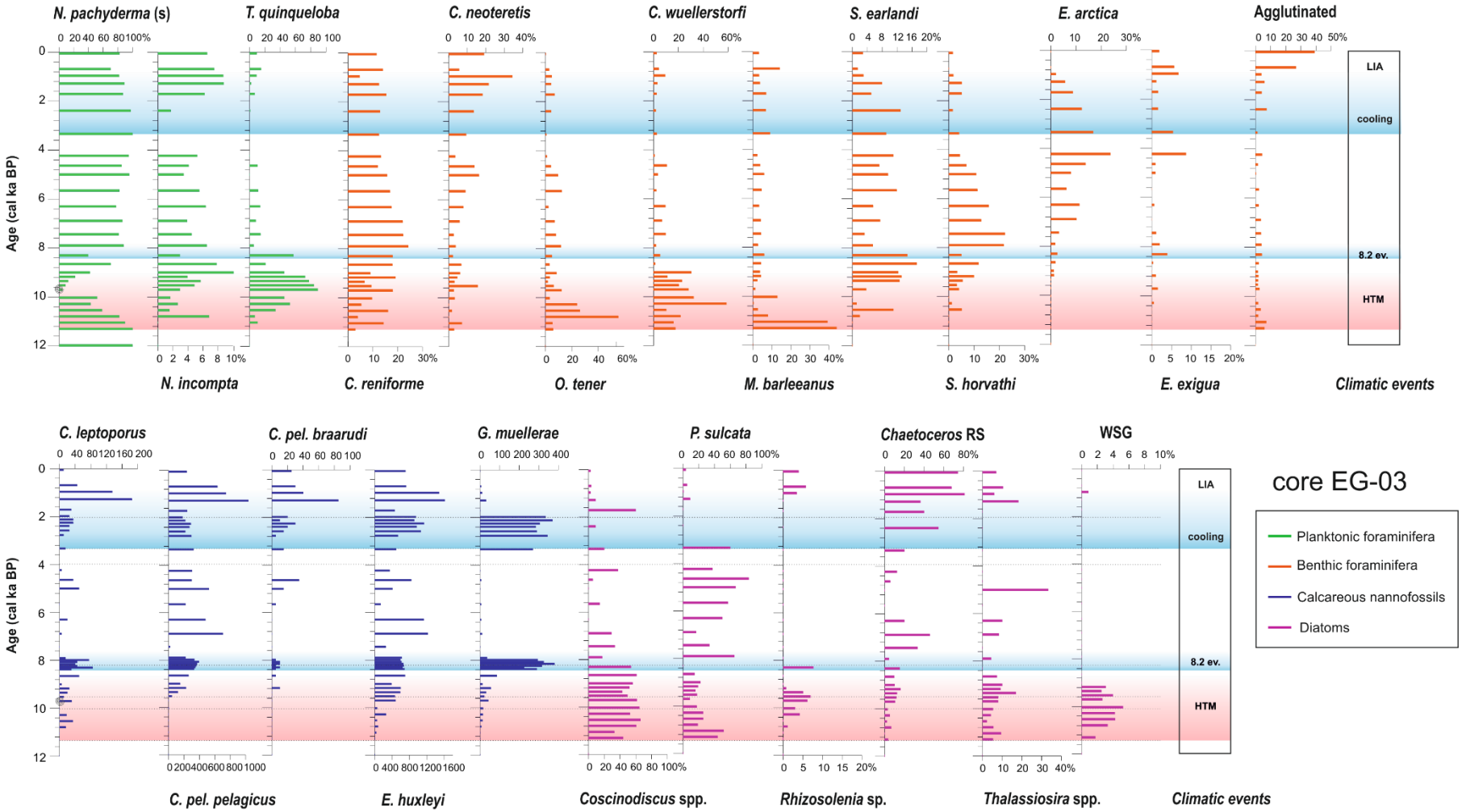

Fig. 6 Down-core micropaleontological composition of EG-03, records plotted versus age. Dotted lines indicate the main events discussed in the text. Blue areas represent colder periods, red areas represent warmer periods. WSG = warm species group. The spiral on the left identifies the pteropod presence

A diatom spike is registered in core EG-02 at ca. 10.4k cal a BP (110 cm, Fig. 2B) and in core EG-03 at ca. 10.0k cal a BP (220 cm, Fig. 2C). Another diatom spike is recorded in core EG-02 at ca. 9.6k cal a BP (90 cm, Fig. 2B) and in core EG-03 at ca. 9.5k cal a BP (200 cm, Fig. 2C). The slightly different ages observed between the two studied cores are probably due to sampling resolution (every 10 cm) rather than to a different age of these bioevents. These events are comparable to those found by Jessen *et al.* (2010) and Carbonara *et al.* (2016) in the western margin of Svalbard and according to Stabell (1986), the diatom high productivity signal can be used as an indicator of the retreat of the polar front at the time of deposition.

The overall increased abundance of diatoms at 10.5-9.2k cal a BP in the studied area corresponds to a period of warmer sea surface temperatures and high primary productivity, also demonstrated by the decrease in cold water species *Neogloboquadrina pachyderma* (s), and a relative increase in the warmer species *N. incompta* and the high productivity species *Turborotalita quinqueloba*. Our data fit well with core GeoB17603-3 results, collected in Kveithola TMF middle slope (Carbonara *et al.*, 2016), recording similar variation in the planktonic assemblage in the same time interval. This period, known as the Holocene Thermal Maximum (HTM, Kaufman *et al.*, 2004; Renssen *et al.*, 2009, 2012) (Fig. 4), has been evidenced in the Nordic Seas in several climate archives in a period comprised between 9-6 cal ka BP (Risebrobakken *et al.*, 2011). The timing of the HTM apparently varied spatially; some records reveal maximum warmth as late as 7.8-6.8k cal a BP southwest of Franz-Josef Land (Duplessy *et al.*, 2001). Sites from the shelf and upper slope of western and northern Svalbard generally show a noticeable, but more limited, influence of AW (Ślubowska *et al.*, 2005; Ślubowska-Woldengen *et al.*, 2007), probably due to the influence of colder and less saline surface waters, originating from the remaining ice caps over Svalbard. The elevated microfossil abundance in early Holocene Arctic Ocean sediments suggests an extraordinarily vigorous water inflow from the South during the HTM, probably both through the Fram Strait and across the Barents Sea (Spielhagen *et al.*, 2011). The HTM mainly reflects the orbital control of the insolation maximum in the early Holocene (Risebrobakken *et al.*, 2011 and references herein) which caused melting water from ice-sheets or inland glaciers. Consequently, the increased input of fresh and turbid waters in the ocean determined the deepening of the nutricline favouring the increase of the *shade flora* mainly represented by *Coscinodiscus* spp. associated with *P. sulcata*.

Abundant pteropod tests of *Limacina helicina* were observed at 9.7k cal a BP (EG-03, 210

cm, Fig. 2C) corresponding to diatom concentration increase. We argue that the preservation of the aragonite test in the sediments may be related to the rapid burial of the pteropod tests by diatom mats.

As for the nannofossils, species diversity at the beginning of the Holocene is low; in particular, diversity is hampered in the Arctic environment by the generally cold-water conditions that are not favourable to the nannoplankton flourishing, therefore, the assemblage is dominated in this period by cold-water adapted taxa such as *Coccolithus pelagicus* s.l. and *Gephyrocapsa muellerae*. *Coccolithus pelagicus* s.l. is generally considered a cold-water indicator in open ocean conditions (McIntyre and Bé, 1967; Roth and Coulbourn, 1982; Samtleben and Bickert, 1990; Samtleben *et al.*, 1995) and *G. muellerae* is associated with cold water (Samtleben and Bickert, 1990; Samtleben *et al.*, 1995; Wells and Okada, 1997). During the HTM, the nannofossil assemblage registers a weak increase of *C. leptoporus*, *G. muellerae* and *Emiliania huxleyi*. *Calcidiscus leptoporus* is reported as having different lower temperature limits (min. 2-11 °C) (McIntyre and Bé, 1967; Samtleben *et al.*, 1995), while *E. huxleyi* is a euryhaline and eurythermal coccolith species (McIntyre and Bé, 1967; Roth and Coulbourn, 1982), with no distinct seasonal abundance changes (Ziveri *et al.*, 1995).

Overall, the comparison among the microfossils both planktonic and benthic indicates a common warming of the water column during the early Holocene, identifying the HTM event at the interval 10.5-9.2k cal a BP (Figs 5, 6).

A decreasing abundance in *C. wuellerstorfi* is recorded in EG-02 and EG-03, from about 10 cal ka BP up to 7.9-7.4k cal a BP (Figs 5, 6) suggesting a weakening in the lateral currents. A similar decreasing trend of *C. wuellerstorfi* was recorded in a core located at 76° N along the SW Svalbard margin by Rasmussen *et al.* (2007).

Starting from about 9.6k cal a BP up to about 8.0k cal a BP, a consistent increase in *Stetsonia horvathi*, *C. reniforme* and *Seabrookia earlandi* has been noted (Figs 5, 6). *Stetsonia horvathi* is a small polar species (<70 µm) which is adapted to live both under permanent or seasonal sea ice, associated with low and unstable organic flux to the seafloor (Table 2) at a water depth >2200 m in the Arctic Ocean. It has been used as a proxy for glacial conditions during the Pleistocene (Polyak *et al.*, 2013; Lazar and Polyak, 2016). The simultaneous presence of planktonic foraminifera and calcareous nannoplankton excludes the possibility of permanent sea ice conditions for this area. The increase in *C. reniforme* suggests a renewal of the cold and salty AW, but might also indicate the establishment of dysoxic or periodic anoxic conditions at the bottom (Hansen and Knudsen, 1995; Hald and Korsun, 1997; Korsun and

Hald, 1998, 2000; Wollenburg *et al.*, 2001; Husum and Hald, 2004). *Seabrookia earlandi* (Fig. S1, photos 18, 19), a small species rarely recorded in the Arctic Sea, is reported by Wollenburg and Mackensen (2009) as living in the hummocky peripheral part of the Håkon Mosby mud volcano located at a water depth of 1265 m on the SW Barents Sea slope, under conditions of anoxic surface sediments and in the presence of symbiotic methane and sulphur oxidizing bacteria. The increase in these species could indicate a period of oligotrophic conditions at the sea bottom that was associated here with the 8.2k cal a BP cold event.

The increase in the cold nannofossil species *G. muellerae,* at about 8.8-8.0k cal a BP (Figs 5, 6), suggests cooling conditions in the surface waters as well. The species *G. muellerae* is presently related to subarctic cold water (Bollmann, 1997; Henderiks and Bollmann, 2004), although the milder ecological preference of *G. muellerae* has been reported (e.g. Flores *et al.*, 1997; Dylmer *et al.*, 2013). This interval is also characterised by a significant peak of reworked nannofossils, a decrease in diatom concentration (Fig. 2B,C), a neat increase of *N. pachyderma* (s), and a decrease in warmer planktonic species (*T. quinqueloba* and subordinately *N. incompta*) (Figs 5, 6). In addition, the sharp decrease in smectite content in these levels could also suggest the reduced influence of AW (Fig. 2B, C). All this evidences lead us to associate this interval to the cold event which occurred in the Northern Hemisphere at about 8.2k cal a BP (Rohling and Pälike, 2005; Ellison, 2006). This interpretation is also supported by the magnetic susceptibility curve of both cores EG-02 and EG-03, showing a characteristic peak during the Holocene at 55 cm and 147 cm respectively (Fig. 2 B, C), dated 8.2k cal a BP in the Western Svalbard slope (Jessen *et al.*, 2010).

From 8.2k cal a BP up to about 4.0k cal a BP, a decrease in *S. horvathi* and *C. reniforme* is recorded in core EG-03 together with a relative increase in the benthic foraminifera *Epistominella arctica, C. neoteretis* and *E. exigua* (Figs 5, 6). *Epistominella arctica* occurs in seasonally ice-free Arctic areas with low to no bottom current activity and together with *E. exigua* may also feed on phytodetritus (Wollenburg and Mackensen, 1998; Cornelius and Gooday, 2004). *Epistominella arctica* is considered to have a transitional ecological strategy from permanent to seasonal sea ice conditions (Wollenburg and Kuhnt, 2000). Its increasing abundance in the studied cores seems to indicate a reduction of the oligotrophic conditions previously suggested by *S. horvathi,* possibly related to the variation of the year-round ice cover of the upper water column. Furthermore, the increasing occurrence of *C. neoteretis* and the relative decrease in *C. reniforme* suggest the increasing influence of the warmer subsurface bottom water. The decrease in *G. mullerae* together with a weak drop in *C. pelagicus* s.l. and a rise in *P. sulcata* suggest warmer conditions for the upper water column as well. This is in

agreement with Sarnthein *et al.* (2003) who found evidence of extended phases of general slight warming during the cool Late Holocene and in particular, from 6.5 to 4.2k cal a BP, studying in detail a sedimentary sequence located in the nearby area at 75°N.

The upper sequence of EG-03, from about 3.2k cal a BP (the last 60 cm), is characterised by a further increase in *C. neoteretis* and by a decrease in *E. arctica* (Fig. 6). At the same time, in core EG-02 *E. exigua* increases in agreement with an increase in diatom concentration described below (Fig. 5), indicating a strong seasonal pulse of fresh phytodetritus for this period (Table 2). In this interval, the high abundance of agglutinated foraminifera occurs (mainly *Recurvoides turbinatus, Hormosinella guttifera* and *Reophax* spp.) (Fig. S1, photos 21-28), their abundance (recorded only in the more recent sediments) could indicate a weak diagenetic process that generally tends to disintegrate the tests towards the bottom of the core.

From 3.2k cal a BP to 2k cal a BP *G. muellerae* shows a general increase, suggesting a new cooling trend in the studied area (Fig. 4, 6). This period should correspond to the so-called Cool Late Holocene (Andersen *et al.*, 2004), known also as the Neoglacial cold event. Further evidence, however, is needed to support this interpretation.

In the uppermost 20 cm of cores EG-02 and EG-03 there is a sharp increase in diatoms, having the highest concentration recorded within each core here (Figs 2B, C). Even though there is a significant difference in the age of the diatom peaks, the association is characterised mainly by *Chaetoceros* RS and, subordinately by *T. nitszchioides*, *Thalassiosira* spp. and *Rhizosolenia* spp. (Figs 5, 6; Table S5). *Chaetoceros* is one of the most abundant diatom genera in modern oceans; it is present in most environments from coastal temperate to polar regions. *Chaetoceros* RS have been traditionally interpreted as indicative of very high primary productivity (Koç and Schrader, 1990; Williams, 1986; De Sève, 1999). Phytoplankton blooms large enough to deplete nutrients are rare in polar areas and depend on the increased stratification of the upper water column and the presence of a shallow mixed layer (Leventer *et al.*, 1996). In polar regions, the abundance of over 20% *Chaetoceros* RS could be related to sea ice duration greater than 3 months per year, with an optimum coverage of 3-9 months per year (Armand *et al.*, 2005). In this sense, Leventer *et al.* (1996) suggested that this high abundance could be related with surface water stratification produced by sea ice melt water, in agreement with the presence of *Rhizosolenia* spp., which has been considered a shadow species adapted to live in the lower photic zones under conditions of stratification (Kemp *et al.*, 2000). Moreover, *Thalassionema* spp. (not shown) has been reported as a cosmopolitan species, Bárcena and Abrantes (1998) considered that the species could be associated with the

occasional upwelling and/or fresh water discharge; this assumption could be in agreement with seasonal sea-ice melting. The very last sample in core EG-02 dates at 1.6k cal a BP.

The last sample of core EG-03 dates at 0.05k cal a BP. The youngest cold event recorded dates at 0.6k cal a BP (10 cm) and it is characterized by a decrease in the nannofossil total abundance together with a decrease in the warm taxa as *N. incompta* and *Coscinodiscus* spp. (Fig. 6). This short cold spell is interpreted as the expression of the Little Ice Age (LIA) (Fig. 4), recorded in the Arctic sediments, southwest Svalbard.

Conclusions

The integrated micropalaeontological (planktonic and benthic foraminifera, calcareous nannoplankton and diatoms) and sedimentological investigations (sediment facies, magnetic susceptibility and clay minerals) of three sediment cores (EG-01, EG-02 and EG-03) recovered on the middle/upper slope of the Storfjorden TMF, add new data to the Late Quaternary reconstruction of the palaeoenvironmental and palaeoceanographic conditions of this region.

Three intervals of significant palaeoenvironmental/climate change were identified: Late Weichselian (44-32 cal ka BP), the post LGM deglaciation (16.2-11.7 cal ka BP) and the Holocene Interglacial (11.7 cal ka BP-Recent).

The Interglacial MIS 3 is characterised by several stratigraphic discontinuities indicating sediment erosion and/or non-deposition related to the high-energy meltwater release and/or re-depositional processes occurring in a minor gully of the Storfjorden Trough Mouth Fan.

The post LGM conditions are dominated by a massive input of terrigenous sediments (plumites of the MWP-1A) that largely diluted the biogenic fraction in the sedimentary record, determining environmental conditions hostile to the bio-productivity and test preservation. Climatic amelioration during the Bølling-Allerød warm interstadials are depicted by the progressive increase of the smectite content in the clay mineral assemblage confirming increasing influence of the Atlantic Water inflow.

The early Holocene is characterized by a sharp reprise of the productivity, with a prominent flowering of diatoms signing the Holocene Thermal Maximum (HTM) at 10.4-9.5 cal ka BP. The occurrence of small benthic foraminifera species such as *Stetsonia horvathi* and *Seabrookia earlandi*, suggests progressive oligotrophic bottom conditions after the HTM, whereas cooling condition of surface waters during 8.3-8.2 cal ka BP and at 2.4 cal ka BP are indicated by the increased presence of the cold nannofossil species *Gephyrocapsa muellerae* and the planktonic

foraminifer *Neogloboquadrina pachyderma* (s). High primary productivity is again recorded by the sharp increase of *Chaetoceros* RS during the late Holocene at about 2.4-1.0k cal a BP suggesting a seasonal sea-ice melting. Cooling conditions of the surface water masses at about 0.6k cal a BP are identified by a decrease in the nannofossil total abundance together with a decrease in the warm-water taxa as *Neogloboquadrina incompta* and *Coscinodiscus* spp. According to the age model, this cold spell corresponds to the Little Ice Age.

Acknowledgments

This study was supported by the Italian projects OGS-EGLACOM and PNRA-MELTSTORM, the Spanish SVAIS (POL2006-07390), NICESTREAMS, and DEGLABAR (CTM2010-17386) projects, the Danish GEUS project "Foraminifera in Artic Ocean", and "CORIBAR-DK", CARLSBERG project, n. 2012_01_0315. Special thanks are addressed to A. Camerlenghi for his continuous scientific support and encouragement. Many thanks to Karolyn Close for the linguistic revision.

References

Abrantes F. 1988. Diatom assemblages as upwelling indicators in surface sediments off Portugal. *Marine Geology* **85**: 15-39.

Andersen C, Koç N, Jennings A *et al.* 2004. Nonuniform response of the major surface currents in the Nordic Seas to insolation forcing: Implications for the Holocene climate variability. *Paleoceanography* **19**: 1–16. doi:10.1029/2002PA000873

Armand LK, Crosta X, Romero O *et al.* 2005. The biogeography of major diatom taxa in Southern Ocean sediments: 1. Sea ice related species. *Palaeogeography. Palaeoclimatology. Palaeoecology* **223**: 93-126. doi:10.1016/j.palaeo.2005.02.015

Bárcena MA, Abrantes F. 1998. Evidence of a high-productivity area off the coast of Malaga from studies of diatoms in surface sediments. *Marine Micropaleontology* **35**: 91-103. doi:10.1016/S0377-8398(98)00012-7

Baumann K-H, Matthiessen J. 1992. Variations in surface water mass conditions in the Norwegian Sea: Evidence from Holocene coccolith and dinoflagellate cyst assemblages. *Marine Micropaleontology* **20 (2)**: 129-146.

Bollmann J. 1997. Morphology and biogeography of Gephirocapsa coccoliths in Holocene sediments. *Science* **29**: 319-350. doi:10.1016/S0377-8398(96)00028-X

Broecker WS, Denton GH, Edwards RL *et al.* 2010. Putting the Younger Dryas cold event into context. *Quaternary Science Review* **29**: 1078-1081. doi:10.1016/j.quascirev.2010.02.019

Caralp M. 1989. Abundance of *Bulimina exilis* and *Melonis barleeanum*: relationship to the quality of marine organic matter. *Geo-Marine Letters* **9**: 7–43.

Carbonara K, Mezgec K, Varagona G *et al.* 2016. Palaeoclimatic changes in Kveithola, Svalbard, during the Late Pleistocene deglaciation and Holocene: Evidences from microfossil and sedimentary records. *Palaeogeography Palaeoclimatology Palaeoecology* **463**: 136-149. doi.org/10.1016/j.palaeo.2016.10.003

Chauhan T, Rasmussen TL, Noormets R. 2016. Palaeoceanography of the Barents Sea continental margin, north of Nordaustlandet, Svalbard, during the last 74 ka. *Boreas* **45**: 76–99. doi:10.1111/bor.12135. ISSN 0300-9483

Cornelius N, Gooday AJ. 2004. "Live" (stained) deep-sea benthic foraminiferans in the western Weddell Sea: Trends in abundance, diversity and taxonomic composition along a depth transect. *Deep-Sea Research Part II* **51**: 1571-1602. doi:10.1016/j.dsr2.2004.06.024

Darling KF, Kucera M, Kroon D *et al.* 2006. A resolution for the coiling direction paradox in *Neogloboquadrina pachyderma*. *Paleoceanography* **21**: PA2011. doi:10.1029/2005PA001189

de Kaenel EP, Villa G. 1996. Oligocene-Miocene calcareous nannofossil biostratigraphy and paleoecology from the Iberia Abyssal Plain. In *Proceedings of the Ocean Drilling Program, Scientific Results, College Station, TX (Ocean Drilling Program)*, Whitmarsh RB, Sawyer DS, Klaus A, Masson DG (eds) **149**: 79-145, doi:10.2973/odp.proc.sr.149.208.1996

De Sève MA. 1999. Transfer function between surface sediment diatom assemblages and sea-surface temperature and salinity of the Labrador Sea. *Marine Micropaleontology* **36**: 249-267. doi:10.1016/S0377-8398(99)00005-5

Dowdeswell JA, Whittington RJ, Jennings AE *et al.* 2000. An origin for laminated glacimarine sediments through sea-ice build-up and suppressed iceberg rafting. *Sedimentology* **47**: 557-576. doi:10.1046/j.1365-3091.2000.00306.x

Duplessy JC, Ivanova E, Murdmaa I *et al.* 2001. Holocene paleoceanography of the northern Barents Sea and variations of the northward heat transport by the Atlantic Ocean. *Boreas* **30**: 1-16. doi:10.1111/j.1502-3885.2001.tb00984.x

Dylmer CV, Giraudeau J, Eynaud F *et al*. 2013. Northward advection of Atlantic water in the eastern Nordic Seas over the last 3000 yr. *Climate of the Past* **9**: 1505–1518. doi:10.5194/cp-9-15052013

Ellison CRW. 2006. Surface and Deep Ocean Interactions During the Cold Climate Event 8200 Years Ago. *Science* **312**: 1929–1932. doi:10.1126/science.1127213

Fagel N, Robert C, Preda M *et al.* 2001. Smectite composition as a tracer of deep circulation: The case of the Northern North Atlantic. *Marine Geology* **172**: 309–330. doi:10.1016/S0025-3227(00)00123-7

Feyling-Hanssen RW, Jørgensen JA, Knudsen KL *et al.* 1971: Late quaternary foraminifera from Vendsyssel, Denmark and Sandnes, Norway. *Bulletin of the Geological Society of Denmark* **21**: 67–317.

Flores JA, Sierro FJ, Francés G *et al.* 1997. The last 100,000 years in the western Mediterranean: sea surface water and frontal dynamics as reveales by coccolithophores. *Marine Micropaleontology* **29**: 351–366.

Gard G, Backman J. 1990. Synthesis of Arctic and Sub-Arctic Coccolith Biochronology and History of North Atlantic Drift Water Influx during the Last 500.000 Years. In *Geological History of the Polar Oceans: Arctic versus Antarctic*, Bleil U, Thiede J (eds). NATO ASI Series **308**: 417-436.

Giraudeau J, Jennings AE, Andrews JT. 2004. Timing and mechanisms of surface and intermediate water circulation changes in the Nordic Seas over the last 10,000 years: a view from the north Iceland shelf. *Quaternary Science Reviews* **23**: 2127–2139.

Gooday AJ. 1993. Deep-sea benthic foraminiferal species which exploit phytodetritus: Characteristic features and controls on distribution. *Marine Micropaleontology* **22**: 187–205.

Groot DE, Aagaard-Sørensen S, Husum K. 2014. Reconstruction of Atlantic water variability during the Holocene in the western Barents Sea. *Climate of the Past* **10:** 51–62. doi:10.5194/cp-10-51-2014.

Hald M, Korsun, S. 1997. Distribution of modern benthic foraminifera from fjords of Svalbard, European Arctic. *Journal of Foraminiferal Research* **27**: 101–122. doi:10.2113/gsjfr.27.2.101

Hansen A, Knudsen KL. 1995. Recent foraminiferal distribution in Freemansundet and Early Holocene stratigraphy on Edgeøya, Svalbard. *Polar Research* **14**: 215–238. doi:10.1111/j.1751-8369.1995.tb00690.x

Hemleben Ch, Spindler M, Anderson OR. 1989. *Modern Planktonic Foraminifera*. Springer Verlag: Berlin.

Henderiks J, Bollmann J. 2004. The Gephyrocapsa sea surface palaeothermometer put to the test: Comparison with alkenone and foraminifera proxies off NW Africa. *Marine Micropaleontology* **50**: 161–184. doi:10.1016/S0377-8398(03)00070-7

Hjelstuen BO, Elverhøi A, Faleide JI. 1996. Cenozoic erosion and sedimentary yield in the drainage area of the Storfjorden Fan. *Global and Planetary Change* **12**: 95-116.

Husum K, Hald M. 2004. A continuous marine record 8000–1600 cal. yr BP from the Malangenfjord, north Norway: foraminiferal and isotopic evidence. *The Holocene* **14**: 877–887. doi:10.1191/0959683604hl752rp

Husum K, Hald M, Stein R *et al.* 2015. Recent benthic foraminifera in the Arctic Ocean and Kara Sea continental margin. *Arktos* **1**: 5. doi:10.1007/s41063-015-0005-9

Ishman SE, Foley KM, 1996. Modern benthic foraminifer distribution in the Amerasian Basin, Arctic Ocean. *Micropaleontology* **42**: 206–220.

Jennings AE, Weiner NJ, Helgadottir *et al.* 2004. Modern Foraminiferal faunas of the southwestern to northern Iceland shelf: oceanographic and environmental controls. *Journal of Foraminiferal Research* **34**: 180–207.

Jessen SP, Rasmussen TL, Nielsen T *et al.* 2010. A new Late Weichselian and Holocene marine chronology for the western Svalbard slope 30,000-0 cal years BP. *Quaternary Science Review* **29**: 1301–1312. doi:10.1016/j.quascirev.2010.02.020

Junttila J, Aagaard-Sørensen S, Husum K *et al.* 2010. Late Glacial-Holocene clay minerals elucidating glacial history in the SW Barents Sea. *Marine Geology* **276**: 71–85. doi:10.1016/j.margeo.2010.07.009

Kaufman DS, Ager TA, Anderson NJ *et al.* 2004. Holocene thermal maximum in the western Arctic (0-180°W). *Quaternary Science Review* **23**: 529–560. doi:10.1016/j.quascirev.2003.09.007

Kemp AES, Pike J, Pearce RB, Lange CB. 2000. The "Fall dump" - A new perspective on the role of a "shade flora" in the annual cycle of diatom production and export flux. *Deep Sea Research Part II* **47**: 2129–2154. doi:10.1016/S0967-0645(00)00019-9

Kemp AES, Villareal TA. 2013. High diatom production and export in stratified waters - A potential negative feedback to global warming. *Progress in Oceanography* **119**: 4–23. doi:10.1016/j.pocean.2013.06.004

Kienast M, Hanebuth TJJ, Pelejero C *et al.*, 2003. Synchroneity of meltwater pulse 1a and the Bølling warming: New evidence from the South China Sea. *Geology* **31**: 67–70. doi:10.1130/0091-7613(2003)031<0067:SOMPAT>2.0.CO;2

Klitgaard Kristensen DK, Rasmussen TL, Koç N. 2013. Palaeoceanographic changes in the northern Barents Sea during the last 16 000 years – new constraints on the last deglaciation of the Svalbard–Barents Sea Ice Sheet. Boreas **42**: 798–813. doi:10.1111/j.1502-3885.2012.00307.x.

Knies J, Matthiesson J, Vogt C *et al.* 2009. The Pliocene glaciation of the Barents Sea-Svalbard region: a new model based on revised chronostratigraphy. *Quaternary Science Review* **28**:812–829.

Koç N, Schrader H. 1990. Surface Sediment Diatom Distribution and Holocene Paleotemperature Variations in the Greenland, Iceland and Norwegian Sea. *Paleoceanography* **5**: 557–580. doi:10.1029/PA005i004p00557

Kohfeld KE, Fairbanks RG, Smith SL *et al.* 1996. *Neogloboquadrina pachyderma* (sinistral coiling) as paleoceanographic tracers in polar oceans: Evidence from Northeast Water Polynya plankton tows, sediment traps, and surface sediments. *Paleoceanography* **11(6)**: 679-699.

Korsun S, Hald M. 2000. Seasonal dynamics of benthic foraminifera in a glacially fed fjord of Svalbard, European Arctic. *Journal of Foraminiferal Research* **30**: 251–271. doi:10.2113/0300251

Korsun S, Hald M. 1998. Modern benthic foraminifera off Novaya Zemlya tidewater glaciers, Russian Arctic. *Arctic and Alpine Research* **30(1)**: 61–77. doi:10.2307/1551746

Korsun SA, Pogodina IA, Forman SL *et al*. 1995. Recent foraminifera in glaciomarine sediments from three arctic fjords of Novaja Zemlja and Svalbard. *Polar Research* **14(1)**: 15-31.

Laberg JS, Vorren TO. 1996. The glacier-fed fan at the mouth of Storfjorden trough, western Barents Sea: a comparative study. *Geologische Rundschau* **85(2)**: 338–349. doi:10.1007/BF02422239

Lagoe MB. 1977. Recent benthic foraminifera from the Central Arctic Ocean. *Journal of Foraminiferal Research* **7(2)**: 106-129.

Lagoe MB. 1979. Recent Benthonic Foraminiferal Biofacies in the Arctic Ocean. *Micropaleontology* **25 (2)**, 214-224.

Lazar KB, Polyak L. 2016. Pleistocene benthic foraminifers in the Arctic Ocean: Implications for sea-ice and circulation history. *Marine Micropaleontology* **126**: 19–30. doi:10.1016/j.marmicro.2016.04.004

Leventer A, Domack EW, Ishman SE *et al.* 1996. Productivity cycles of 200-300 years in the Antarctic Peninsula region: Understanding linkages among the sun, atmosphere, oceans, sea ice, and biota. *Bulletin of the Geological Society of America* **108**: 1626–1644. doi:10.1130/0016-7606(1996)108<1626:PCOYIT>2.3.CO;2

Loeblich Jr AR, Tappan H. 1987. *Foraminiferal Genera and their Classification*. Van Reinhold Company: New York.

Lubinski DJ, Polyak L, Forman SL. 2001. Freshwater and Atlantic Water inflows to the deep northern Barents and Kara seas since ca 13 14C ka: foraminifera and stable isotopes. *Quaternary Science Review* **20**: 1851–1879. doi:10.1016/S0277-3791(01)00016-6

Lucchi RG, Camerlenghi A, Rebesco M *et al.* 2013. Postglacial sedimentary processes on the Storfjorden and Kveithola trough mouth fans: Significance of extreme glacimarine sedimentation. *Global and Planetary Change* **111**: 309–326. doi:10.1016/j.gloplacha.2013.10.008

Lucchi RG, Sagnotti L, Camerlenghi A *et al.* 2015. Marine sedimentary record of Meltwater Pulse 1a along the NW Barents Sea continental margin. *Arktos* **1**: 7. doi:10.1007/s41063-015-0008-6

Lutze GF, Thiel H. 1989. Epibenthic foraminifera from elevated microhabitats: *Cibicidoides wuellerstorfi* and *Planulina ariminensis*. *Journal of Foraminiferal Research* **19**:153–158.

Mackensen A, Sejrup HP, Jansen E. 1985. The distribution of living benthic foraminifera on the continental slope and rise off southwest Norway. *Marine Micropaleontology* **9**: 275–306. doi:10.1016/0377-8398(85)90001-5

Mangerud J, Gulliksen S. 1975. Apparent radiocarbon ages of recent marine shells from Norway, Spitbergen, and Arctic Canada. *Quaternary Research* **5**: 263–273.

McIntyre A, Bé AWH. 1967. Modern coccolithophoridae of the atlantic ocean - I. Placoliths and cyrtoliths. *Deep Sea Research Oceanography Abstract* **14**: 561–597. doi:10.1016/0011-7471(67)90065-4

McQuoid MR, Nordbergb K. 2003. The diatom *Paralia sulcata* as an environmental indicator species in coastal sediments. *Estuarine, Coastal and Shelf Science* **56 (2)**: 339–354. doi:10.1016/S0272-7714(02)00187-7

Murray J. 2006. *Ecology and Applications of Benthic Foraminifera*. Cambridge University Press: Cambridge, New York, Melbourne.

Osterman LE, Poore RZ, Foley KM. 1999. Distribution of benthic foraminifers (> 125 μm) in the surface sediments of the Arctic Ocean. *United States Geological Survey Bulletin* **2164**, 28 pp.

Pedrosa MT, Camerlenghi A, De Mol B *et al.* 2011. Seabed morphology and shallow sedimentary structure of the Storfjorden and Kveithola trough-mouth fans (North West Barents Sea). *Marine Geology* **286**: 65–81. doi:10.1016/j.margeo.2011.05.009

Pogodina IA. 1999. Distribution of benthonic and planktonic foraminifera in deposits of the Storfjord trough, in the western Barents Sea. *Polish Polar Studies*, XXVI Polar Symposium, Lublin, June 1999, 203-214.

Polyak L, Best KM, Crawford KA *et al.* 2013. Quaternary history of sea ice in the western Arctic Ocean based on foraminifera. *Quaternary Science Review* **79**: 145–156. doi:10.1016/j.quascirev.2012.12.018

Polyak L, Korsun S, Febo LA *et al.* 2002: Benthic foraminiferal assemblages from the southern Kara Sea, a river-influenced Arctic marine environment. *Journal of Foraminiferal Research* **32**: 252–273.

Rae JWB, Sarnthein M, Foster GL *et al.* 2014. Deep water formation in the North Pacific and deglacial CO_2 rise. *Paleoceanography* **29**:645–667.

Rahmstorf S. 2002. Ocean circulation and climate during the past 120,000 years. *Nature* **419**: 207–214.

Rasmussen TL, Thomsen E. 2015. Palaeoceanographic development in Storfjorden, Svalbard, during the deglaciation and Holocene: Evidence from benthic foraminiferal records. *Boreas* **44**: 24–44. doi:10.1111/bor.12098

Rasmussen TL, Thomsen E, Ślubowska MA *et al.* 2007. Paleoceanographic evolution of the SW Svalbard margin (76°N) since 20,000 ^{14}C yr BP. *Quaternary Research* **67**: 100–114. doi:10.1016/j.yqres.2006.07.002

Rasmussen TL, Thomsen E, Skirbekk K *et al.* 2014. Spatial and temporal distribution of Holocene temperature maxima in the northern Nordic seas: interplay of Atlantic-, Arctic- and polar water masses. *Quaternary Science Reviews* **92**: 280-291. doi: 10.1016/j.quascirev.2013.10.034

Reimer P J, Baillie MGL, Bard E. *et al.* 2009. IntCal09 and Marine09 radiocarbon age calibration curves, 0–50,000 years cal BP. *Radiocarbon* **51**: 1111–1150. doi:10.2458/azu_js_rc.51.3569

Renssen H, Seppä H, Crosta X *et al.* 2012. Global characterization of the Holocene Thermal Maximum. *Quaternary Science Review* **48**: 7–19. doi:10.1016/j.quascirev.2012.05.022

Renssen H, Seppä H, Heiri O *et al.* 2009. The spatial and temporal complexity of the Holocene thermal maximum. *Nature Geoscience* **2**: 411–414. doi:10.1038/ngeo513

Risebrobakken B, Dokken T, Smedsrud LH *et al.* 2011. Early Holocene temperature variability in the Nordic Seas: The role of oceanic heat advection versus changes in orbital forcing. *Paleoceanography* **26**: PA4206. doi:10.1029/2011PA002117

Rohling EJ, Pälike H. 2005. Centennial-scale climate cooling with a sudden cold event around 8,200 years ago. *Nature* **434**: 975–979. doi:10.1038/nature03421

Roth PH, Coulbourn WT. 1982. Floral and solution patterns of coccoliths in surface sediments of the North Pacific. *Marine Micropaleontology* **7**: 1–52. doi:10.1016/0377-8398(82)90014-7

Sagnotti L, Macrì P, Lucchi RG *et al.* 2011. A Holocene paleosecular variation record from the northwestern Barents Sea continental margin. *Geochemistry Geophysics Geosystems* **12 (11)**: Q11Z33.

Saloranta TM, Svendsen H. 2001. Across the Arctic front west of Spitsbergen: high-resolution CTD sections from 1998–2000. *Polar Research* **20(2)**: 177–184.

Samtleben C, Bickert T. 1990. Coccoliths in sediment traps from the Norwegian Sea. Marine *Micropaleontology* **16**: 39–64. doi:10.1016/0377-8398(90)90028-K

Samtleben C, Schäfer P, Andruleit H *et al.* 1995. Plankton in the Norwegian-Greenland Sea: from living communities to sediment assemblages -an actualistic approach. *Geologische Rundschau* **84**: 108–136. doi:10.1007/BF00192245

Sarnthein M. 2011. Northern Meltwater Pulse, CO_2, and changes in Atlantic convection. *Science* **331**:156–158.

Sarnthein M, Van Kreveld S, Erlenkeuser H *et al.* 2003. Centennial-to-millennial-scale periodicities of Holocene climate and sediment injections off the western Barents shelf, 75°N. *Boreas* **32**: 447–461. doi:10.1111/j.1502-3885.2003.tb01227.x

Schiebel R, Hemleben C. 2000. Interannual variability of planktic foraminiferal populations and test flux in the eastern North Atlantic Ocean (JGOFS). *Deep-Sea Research Part II* **47**: 1809– 1852.

Schiebel R, Waniek J, Bork M. *et al.* 2001. Planktic foraminiferal production stimulated by chlorophyll redistribution and entrainment of nutrients. *Deep-Sea Research Part I* **48**: 721–740.

Schrader HJ, Gersonde R. 1978. Diatoms and silicoflagellates. In *Micropaleontological Counting Methods and Techniques: An Exercise of an Eight Metres Section of the Lower Pliocene of Cap Rossello, Sicily*, Zachariasse WJ *et al* (eds). *Utrecht Micropaleontological Bulletin* **17**:129-176.

Schröder-Adams CJ, Cole FE, Medioli FS *et al.* 1990. Recent Arctic shelf foraminifera: Seasonally ice covered areas vs. perennially ice covered areas. *Journal of Foraminiferal Research* **20(1)**: 8– 36.

Scott DB, Vilks G. 1991. Benthic foraminifera in the surface sediments of the deep sea Arctic Ocean. *Journal of Foraminiferal Research* **21**: 20-38.

Scott DB, Schell T, Rochon A *et al.* 2008. Modern benthic foraminifera in the surface sediments of the Beaufort Shelf, slope and Mackenzie Trough, Beaufort Sea, Canada: taxonomy and summary of surficial distributions. *Journal of Foraminiferal Research* **38**: 228–250.

Sejrup H-P, Fjaeran T, Hald M *et al.* 1981. Benthonic foraminifera in surface samples from the Norwegian continental margin between 62 degrees N and 65 degrees N. *Journal of Foraminiferal Research* **11**: 277–295. doi:10.2113/gsjfr.11.4.277

Ślubowska MA, Koç N, Rasmussen TL *et al.* 2005. Changes in the flow of Atlantic water into the Arctic Ocean since the last deglaciation: Evidence from the northern Svalbard continental margin, 80°N. *Paleoceanography* **20**: 1–16. doi:10.1029/2005PA001141

Ślubowska-Woldengen M, Rasmussen TL, Koç N *et al.* 2007. Advection of Atlantic Water to the western and northern Svalbard shelf since 17,500 cal yr BP. *Quaternary Science Review* 26: 463–478. doi:10.1016/j.quascirev.2006.09.009

Ślubowska-Woldengen M, Koç N, Rasmussen TL *et al*. 2008. Timeslice reconstructions of ocean circulation changes on the continental shelf in the Nordic and Barents Seas during the last 16,000 cal yr B.P. *Quaternary Science Reviews* **27**: 1476–1492. doi:10.1016/j.quascirev.2008.04.015

Spielhagen RF, Werner K, Sørensen SA *et al.* 2011. Enhanced modern heat transfer to the Arctic by warm Atlantic Water. *Science* **331**: 450–453. doi:10.1126/science.1197397

Stabell B. 1986. A diatom maximum horizon in upper quaternary deposits. *Geologische Rundschau* **75**: 175–184. doi:10.1007/BF01770186

Steinsund PI. 1994: *Benthic foraminifera in surface sediments of the Barents and Kara seas: Modern and late Quaternary applications*. PhD thesis, University of Tromsø.

Stuiver M, Reimer PJ. 1993. Extended ^{14}C database and revised CALIB radiocarbon calibration program. *Radiocarbon* **35**: 215–230.

Tomas CR. 1997. *Identifying Marine Phytoplankton*. Academic Press: New York.

Thomas E, Booth L, Maslin M *et al.* 1995. Northeastern Atlantic benthic foraminifera during the last 45,000 years: changes in productivity seen from the bottom up. *Paleoceanography* **10**: 545–562.

Thornalley DJR, Bauc HA, Gebbie G *et al.* 2015. A warm and poorly ventilated deep Arctic Mediterranean during the last glacial period. *Science*, **349(6249)**: 706–710. doi:10.1126/science.aaa9554

Villa G, Palandri S, Wise SW. 2005. Quaternary calcareous nannofossils from Periantarctic basins: Paleoecological and paleoclimatic implications. *Marine Micropaleontology* **56**: 103–121. doi:10.1016/j.marmicro.2005.03.006

Villa G, Persico D, Wise SW *et al.* 2012. Calcareous nannofossil evidence for Marine Isotope Stage 31 (1Ma) in Core AND-1B, ANDRILL McMurdo Ice Shelf Project (Antarctica). *Global and Planetary Change* **96–97**: 75–86. doi:10.1016/j.gloplacha.2009.12.003

Vogt C, Knies J. 2009. Sediment pathways in the western Barents Sea inferred from clay mineral assemblages in surface sediments. *Norwegian Journal of Geology* **89**: 41–55.

Wells P, Okada H. 1997. Response of nannoplankton to major changes in sea-surface temperature and movements of hydrological fronts over Site DSDP 594 (south Chatham Rise, southeastern New Zealand), during the last 130 kyr. *Marine Micropaleontology* **32**: 341–363. doi:10.1016/S0377-8398(97)00025-X

Werner K, Spielhagen RF, Bauch D *et al.* 2013. Atlantic Water advection versus sea-ice advances in the eastern Fram Strait during the last 9 ka: Multiproxy evidence for a two-phase Holocene. *Paleoceanography* **28**: 283–295. doi:10.1002/palo.20028

Williams KM. 1986. Recent Arctic marine diatom assemblages from bottom sediments in Baffin Bay and Davis Strait. *Marine Micropaleontology* **10**: 327–341. doi:10.1016/0377-8398(86)90035-6

Wollenburg JE, Kuhnt W. 2000. The response of benthic foraminifers to carbon flux and primary production in the Arctic Ocean. *Marine Micropaleontology* **40**: 189-231. doi:10.1016/S0377-8398(00)00039-6

Wollenburg JE, Mackensen A. 1998. Living benthic foraminifers from the central Arctic Ocean: Faunal composition, standing stock and diversity. *Marine Micropaleontology* **34**: 153–185. doi:10.1016/S0377-8398(98)00007-3

Wollenburg JE, Mackensen A. 2009. The ecology and distribution of benthic foraminifera at the Håkon Mosby mud volcano (SW Barents Sea slope). *Deep-Sea Research Part I* **56**: 1336–1370. doi:10.1016/j.dsr.2009.02.004

Wollenburg JE, Knies J, Mackensen A. 2004. High-resolution paleoproductivity fluctuations during the past 24 kyr as indicated by benthic foraminifera in the marginal Arctic Ocean. *Palaeogeography Palaeoclimatology Palaeoecology* **204**: 209–238. doi:10.1016/S0031-0182(03)00726-0

Wollenburg JE, Kuhnt W, Mackensen A. 2001. Changes in Arctic Ocean paleoproductivity and hydrography during the last 145 kyr: The benthic foraminiferal record. *Paleoceanography* **16(1)**: 65-77, doi10.1029/1999PA000454.

Zamelczyk K, Rasmussen TL, Husum K et *al.* 2012. Paleoceanographic changes and calcium carbonate dissolution in the central Fram Strait during the last 20 ka. *Quaternary Research* **78**: 405–416. doi:10.1016/j.yqres.2012.07.006

Ziveri P, Thunell RC, Rio D. 1995. Export production of coccolithophores in an upwelling region: Results from San Pedro Basin, Southern California Borderlands. *Marine Micropaleontology* **24**: 335–358. doi:10.1016/0377-8398(94)00017-H

CHAPTER VI

Case study 4: Bellsund Drift, West of Svalbard (PREPARED project)

6.1 Introduction

The Upper Pleistocene and Holocene distribution of calcareous nannofossils has been investigated in a Calypso piston core, raised from the Bellsund drift, located west of Svalbard, South of the Fram Strait, where significant water mass exchanges affect the Arctic climate. The core is thought to contain an expanded stratigraphic sequence that is suitable for high-resolution palaeoclimatic and palaeoenvironmental reconstructions of the recent past climatic oscillations. Contourite drifts are ideal areas to address palaeoceanographic and palaeoclimatic studies since these sedimentary deposits typically form along the pathways of major bottom currents (Laberg et al., 2005; Rebesco and Camerlenghi, 2008); they are characterized by relatively high and continuous accumulation rates generating expanded sedimentary sequences, in contrast to adjacent condensed pelagic sequences (Knutz, 2008).

In the present study, we combine calcareous nannofossil data with lithological characteristics, using the magnetic susceptibility of the sediments and AMS ^{14}C dating for age model reconstructions. The aim is to investigate the climate variations occurred during the last 38.8 cal ky BP (from Marine Isotope Stage, MIS 3 to MIS 1) and to define an age model for along slope stratigraphic cross correlation, still lacking in this area. A detailed reconstruction of the last glacial and Holocene history is central in improving our understanding of past climate change.

6.2 Study area

The Bellsund drift is located on the continental slope between 1200 and 1800 mbsl. It represents a valuable high-resolution sedimentary and climate archive, located along the continental margin West of Spitsbergen, where important Atlantic and Arctic water masses exchanges and interactions affect the climate. Contourite drifts are well known throughout the world oceans, occurring anywhere from the abyssal area to shelf settings. They are often well developed along the continental slope where bottom currents are confined (Faugères and Stow, 2008). Rebesco et al. (2013) indicated that along the western slope of Svalbard, the Norwegian Sea Deep Water mass is episodically ventilated by dense and turbid shelf waters (brine) forming in the shelf area during wintertime and episodically cascading the slope towards deeper environments. This

down-slope process episodically feeds the West Spitsbergen Current (WSC) moving along the NW Barents Sea slope, it is responsible for the formation of contourite and accumulation of contourite drifts. The onset and growth of the contourite drifts located along the West Spitsbergen slope is inferred to occur at about 1.3 Ma in relation with the Early Pleistocene glacial expansion recorded in the area. The contouritic drifts along the NW Svalbard area are located between Trough Mouth Fan (TMF) areas. The lack of mounded contouritic deposits on the continental slope offshore TMFs like the Storfjorden, is related to the consecutive morphological erosion generated by the glacigenic debris flows that descend the slope during periods of glacial maximum in the case of shelf edge glaciations. The Bellsund drift is inferred to contain the record of the regional palaeoceanographic and palaeoclimatic history.

The Fram Strait is the only deep-sea open gate through which water masses are exchanged between the North Atlantic and Arctic Oceans. Warm Atlantic waters, forming the WSC, are advected northward across the eastern side of the Fram Strait. The warm WSC is responsible for almost ice-free conditions in the West and North Svalbard area during winter, exerting a strong control on Arctic climate (IPCC, 2007). A branch of the WSC mixes with Polar water moving North of Svalbard and enters the Barents Sea, East of Spitsbergen, forming the Eastern Spitsbergen Current (ESC) (Fig. 1).

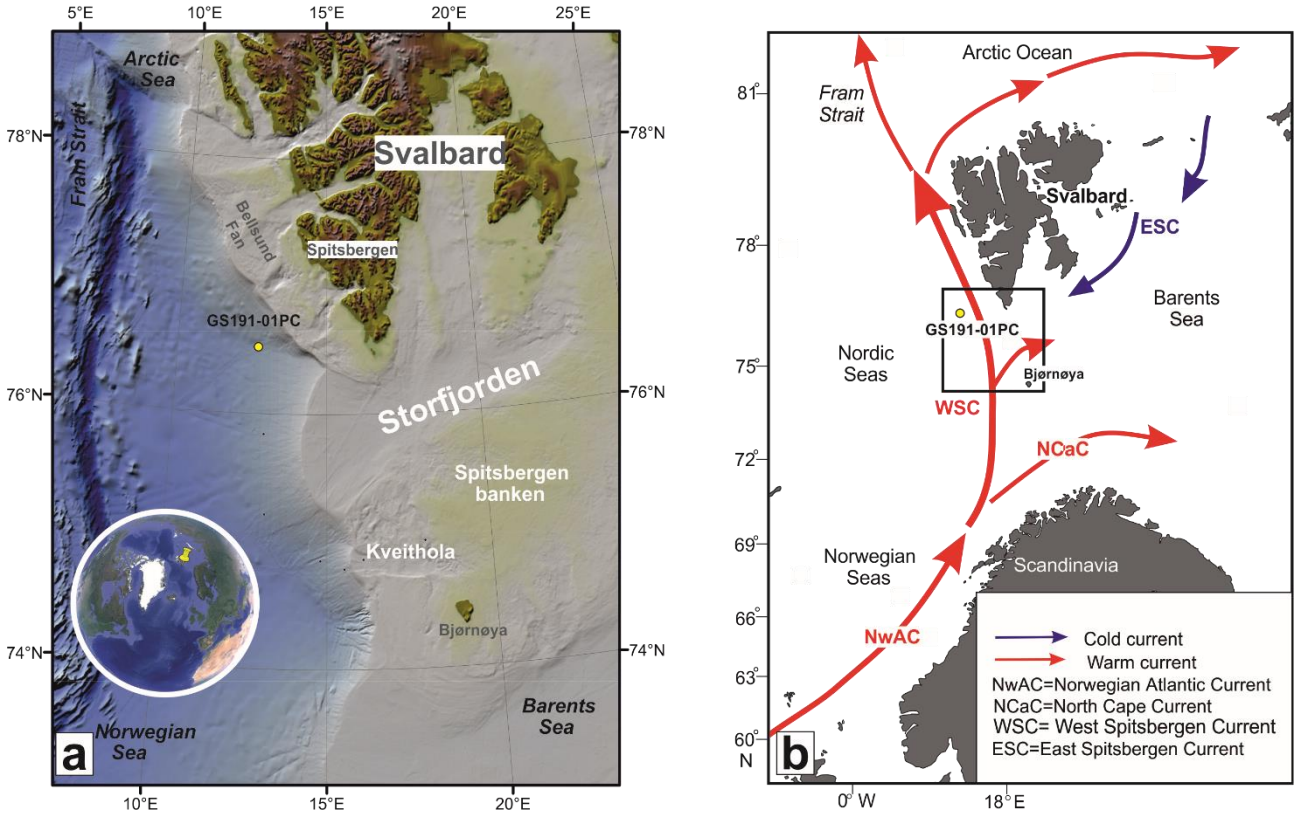

Fig. 1 Location of the study area. Yellow dot indicates the location of the studied core GS191-01PC. b Oceanographic circulation in the NW Barents Sea. The black box indicates the study area.

6.3 Material and age model

This study is based on the investigation of a 1967 cm-long Calypso piston core (GS191-01PC), recovered on the crest of the Bellsund sediment drift during the Eurofleets-2 PREPARED cruise (Tromsø–Tromsø, June 5–15, 2014) on board the Norwegian R/V G.O. Sars (Table 1, Fig. 1).

Core ID	Lat. N	Long. E	Water depth (m)	Total recovery (cm)	Location
GS191-01PC	76° 31.30'	12° 44.30'	1647	1967	Bellsund Drift

Table 1 Site locations, water depth and total length of sediment core investigated in this study.

The core was opened and visually logged and analyzed with a multi sensor core logger to measure the magnetic susceptibility. Sediment samples were collected regularly at 10 cm interval and analyzed for sedimentological characteristics and calcareous nannofossil content.

The sedimentary sequence contains at the base (1967–1165 cm bsf) the record of the MIS 3 (38.8–27 ka BP), characterized by alternated contouritic sedimentation (bioturbated sediments with marine derived organic matter content) and reworked sediments suggesting “anomalous”,

not fully interglacial conditions with glacial front proximal to the shelf edge. Above this interval (1165–912 cm bsf), the deposition consists of slightly bioturbated sediments with abundant sparse IRD, locally organized into layers as between 1060–1130 cm bsf, where the sediments appear also laminated. This interval is topped by a nearly 20 cm-thick layer of oxidized sediments that, according to core correlation and age model, corresponds to oxidized layer OX2 of Lucchi et al. (2013). Laminated sediments correspond to the transition from fully glacial to interglacial conditions, indicating a deglaciation phase. The Holocene interval is characterized by crudely layered and bioturbated sediments, suggesting the presence of bottom currents and palaeoenvironmental conditions favorable to bioactivity (Lucchi et al., 2013) (Fig. 2).

Two oxidized layers were identified: OX-1 at 618 cm and OX-2 at 930 cm.

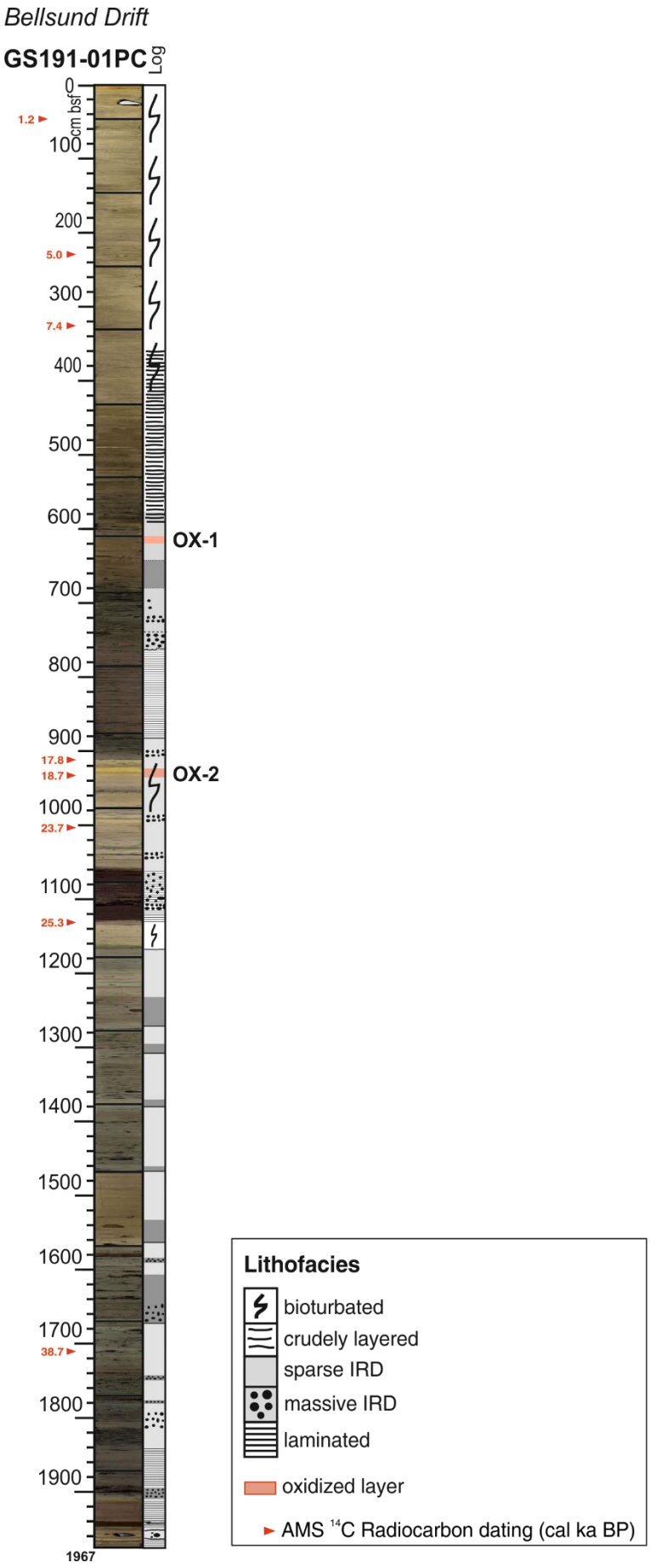

Fig. 2 Lithological log of the investigated piston core with ^{14}C dates indicated.

A total of 196 smear slides were prepared as indicated in Chapter II. A number of ecological indices were calculated and considered for environmental reconstruction:

- the ratio between *Emiliania huxleyi* and *Coccolithus pelagicus* s.l. (H/P ratio) that, in the Nordic Seas fossil assemblages, gives indication on the location of the Arctic Front (Andruleit and Baumann, 1998) separating the seasonally sea ice covered Polar and Arctic water from the warmer and saltier Atlantic-derived water;
- the dominance and Shannon Wiener diversity indices were calculated from species relative abundance, using the software PAST (Hammer et al., 2001).

Eight-accelerator mass spectrometry (AMS) ^{14}C dating on foraminifera supported the chronostratigraphy for this study (Table 2). The ^{14}C ages have been corrected for the ocean-reservoir effect and calibrated with the software Calib 7.1 (Stuiver and Reimer, 1993), using the Marine13 calibration curve (Reimer, 2013) and applying an average marine regional reservoir effect $\Delta R = 88 \pm 37$ years, obtained from the Marine Reservoir Correction Database of Calib 7.1 for the north-western Barents Sea area (Mangerud and Gulliksen, 1975). The ages are reported in calendar years and indicated the following as cal ka BP, where the time-zero corresponds, by convention, to 1950 AD. An age model was developed by linear interpolation between the calibrated radiocarbon horizons.

Measurements for magnetic susceptibility and palaeomagnetic/rock magnetic parameters were performed on u-channels, collected along the central part of the split sections. The low-field magnetic susceptibility (κ) was measured using a Bartington magnetic susceptibility meter equipped with probe MS2C. The low-field magnetic susceptibility intensities mostly depend on the concentration of ferromagnetic minerals; however, κ values are determined by the contribution of all the rock forming minerals, in proportion to their relative abundance and specific magnetic susceptibility.

Lab. code	Depth (cm)	Material	^{14}C Age	Age error	1 σ cal age (cal a BP)	2 σ cal age (cal a BP)	Median probability (cal a BP)
OS-123414	45	Foraminifera	1740	40	1166-1271	1074-1305	1212
OS-123438	231	Foraminifera	4850	30	4912-5087/ 5093-5114	4859-5209	5017
OS-123439	322	Foraminifera	7030	30	7408-7494	7360-7551	7450

OS-123440	915	Foraminifera	15150	55	17758-17944	17636-18027	17841
OS-123412	934	Foraminifera	15900	150	18516-18827	18322-18967	18666
OS-123527	1053	Foraminifera	20200	100	23587-23888	23436-24032	23736
OS-123526	1137	Foraminifera	21500	120	25209-25524	25030-25664	25359
OS-123407	1713	Foraminifera	34900	1500	36966-40388	35522-41726	38722

Table 2 Radiocarbon dates and calendar year calibrations for the studied cores.

6.4 Results

The dominant calcareous nannofossil taxa are *Emiliania huxleyi*, followed by *Coccolithus pelagicus* s.l., *Gephyrocapsa oceanica*, small *Gephyrocapsa* spp., *Calcidiscus leptoporus* and *Gephyrocapsa muellerae*. *Braarudosphaera bigelowii*, *Gephyrocapsa caribbeanica*, *Helicosphaera carteri* and *Syracosphaera* spp. are present in low percentages (less than 2%). Here we considered only the dominant species, as they are the most significant taxa for palaeoenvironmental interpretations. The assemblage includes Palaeogene and Cretaceous reworked taxa (*Discoaster binodosus*, *Arkhangelskiella maastrichtiana*, *Biscutum* spp., *Staurolithites* spp., *Eiffellithus* spp., *Microrhabdulus* spp., *Tranolithus* spp., *Watznaueria* spp., *Zeugrhabdotus* spp.), abundant in the interval 1200-900 cm (Fig. 3).

The calcareous nannofossil total abundance (without reworking), calculated on number of specimens per fixed area, spans from 0 to 10137 coccoliths/10 mm^2 through the record, presenting an increasing trend towards the top of the core (Fig. 3).

The interval from 1967-1165 cm is characterized by low nannofossil abundance, with predominant *E. huxleyi* (up to 100%) that shows a distinguishing pattern, tending to 0 every 20-200 cm. The interval from 1165-570 cm is still characterized by low coccolith abundance with dominant *E. huxleyi* (up to 100%) and some *C. pelagicus* s.l. peaks, along with an increase of total reworking (Fig. 3).

In the upper part of the core, between 570-0 cm, the total abundance increases considerably. A reduction of *E. huxleyi* as percentage occurs (ca. 63%), along with an increase of *C. pelagicus* s.l. (ca. 31%) and *C. leptoporus* (up to 5%), both as percentage and as number of coccoliths/10 mm^2. *Gephyrocapsa oceanica* shows a rise between 540-280 cm (up to 12%), followed by an

increase, as number of coccoliths/10 mm^2, of small *Gephyrocapsa* spp. between 260-0 cm (Fig. 3).

A main crossover between dominance and diversity indices occurs at 460 cm. The H/P ratio spans from -0.19 to 2.85 through the core. An abrupt H/P ratio decrease is shown within the interlaminated lithofacies and a descending trend is shown toward the top of the core (Fig. 3).

The magnetic susceptibility record shows higher and more variable values in the interval 1967-570 cm, whereas the upper section is characterized by nearly constant values (Fig. 3).

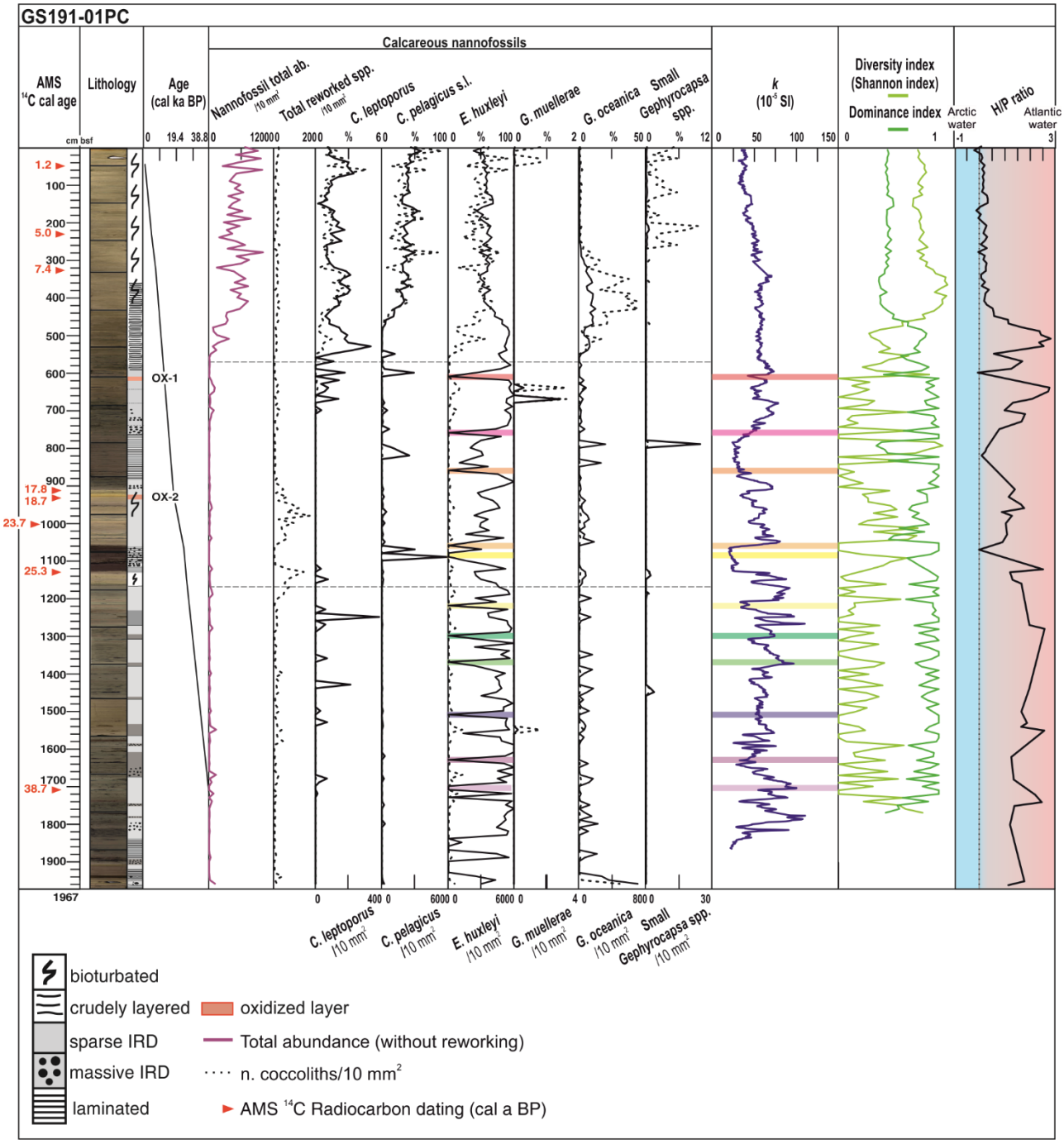

Fig. 3 Abundances of calcareous nannofossils for the investigated core, plotted versus depth. Age-depth plot is shown. Red arrows indicate calibrated calendar ages dated by AMS ^{14}C (see Table 2 for details). Dotted curves indicate nannofossil absolute abundance, expressed as n. of coccoliths/10 mm^2 in the slide. The magnetic susceptibility (κ), dominance and Shannon Wiener diversity indices and H/P ratio are shown. The horizontal dotted lines and the colored rectangles correspond to time interval limits, commented in the discussions.

6.5 Discussion

The investigated core contains an expanded sedimentary sequence that includes sediments spanning MIS 3–1. On the basis of the age model, the variations in nannofossil assemblage and sedimentary evidences, three intervals during the last 38.8 cal ky BP are identified: MIS 3

(38.8-25.9 cal ka BP), MIS 2 (25.9-11.7 cal ka BP) and MIS 1 or Holocene (11.7-1.2 cal ka BP).

6.5.1 MIS 3

Marine Isotope Stage 3, a period that lasted between 60 and 27 cal ka BP during the last glacial cycle, experienced several abrupt climatic variations (Van Meerbeeck et al., 2008), as indicated by the diffuse presence of Mass Transport Deposits between 1967 cm and 1165 cm.

The general very low abundance of calcareous nannofossils confirms the noticeable climatic variability of this "cold" interglacial stage. The two Heinrich Events indicated as H3 at ca. 31 cal ka BP and H4 at 38 cal ka BP (Hemming, 2004), were identified in the core corresponding to minima of *Emiliania huxleyi* and peaks of magnetic susceptibility (Fig. 4).

Other four *E. huxleyi* minima are recorded during MIS 3, but any clear climatic correlations was identified. In these four intervals, the *E. huxleyi* is considered not in situ and its distribution pattern probably reflects the response of glacial dynamic with sediment erosion and re-deposition. The lower values (often proximal to zero) may reflect a halt in the terrigenous input during the colder periods within MIS 3.

The coccolith dimensions correlate well with the sortable silt grain size distribution indicated in this area by Jessen and Rasmussen (2015): intervals with low coccolith abundance relate with periods of climate cooling and freshening of the surface water in the Nordic Seas, in agreement with high magnetic susceptibility value. The H/P ratio is here overestimated owing to the virtual absence of *C. pelagicus* s.l. and, therefore, is not indicative of the front location.

6.5.2 MIS 2

The period between 25.9 and 11.7 cal ka BP was characterized by glacial conditions, with overall low coccolith abundance. Three Heinrich Events, H0 (YD) at ca. 12 cal ka BP, H1 at 16.8 al ka BP and H2 at 24 cal ka BP (Hemming, 2004), correlate with three minima of *E. huxleyi* (Fig. 4). Other two *E. huxleyi* minima are detected at 15 cal ka BP and 24.5 cal ka BP. Most of these minima are positively correlated with the magnetic susceptibility increase, suggesting cold environmental conditions. On glaciated margins, sediment mass transportation and meltwater plumes significantly influences the magnetic susceptibility (Jessen et al., 2010; Rasmussen et al., 2007).

The noticeable presence of reworked taxa during this interval could suggest a melting event; owing to their extreme small size, coccoliths may have been eroded from Cretaceous and Palaeogene formations by the ice sheet. The presence of two oxidized layers marks the

inception of deglaciation (OX-2) at ca. 18 cal ka BP and the Younger Dryas event (OX-1) (Fig. 3) at ca. 12 cal ka BP as indicated by Lucchi et al. (2013) in the area South of Svalbard. The latter, according to Hemming (2004), corresponds to the Heinrich Event H0 (Fig. 4). The oxidized layers suggest the intensification of deep currents, transporting oxygen to the bottom. The nannofossil assemblage is of low diversity during MIS 2, as expected for a glacial phase. The H/P ratio is still overestimated due to the virtual absence of *C. pelagicus* s.l..

6.5.3 MIS 1

At the Younger Dryas/Holocene boundary (11.7 cal ka BP), the increase of coccolith abundance indicates an influence of warm Atlantic water, which probably resulted in thinning and reduction of the sea ice. The assemblage is more diverse than the in previous MIS 3 and 2, confirming Holocene interglacial conditions. The magnetic susceptibility shows a less variable trend, reflecting stable environmental conditions. *Coccolithus pelagicus* s.l., *E. huxleyi* and gephyrocapsids are the most important taxa in the assemblage from 10 to 6.5 cal ka BP, in agreement with the results obtained by Baumann and Matthiessen (1992) in neighboring areas.

The increase in absolute number of coccoliths during the Holocene indicates that the inflow of relatively warm Atlantic water became permanently established. Unfortunately, the H/P ratio discredits this interpretation. The increase of the cold-water species *C. pelagicus* s.l. shows conditions similar to those of the present day Arctic domain (Baumann and Matthiessen, 1992).

During the Holocene, the sediments are IRD-free indicating that few, if any, icebergs entered the western Svalbard margin in this period.

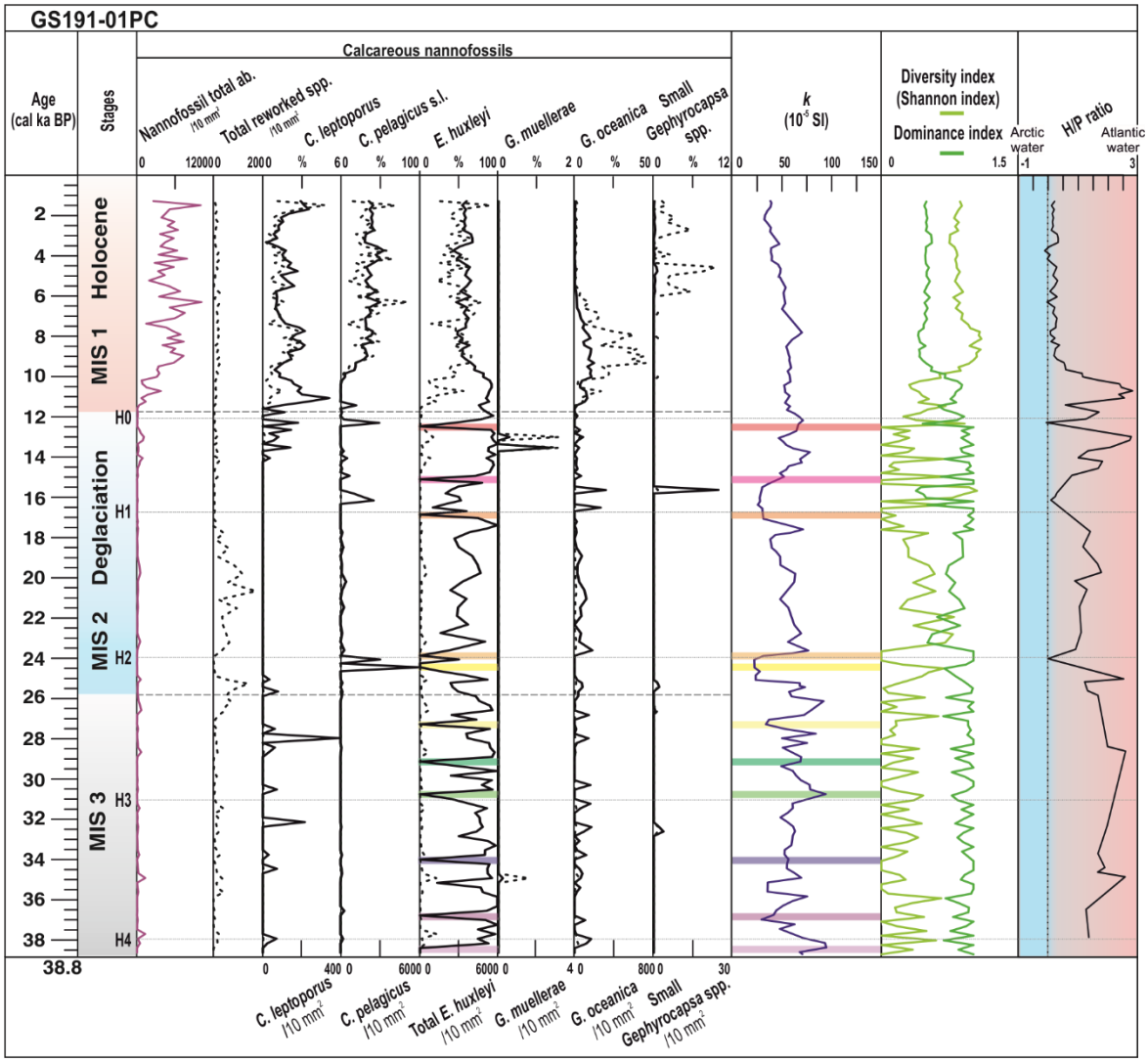

Fig. 4 Abundances of calcareous nannofossils for the investigated core, plotted versus age. Dotted curves indicate nannofossil absolute abundance, expressed as n. of coccoliths/10 mm^2 in the slide. The magnetic susceptibility (κ), dominance and Shannon Wiener diversity indices and H/P ratio are shown. The horizontal dotted lines and the colored rectangles correspond to time interval limits, commented in the text. MIS= Marine Isotope Stage; H= Heinrich events.

6. Conclusions

The 1967-cm long Calypso piston core, collected from the Bellsund Drift (GS191-01PC) contains an expanded sedimentary record dating 38.8-1.2 cal ka BP.

During MIS 3 and 2 (38.8-11.7 cal ka BP) calcareous nannofossil abundance was very low and interpreted as reworked; minima of *E. huxleyi* correlate with five Heinrich Events. Most of these minima are positively correlated with magnetic susceptibility increase, suggesting cold environmental conditions. The correlation of the timing of the *E. huxleyi* minima and the peaks of magnetic susceptibility with the Heinrich events may be seen as the response of glacial dynamic and erosion that is relented during colder periods within MIS 3.

The presence of reworked taxa during the lower part of MIS 2 could suggest a melting event and the two oxidized layers, in this interval, mark the inception of deglaciation (OX-2) at ca. 18 cal ka BP and the Younger Dryas event (OX-1) at ca. 12 cal ka BP, respectively. Both events may represent the intensification of deep currents that carried oxygen to the sea bottom.

During the Holocene, the coccolith abundance increased considerably, signifying that the inflow of relatively warm Atlantic water became permanently established.

The H/P ratio is not reliable enough, owing to *C. pelagicus* s.l. virtual absence, contrasting our interpretation.

References

Andruleit, H.A., Baumann, K.H., 1998. History of the last deglaciation and holocene in the Nordic seas as revealed by coccolithophore assemblages. Mar. Micropaleontol. 35, 179–201. doi:10.1016/S0377-8398(98)00021-8

Baumann, K.H., Matthiessen, J., 1992. Variations in surface water mass conditions in the Norwegian Sea: Evidence from Holocene coccolith and dinoflagellate cyst assemblages. Mar. Micropaleontol. 20, 129–146. doi:10.1016/0377-8398(92)90003-3

Faugères, J.C., Stow, D.A. V, 2008. Chapter 14 Contourite Drifts. Nature, Evolution and Controls. Dev. Sedimentol. doi:10.1016/S0070-4571(08)10014-0

Hammer, Ø., Harper, D.A.T., Ryan, P.D., 2001. PAST: Palaeontological statistics software package for education and data analysis. Palaeontol. Electron. 4, 1–9. doi:10.1163/001121611X566785

Hemming, S.R., 2004. Heinrich events: Massive late Pleistocene detritus layers of the North Atlantic and their global climate imprint. Rev. Geophys. 42, RG1005. doi:10.1029/2003RG000128

IPCC, 2007. Climate Change 2007 - The Physical Science Basis: Working Group I Contribution to the Fourth Assessment Report of the IPCC (Climate Change 2007), Cambridge University Press Cambridge United Kingdom and New York NY USA.

Jessen, S.P., Rasmussen, T.L., 2015. Sortable silt cycles in Svalbard slope sediments 74-0 ka. J. Quat. Sci. 30, 743–753. doi:10.1002/jqs.2807

Jessen, S.P., Rasmussen, T.L., Nielsen, T., Solheim, A., 2010. A new Late Weichselian and Holocene marine chronology for the western Svalbard slope 30,000-0 cal years BP. Quat. Sci. Rev. 29, 1301–1312. doi:10.1016/j.quascirev.2010.02.020

Knutz, P.C., 2008. Chapter 24 Palaeoceanographic Significance of Contourite Drifts. Dev. Sedimentol. doi:10.1016/S0070-4571(08)10024-3

Laberg, J.S., Stoker, M.S., Dahlgren, K.I.T., de Haas, H., Haflidason, H., Hjelstuen, B.O., Nielsen, T., Shannon, P.M., Vorren, T.O., van Weering, T.C.E., Ceramicola, S., 2005. Cenozoic along slope processes and sedimentation on the NW European Atlantic margin. Mar. Pet. Geol. doi:10.1016/j.marpetgeo.2005.01.008

Lucchi, R.G., Camerlenghi, A., Rebesco, M., Colmenero-Hidalgo, E., Sierro, F.J., Sagnotti, L., Urgeles, R., Melis, R., Morigi, C., Bàrcena, M.A., Giorgetti, G., Villa, G., Persico, D., Flores, J.A., Rigual-Hernandez, A.S., Pedrosa, M.T., Macri, P., Caburlotto, A., 2013. Postglacial sedimentary processes on the Storfjorden and Kveithola trough mouth fans: Significance of extreme glacimarine sedimentation. Glob. Planet. Change 111, 309–326. doi:10.1016/j.gloplacha.2013.10.008

Mangerud, J., Gulliksen, S., 1975. Apparent radiocarbon ages of recent marine shells from Norway, Spitsbergen, and Arctic Canada. Quat. Res. 5, 263–273. doi:10.1016/0033-5894(75)90028-9

Rasmussen, T.L., Thomsen, E., Ślubowska, M.A., Jessen, S., Solheim, A., Koç, N., 2007. Paleoceanographic evolution of the SW Svalbard margin (76°N) since 20,000 14C yr BP. Quat. Res. 67, 100–114. doi:10.1016/j.yqres.2006.07.002

Rebesco, M., Camerlenghi, A., 2008. Late Pliocene margin development and mega debris flow deposits on the Antarctic continental margins: Evidence of the onset of the modern Antarctic Ice Sheet? Palaeogeogr. Palaeoclimatol. Palaeoecol. 260, 149–167. doi:10.1016/j.palaeo.2007.08.009

Rebesco, M., Wåhlin, A., Laberg, J.S., Schauer, U., Beszczynska-Mller, A., Lucchi, R.G., Noormets, R., Accettella, D., Zarayskaya, Y., Diviacco, P., 2013. Quaternary contourite drifts of the Western Spitsbergen margin. Deep. Res. Part I Oceanogr. Res. Pap. 79, 156–168. doi:10.1016/j.dsr.2013.05.013

Reimer, P., 2013. IntCal13 and Marine13 Radiocarbon Age Calibration Curves 0–50,000 Years cal BP. Radiocarbon 55, 1869–1887. doi:10.2458/azu_js_rc.55.16947

Stuiver, M., Reimer, P.J., 1993. Extended ^{14}C data base and revised CALIB 3.0 14C age calibration program. Radiocarbon 35, 215–230.

Van Meerbeeck, C.J., Renssen, H., Roche, D.M., 2008. How did Marine Isotope Stage 3 and Last Glacial Maximum climates differ? Perspectives from equilibrium simulations. Clim. Past Discuss. 4, 1115–1158. doi:10.5194/cpd-4-1115-2008

CHAPTER VII

Late Pleistocene and Holocene climate variability in the Barents Sea as revealed by coccolithophore assemblages

Coccolithophore assemblages were investigated in 8 sediment cores from the Arctic Ocean. Two of these cores, GeoB17603-3, in the following indicated as 17603-3, and GS191-01PC (Fig. 1), having a well-constrained absolute chronology for the last ca. 14 cal ka BP, were selected as the best representative succession of the Late Pleistocene deglaciation and Holocene interglacial calcareous nannofossil variations to identify the palaeoclimatic conditions of this time interval at high northern latitude.

The calcareous nannofossil assemblages are generally of low diversity; *Emiliania huxleyi* and *Coccolithus pelagicus* s.l. together usually comprise more than 80% of the assemblage for most of the studied interval, however their co-variation is indicative in the high latitude Holocene reconstruction. Other significant taxa, such as *Gephyrocapsa oceanica*, *G. muellerae* and small *Gephyrocapsa* spp., contribute to reach the goal (Fig. 2).

Sparse occurrences of coccolithophores together with reworked pre-Quaternary taxa are observed during the deglaciation phase (Figg. 1-2), indicating harsh environmental conditions with dominant influence of meltwater. During Late Pleistocene, *G. muellerae* reaches its highest abundances, supporting deglaciation evidences. In both cores the assemblages are characterized by dominance of *E. huxleyi*, showing a similar decrease during the Younger Dryas, correlated by some authors with the H0 event (Hemming, 2004) (Fig. 2).

At the transition from Late Pleistocene to Holocene, a considerable coccolithophore increase (three/fourfold) occurs in both cores, suggesting ice-free conditions (Fig. 2). A change in the composition of the coccolithophore assemblages corresponds to the establishment of modern conditions, as supported also by the diversity index increase starting from about 10 cal ka BP (Fig. 2). The investigated sections evidenced comparable behavior of the coccolithophore assemblages, most of the species showing the same trend, except for small *Gephyrocapsa* spp., occurring between about 11.7-9.2 cal ka BP in core 17603-3 only (Fig. 2). *Emiliania huxleyi* is the most important contributor of the assemblages making up more than 65% of the total coccolithophores. The abundance of *C. pelagicus* s.l. significantly increases in both cores from around 9.3 cal ka BP, in agreement with earlier findings in the region (Andruleit and Baumann,

1998). The occurrence of *G. oceanica* is characterized by a maximum between 9.3-7.4 cal k BP (Fig. 2).

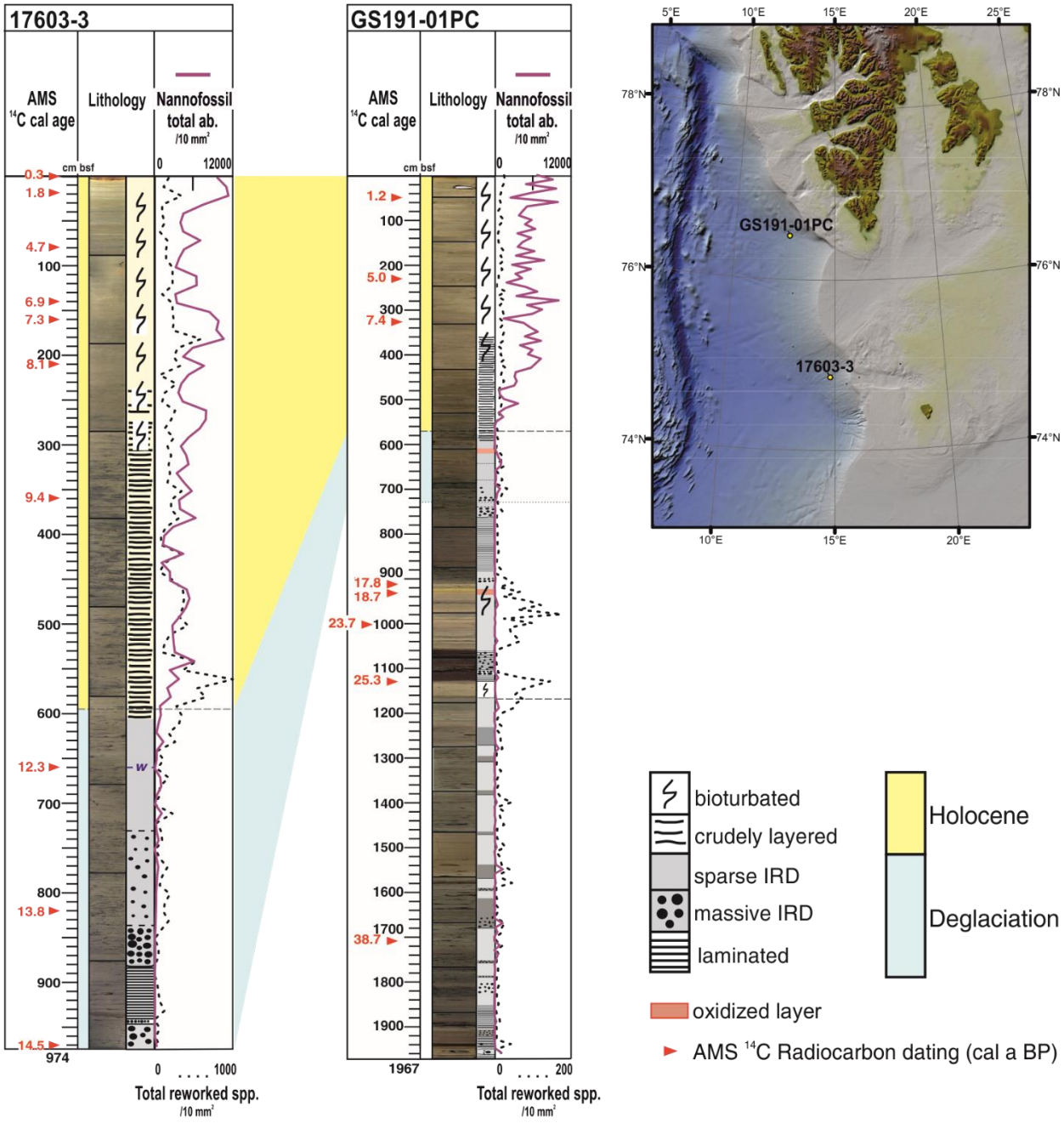

Fig. 1 Lithological logs, nannofossil total abundance and total reworked taxa plots for cores 17603-3 and GS191-01PC. The horizontal dotted lines correspond to time interval limits, commented in the text. The map with locations of the investigated cores is shown.

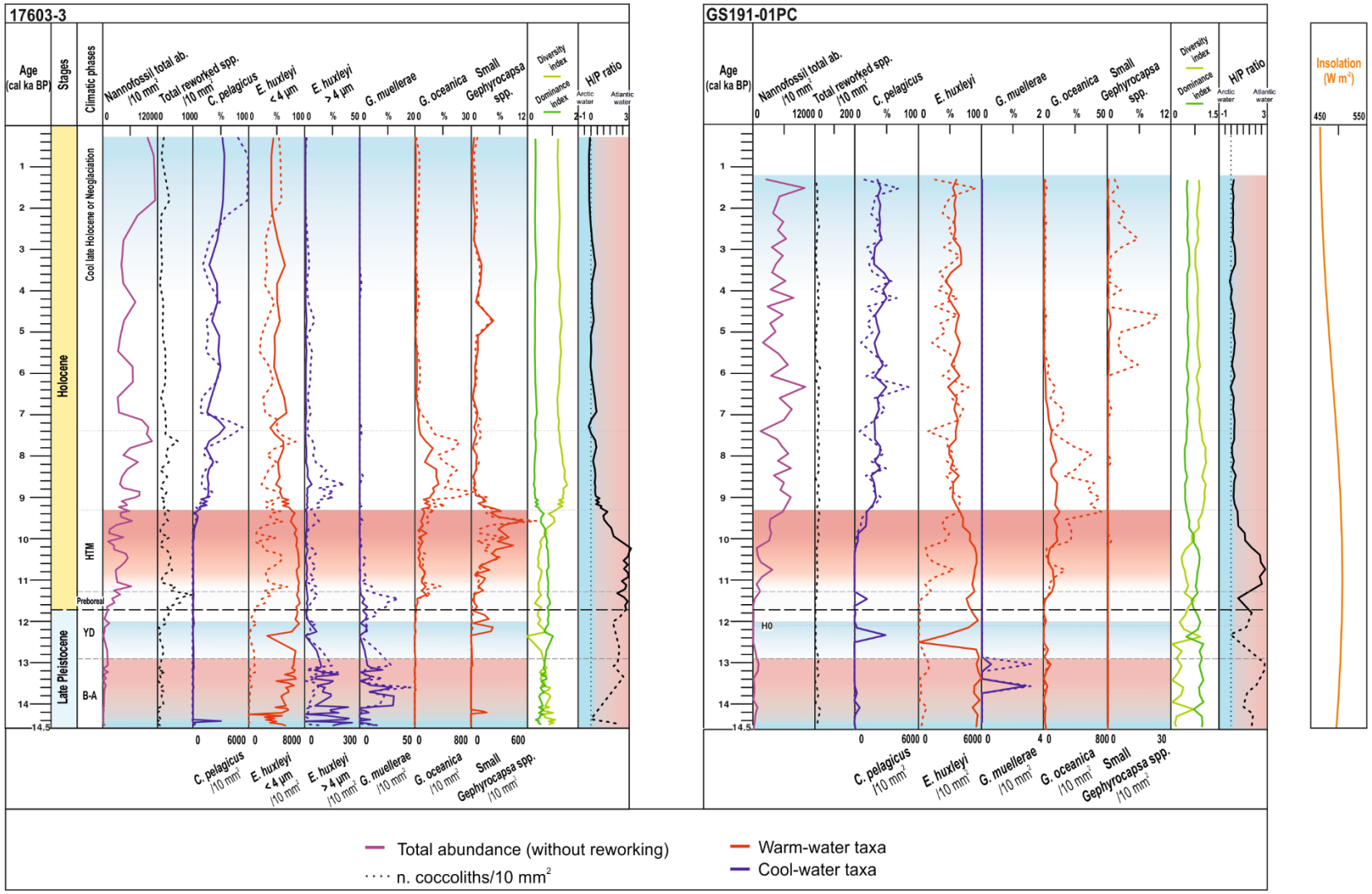

Fig. 2 Comparison of the coccolith abundance results of the two cores 17603-3 and GS191-01PC, plotted versus calendar age. The lower part of the H/P ratio curve is dotted due to the absence of *C. pelagicus*, commented in the text. The summer insolation curve at 65° N for the studied interval, following Laskar et al. (2004), is shown in orange on the right of the figure. B-A= Bølling-Allerød; YD= Younger Dryas; HTM= Holocene Thermal Maximum.

The changes in the assemblage structure can be described through the ratio variations of the two dominant species *E. huxleyi* and *C. pelagicus* (H/P ratio). In the Late Pleistocene, the coccolithophore concentrations are generally too low to determine reliable ratios. At the transition to Holocene, the H/P ratio shows a maximum in both cores and it decreases from ca. 10.2 cal ka BP towards the top of the cores (Fig. 2). These observations suggest the conditions for coccolithophore growth persisted harsh until the end of the Late Pleistocene, probably due to the presence of extensive sea-ice cover. A consistent warming occurred at the onset of the Holocene, probably related to the inflow of warmer waters from the North Atlantic at ca. 11.5 cal ka BP.

Several records, based on stable isotopes from throughout the Nordic seas, indicate that the late glacial interval was punctuated by numerous meltwater events, due to the decay of the surrounding ice-sheets (Sarnthein and Altenbach, 1995). Reduced seawater salinity, associated to ice melting, has probably disadvantaged coccolithophore growth. During the Bølling-Allerød interstadial (Fig. 2), the surface conditions were relatively cold and turbid due to detrital plumes of meltwaters.

The initial Holocene warming, as indicated by coccolithophore increase, seem to occur nearly synchronously along the path of the WSC. This is also supported by the relatively high H/P ratio measured in the cores directly influenced from the Atlantic inflow, corresponding to the Holocene Thermal Maximum (HTM) (Jansen et al., 2009; Kaufman et al., 2004; Rasmussen and Thomsen, 2014; Wanner et al., 2008) (Fig. 2). Diatom-based Sea surface temperature (SST) estimates indicate a noticeable increase in SST during early Holocene (Koç and Schrader, 1990), that is in good agreement with the presented nannofossil findings, probably in relation to summer insolation maximum at that time (Fig. 2).

Following the HTM, the H/P ratio shows low values, in agreement with a slight decrease in nannofossil abundances, indicating a brief drop in SST. This is not in full agreement with high middle-late Holocene H/P values observed in cores from the Norwegian Sea during the same interval (Andruleit and Baumann, 1998). This discrepancy may be explained by the high sedimentation rate of the studied cores, compared to the condensed sediments of the above-mentioned Norwegian Sea cores. However, in general, the coccolith records from core 17603-3 and GS191-01PC indicate an early Holocene temperature increase, followed by a gradual cooling through the middle-late Holocene interval.

The onset of the Neoglaciation interval is thought to have been caused by reduced solar radiation; by the micropalaeontological point of view, harsh, cool late Holocene conditions are suggested by the high abundance of *C. pelagicus* s.l. and the rare warm-water taxa (*G. oceanica* and small *Gephyrocapsa* spp.). A future higher sampling resolution in the upper part of the cores could provide more exhaustive information on this very short climatic episode. A detailed time resolution

is needed if we want to establish how present climatic changes are comparable to those of the most recent geological past.

In the following, a summary of the recognized climatic changes is presented for the last 14.5 cal ky BP (Fig. 3), along the northwestern Barents Sea, obtained through the study of calcareous nannofossils:

- **Deglaciation phase:** harsh climatic condition and extensive sea-ice cover
    - H/P not reliable
    - Sparse occurrences of coccolithophores
    - *G. muellerae* highest abundance
    - Dominance of *E.huxleyi*
- **YD**
    - Decrease of *E. huxleyi*
- **Holocene**
    - since 11.5 cal ka BP H/P increase
        - HTM:
            - summer insolation maximum
            - SST increase
            - H/P peak at ca. 10.2 cal ka BP
            - since ca. 10 cal ka BP diversity index increase
    - from around 9.3 cal ka BP *C. pelagicus* s.l. significant increase
    - 9.3-7.4 cal ka BP *G. oceanica* maximum
        - Neoglaciation:
            - *C. pelagicus* s.l. high abundance
            - rare warm-water taxa

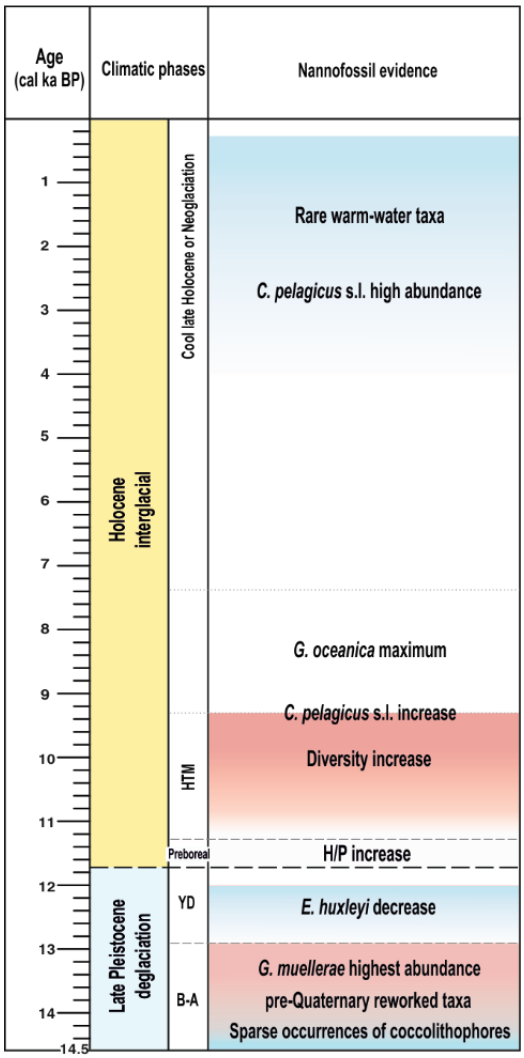

Fig. 3 Summary of the recognized climatic changes for the last 14.5 cal ky BP and relative nannofossil evidence.

References

Andruleit, H.A., Baumann, K.H., 1998. History of the last deglaciation and holocene in the Nordic seas as revealed by coccolithophore assemblages. Mar. Micropaleontol. 35, 179–201. doi:10.1016/S0377-8398(98)00021-8

Hemming, S.R., 2004. Heinrich events: Massive late Pleistocene detritus layers of the North Atlantic and their global climate imprint. Rev. Geophys. 42, RG1005. doi:10.1029/2003rg000128

Jansen, E., Andersson, C., Moros, M., Nisancioglu, K.H., Nyland, B.F., Telford, R.J., 2009. The Early to Mid-Holocene Thermal Optimum in the North Atlantic, in: Natural Climate Variability and Global Warming: A Holocene Perspective. pp. 123–137. doi:10.1002/9781444300932.ch5

Kaufman, D.S., Ager, T.A., Anderson, N.J., Anderson, P.M., Andrews, J.T., Bartlein, P.J., Brubaker, L.B., Coats, L.L., Cwynar, L.C., Duvall, M.L., Dyke, A.S., Edwards, M.E., Eisner, W.R., Gajewski, K., Geirsdöttir, A., Hu, F.S., Jennings, A.E., Kaplan, M.R., Kerwin, M.W., Lozhkin, A. V., MacDonald, G.M., Miller, G.H., Mock, C.J., Oswald, W.W., Otto-Bliesner, B.L., Porinchu, D.F., Rhland, K., Smol, J.P., Steig, E.J., Wolfe, B.B., 2004. Holocene thermal maximum in the western Arctic (0-180°W). Quat. Sci. Rev. 23, 529–560. doi:10.1016/j.quascirev.2003.09.007

Koç, N., Schrader, H., 1990. Surface Sediment Diatom Distribution and Holocene Paleotemperature Variations in the Greenland, Iceland and Norwegian Sea. Paleoceanography 5, 557–580. doi:10.1029/PA005i004p00557

Laskar, J., Robutel, P., Joutel, F., Gastineau, M., Correia, a C.M., Levrard, B., 2004. Astrophysics A long-term numerical solution for the insolation. Astronomy 285, 261–285. doi:10.1051/0004-6361

Rasmussen, T.L., Thomsen, E., 2014. Brine formation in relation to climate changes and ice retreat during the last 15,000years in Storfjorden, Svalbard, 76-78N. Paleoceanography 29, 911–929. doi:10.1002/2014PA002643

Sarnthein, M., Altenbach, A., 1995. Late Quaternary changes in surface water and deep water masses of the Nordic Seas and north-eastern North Atlantic: a review. Geol. Rundschau 84, 89–107. doi:10.1007/BF00192244

Sarnthein, M., Van Kreveld, S., Erlenkeuser, H., Grootes, P.M., Kucera, M., Pflauman, U., Schulz, M., 2003. Centennial-to-millennial-scale periodicities of Holocene climate and sediment injections off the western Barents shelf, 75°N. Boreas 32, 447–461. doi:10.1111/j.1502-3885.2003.tb01227.x

Wanner, H., Beer, J., Bütikofer, J., Crowley, T.J., Cubasch, U., Flückiger, J., Goosse, H., Grosjean, M., Joos, F., Kaplan, J.O., Küttel, M., Müller, S.A., Prentice, I.C., Solomina, O., Stocker, T.F., Tarasov, P., Wagner, M., Widmann, M., 2008. Mid- to Late Holocene climate change: an overview. Quat. Sci. Rev. 27, 1791–1828. doi:10.1016/j.quascirev.2008.06.013

SUPPLEMENTARY A- GeoB17601-5 nannofossil abundance

Sample	Depth (cm)	Fields	*Coccolithus pelagicus pelagicus*	*Emiliania huxleyi* < 4 µm	*Emiliania huxleyi* > 4µm	*Gephyrocapsa caribbeanica*	*Gephyrocapsa muellerae*	Reworked	Small *Gephyrocapsa* spp. (<3)	Small *Reticulofenestra* spp.	*Thoracosphaera* spp.	Total *E. huxleyi*	Total abundance (with reworked)	Total abundance (NO reworked)
GeoB17601-5-1, 0-1	0	200	362	908	31	5	2	15	67	0	0	939	1390	1375
GeoB17601-5-1, 10-11	10	200	155	653	21	3	3	17	42	0	0	674	894	877
GeoB17601-5-1, 20-21	20	200	240	580	5	2	7	7	36	0	0	585	877	870
GeoB17601-5-1, 30-31	30	200	35	233	29	0	14	13	10	0	0	262	334	321
GeoB17601-5-1, 40-41	40	200	0	34	5	0	1	6	0	0	0	39	46	40
GeoB17601-5-2, 51-52	51	200	0	25	1	0	0	4	0	0	0	26	30	26
GeoB17601-5-2, 60-61	60	200	0	10	0	0	0	2	0	0	0	10	12	10
GeoB17601-5-2, 70-71	70	200	0	47	8	0	0	7	0	0	0	55	62	55
GeoB17601-5-2, 80-81	80	200	0	43	3	0	3	5	0	0	0	46	54	49

GeoB17601-5-2, 90-91	90	200	0	49	10	0	4	2	0	0	0	59	65	63
GeoB17601-5-2, 100-101	100	200	0	27	12	0	3	3	0	0	0	39	45	42
GeoB17601-5-2, 110-111	110	200	0	39	6	0	2	2	0	0	1	45	50	48
GeoB17601-5-2, 120-121	120	200	0	118	29	0	5	3	0	0	0	147	155	152
GeoB17601-5-2, 130-131	130	200	0	36	1	0	3	5	0	0	0	37	45	40
GeoB17601-5-2, 140-141	140	200	0	19	1	0	0	4	0	0	0	20	24	20
GeoB17601-5-3, 152-153	152	200	0	15	0	0	0	10	0	0	0	15	25	15
GeoB17601-5-3, 160-161	160	200	0	19	6	0	1	11	0	0	0	25	37	26
GeoB17601-5-3, 170-171	170	200	0	33	10	0	2	4	0	0	0	43	49	45
GeoB17601-5-3, 180-181	180	200	0	3	0	0	0	1	0	0	0	3	4	3
GeoB17601-5-3, 190-191	190	200	0	3	0	0	0	7	0	0	0	3	10	3
GeoB17601-5-3, 200-201	200	200	0	9	0	0	0	6	0	0	0	9	15	9
GeoB17601-5-3, 210-211	210	200	0	5	0	0	2	5	0	0	0	5	12	7
GeoB17601-5-3, 220-221	220	200	0	3	1	0	0	5	0	0	0	4	9	4
GeoB17601-5-3, 230-231	230	200	0	1	0	0	0	4	0	0	0	1	5	1
GeoB17601-5-3, 240-241	240	200	0	1	0	0	0	9	0	0	0	1	10	1
GeoB17601-5-3, 250-251	250	200	0	3	0	0	0	5	0	0	0	3	8	3
GeoB17601-5-4, 282-283	282	200	0	1	0	0	0	5	0	0	0	1	6	1
GeoB17601-5-4, 290-291	290	200	0	3	0	0	0	15	0	0	0	3	18	3
GeoB17601-5-4, 300-301	300	200	0	5	0	0	0	10	0	0	0	5	15	5
GeoB17601-5-4, 310-311	310	200	0	2	0	0	0	11	0	0	0	2	13	2
GeoB17601-5-4, 320-321	320	200	0	2	0	0	1	9	0	0	0	2	12	3

GeoB17601-5-4, 330-331	330	200	0	5	0	0	0	20	0	0	0	5	25	5
GeoB17601-5-4, 340-341	340	200	1	2	1	0	0	14	0	0	0	3	18	4
GeoB17601-5-5, 352-353	352	200	0	4	0	0	1	24	0	1	0	4	30	6
GeoB17601-5-5, 360-361	360	200	0	5	2	0	0	13	0	0	0	7	20	7
GeoB17601-5-5, 370-371	370	200	0	1	0	0	0	7	0	0	0	1	8	1
GeoB17601-5-5, 380-381	380	200	1	3	0	0	1	18	0	0	0	3	23	5
GeoB17601-5-5, 390-391	390	200	0	4	1	0	0	23	0	1	0	5	29	6
GeoB17601-5-5, 400-401	400	200	0	0	0	0	0	26	0	0	0	0	26	0
GeoB17601-5-5, 410-411	410	200	0	0	0	0	0	15	0	0	0	0	15	0
GeoB17601-5-5, 420-421	420	200	0	0	0	0	0	17	0	0	0	0	17	0
GeoB17601-5-5, 430-431	430	200	0	3	0	0	0	18	0	0	0	3	21	3
GeoB17601-5-5, 440-441	440	200	0	7	0	0	0	20	0	0	0	7	27	7
GeoB17601-5-6, 452-453	452	200	0	5	1	0	0	27	0	0	1	6	34	7
GeoB17601-5-6, 460-461	460	200	0	5	1	0	0	25	0	0	0	6	31	6
GeoB17601-5-6, 470-471	470	200	0	3	0	0	0	15	0	0	0	3	18	3
GeoB17601-5-6, 480-481	480	200	0	2	0	0	0	6	0	0	0	2	8	2
GeoB17601-5-6, 490-491	490	200	0	5	0	0	0	22	0	0	0	5	27	5
GeoB17601-5-6, 500-501	500	200	0	1	0	0	0	30	0	0	0	1	31	1
GeoB17601-5-6, 510-511	510	200	1	1	0	0	0	31	0	0	2	1	35	4
GeoB17601-5-6, 520-521	520	200	2	11	0	0	0	12	0	0	0	11	25	13

Sample	Depth (cm)	Observed surface (mm^2)	*C. pel. pelagicus*/10 mm^2	*E. huxleyi* < 4 µm/10 mm^2	*E. huxleyi* > 4µm/10 mm^2	*G. caribbeanica*/10 mm^2	*G. muellerae*/10 mm^2	Reworked/10 mm^2	Small *Gephyrocapsa* spp. (<3)/10 mm^2	Small *Reticulofenestra* spp./10 mm^2	*Thoracosphaera* spp. /10 mm^2	Total *E. huxleyi* /10 mm^2	Total abundance (with reworked) /10 mm^2	Total abundance (NO reworked) /10 mm^2
GeoB17601-5-1, 0-1	0	6,28	576,43	1445,86	49,36	7,96	3,18	23,89	106,69	0,00	0,00	1495,22	2213,38	2189,49
GeoB17601-5-1, 10-11	10	6,28	246,82	1039,81	33,44	4,78	4,78	27,07	66,88	0,00	0,00	1073,25	1423,57	1396,50
GeoB17601-5-1, 20-21	20	6,28	382,17	923,57	7,96	3,18	11,15	11,15	57,32	0,00	0,00	931,53	1396,50	1385,35
GeoB17601-5-1, 30-31	30	6,28	55,73	371,02	46,18	0,00	22,29	20,70	15,92	0,00	0,00	417,20	531,85	511,15
GeoB17601-5-1, 40-41	40	6,28	0,00	54,14	7,96	0,00	1,59	9,55	0,00	0,00	0,00	62,10	73,25	63,69
GeoB17601-5-2, 51-52	51	6,28	0,00	39,81	1,59	0,00	0,00	6,37	0,00	0,00	0,00	41,40	47,77	41,40
GeoB17601-5-2, 60-61	60	6,28	0,00	15,92	0,00	0,00	0,00	3,18	0,00	0,00	0,00	15,92	19,11	15,92
GeoB17601-5-2, 70-71	70	6,28	0,00	74,84	12,74	0,00	0,00	11,15	0,00	0,00	0,00	87,58	98,73	87,58
GeoB17601-5-2, 80-81	80	6,28	0,00	68,47	4,78	0,00	4,78	7,96	0,00	0,00	0,00	73,25	85,99	78,03
GeoB17601-5-2, 90-91	90	6,28	0,00	78,03	15,92	0,00	6,37	3,18	0,00	0,00	0,00	93,95	103,50	100,32
GeoB17601-5-2, 100-101	100	6,28	0,00	42,99	19,11	0,00	4,78	4,78	0,00	0,00	0,00	62,10	71,66	66,88
GeoB17601-5-2, 110-111	110	6,28	0,00	62,10	9,55	0,00	3,18	3,18	0,00	0,00	1,59	71,66	79,62	76,43

GeoB17601-5-2, 120-121	120	6,28	0,00	187,90	46,18	0,00	7,96	4,78	0,00	0,00	0,00	234,08	246,82	242,04
GeoB17601-5-2, 130-131	130	6,28	0,00	57,32	1,59	0,00	4,78	7,96	0,00	0,00	0,00	58,92	71,66	63,69
GeoB17601-5-2, 140-141	140	6,28	0,00	30,25	1,59	0,00	0,00	6,37	0,00	0,00	0,00	31,85	38,22	31,85
GeoB17601-5-3, 152-153	152	6,28	0,00	23,89	0,00	0,00	0,00	15,92	0,00	0,00	0,00	23,89	39,81	23,89
GeoB17601-5-3, 160-161	160	6,28	0,00	30,25	9,55	0,00	1,59	17,52	0,00	0,00	0,00	39,81	58,92	41,40
GeoB17601-5-3, 170-171	170	6,28	0,00	52,55	15,92	0,00	3,18	6,37	0,00	0,00	0,00	68,47	78,03	71,66
GeoB17601-5-3, 180-181	180	6,28	0,00	4,78	0,00	0,00	0,00	1,59	0,00	0,00	0,00	4,78	6,37	4,78
GeoB17601-5-3, 190-191	190	6,28	0,00	4,78	0,00	0,00	0,00	11,15	0,00	0,00	0,00	4,78	15,92	4,78
GeoB17601-5-3, 200-201	200	6,28	0,00	14,33	0,00	0,00	0,00	9,55	0,00	0,00	0,00	14,33	23,89	14,33
GeoB17601-5-3, 210-211	210	6,28	0,00	7,96	0,00	0,00	3,18	7,96	0,00	0,00	0,00	7,96	19,11	11,15
GeoB17601-5-3, 220-221	220	6,28	0,00	4,78	1,59	0,00	0,00	7,96	0,00	0,00	0,00	6,37	14,33	6,37
GeoB17601-5-3, 230-231	230	6,28	0,00	1,59	0,00	0,00	0,00	6,37	0,00	0,00	0,00	1,59	7,96	1,59
GeoB17601-5-3, 240-241	240	6,28	0,00	1,59	0,00	0,00	0,00	14,33	0,00	0,00	0,00	1,59	15,92	1,59
GeoB17601-5-3, 250-251	250	6,28	0,00	4,78	0,00	0,00	0,00	7,96	0,00	0,00	0,00	4,78	12,74	4,78
GeoB17601-5-4, 282-283	282	6,28	0,00	1,59	0,00	0,00	0,00	7,96	0,00	0,00	0,00	1,59	9,55	1,59
GeoB17601-5-4, 290-291	290	6,28	0,00	4,78	0,00	0,00	0,00	23,89	0,00	0,00	0,00	4,78	28,66	4,78
GeoB17601-5-4, 300-301	300	6,28	0,00	7,96	0,00	0,00	0,00	15,92	0,00	0,00	0,00	7,96	23,89	7,96
GeoB17601-5-4, 310-311	310	6,28	0,00	3,18	0,00	0,00	0,00	17,52	0,00	0,00	0,00	3,18	20,70	3,18
GeoB17601-5-4, 320-321	320	6,28	0,00	3,18	0,00	0,00	1,59	14,33	0,00	0,00	0,00	3,18	19,11	4,78
GeoB17601-5-4, 330-331	330	6,28	0,00	7,96	0,00	0,00	0,00	31,85	0,00	0,00	0,00	7,96	39,81	7,96
GeoB17601-5-4, 340-341	340	6,28	1,59	3,18	1,59	0,00	0,00	22,29	0,00	0,00	0,00	4,78	28,66	6,37
GeoB17601-5-5, 352-353	352	6,28	0,00	6,37	0,00	0,00	1,59	38,22	0,00	1,59	0,00	6,37	47,77	9,55

GeoB17601-5-5, 360-361	360	6,28	0,00	7,96	3,18	0,00	0,00	20,70	0,00	0,00	0,00	11,15	31,85	11,15
GeoB17601-5-5, 370-371	370	6,28	0,00	1,59	0,00	0,00	0,00	11,15	0,00	0,00	0,00	1,59	12,74	1,59
GeoB17601-5-5, 380-381	380	6,28	1,59	4,78	0,00	0,00	1,59	28,66	0,00	0,00	0,00	4,78	36,62	7,96
GeoB17601-5-5, 390-391	390	6,28	0,00	6,37	1,59	0,00	0,00	36,62	0,00	1,59	0,00	7,96	46,18	9,55
GeoB17601-5-5, 400-401	400	6,28	0,00	0,00	0,00	0,00	0,00	41,40	0,00	0,00	0,00	0,00	41,40	0,00
GeoB17601-5-5, 410-411	410	6,28	0,00	0,00	0,00	0,00	0,00	23,89	0,00	0,00	0,00	0,00	23,89	0,00
GeoB17601-5-5, 420-421	420	6,28	0,00	0,00	0,00	0,00	0,00	27,07	0,00	0,00	0,00	0,00	27,07	0,00
GeoB17601-5-5, 430-431	430	6,28	0,00	4,78	0,00	0,00	0,00	28,66	0,00	0,00	0,00	4,78	33,44	4,78
GeoB17601-5-5, 440-441	440	6,28	0,00	11,15	0,00	0,00	0,00	31,85	0,00	0,00	0,00	11,15	42,99	11,15
GeoB17601-5-6, 452-453	452	6,28	0,00	7,96	1,59	0,00	0,00	42,99	0,00	0,00	1,59	9,55	54,14	11,15
GeoB17601-5-6, 460-461	460	6,28	0,00	7,96	1,59	0,00	0,00	39,81	0,00	0,00	0,00	9,55	49,36	9,55
GeoB17601-5-6, 470-471	470	6,28	0,00	4,78	0,00	0,00	0,00	23,89	0,00	0,00	0,00	4,78	28,66	4,78
GeoB17601-5-6, 480-481	480	6,28	0,00	3,18	0,00	0,00	0,00	9,55	0,00	0,00	0,00	3,18	12,74	3,18
GeoB17601-5-6, 490-491	490	6,28	0,00	7,96	0,00	0,00	0,00	35,03	0,00	0,00	0,00	7,96	42,99	7,96
GeoB17601-5-6, 500-501	500	6,28	0,00	1,59	0,00	0,00	0,00	47,77	0,00	0,00	0,00	1,59	49,36	1,59
GeoB17601-5-6, 510-511	510	6,28	1,59	1,59	0,00	0,00	0,00	49,36	0,00	0,00	3,18	1,59	55,73	6,37
GeoB17601-5-6, 520-521	520	6,28	3,18	17,52	0,00	0,00	0,00	19,11	0,00	0,00	0,00	17,52	39,81	20,70

Sample	Depth (cm)	% *C. pel. pelagicus*	% *E. huxleyi* < 4 µm	% *E. huxleyi* > 4µm	% *G. caribbeanica*	% *G. muellerae*	% Reworked	% Small *Gephyrocapsa* spp. (<3)	% Small *Reticulofenestra* spp.	% *Thoracosphaera* spp.	% Total *E. huxleyi*	% Total abundance (NO reworked)
GeoB17601-5-1, 0-1	0	0,28373	26,04	65,32	2,23	0,36	0,14	1,08	4,82	0,00	67,55	98,92
GeoB17601-5-1, 10-11	10	0,44115	17,34	73,04	2,35	0,34	0,34	1,90	4,70	0,00	75,39	98,10
GeoB17601-5-1, 20-21	20	0,4497	27,37	66,13	0,57	0,23	0,80	0,80	4,10	0,00	66,70	99,20
GeoB17601-5-1, 30-31	30	1,18079	10,48	69,76	8,68	0,00	4,19	3,89	2,99	0,00	78,44	96,11
GeoB17601-5-1, 40-41	40	8,57357	0,00	73,91	10,87	0,00	2,17	13,04	0,00	0,00	84,78	86,96
GeoB17601-5-2, 51-52	51	13,1461	0,00	83,33	3,33	0,00	0,00	13,33	0,00	0,00	86,67	86,67
GeoB17601-5-2, 60-61	60	32,8653	0,00	83,33	0,00	0,00	0,00	16,67	0,00	0,00	83,33	83,33
GeoB17601-5-2, 70-71	70	6,36103	0,00	75,81	12,90	0,00	0,00	11,29	0,00	0,00	88,71	88,71
GeoB17601-5-2, 80-81	80	7,30341	0,00	79,63	5,56	0,00	5,56	9,26	0,00	0,00	85,19	90,74
GeoB17601-5-2, 90-91	90	6,06745	0,00	75,38	15,38	0,00	6,15	3,08	0,00	0,00	90,77	96,92
GeoB17601-5-2, 100-101	100	8,76409	0,00	60,00	26,67	0,00	6,67	6,67	0,00	0,00	86,67	93,33
GeoB17601-5-2, 110-111	110	7,88768	0,00	78,00	12,00	0,00	4,00	4,00	0,00	0,00	90,00	96,00
GeoB17601-5-2, 120-121	120	2,54441	0,00	76,13	18,71	0,00	3,23	1,94	0,00	0,00	94,84	98,06

GeoB17601-5-2, 130-131	130	8,76409	0,00	80,00	2,22	0,00	6,67	11,11	0,00	0,00	82,22	88,89
GeoB17601-5-2, 140-141	140	16,4327	0,00	79,17	4,17	0,00	0,00	16,67	0,00	0,00	83,33	83,33
GeoB17601-5-3, 152-153	152	15,7754	0,00	60,00	0,00	0,00	0,00	40,00	0,00	0,00	60,00	60,00
GeoB17601-5-3, 160-161	160	10,659	0,00	51,35	16,22	0,00	2,70	29,73	0,00	0,00	67,57	70,27
GeoB17601-5-3, 170-171	170	8,04865	0,00	67,35	20,41	0,00	4,08	8,16	0,00	0,00	87,76	91,84
GeoB17601-5-3, 180-181	180	98,596	0,00	75,00	0,00	0,00	0,00	25,00	0,00	0,00	75,00	75,00
GeoB17601-5-3, 190-191	190	39,4384	0,00	30,00	0,00	0,00	0,00	70,00	0,00	0,00	30,00	30,00
GeoB17601-5-3, 200-201	200	26,2923	0,00	60,00	0,00	0,00	0,00	40,00	0,00	0,00	60,00	60,00
GeoB17601-5-3, 210-211	210	32,8653	0,00	41,67	0,00	0,00	16,67	41,67	0,00	0,00	41,67	58,33
GeoB17601-5-3, 220-221	220	43,8204	0,00	33,33	11,11	0,00	0,00	55,56	0,00	0,00	44,44	44,44
GeoB17601-5-3, 230-231	230	78,8768	0,00	20,00	0,00	0,00	0,00	80,00	0,00	0,00	20,00	20,00
GeoB17601-5-3, 240-241	240	39,4384	0,00	10,00	0,00	0,00	0,00	90,00	0,00	0,00	10,00	10,00
GeoB17601-5-3, 250-251	250	49,298	0,00	37,50	0,00	0,00	0,00	62,50	0,00	0,00	37,50	37,50
GeoB17601-5-4, 282-283	282	65,7307	0,00	16,67	0,00	0,00	0,00	83,33	0,00	0,00	16,67	16,67
GeoB17601-5-4, 290-291	290	21,9102	0,00	16,67	0,00	0,00	0,00	83,33	0,00	0,00	16,67	16,67
GeoB17601-5-4, 300-301	300	26,2923	0,00	33,33	0,00	0,00	0,00	66,67	0,00	0,00	33,33	33,33
GeoB17601-5-4, 310-311	310	30,3372	0,00	15,38	0,00	0,00	0,00	84,62	0,00	0,00	15,38	15,38
GeoB17601-5-4, 320-321	320	32,8653	0,00	16,67	0,00	0,00	8,33	75,00	0,00	0,00	16,67	25,00
GeoB17601-5-4, 330-331	330	15,7754	0,00	20,00	0,00	0,00	0,00	80,00	0,00	0,00	20,00	20,00
GeoB17601-5-4, 340-341	340	21,9102	5,56	11,11	5,56	0,00	0,00	77,78	0,00	0,00	16,67	22,22
GeoB17601-5-5, 352-353	352	13,1461	0,00	13,33	0,00	0,00	3,33	80,00	0,00	3,33	13,33	20,00
GeoB17601-5-5, 360-361	360	19,7192	0,00	25,00	10,00	0,00	0,00	65,00	0,00	0,00	35,00	35,00

GeoB17601-5-5, 370-371	370	49,298	0,00	12,50	0,00	0,00	0,00	87,50	0,00	0,00	12,50	12,50
GeoB17601-5-5, 380-381	380	17,1471	4,35	13,04	0,00	0,00	4,35	78,26	0,00	0,00	13,04	21,74
GeoB17601-5-5, 390-391	390	13,5994	0,00	13,79	3,45	0,00	0,00	79,31	0,00	3,45	17,24	20,69
GeoB17601-5-5, 400-401	400	15,1686	0,00	0,00	0,00	0,00	0,00	100,00	0,00	0,00	0,00	0,00
GeoB17601-5-5, 410-411	410	26,2923	0,00	0,00	0,00	0,00	0,00	100,00	0,00	0,00	0,00	0,00
GeoB17601-5-5, 420-421	420	23,1991	0,00	0,00	0,00	0,00	0,00	100,00	0,00	0,00	0,00	0,00
GeoB17601-5-5, 430-431	430	18,7802	0,00	14,29	0,00	0,00	0,00	85,71	0,00	0,00	14,29	14,29
GeoB17601-5-5, 440-441	440	14,6068	0,00	25,93	0,00	0,00	0,00	74,07	0,00	0,00	25,93	25,93
GeoB17601-5-6, 452-453	452	11,5995	0,00	14,71	2,94	0,00	0,00	79,41	0,00	0,00	17,65	20,59
GeoB17601-5-6, 460-461	460	12,7221	0,00	16,13	3,23	0,00	0,00	80,65	0,00	0,00	19,35	19,35
GeoB17601-5-6, 470-471	470	21,9102	0,00	16,67	0,00	0,00	0,00	83,33	0,00	0,00	16,67	16,67
GeoB17601-5-6, 480-481	480	49,298	0,00	25,00	0,00	0,00	0,00	75,00	0,00	0,00	25,00	25,00
GeoB17601-5-6, 490-491	490	14,6068	0,00	18,52	0,00	0,00	0,00	81,48	0,00	0,00	18,52	18,52
GeoB17601-5-6, 500-501	500	12,7221	0,00	3,23	0,00	0,00	0,00	96,77	0,00	0,00	3,23	3,23
GeoB17601-5-6, 510-511	510	11,2681	2,86	2,86	0,00	0,00	0,00	88,57	0,00	0,00	2,86	11,43
GeoB17601-5-6, 520-521	520	15,7754	8,00	44,00	0,00	0,00	0,00	48,00	0,00	0,00	44,00	52,00

Sample	Depth (cm)	H/P ratio	Dominance index	Shannon diversity index	CEX *C. pel.*(modif. Dittert et al., 1999)
GeoB17601-5-1, 0-1	0	0,41396	0,50	0,94	0,98
GeoB17601-5-1, 10-11	10	0,63833	0,57	0,88	0,98
GeoB17601-5-1, 20-21	20	0,38694	0,51	0,88	0,97
GeoB17601-5-1, 30-31	30	0,87423	0,51	1,06	0,98
GeoB17601-5-1, 40-41	40		0,58	0,81	1,00
GeoB17601-5-2, 51-52	51		0,71	0,53	1,00
GeoB17601-5-2, 60-61	60		0,72	0,45	1,00
GeoB17601-5-2, 70-71	70		0,60	0,72	1,00
GeoB17601-5-2, 80-81	80		0,65	0,72	1,00
GeoB17601-5-2, 90-91	90		0,60	0,78	1,00
GeoB17601-5-2, 100-101	100		0,44	1,02	1,00
GeoB17601-5-2, 110-111	110		0,63	0,78	1,00
GeoB17601-5-2, 120-121	120		0,62	0,71	1,00

GeoB17601-5-2, 130-131	130		0,66	0,69	1,00
GeoB17601-5-2, 140-141	140		0,66	0,62	1,00
GeoB17601-5-3, 152-153	152		0,52	0,67	1,00
GeoB17601-5-3, 160-161	160		0,38	1,10	1,00
GeoB17601-5-3, 170-171	170		0,50	0,93	1,00
GeoB17601-5-3, 180-181	180		0,63	0,56	1,00
GeoB17601-5-3, 190-191	190		0,58	0,61	1,00
GeoB17601-5-3, 200-201	200		0,52	0,67	1,00
GeoB17601-5-3, 210-211	210		0,38	1,03	1,00
GeoB17601-5-3, 220-221	220		0,43	0,94	1,00
GeoB17601-5-3, 230-231	230		0,68	0,50	1,00
GeoB17601-5-3, 240-241	240		0,82	0,33	1,00
GeoB17601-5-3, 250-251	250		0,53	0,66	1,00
GeoB17601-5-4, 282-283	282		0,72	0,45	1,00
GeoB17601-5-4, 290-291	290		0,72	0,45	1,00
GeoB17601-5-4, 300-301	300		0,56	0,64	1,00
GeoB17601-5-4, 310-311	310		0,74	0,43	1,00
GeoB17601-5-4, 320-321	320		0,60	0,72	1,00
GeoB17601-5-4, 330-331	330		0,68	0,50	1,00
GeoB17601-5-4, 340-341	340	0,47712	0,62	0,76	0,46
GeoB17601-5-5, 352-353	352		0,66	0,67	1,00
GeoB17601-5-5, 360-361	360		0,50	0,86	1,00

GeoB17601-5-5, 370-371	370		0,78	0,38	1,00
GeoB17601-5-5, 380-381	380	0,47712	0,63	0,73	0,52
GeoB17601-5-5, 390-391	390		0,65	0,69	1,00
GeoB17601-5-5, 400-401	400		1,00	0,00	
GeoB17601-5-5, 410-411	410		1,00	0,00	
GeoB17601-5-5, 420-421	420		1,00	0,00	
GeoB17601-5-5, 430-431	430		0,76	0,41	1,00
GeoB17601-5-5, 440-441	440		0,62	0,57	1,00
GeoB17601-5-6, 452-453	452		0,65	0,67	1,00
GeoB17601-5-6, 460-461	460		0,68	0,58	1,00
GeoB17601-5-6, 470-471	470		0,72	0,45	1,00
GeoB17601-5-6, 480-481	480		0,63	0,56	1,00
GeoB17601-5-6, 490-491	490		0,70	0,48	1,00
GeoB17601-5-6, 500-501	500		0,94	0,14	1,00
GeoB17601-5-6, 510-511	510	0	0,79	0,47	0,36
GeoB17601-5-6, 520-521	520	0,74036	0,43	0,92	0,69

SUPPLEMENTARY B- GeoB17603-3 microfossil abundances

Calcareous nannofossils

Sample	Depth (cm)	Fields	*Braarudosphaera bigelowii*	*Calcidiscus leptoporus*	*Coccolithus pelagicus braarudi*	*Coccolithus pelagicus pelagicus*	*Emiliania huxleyi* < 4 µm	*Emiliania huxleyi* > 4µm	*Gephyrocapsa muellerae*	*Gephyrocapsa oceanica*	*Helicosphaera carteri*	Reworked Cenozoic	Reworked Cretaceous	Small *Gephyrocapsa* spp. (<3)	*Syracosphaera* spp.	*Thoracosphaera* spp.	Total *E. huxleyi*	Total *C. pelagicus*	Total abundance (with reworked)	Total abundance (NO reworked)	Total Reworked
GeoB17603-3-1, 0-1	0	200	1	89	11	3230	2731	4	0	14	1	6	5	42	10	12	2735	3241	6156	6145	11
GeoB17603-3-1, 10-11	10	200	0	107	3	3950	2863	0	0	42	0	1	6	18	14	11	2863	3953	7015	7008	7
GeoB17603-3-1, 20-21	20	200	0	246	7	3883	2949	0	0	35	0	9	12	38	40	9	2949	3890	7228	7207	21
GeoB17603-3-1, 30-31	30	200	0	203	4	2391	2063	2	0	23	0	5	1	40	16	7	2065	2395	4755	4749	6
GeoB17603-3-1, 40-41	40	200	0	60	7	1213	1486	7	0	16	0	3	3	18	0	5	1493	1220	2818	2812	6
GeoB17603-3-1, 50-51	50	200	1	38	1	736	1651	13	0	9	0	4	4	58	6	5	1664	737	2526	2518	8
GeoB17603-3-1, 60-61	60	200	0	55	9	1191	1424	4	1	23	0	1	3	56	6	16	1428	1200	2789	2785	4
GeoB17603-3-1, 70-71	70	200	1	93	6	1944	2307	10	0	38	0	5	5	47	5	3	2317	1950	4464	4454	10
GeoB17603-3-1, 80-81	80	200	0	90	3	972	1615	31	0	13	0	7	2	137	3	5	1646	975	2878	2869	9
GeoB17603-3-2, 90-91	90	200	0	80	1	1128	1114	5	0	8	0	4	5	35	4	10	1119	1129	2394	2385	9

GeoB17603-3-2, 100-101	100	200	1	49	3	935	976	22	0	23	0	9	5	30	3	14	998	938	2070	2056	14
GeoB17603-3-2, 110-111	110	200	0	60	5	2006	1868	17	0	45	0	6	8	35	9	25	1885	2011	4084	4070	14
GeoB17603-3-2, 120-121	120	200	2	55	6	1701	2220	16	0	44	0	5	9	38	3	21	2236	1707	4120	4106	14
GeoB17603-3-2, 130-131	130	200	1	24	5	655	1294	7	0	17	0	1	5	8	0	5	1301	660	2022	2016	6
GeoB17603-3-2, 140-141	140	200	1	26	1	548	1490	18	0	47	0	10	4	31	1	5	1508	549	2182	2168	14
GeoB17603-3-2, 150-151	150	200	1	42	2	2419	2702	10	0	99	0	6	8	64	4	15	2712	2421	5372	5358	14
GeoB17603-3-2, 160-161	160	200	0	63	10	3547	2427	7	1	141	0	4	11	42	2	9	2434	3557	6264	6249	15
GeoB17603-3-2, 170-171	170	200	0	45	8	2806	2905	8	1	178	0	5	9	72	2	13	2913	2814	6052	6038	14
GeoB17603-3-2, 180-181	180	200	1	69	13	1935	4240	25	0	393	1	23	13	51	8	18	4265	1948	6790	6754	36
GeoB17603-3-3, 190-191	190	200	1	85	5	874	2330	31	0	354	0	7	11	15	5	9	2361	879	3727	3709	18
GeoB17603-3-3, 200-201	200	200	0	50	4	833	1617	26	0	200	3	10	5	35	5	8	1643	837	2796	2781	15
GeoB17603-3-3, 210-211	210	200	1	138	12	1743	2552	35	0	257	0	9	11	54	1	23	2587	1755	4836	4816	20
GeoB17603-3-3, 220-221	220	200	0	97	2	932	1781	71	0	377	0	2	2	37	3	11	1852	934	3315	3311	4
GeoB17603-3-3, 230-231	230	200	0	66	3	679	1471	52	2	299	0	10	7	13	8	13	1523	682	2623	2606	17
GeoB17603-3-3, 240-241	240	200	0	69	1	645	1137	133	0	291	0	4	4	22	10	5	1270	646	2321	2313	8
GeoB17603-3-3, 250-251	250	200	1	59	13	726	1604	45	0	264	0	1	5	16	6	6	1649	739	2746	2740	6
GeoB17603-3-3, 260-261	260	200	0	128	2	1392	2830	97	0	513	0	5	11	46	10	15	2927	1394	5049	5033	16
GeoB17603-3-3, 270-271	270	200	1	129	3	1335	2966	62	0	425	0	5	8	52	10	7	3028	1338	5003	4990	13
GeoB17603-3-3, 280-281	280	200	1	97	1	1058	2664	95	0	355	0	2	6	114	4	14	2759	1059	4411	4403	8
GeoB17603-3-4, 290-291	290	200	0	131	4	503	2385	48	0	155	0	6	9	85	4	4	2433	507	3334	3319	15
GeoB17603-3-4, 300-301	300	200	0	41	8	636	1541	52	0	190	1	6	4	82	2	4	1593	644	2567	2557	10
GeoB17603-3-4, 310-311	310	200	0	65	4	523	2230	39	0	165	0	6	7	50	0	6	2269	527	3095	3082	13

GeoB17603-3-4, 320-321	320	200	1	44	6	809	2035	44	2	269	0	5	6	73	3	13	2079	815	3310	3299	11
GeoB17603-3-4, 330-331	330	200	0	23	31	213	1579	48	0	163	0	9	3	82	6	5	1627	244	2162	2150	12
GeoB17603-3-4, 340-341	340	200	0	20	24	349	2149	19	0	104	0	4	6	150	2	11	2168	373	2838	2828	10
GeoB17603-3-4, 350-351	350	200	2	30	5	272	2876	25	0	178	1	12	9	213	6	10	2901	277	3639	3618	21
GeoB17603-3-4, 360-361	360	200	0	32	4	98	1994	29	0	120	1	8	5	101	1	2	2023	102	2395	2382	13
GeoB17603-3-4, 370-371	370	200	0	17	13	203	1952	35	0	108	0	6	7	145	2	3	1987	216	2491	2478	13
GeoB17603-3-4, 380-381	380	200	1	31	22	256	3047	46	2	131	0	11	8	437	9	9	3093	278	4010	3991	19
GeoB17603-3-5, 390-391	390	200	0	22	2	73	1468	27	0	78	1	8	1	129	0	1	1495	75	1810	1801	9
GeoB17603-3-5, 400-401	400	200	0	13	1	20	800	10	0	24	0	4	1	54	2	0	810	21	929	924	5
GeoB17603-3-5, 410-411	410	200	0	7	1	13	667	6	0	51	0	3	2	56	2	0	673	14	808	803	5
GeoB17603-3-5, 420-421	420	200	0	16	2	39	2428	4	0	59	0	13	8	225	5	2	2432	41	2801	2780	21
GeoB17603-3-5, 430-431	430	200	0	10	0	0	584	3	1	28	0	8	0	38	0	0	587	0	672	664	8
GeoB17603-3-5, 440-441	440	200	0	12	0	0	1265	8	1	46	0	4	0	133	7	0	1273	0	1476	1472	4
GeoB17603-3-5, 450-451	450	200	0	12	1	0	1350	32	0	31	0	12	3	81	4	0	1382	1	1526	1511	15
GeoB17603-3-5, 460-461	460	200	1	36	0	3	2820	35	0	90	1	21	1	141	3	1	2855	3	3153	3131	22
GeoB17603-3-5, 470-471	470	200	0	35	0	4	3079	13	3	64	0	18	5	198	1	2	3092	4	3422	3399	23
GeoB17603-3-5, 480-481	480	200	1	37	3	5	2779	21	3	87	0	20	2	120	0	4	2800	8	3082	3060	22
GeoB17603-3-6, 490-491	490	200	0	48	2	1	2250	36	2	64	0	18	1	47	1	2	2286	3	2472	2453	19
GeoB17603-3-6, 500-501	500	200	0	35	1	3	1510	25	0	80	0	24	2	69	2	2	1535	4	1753	1727	26
GeoB17603-3-6, 510-511	510	200	0	72	0	2	1560	18	3	96	0	12	0	17	5	2	1578	2	1787	1775	12
GeoB17603-3-6, 520-521	520	200	0	33	0	2	1654	31	4	71	0	5	3	56	1	1	1685	2	1861	1853	8
GeoB17603-3-6, 530-531	530	200	0	32	0	7	1792	7	1	73	0	4	2	49	0	5	1799	7	1972	1966	6

GeoB17603-3-6, 540-541	540	200	0	33	0	6	3491	38	7	228	0	29	3	59	4	8	3529	6	3906	3874	32
GeoB17603-3-6, 550-551	550	200	0	8	0	3	1344	18	4	57	1	21	1	39	3	1	1362	3	1500	1478	22
GeoB17603-3-6, 560-561	560	200	1	11	14	5	2101	42	11	145	3	53	8	17	1	4	2143	19	2416	2355	61
GeoB17603-3-6, 570-571	570	200	0	8	0	3	1142	29	22	16	0	27	6	8	4	1	1171	3	1266	1233	33
GeoB17603-3-6, 580-581	580	200	0	4	0	2	1471	18	15	25	0	33	7	11	1	5	1489	2	1592	1552	40
GeoB17603-3-7, 590-591	590	200	0	20	0	1	454	11	15	3	0	14	3	7	0	2	465	1	530	513	17
GeoB17603-3-7, 600-601	600	200	0	27	0	1	542	5	8	5	0	18	3	3	0	3	547	1	615	594	21
GeoB17603-3-7, 610-611	610	200	0	1	0	0	329	4	10	1	0	16	3	11	1	2	333	0	378	359	19
GeoB17603-3-7, 620-621	620	200	0	1	0	1	156	4	4	1	0	8	3	7	0	0	160	1	185	174	11
GeoB17603-3-7, 630-631	630	200	0	0	15	1	776	36	3	1	0	11	5	4	0	0	812	16	852	836	16
GeoB17603-3-7, 640-641	640	200	0	0	0	0	162	14	5	0	0	1	1	9	0	1	176	0	193	191	2
GeoB17603-3-7, 650-651	650	200	0	1	0	0	146	19	4	1	1	5	2	8	0	1	165	0	188	181	7
GeoB17603-3-7, 660-661	660	200	0	0	0	0	1	0	0	0	0	1	1	0	0	0	1	0	3	1	2
GeoB17603-3-7, 670-671	670	200	0	2	0	3	462	56	10	0	0	4	7	1	0	2	518	3	547	536	11
GeoB17603-3-7, 680-681	680	200	0	2	4	1	509	90	18	3	0	1	3	2	0	0	599	5	633	629	4
GeoB17603-3-8, 690-691	690	200	0	2	0	3	151	26	8	0	0	3	1	0	0	0	177	3	194	190	4
GeoB17603-3-8, 700-701	700	200	0	0	0	0	30	3	3	0	0	0	0	0	0	0	33	0	36	36	0
GeoB17603-3-8, 710-711	710	200	0	3	0	0	561	110	2	0	0	2	12	0	0	0	671	0	690	676	14
GeoB17603-3-8, 720-721	720	200	0	0	0	0	68	31	2	0	0	1	1	0	1	0	99	0	104	102	2
GeoB17603-3-8, 730-731	730	200	0	1	0	0	147	17	7	0	0	0	5	0	0	1	164	0	178	173	5
GeoB17603-3-8, 740-741	740	200	0	1	1	0	321	33	13	1	0	3	3	0	0	0	354	1	376	370	6
GeoB17603-3-8, 750-751	750	200	0	0	0	0	2	1	0	0	0	0	1	0	0	0	3	0	4	3	1

GeoB17603-3-8, 760-761	760	200	0	2	0	0	130	39	4	0	0	2	2	0	0	0	169	0	179	175	4
GeoB17603-3-8, 770-771	770	200	0	1	0	0	281	39	13	1	0	3	7	0	0	0	320	0	345	335	10
GeoB17603-3-8, 780-781	780	200	0	0	0	2	167	44	29	0	0	1	5	0	0	0	211	2	248	242	6
GeoB17603-3-9, 790-791	790	200	0	0	0	0	132	30	16	1	0	1	3	0	1	1	162	0	185	181	4
GeoB17603-3-9, 800-801	800	200	0	0	0	0	101	22	5	0	0	2	10	0	0	0	123	0	140	128	12
GeoB17603-3-9, 810-811	810	200	0	1	0	0	89	32	10	0	0	1	7	0	0	0	121	0	140	132	8
GeoB17603-3-9, 820-821	820	200	0	0	0	0	66	26	14	0	0	1	6	0	0	0	92	0	113	106	7
GeoB17603-3-9, 830-831	830	200	0	0	0	0	61	8	11	0	0	2	9	0	0	0	69	0	91	80	11
GeoB17603-3-9, 840-841	840	200	0	0	0	0	30	24	3	0	0	1	4	0	0	0	54	0	62	57	5
GeoB17603-3-9, 850-851	850	200	0	0	0	0	7	3	0	0	0	0	0	0	0	0	10	0	10	10	0
GeoB17603-3-9, 860-861	860	200	0	0	0	0	35	11	0	0	0	2	1	0	0	0	46	0	49	46	3
GeoB17603-3-9, 870-871	870	200	0	0	0	0	28	10	1	0	0	0	3	1	0	0	38	0	43	40	3
GeoB17603-3-9, 880-881	880	200	0	0	0	0	18	9	1	0	0	0	0	1	1	0	27	0	30	30	0
GeoB17603-3-10, 890-891	890	200	0	0	0	0	0	0	0	0	0	0	0	0	0	0	0	0	0	0	0
GeoB17603-3-10, 900-901	900	200	0	0	0	0	6	2	0	0	0	0	2	0	0	0	8	0	10	8	2
GeoB17603-3-10, 910-911	910	200	0	0	0	0	2	2	0	0	0	0	3	0	0	0	4	0	7	4	3
GeoB17603-3-10, 920-921	920	200	0	0	0	0	13	11	0	0	0	0	4	0	0	0	24	0	28	24	4
GeoB17603-3-10, 930-931	930	200	0	0	0	0	8	9	1	0	0	1	7	0	0	0	17	0	26	18	8
GeoB17603-3-10, 940-941	940	200	0	0	0	1	1	0	0	0	0	0	0	0	0	0	1	1	2	2	0
GeoB17603-3-10, 950-951	950	200	0	0	0	0	10	11	0	0	0	0	4	0	0	1	21	0	26	22	4
GeoB17603-3-10, 960-961	960	200	0	0	0	1	16	8	1	0	0	0	1	0	0	0	24	1	27	26	1
GeoB17603-3-10, 970-971	970	200	0	0	0	2	129	49	10	0	0	0	4	0	0	0	178	2	194	190	4

Sample	Depth (cm)	Observed surface (mm^2)	*B. bigelowii*/10 mm^2	*C. leptoporus*/10 mm^2	*C. pel. braarudi*/10 mm^2	*C. pel. pelagicus*/10 mm^2	*E. huxleyi* < 4 µm/10 mm^2	*E. huxleyi* > 4µm/10 mm^2	*G. muellerae*/10 mm^2	*G. oceanica*/10 mm^2	*H. carteri*/10 mm^2	Reworked Cenozoic/10 mm^2	Reworked Cretaceous/10 mm^2	Small *Gephyrocapsa* spp. (<3)/10 mm^2	*Syracosphaera* spp./10 mm^2	*Thoracosphaera* spp. /10 mm^2
GeoB17603-3-1, 0-1	0	6,28	1,6	141,7	17,5	5143,3	4348,7	6,4	0,0	22,3	1,6	9,6	8,0	66,9	15,9	19,1
GeoB17603-3-1, 10-11	10	6,28	0,0	170,4	4,8	6289,8	4558,9	0,0	0,0	66,9	0,0	1,6	9,6	28,7	22,3	17,5
GeoB17603-3-1, 20-21	20	6,28	0,0	391,7	11,1	6183,1	4695,9	0,0	0,0	55,7	0,0	14,3	19,1	60,5	63,7	14,3
GeoB17603-3-1, 30-31	30	6,28	0,0	323,2	6,4	3807,3	3285,0	3,2	0,0	36,6	0,0	8,0	1,6	63,7	25,5	11,1
GeoB17603-3-1, 40-41	40	6,28	0,0	95,5	11,1	1931,5	2366,2	11,1	0,0	25,5	0,0	4,8	4,8	28,7	0,0	8,0
GeoB17603-3-1, 50-51	50	6,28	1,6	60,5	1,6	1172,0	2629,0	20,7	0,0	14,3	0,0	6,4	6,4	92,4	9,6	8,0
GeoB17603-3-1, 60-61	60	6,28	0,0	87,6	14,3	1896,5	2267,5	6,4	1,6	36,6	0,0	1,6	4,8	89,2	9,6	25,5
GeoB17603-3-1, 70-71	70	6,28	1,6	148,1	9,6	3095,5	3673,6	15,9	0,0	60,5	0,0	8,0	8,0	74,8	8,0	4,8
GeoB17603-3-1, 80-81	80	6,28	0,0	143,3	4,8	1547,8	2571,7	49,4	0,0	20,7	0,0	11,1	3,2	218,2	4,8	8,0
GeoB17603-3-2, 90-91	90	6,28	0,0	127,4	1,6	1796,2	1773,9	8,0	0,0	12,7	0,0	6,4	8,0	55,7	6,4	15,9
GeoB17603-3-2, 100-101	100	6,28	1,6	78,0	4,8	1488,9	1554,1	35,0	0,0	36,6	0,0	14,3	8,0	47,8	4,8	22,3
GeoB17603-3-2, 110-111	110	6,28	0,0	95,5	8,0	3194,3	2974,5	27,1	0,0	71,7	0,0	9,6	12,7	55,7	14,3	39,8
GeoB17603-3-2, 120-121	120	6,28	3,2	87,6	9,6	2708,6	3535,0	25,5	0,0	70,1	0,0	8,0	14,3	60,5	4,8	33,4

GeoB17603-3-2, 130-131	130	6,28	1,6	38,2	8,0	1043,0	2060,5	11,1	0,0	27,1	0,0	1,6	8,0	12,7	0,0	8,0
GeoB17603-3-2, 140-141	140	6,28	1,6	41,4	1,6	872,6	2372,6	28,7	0,0	74,8	0,0	15,9	6,4	49,4	1,6	8,0
GeoB17603-3-2, 150-151	150	6,28	1,6	66,9	3,2	3851,9	4302,5	15,9	0,0	157,6	0,0	9,6	12,7	101,9	6,4	23,9
GeoB17603-3-2, 160-161	160	6,28	0,0	100,3	15,9	5648,1	3864,6	11,1	1,6	224,5	0,0	6,4	17,5	66,9	3,2	14,3
GeoB17603-3-2, 170-171	170	6,28	0,0	71,7	12,7	4468,2	4625,8	12,7	1,6	283,4	0,0	8,0	14,3	114,6	3,2	20,7
GeoB17603-3-2, 180-181	180	6,28	1,6	109,9	20,7	3081,2	6751,6	39,8	0,0	625,8	1,6	36,6	20,7	81,2	12,7	28,7
GeoB17603-3-3, 190-191	190	6,28	1,6	135,4	8,0	1391,7	3710,2	49,4	0,0	563,7	0,0	11,1	17,5	23,9	8,0	14,3
GeoB17603-3-3, 200-201	200	6,28	0,0	79,6	6,4	1326,4	2574,8	41,4	0,0	318,5	4,8	15,9	8,0	55,7	8,0	12,7
GeoB17603-3-3, 210-211	210	6,28	1,6	219,7	19,1	2775,5	4063,7	55,7	0,0	409,2	0,0	14,3	17,5	86,0	1,6	36,6
GeoB17603-3-3, 220-221	220	6,28	0,0	154,5	3,2	1484,1	2836,0	113,1	0,0	600,3	0,0	3,2	3,2	58,9	4,8	17,5
GeoB17603-3-3, 230-231	230	6,28	0,0	105,1	4,8	1081,2	2342,4	82,8	3,2	476,1	0,0	15,9	11,1	20,7	12,7	20,7
GeoB17603-3-3, 240-241	240	6,28	0,0	109,9	1,6	1027,1	1810,5	211,8	0,0	463,4	0,0	6,4	6,4	35,0	15,9	8,0
GeoB17603-3-3, 250-251	250	6,28	1,6	93,9	20,7	1156,1	2554,1	71,7	0,0	420,4	0,0	1,6	8,0	25,5	9,6	9,6
GeoB17603-3-3, 260-261	260	6,28	0,0	203,8	3,2	2216,6	4506,4	154,5	0,0	816,9	0,0	8,0	17,5	73,2	15,9	23,9
GeoB17603-3-3, 270-271	270	6,28	1,6	205,4	4,8	2125,8	4722,9	98,7	0,0	676,8	0,0	8,0	12,7	82,8	15,9	11,1
GeoB17603-3-3, 280-281	280	6,28	1,6	154,5	1,6	1684,7	4242,0	151,3	0,0	565,3	0,0	3,2	9,6	181,5	6,4	22,3
GeoB17603-3-4, 290-291	290	6,28	0,0	208,6	6,4	801,0	3797,8	76,4	0,0	246,8	0,0	9,6	14,3	135,4	6,4	6,4
GeoB17603-3-4, 300-301	300	6,28	0,0	65,3	12,7	1012,7	2453,8	82,8	0,0	302,5	1,6	9,6	6,4	130,6	3,2	6,4
GeoB17603-3-4, 310-311	310	6,28	0,0	103,5	6,4	832,8	3551,0	62,1	0,0	262,7	0,0	9,6	11,1	79,6	0,0	9,6
GeoB17603-3-4, 320-321	320	6,28	1,6	70,1	9,6	1288,2	3240,4	70,1	3,2	428,3	0,0	8,0	9,6	116,2	4,8	20,7
GeoB17603-3-4, 330-331	330	6,28	0,0	36,6	49,4	339,2	2514,3	76,4	0,0	259,6	0,0	14,3	4,8	130,6	9,6	8,0
GeoB17603-3-4, 340-341	340	6,28	0,0	31,8	38,2	555,7	3422,0	30,3	0,0	165,6	0,0	6,4	9,6	238,9	3,2	17,5

GeoB17603-3-4, 350-351	350	6,28	3,2	47,8	8,0	433,1	4579,6	39,8	0,0	283,4	1,6	19,1	14,3	339,2	9,6	15,9
GeoB17603-3-4, 360-361	360	6,28	0,0	51,0	6,4	156,1	3175,2	46,2	0,0	191,1	1,6	12,7	8,0	160,8	1,6	3,2
GeoB17603-3-4, 370-371	370	6,28	0,0	27,1	20,7	323,2	3108,3	55,7	0,0	172,0	0,0	9,6	11,1	230,9	3,2	4,8
GeoB17603-3-4, 380-381	380	6,28	1,6	49,4	35,0	407,6	4851,9	73,2	3,2	208,6	0,0	17,5	12,7	695,9	14,3	14,3
GeoB17603-3-5, 390-391	390	6,28	0,0	35,0	3,2	116,2	2337,6	43,0	0,0	124,2	1,6	12,7	1,6	205,4	0,0	1,6
GeoB17603-3-5, 400-401	400	6,28	0,0	20,7	1,6	31,8	1273,9	15,9	0,0	38,2	0,0	6,4	1,6	86,0	3,2	0,0
GeoB17603-3-5, 410-411	410	6,28	0,0	11,1	1,6	20,7	1062,1	9,6	0,0	81,2	0,0	4,8	3,2	89,2	3,2	0,0
GeoB17603-3-5, 420-421	420	6,28	0,0	25,5	3,2	62,1	3866,2	6,4	0,0	93,9	0,0	20,7	12,7	358,3	8,0	3,2
GeoB17603-3-5, 430-431	430	6,28	0,0	15,9	0,0	0,0	929,9	4,8	1,6	44,6	0,0	12,7	0,0	60,5	0,0	0,0
GeoB17603-3-5, 440-441	440	6,28	0,0	19,1	0,0	0,0	2014,3	12,7	1,6	73,2	0,0	6,4	0,0	211,8	11,1	0,0
GeoB17603-3-5, 450-451	450	6,28	0,0	19,1	1,6	0,0	2149,7	51,0	0,0	49,4	0,0	19,1	4,8	129,0	6,4	0,0
GeoB17603-3-5, 460-461	460	6,28	1,6	57,3	0,0	4,8	4490,4	55,7	0,0	143,3	1,6	33,4	1,6	224,5	4,8	1,6
GeoB17603-3-5, 470-471	470	6,28	0,0	55,7	0,0	6,4	4902,9	20,7	4,8	101,9	0,0	28,7	8,0	315,3	1,6	3,2
GeoB17603-3-5, 480-481	480	6,28	1,6	58,9	4,8	8,0	4425,2	33,4	4,8	138,5	0,0	31,8	3,2	191,1	0,0	6,4
GeoB17603-3-6, 490-491	490	6,28	0,0	76,4	3,2	1,6	3582,8	57,3	3,2	101,9	0,0	28,7	1,6	74,8	1,6	3,2
GeoB17603-3-6, 500-501	500	6,28	0,0	55,7	1,6	4,8	2404,5	39,8	0,0	127,4	0,0	38,2	3,2	109,9	3,2	3,2
GeoB17603-3-6, 510-511	510	6,28	0,0	114,6	0,0	3,2	2484,1	28,7	4,8	152,9	0,0	19,1	0,0	27,1	8,0	3,2
GeoB17603-3-6, 520-521	520	6,28	0,0	52,5	0,0	3,2	2633,8	49,4	6,4	113,1	0,0	8,0	4,8	89,2	1,6	1,6
GeoB17603-3-6, 530-531	530	6,28	0,0	51,0	0,0	11,1	2853,5	11,1	1,6	116,2	0,0	6,4	3,2	78,0	0,0	8,0
GeoB17603-3-6, 540-541	540	6,28	0,0	52,5	0,0	9,6	5558,9	60,5	11,1	363,1	0,0	46,2	4,8	93,9	6,4	12,7
GeoB17603-3-6, 550-551	550	6,28	0,0	12,7	0,0	4,8	2140,1	28,7	6,4	90,8	1,6	33,4	1,6	62,1	4,8	1,6
GeoB17603-3-6, 560-561	560	6,28	1,6	17,5	22,3	8,0	3345,5	66,9	17,5	230,9	4,8	84,4	12,7	27,1	1,6	6,4

GeoB17603-3-6, 570-571	570	6,28	0,0	12,7	0,0	4,8	1818,5	46,2	35,0	25,5	0,0	43,0	9,6	12,7	6,4	1,6
GeoB17603-3-6, 580-581	580	6,28	0,0	6,4	0,0	3,2	2342,4	28,7	23,9	39,8	0,0	52,5	11,1	17,5	1,6	8,0
GeoB17603-3-7, 590-591	590	6,28	0,0	31,8	0,0	1,6	722,9	17,5	23,9	4,8	0,0	22,3	4,8	11,1	0,0	3,2
GeoB17603-3-7, 600-601	600	6,28	0,0	43,0	0,0	1,6	863,1	8,0	12,7	8,0	0,0	28,7	4,8	4,8	0,0	4,8
GeoB17603-3-7, 610-611	610	6,28	0,0	1,6	0,0	0,0	523,9	6,4	15,9	1,6	0,0	25,5	4,8	17,5	1,6	3,2
GeoB17603-3-7, 620-621	620	6,28	0,0	1,6	0,0	1,6	248,4	6,4	6,4	1,6	0,0	12,7	4,8	11,1	0,0	0,0
GeoB17603-3-7, 630-631	630	6,28	0,0	0,0	23,9	1,6	1235,7	57,3	4,8	1,6	0,0	17,5	8,0	6,4	0,0	0,0
GeoB17603-3-7, 640-641	640	6,28	0,0	0,0	0,0	0,0	258,0	22,3	8,0	0,0	0,0	1,6	1,6	14,3	0,0	1,6
GeoB17603-3-7, 650-651	650	6,28	0,0	1,6	0,0	0,0	232,5	30,3	6,4	1,6	1,6	8,0	3,2	12,7	0,0	1,6
GeoB17603-3-7, 660-661	660	6,28	0,0	0,0	0,0	0,0	1,6	0,0	0,0	0,0	0,0	1,6	1,6	0,0	0,0	0,0
GeoB17603-3-7, 670-671	670	6,28	0,0	3,2	0,0	4,8	735,7	89,2	15,9	0,0	0,0	6,4	11,1	1,6	0,0	3,2
GeoB17603-3-7, 680-681	680	6,28	0,0	3,2	6,4	1,6	810,5	143,3	28,7	4,8	0,0	1,6	4,8	3,2	0,0	0,0
GeoB17603-3-8, 690-691	690	6,28	0,0	3,2	0,0	4,8	240,4	41,4	12,7	0,0	0,0	4,8	1,6	0,0	0,0	0,0
GeoB17603-3-8, 700-701	700	6,28	0,0	0,0	0,0	0,0	47,8	4,8	4,8	0,0	0,0	0,0	0,0	0,0	0,0	0,0
GeoB17603-3-8, 710-711	710	6,28	0,0	4,8	0,0	0,0	893,3	175,2	3,2	0,0	0,0	3,2	19,1	0,0	0,0	0,0
GeoB17603-3-8, 720-721	720	6,28	0,0	0,0	0,0	0,0	108,3	49,4	3,2	0,0	0,0	1,6	1,6	0,0	1,6	0,0
GeoB17603-3-8, 730-731	730	6,28	0,0	1,6	0,0	0,0	234,1	27,1	11,1	0,0	0,0	0,0	8,0	0,0	0,0	1,6
GeoB17603-3-8, 740-741	740	6,28	0,0	1,6	1,6	0,0	511,1	52,5	20,7	1,6	0,0	4,8	4,8	0,0	0,0	0,0
GeoB17603-3-8, 750-751	750	6,28	0,0	0,0	0,0	0,0	3,2	1,6	0,0	0,0	0,0	0,0	1,6	0,0	0,0	0,0
GeoB17603-3-8, 760-761	760	6,28	0,0	3,2	0,0	0,0	207,0	62,1	6,4	0,0	0,0	3,2	3,2	0,0	0,0	0,0
GeoB17603-3-8, 770-771	770	6,28	0,0	1,6	0,0	0,0	447,5	62,1	20,7	1,6	0,0	4,8	11,1	0,0	0,0	0,0
GeoB17603-3-8, 780-781	780	6,28	0,0	0,0	0,0	3,2	265,9	70,1	46,2	0,0	0,0	1,6	8,0	0,0	0,0	0,0

GeoB17603-3-9, 790-791	790	6,28	0,0	0,0	0,0	0,0	210,2	47,8	25,5	1,6	0,0	1,6	4,8	0,0	1,6	1,6
GeoB17603-3-9, 800-801	800	6,28	0,0	0,0	0,0	0,0	160,8	35,0	8,0	0,0	0,0	3,2	15,9	0,0	0,0	0,0
GeoB17603-3-9, 810-811	810	6,28	0,0	1,6	0,0	0,0	141,7	51,0	15,9	0,0	0,0	1,6	11,1	0,0	0,0	0,0
GeoB17603-3-9, 820-821	820	6,28	0,0	0,0	0,0	0,0	105,1	41,4	22,3	0,0	0,0	1,6	9,6	0,0	0,0	0,0
GeoB17603-3-9, 830-831	830	6,28	0,0	0,0	0,0	0,0	97,1	12,7	17,5	0,0	0,0	3,2	14,3	0,0	0,0	0,0
GeoB17603-3-9, 840-841	840	6,28	0,0	0,0	0,0	0,0	47,8	38,2	4,8	0,0	0,0	1,6	6,4	0,0	0,0	0,0
GeoB17603-3-9, 850-851	850	6,28	0,0	0,0	0,0	0,0	11,1	4,8	0,0	0,0	0,0	0,0	0,0	0,0	0,0	0,0
GeoB17603-3-9, 860-861	860	6,28	0,0	0,0	0,0	0,0	55,7	17,5	0,0	0,0	0,0	3,2	1,6	0,0	0,0	0,0
GeoB17603-3-9, 870-871	870	6,28	0,0	0,0	0,0	0,0	44,6	15,9	1,6	0,0	0,0	0,0	4,8	1,6	0,0	0,0
GeoB17603-3-9, 880-881	880	6,28	0,0	0,0	0,0	0,0	28,7	14,3	1,6	0,0	0,0	0,0	0,0	1,6	1,6	0,0
GeoB17603-3-10, 890-891	890	6,28	0,0	0,0	0,0	0,0	0,0	0,0	0,0	0,0	0,0	0,0	0,0	0,0	0,0	0,0
GeoB17603-3-10, 900-901	900	6,28	0,0	0,0	0,0	0,0	9,6	3,2	0,0	0,0	0,0	0,0	3,2	0,0	0,0	0,0
GeoB17603-3-10, 910-911	910	6,28	0,0	0,0	0,0	0,0	3,2	3,2	0,0	0,0	0,0	0,0	4,8	0,0	0,0	0,0
GeoB17603-3-10, 920-921	920	6,28	0,0	0,0	0,0	0,0	20,7	17,5	0,0	0,0	0,0	0,0	6,4	0,0	0,0	0,0
GeoB17603-3-10, 930-931	930	6,28	0,0	0,0	0,0	0,0	12,7	14,3	1,6	0,0	0,0	1,6	11,1	0,0	0,0	0,0
GeoB17603-3-10, 940-941	940	6,28	0,0	0,0	0,0	1,6	1,6	0,0	0,0	0,0	0,0	0,0	0,0	0,0	0,0	0,0
GeoB17603-3-10, 950-951	950	6,28	0,0	0,0	0,0	0,0	15,9	17,5	0,0	0,0	0,0	0,0	6,4	0,0	0,0	1,6
GeoB17603-3-10, 960-961	960	6,28	0,0	0,0	0,0	1,6	25,5	12,7	1,6	0,0	0,0	0,0	1,6	0,0	0,0	0,0
GeoB17603-3-10, 970-971	970	6,28	0,0	0,0	0,0	3,2	205,4	78,0	15,9	0,0	0,0	0,0	6,4	0,0	0,0	0,0

Sample	Depth (cm)	Observed surface (mm^2)	Total *E. huxleyi* /10 mm^2	Total *C. pelagicus* /10 mm^2	Total abundance (with reworked) /10 mm^2	Total abundance (NO reworked) /10 mm^2	Total Reworked /10 mm^2
GeoB17603-3-1, 0-1	0	6,28	4355,1	5160,8	9802,5	9785,0	17,5
GeoB17603-3-1, 10-11	10	6,28	4558,9	6294,6	11170,4	11159,2	11,1
GeoB17603-3-1, 20-21	20	6,28	4695,9	6194,3	11509,6	11476,1	33,4
GeoB17603-3-1, 30-31	30	6,28	3288,2	3813,7	7571,7	7562,1	9,6
GeoB17603-3-1, 40-41	40	6,28	2377,4	1942,7	4487,3	4477,7	9,6
GeoB17603-3-1, 50-51	50	6,28	2649,7	1173,6	4022,3	4009,6	12,7
GeoB17603-3-1, 60-61	60	6,28	2273,9	1910,8	4441,1	4434,7	6,4
GeoB17603-3-1, 70-71	70	6,28	3689,5	3105,1	7108,3	7092,4	15,9
GeoB17603-3-1, 80-81	80	6,28	2621,0	1552,5	4582,8	4568,5	14,3
GeoB17603-3-2, 90-91	90	6,28	1781,8	1797,8	3812,1	3797,8	14,3
GeoB17603-3-2, 100-101	100	6,28	1589,2	1493,6	3296,2	3273,9	22,3

GeoB17603-3-2, 110-111	110	6,28	3001,6	3202,2	6503,2	6480,9	22,3
GeoB17603-3-2, 120-121	120	6,28	3560,5	2718,2	6560,5	6538,2	22,3
GeoB17603-3-2, 130-131	130	6,28	2071,7	1051,0	3219,7	3210,2	9,6
GeoB17603-3-2, 140-141	140	6,28	2401,3	874,2	3474,5	3452,2	22,3
GeoB17603-3-2, 150-151	150	6,28	4318,5	3855,1	8554,1	8531,8	22,3
GeoB17603-3-2, 160-161	160	6,28	3875,8	5664,0	9974,5	9950,6	23,9
GeoB17603-3-2, 170-171	170	6,28	4638,5	4480,9	9636,9	9614,6	22,3
GeoB17603-3-2, 180-181	180	6,28	6791,4	3101,9	10812,1	10754,8	57,3
GeoB17603-3-3, 190-191	190	6,28	3759,6	1399,7	5934,7	5906,1	28,7
GeoB17603-3-3, 200-201	200	6,28	2616,2	1332,8	4452,2	4428,3	23,9
GeoB17603-3-3, 210-211	210	6,28	4119,4	2794,6	7700,6	7668,8	31,8
GeoB17603-3-3, 220-221	220	6,28	2949,0	1487,3	5278,7	5272,3	6,4
GeoB17603-3-3, 230-231	230	6,28	2425,2	1086,0	4176,8	4149,7	27,1
GeoB17603-3-3, 240-241	240	6,28	2022,3	1028,7	3695,9	3683,1	12,7
GeoB17603-3-3, 250-251	250	6,28	2625,8	1176,8	4372,6	4363,1	9,6
GeoB17603-3-3, 260-261	260	6,28	4660,8	2219,7	8039,8	8014,3	25,5
GeoB17603-3-3, 270-271	270	6,28	4821,7	2130,6	7966,6	7945,9	20,7
GeoB17603-3-3, 280-281	280	6,28	4393,3	1686,3	7023,9	7011,1	12,7
GeoB17603-3-4, 290-291	290	6,28	3874,2	807,3	5308,9	5285,0	23,9
GeoB17603-3-4, 300-301	300	6,28	2536,6	1025,5	4087,6	4071,7	15,9
GeoB17603-3-4, 310-311	310	6,28	3613,1	839,2	4928,3	4907,6	20,7
GeoB17603-3-4, 320-321	320	6,28	3310,5	1297,8	5270,7	5253,2	17,5

GeoB17603-3-4, 330-331	330	6,28	2590,8	388,5	3442,7	3423,6	19,1
GeoB17603-3-4, 340-341	340	6,28	3452,2	593,9	4519,1	4503,2	15,9
GeoB17603-3-4, 350-351	350	6,28	4619,4	441,1	5794,6	5761,1	33,4
GeoB17603-3-4, 360-361	360	6,28	3221,3	162,4	3813,7	3793,0	20,7
GeoB17603-3-4, 370-371	370	6,28	3164,0	343,9	3966,6	3945,9	20,7
GeoB17603-3-4, 380-381	380	6,28	4925,2	442,7	6385,4	6355,1	30,3
GeoB17603-3-5, 390-391	390	6,28	2380,6	119,4	2882,2	2867,8	14,3
GeoB17603-3-5, 400-401	400	6,28	1289,8	33,4	1479,3	1471,3	8,0
GeoB17603-3-5, 410-411	410	6,28	1071,7	22,3	1286,6	1278,7	8,0
GeoB17603-3-5, 420-421	420	6,28	3872,6	65,3	4460,2	4426,8	33,4
GeoB17603-3-5, 430-431	430	6,28	934,7	0,0	1070,1	1057,3	12,7
GeoB17603-3-5, 440-441	440	6,28	2027,1	0,0	2350,3	2343,9	6,4
GeoB17603-3-5, 450-451	450	6,28	2200,6	1,6	2429,9	2406,1	23,9
GeoB17603-3-5, 460-461	460	6,28	4546,2	4,8	5020,7	4985,7	35,0
GeoB17603-3-5, 470-471	470	6,28	4923,6	6,4	5449,0	5412,4	36,6
GeoB17603-3-5, 480-481	480	6,28	4458,6	12,7	4907,6	4872,6	35,0
GeoB17603-3-6, 490-491	490	6,28	3640,1	4,8	3936,3	3906,1	30,3
GeoB17603-3-6, 500-501	500	6,28	2444,3	6,4	2791,4	2750,0	41,4
GeoB17603-3-6, 510-511	510	6,28	2512,7	3,2	2845,5	2826,4	19,1
GeoB17603-3-6, 520-521	520	6,28	2683,1	3,2	2963,4	2950,6	12,7
GeoB17603-3-6, 530-531	530	6,28	2864,6	11,1	3140,1	3130,6	9,6
GeoB17603-3-6, 540-541	540	6,28	5619,4	9,6	6219,7	6168,8	51,0

GeoB17603-3-6, 550-551	550	6,28	2168,8	4,8	2388,5	2353,5	35,0
GeoB17603-3-6, 560-561	560	6,28	3412,4	30,3	3847,1	3750,0	97,1
GeoB17603-3-6, 570-571	570	6,28	1864,6	4,8	2015,9	1963,4	52,5
GeoB17603-3-6, 580-581	580	6,28	2371,0	3,2	2535,0	2471,3	63,7
GeoB17603-3-7, 590-591	590	6,28	740,4	1,6	843,9	816,9	27,1
GeoB17603-3-7, 600-601	600	6,28	871,0	1,6	979,3	945,9	33,4
GeoB17603-3-7, 610-611	610	6,28	530,3	0,0	601,9	571,7	30,3
GeoB17603-3-7, 620-621	620	6,28	254,8	1,6	294,6	277,1	17,5
GeoB17603-3-7, 630-631	630	6,28	1293,0	25,5	1356,7	1331,2	25,5
GeoB17603-3-7, 640-641	640	6,28	280,3	0,0	307,3	304,1	3,2
GeoB17603-3-7, 650-651	650	6,28	262,7	0,0	299,4	288,2	11,1
GeoB17603-3-7, 660-661	660	6,28	1,6	0,0	4,8	1,6	3,2
GeoB17603-3-7, 670-671	670	6,28	824,8	4,8	871,0	853,5	17,5
GeoB17603-3-7, 680-681	680	6,28	953,8	8,0	1008,0	1001,6	6,4
GeoB17603-3-8, 690-691	690	6,28	281,8	4,8	308,9	302,5	6,4
GeoB17603-3-8, 700-701	700	6,28	52,5	0,0	57,3	57,3	0,0
GeoB17603-3-8, 710-711	710	6,28	1068,5	0,0	1098,7	1076,4	22,3
GeoB17603-3-8, 720-721	720	6,28	157,6	0,0	165,6	162,4	3,2
GeoB17603-3-8, 730-731	730	6,28	261,1	0,0	283,4	275,5	8,0
GeoB17603-3-8, 740-741	740	6,28	563,7	1,6	598,7	589,2	9,6
GeoB17603-3-8, 750-751	750	6,28	4,8	0,0	6,4	4,8	1,6
GeoB17603-3-8, 760-761	760	6,28	269,1	0,0	285,0	278,7	6,4

GeoB17603-3-8, 770-771	770	6,28	509,6	0,0	549,4	533,4	15,9
GeoB17603-3-8, 780-781	780	6,28	336,0	3,2	394,9	385,4	9,6
GeoB17603-3-9, 790-791	790	6,28	258,0	0,0	294,6	288,2	6,4
GeoB17603-3-9, 800-801	800	6,28	195,9	0,0	222,9	203,8	19,1
GeoB17603-3-9, 810-811	810	6,28	192,7	0,0	222,9	210,2	12,7
GeoB17603-3-9, 820-821	820	6,28	146,5	0,0	179,9	168,8	11,1
GeoB17603-3-9, 830-831	830	6,28	109,9	0,0	144,9	127,4	17,5
GeoB17603-3-9, 840-841	840	6,28	86,0	0,0	98,7	90,8	8,0
GeoB17603-3-9, 850-851	850	6,28	15,9	0,0	15,9	15,9	0,0
GeoB17603-3-9, 860-861	860	6,28	73,2	0,0	78,0	73,2	4,8
GeoB17603-3-9, 870-871	870	6,28	60,5	0,0	68,5	63,7	4,8
GeoB17603-3-9, 880-881	880	6,28	43,0	0,0	47,8	47,8	0,0
GeoB17603-3-10, 890-891	890	6,28	0,0	0,0	0,0	0,0	0,0
GeoB17603-3-10, 900-901	900	6,28	12,7	0,0	15,9	12,7	3,2
GeoB17603-3-10, 910-911	910	6,28	6,4	0,0	11,1	6,4	4,8
GeoB17603-3-10, 920-921	920	6,28	38,2	0,0	44,6	38,2	6,4
GeoB17603-3-10, 930-931	930	6,28	27,1	0,0	41,4	28,7	12,7
GeoB17603-3-10, 940-941	940	6,28	1,6	1,6	3,2	3,2	0,0
GeoB17603-3-10, 950-951	950	6,28	33,4	0,0	41,4	35,0	6,4
GeoB17603-3-10, 960-961	960	6,28	38,2	1,6	43,0	41,4	1,6
GeoB17603-3-10, 970-971	970	6,28	283,4	3,2	308,9	302,5	6,4

Sample	Depth (cm)	% *B. bigelowii*	% *C. leptoporus*	% *C. pel. braarudi*	% *C. pel. pelagicus*	% *E. huxleyi* < 4 µm	% *E. huxleyi* > 4µm	% *G. muellerae*	% *G. oceanica*	% *H. carteri*	% Reworked Cenozoic	% Reworked Cretaceous	% Small *Gephyrocapsa* spp. (<3)	% *Syracosphaera* spp.	% *Thoracosphaera* spp.
GeoB17603-3-1, 0-1	0	0,02	1,45	0,18	52,47	44,36	0,06	0,00	0,23	0,02	0,10	0,08	0,68	0,16	0,19
GeoB17603-3-1, 10-11	10	0,00	1,53	0,04	56,31	40,81	0,00	0,00	0,60	0,00	0,01	0,09	0,26	0,20	0,16
GeoB17603-3-1, 20-21	20	0,00	3,40	0,10	53,72	40,80	0,00	0,00	0,48	0,00	0,12	0,17	0,53	0,55	0,12
GeoB17603-3-1, 30-31	30	0,00	4,27	0,08	50,28	43,39	0,04	0,00	0,48	0,00	0,11	0,02	0,84	0,34	0,15
GeoB17603-3-1, 40-41	40	0,00	2,13	0,25	43,04	52,73	0,25	0,00	0,57	0,00	0,11	0,11	0,64	0,00	0,18
GeoB17603-3-1, 50-51	50	0,04	1,50	0,04	29,14	65,36	0,51	0,00	0,36	0,00	0,16	0,16	2,30	0,24	0,20
GeoB17603-3-1, 60-61	60	0,00	1,97	0,32	42,70	51,06	0,14	0,04	0,82	0,00	0,04	0,11	2,01	0,22	0,57
GeoB17603-3-1, 70-71	70	0,02	2,08	0,13	43,55	51,68	0,22	0,00	0,85	0,00	0,11	0,11	1,05	0,11	0,07
GeoB17603-3-1, 80-81	80	0,00	3,13	0,10	33,77	56,12	1,08	0,00	0,45	0,00	0,24	0,07	4,76	0,10	0,17
GeoB17603-3-2, 90-91	90	0,00	3,34	0,04	47,12	46,53	0,21	0,00	0,33	0,00	0,17	0,21	1,46	0,17	0,42
GeoB17603-3-2, 100-101	100	0,05	2,37	0,14	45,17	47,15	1,06	0,00	1,11	0,00	0,43	0,24	1,45	0,14	0,68

GeoB17603-3-2, 110-111	110	0,00	1,47	0,12	49,12	45,74	0,42	0,00	1,10	0,00	0,15	0,20	0,86	0,22	0,61
GeoB17603-3-2, 120-121	120	0,05	1,33	0,15	41,29	53,88	0,39	0,00	1,07	0,00	0,12	0,22	0,92	0,07	0,51
GeoB17603-3-2, 130-131	130	0,05	1,19	0,25	32,39	64,00	0,35	0,00	0,84	0,00	0,05	0,25	0,40	0,00	0,25
GeoB17603-3-2, 140-141	140	0,05	1,19	0,05	25,11	68,29	0,82	0,00	2,15	0,00	0,46	0,18	1,42	0,05	0,23
GeoB17603-3-2, 150-151	150	0,02	0,78	0,04	45,03	50,30	0,19	0,00	1,84	0,00	0,11	0,15	1,19	0,07	0,28
GeoB17603-3-2, 160-161	160	0,00	1,01	0,16	56,63	38,75	0,11	0,02	2,25	0,00	0,06	0,18	0,67	0,03	0,14
GeoB17603-3-2, 170-171	170	0,00	0,74	0,13	46,36	48,00	0,13	0,02	2,94	0,00	0,08	0,15	1,19	0,03	0,21
GeoB17603-3-2, 180-181	180	0,01	1,02	0,19	28,50	62,44	0,37	0,00	5,79	0,01	0,34	0,19	0,75	0,12	0,27
GeoB17603-3-3, 190-191	190	0,03	2,28	0,13	23,45	62,52	0,83	0,00	9,50	0,00	0,19	0,30	0,40	0,13	0,24
GeoB17603-3-3, 200-201	200	0,00	1,79	0,14	29,79	57,83	0,93	0,00	7,15	0,11	0,36	0,18	1,25	0,18	0,29
GeoB17603-3-3, 210-211	210	0,02	2,85	0,25	36,04	52,77	0,72	0,00	5,31	0,00	0,19	0,23	1,12	0,02	0,48
GeoB17603-3-3, 220-221	220	0,00	2,93	0,06	28,11	53,73	2,14	0,00	11,37	0,00	0,06	0,06	1,12	0,09	0,33
GeoB17603-3-3, 230-231	230	0,00	2,52	0,11	25,89	56,08	1,98	0,08	11,40	0,00	0,38	0,27	0,50	0,30	0,50
GeoB17603-3-3, 240-241	240	0,00	2,97	0,04	27,79	48,99	5,73	0,00	12,54	0,00	0,17	0,17	0,95	0,43	0,22
GeoB17603-3-3, 250-251	250	0,04	2,15	0,47	26,44	58,41	1,64	0,00	9,61	0,00	0,04	0,18	0,58	0,22	0,22
GeoB17603-3-3, 260-261	260	0,00	2,54	0,04	27,57	56,05	1,92	0,00	10,16	0,00	0,10	0,22	0,91	0,20	0,30
GeoB17603-3-3, 270-271	270	0,02	2,58	0,06	26,68	59,28	1,24	0,00	8,49	0,00	0,10	0,16	1,04	0,20	0,14
GeoB17603-3-3, 280-281	280	0,02	2,20	0,02	23,99	60,39	2,15	0,00	8,05	0,00	0,05	0,14	2,58	0,09	0,32
GeoB17603-3-4, 290-291	290	0,00	3,93	0,12	15,09	71,54	1,44	0,00	4,65	0,00	0,18	0,27	2,55	0,12	0,12
GeoB17603-3-4, 300-301	300	0,00	1,60	0,31	24,78	60,03	2,03	0,00	7,40	0,04	0,23	0,16	3,19	0,08	0,16
GeoB17603-3-4, 310-311	310	0,00	2,10	0,13	16,90	72,05	1,26	0,00	5,33	0,00	0,19	0,23	1,62	0,00	0,19
GeoB17603-3-4, 320-321	320	0,03	1,33	0,18	24,44	61,48	1,33	0,06	8,13	0,00	0,15	0,18	2,21	0,09	0,39

GeoB17603-3-4, 330-331	330	0,00	1,06	1,43	9,85	73,03	2,22	0,00	7,54	0,00	0,42	0,14	3,79	0,28	0,23
GeoB17603-3-4, 340-341	340	0,00	0,70	0,85	12,30	75,72	0,67	0,00	3,66	0,00	0,14	0,21	5,29	0,07	0,39
GeoB17603-3-4, 350-351	350	0,05	0,82	0,14	7,47	79,03	0,69	0,00	4,89	0,03	0,33	0,25	5,85	0,16	0,27
GeoB17603-3-4, 360-361	360	0,00	1,34	0,17	4,09	83,26	1,21	0,00	5,01	0,04	0,33	0,21	4,22	0,04	0,08
GeoB17603-3-4, 370-371	370	0,00	0,68	0,52	8,15	78,36	1,41	0,00	4,34	0,00	0,24	0,28	5,82	0,08	0,12
GeoB17603-3-4, 380-381	380	0,02	0,77	0,55	6,38	75,99	1,15	0,05	3,27	0,00	0,27	0,20	10,90	0,22	0,22
GeoB17603-3-5, 390-391	390	0,00	1,22	0,11	4,03	81,10	1,49	0,00	4,31	0,06	0,44	0,06	7,13	0,00	0,06
GeoB17603-3-5, 400-401	400	0,00	1,40	0,11	2,15	86,11	1,08	0,00	2,58	0,00	0,43	0,11	5,81	0,22	0,00
GeoB17603-3-5, 410-411	410	0,00	0,87	0,12	1,61	82,55	0,74	0,00	6,31	0,00	0,37	0,25	6,93	0,25	0,00
GeoB17603-3-5, 420-421	420	0,00	0,57	0,07	1,39	86,68	0,14	0,00	2,11	0,00	0,46	0,29	8,03	0,18	0,07
GeoB17603-3-5, 430-431	430	0,00	1,49	0,00	0,00	86,90	0,45	0,15	4,17	0,00	1,19	0,00	5,65	0,00	0,00
GeoB17603-3-5, 440-441	440	0,00	0,81	0,00	0,00	85,70	0,54	0,07	3,12	0,00	0,27	0,00	9,01	0,47	0,00
GeoB17603-3-5, 450-451	450	0,00	0,79	0,07	0,00	88,47	2,10	0,00	2,03	0,00	0,79	0,20	5,31	0,26	0,00
GeoB17603-3-5, 460-461	460	0,03	1,14	0,00	0,10	89,44	1,11	0,00	2,85	0,03	0,67	0,03	4,47	0,10	0,03
GeoB17603-3-5, 470-471	470	0,00	1,02	0,00	0,12	89,98	0,38	0,09	1,87	0,00	0,53	0,15	5,79	0,03	0,06
GeoB17603-3-5, 480-481	480	0,03	1,20	0,10	0,16	90,17	0,68	0,10	2,82	0,00	0,65	0,06	3,89	0,00	0,13
GeoB17603-3-6, 490-491	490	0,00	1,94	0,08	0,04	91,02	1,46	0,08	2,59	0,00	0,73	0,04	1,90	0,04	0,08
GeoB17603-3-6, 500-501	500	0,00	2,00	0,06	0,17	86,14	1,43	0,00	4,56	0,00	1,37	0,11	3,94	0,11	0,11
GeoB17603-3-6, 510-511	510	0,00	4,03	0,00	0,11	87,30	1,01	0,17	5,37	0,00	0,67	0,00	0,95	0,28	0,11
GeoB17603-3-6, 520-521	520	0,00	1,77	0,00	0,11	88,88	1,67	0,21	3,82	0,00	0,27	0,16	3,01	0,05	0,05
GeoB17603-3-6, 530-531	530	0,00	1,62	0,00	0,35	90,87	0,35	0,05	3,70	0,00	0,20	0,10	2,48	0,00	0,25
GeoB17603-3-6, 540-541	540	0,00	0,84	0,00	0,15	89,38	0,97	0,18	5,84	0,00	0,74	0,08	1,51	0,10	0,20

GeoB17603-3-6, 550-551	550	0,00	0,53	0,00	0,20	89,60	1,20	0,27	3,80	0,07	1,40	0,07	2,60	0,20	0,07
GeoB17603-3-6, 560-561	560	0,04	0,46	0,58	0,21	86,96	1,74	0,46	6,00	0,12	2,19	0,33	0,70	0,04	0,17
GeoB17603-3-6, 570-571	570	0,00	0,63	0,00	0,24	90,21	2,29	1,74	1,26	0,00	2,13	0,47	0,63	0,32	0,08
GeoB17603-3-6, 580-581	580	0,00	0,25	0,00	0,13	92,40	1,13	0,94	1,57	0,00	2,07	0,44	0,69	0,06	0,31
GeoB17603-3-7, 590-591	590	0,00	3,77	0,00	0,19	85,66	2,08	2,83	0,57	0,00	2,64	0,57	1,32	0,00	0,38
GeoB17603-3-7, 600-601	600	0,00	4,39	0,00	0,16	88,13	0,81	1,30	0,81	0,00	2,93	0,49	0,49	0,00	0,49
GeoB17603-3-7, 610-611	610	0,00	0,26	0,00	0,00	87,04	1,06	2,65	0,26	0,00	4,23	0,79	2,91	0,26	0,53
GeoB17603-3-7, 620-621	620	0,00	0,54	0,00	0,54	84,32	2,16	2,16	0,54	0,00	4,32	1,62	3,78	0,00	0,00
GeoB17603-3-7, 630-631	630	0,00	0,00	1,76	0,12	91,08	4,23	0,35	0,12	0,00	1,29	0,59	0,47	0,00	0,00
GeoB17603-3-7, 640-641	640	0,00	0,00	0,00	0,00	83,94	7,25	2,59	0,00	0,00	0,52	0,52	4,66	0,00	0,52
GeoB17603-3-7, 650-651	650	0,00	0,53	0,00	0,00	77,66	10,11	2,13	0,53	0,53	2,66	1,06	4,26	0,00	0,53
GeoB17603-3-7, 660-661	660	0,00	0,00	0,00	0,00	33,33	0,00	0,00	0,00	0,00	33,33	33,33	0,00	0,00	0,00
GeoB17603-3-7, 670-671	670	0,00	0,37	0,00	0,55	84,46	10,24	1,83	0,00	0,00	0,73	1,28	0,18	0,00	0,37
GeoB17603-3-7, 680-681	680	0,00	0,32	0,63	0,16	80,41	14,22	2,84	0,47	0,00	0,16	0,47	0,32	0,00	0,00
GeoB17603-3-8, 690-691	690	0,00	1,03	0,00	1,55	77,84	13,40	4,12	0,00	0,00	1,55	0,52	0,00	0,00	0,00
GeoB17603-3-8, 700-701	700	0,00	0,00	0,00	0,00	83,33	8,33	8,33	0,00	0,00	0,00	0,00	0,00	0,00	0,00
GeoB17603-3-8, 710-711	710	0,00	0,43	0,00	0,00	81,30	15,94	0,29	0,00	0,00	0,29	1,74	0,00	0,00	0,00
GeoB17603-3-8, 720-721	720	0,00	0,00	0,00	0,00	65,38	29,81	1,92	0,00	0,00	0,96	0,96	0,00	0,96	0,00
GeoB17603-3-8, 730-731	730	0,00	0,56	0,00	0,00	82,58	9,55	3,93	0,00	0,00	0,00	2,81	0,00	0,00	0,56
GeoB17603-3-8, 740-741	740	0,00	0,27	0,27	0,00	85,37	8,78	3,46	0,27	0,00	0,80	0,80	0,00	0,00	0,00
GeoB17603-3-8, 750-751	750	0,00	0,00	0,00	0,00	50,00	25,00	0,00	0,00	0,00	0,00	25,00	0,00	0,00	0,00
GeoB17603-3-8, 760-761	760	0,00	1,12	0,00	0,00	72,63	21,79	2,23	0,00	0,00	1,12	1,12	0,00	0,00	0,00

GeoB17603-3-8, 770-771	770	0,00	0,29	0,00	0,00	81,45	11,30	3,77	0,29	0,00	0,87	2,03	0,00	0,00	0,00
GeoB17603-3-8, 780-781	780	0,00	0,00	0,00	0,81	67,34	17,74	11,69	0,00	0,00	0,40	2,02	0,00	0,00	0,00
GeoB17603-3-9, 790-791	790	0,00	0,00	0,00	0,00	71,35	16,22	8,65	0,54	0,00	0,54	1,62	0,00	0,54	0,54
GeoB17603-3-9, 800-801	800	0,00	0,00	0,00	0,00	72,14	15,71	3,57	0,00	0,00	1,43	7,14	0,00	0,00	0,00
GeoB17603-3-9, 810-811	810	0,00	0,71	0,00	0,00	63,57	22,86	7,14	0,00	0,00	0,71	5,00	0,00	0,00	0,00
GeoB17603-3-9, 820-821	820	0,00	0,00	0,00	0,00	58,41	23,01	12,39	0,00	0,00	0,88	5,31	0,00	0,00	0,00
GeoB17603-3-9, 830-831	830	0,00	0,00	0,00	0,00	67,03	8,79	12,09	0,00	0,00	2,20	9,89	0,00	0,00	0,00
GeoB17603-3-9, 840-841	840	0,00	0,00	0,00	0,00	48,39	38,71	4,84	0,00	0,00	1,61	6,45	0,00	0,00	0,00
GeoB17603-3-9, 850-851	850	0,00	0,00	0,00	0,00	70,00	30,00	0,00	0,00	0,00	0,00	0,00	0,00	0,00	0,00
GeoB17603-3-9, 860-861	860	0,00	0,00	0,00	0,00	71,43	22,45	0,00	0,00	0,00	4,08	2,04	0,00	0,00	0,00
GeoB17603-3-9, 870-871	870	0,00	0,00	0,00	0,00	65,12	23,26	2,33	0,00	0,00	0,00	6,98	2,33	0,00	0,00
GeoB17603-3-9, 880-881	880	0,00	0,00	0,00	0,00	60,00	30,00	3,33	0,00	0,00	0,00	0,00	3,33	3,33	0,00
GeoB17603-3-10, 890-891	890	0,00	0,00	0,00	0,00	0,00	0,00	0,00	0,00	0,00	0,00	0,00	0,00	0,00	0,00
GeoB17603-3-10, 900-901	900	0,00	0,00	0,00	0,00	60,00	20,00	0,00	0,00	0,00	0,00	20,00	0,00	0,00	0,00
GeoB17603-3-10, 910-911	910	0,00	0,00	0,00	0,00	28,57	28,57	0,00	0,00	0,00	0,00	42,86	0,00	0,00	0,00
GeoB17603-3-10, 920-921	920	0,00	0,00	0,00	0,00	46,43	39,29	0,00	0,00	0,00	0,00	14,29	0,00	0,00	0,00
GeoB17603-3-10, 930-931	930	0,00	0,00	0,00	0,00	30,77	34,62	3,85	0,00	0,00	3,85	26,92	0,00	0,00	0,00
GeoB17603-3-10, 940-941	940	0,00	0,00	0,00	50,00	50,00	0,00	0,00	0,00	0,00	0,00	0,00	0,00	0,00	0,00
GeoB17603-3-10, 950-951	950	0,00	0,00	0,00	0,00	38,46	42,31	0,00	0,00	0,00	0,00	15,38	0,00	0,00	3,85
GeoB17603-3-10, 960-961	960	0,00	0,00	0,00	3,70	59,26	29,63	3,70	0,00	0,00	0,00	3,70	0,00	0,00	0,00
GeoB17603-3-10, 970-971	970	0,00	0,00	0,00	1,03	66,49	25,26	5,15	0,00	0,00	0,00	2,06	0,00	0,00	0,00

Sample	Depth (cm)	% Total *E. huxleyi*	% Total *C. pelagicus*	% Total abundance (NO reworked)	% Total Reworked
GeoB17603-3-1, 0-1	0	44,43	52,65	99,82	0,18
GeoB17603-3-1, 10-11	10	40,81	56,35	99,90	0,10
GeoB17603-3-1, 20-21	20	40,80	53,82	99,71	0,29
GeoB17603-3-1, 30-31	30	43,43	50,37	99,87	0,13
GeoB17603-3-1, 40-41	40	52,98	43,29	99,79	0,21
GeoB17603-3-1, 50-51	50	65,87	29,18	99,68	0,32
GeoB17603-3-1, 60-61	60	51,20	43,03	99,86	0,14
GeoB17603-3-1, 70-71	70	51,90	43,68	99,78	0,22
GeoB17603-3-1, 80-81	80	57,19	33,88	99,69	0,31
GeoB17603-3-2, 90-91	90	46,74	47,16	99,62	0,38
GeoB17603-3-2, 100-101	100	48,21	45,31	99,32	0,68
GeoB17603-3-2, 110-111	110	46,16	49,24	99,66	0,34

GeoB17603-3-2, 120-121	120	54,27	41,43	99,66	0,34
GeoB17603-3-2, 130-131	130	64,34	32,64	99,70	0,30
GeoB17603-3-2, 140-141	140	69,11	25,16	99,36	0,64
GeoB17603-3-2, 150-151	150	50,48	45,07	99,74	0,26
GeoB17603-3-2, 160-161	160	38,86	56,78	99,76	0,24
GeoB17603-3-2, 170-171	170	48,13	46,50	99,77	0,23
GeoB17603-3-2, 180-181	180	62,81	28,69	99,47	0,53
GeoB17603-3-3, 190-191	190	63,35	23,58	99,52	0,48
GeoB17603-3-3, 200-201	200	58,76	29,94	99,46	0,54
GeoB17603-3-3, 210-211	210	53,49	36,29	99,59	0,41
GeoB17603-3-3, 220-221	220	55,87	28,17	99,88	0,12
GeoB17603-3-3, 230-231	230	58,06	26,00	99,35	0,65
GeoB17603-3-3, 240-241	240	54,72	27,83	99,66	0,34
GeoB17603-3-3, 250-251	250	60,05	26,91	99,78	0,22
GeoB17603-3-3, 260-261	260	57,97	27,61	99,68	0,32
GeoB17603-3-3, 270-271	270	60,52	26,74	99,74	0,26
GeoB17603-3-3, 280-281	280	62,55	24,01	99,82	0,18
GeoB17603-3-4, 290-291	290	72,98	15,21	99,55	0,45
GeoB17603-3-4, 300-301	300	62,06	25,09	99,61	0,39
GeoB17603-3-4, 310-311	310	73,31	17,03	99,58	0,42
GeoB17603-3-4, 320-321	320	62,81	24,62	99,67	0,33
GeoB17603-3-4, 330-331	330	75,25	11,29	99,44	0,56

GeoB17603-3-4, 340-341	340	76,39	13,14	99,65	0,35
GeoB17603-3-4, 350-351	350	79,72	7,61	99,42	0,58
GeoB17603-3-4, 360-361	360	84,47	4,26	99,46	0,54
GeoB17603-3-4, 370-371	370	79,77	8,67	99,48	0,52
GeoB17603-3-4, 380-381	380	77,13	6,93	99,53	0,47
GeoB17603-3-5, 390-391	390	82,60	4,14	99,50	0,50
GeoB17603-3-5, 400-401	400	87,19	2,26	99,46	0,54
GeoB17603-3-5, 410-411	410	83,29	1,73	99,38	0,62
GeoB17603-3-5, 420-421	420	86,83	1,46	99,25	0,75
GeoB17603-3-5, 430-431	430	87,35	0,00	98,81	1,19
GeoB17603-3-5, 440-441	440	86,25	0,00	99,73	0,27
GeoB17603-3-5, 450-451	450	90,56	0,07	99,02	0,98
GeoB17603-3-5, 460-461	460	90,55	0,10	99,30	0,70
GeoB17603-3-5, 470-471	470	90,36	0,12	99,33	0,67
GeoB17603-3-5, 480-481	480	90,85	0,26	99,29	0,71
GeoB17603-3-6, 490-491	490	92,48	0,12	99,23	0,77
GeoB17603-3-6, 500-501	500	87,56	0,23	98,52	1,48
GeoB17603-3-6, 510-511	510	88,30	0,11	99,33	0,67
GeoB17603-3-6, 520-521	520	90,54	0,11	99,57	0,43
GeoB17603-3-6, 530-531	530	91,23	0,35	99,70	0,30
GeoB17603-3-6, 540-541	540	90,35	0,15	99,18	0,82
GeoB17603-3-6, 550-551	550	90,80	0,20	98,53	1,47

GeoB17603-3-6, 560-561	560	88,70	0,79	97,48	2,52
GeoB17603-3-6, 570-571	570	92,50	0,24	97,39	2,61
GeoB17603-3-6, 580-581	580	93,53	0,13	97,49	2,51
GeoB17603-3-7, 590-591	590	87,74	0,19	96,79	3,21
GeoB17603-3-7, 600-601	600	88,94	0,16	96,59	3,41
GeoB17603-3-7, 610-611	610	88,10	0,00	94,97	5,03
GeoB17603-3-7, 620-621	620	86,49	0,54	94,05	5,95
GeoB17603-3-7, 630-631	630	95,31	1,88	98,12	1,88
GeoB17603-3-7, 640-641	640	91,19	0,00	98,96	1,04
GeoB17603-3-7, 650-651	650	87,77	0,00	96,28	3,72
GeoB17603-3-7, 660-661	660	33,33	0,00	33,33	66,67
GeoB17603-3-7, 670-671	670	94,70	0,55	97,99	2,01
GeoB17603-3-7, 680-681	680	94,63	0,79	99,37	0,63
GeoB17603-3-8, 690-691	690	91,24	1,55	97,94	2,06
GeoB17603-3-8, 700-701	700	91,67	0,00	100,00	0,00
GeoB17603-3-8, 710-711	710	97,25	0,00	97,97	2,03
GeoB17603-3-8, 720-721	720	95,19	0,00	98,08	1,92
GeoB17603-3-8, 730-731	730	92,13	0,00	97,19	2,81
GeoB17603-3-8, 740-741	740	94,15	0,27	98,40	1,60
GeoB17603-3-8, 750-751	750	75,00	0,00	75,00	25,00
GeoB17603-3-8, 760-761	760	94,41	0,00	97,77	2,23
GeoB17603-3-8, 770-771	770	92,75	0,00	97,10	2,90

GeoB17603-3-8, 780-781	780	85,08	0,81	97,58	2,42
GeoB17603-3-9, 790-791	790	87,57	0,00	97,84	2,16
GeoB17603-3-9, 800-801	800	87,86	0,00	91,43	8,57
GeoB17603-3-9, 810-811	810	86,43	0,00	94,29	5,71
GeoB17603-3-9, 820-821	820	81,42	0,00	93,81	6,19
GeoB17603-3-9, 830-831	830	75,82	0,00	87,91	12,09
GeoB17603-3-9, 840-841	840	87,10	0,00	91,94	8,06
GeoB17603-3-9, 850-851	850	100,00	0,00	100,00	0,00
GeoB17603-3-9, 860-861	860	93,88	0,00	93,88	6,12
GeoB17603-3-9, 870-871	870	88,37	0,00	93,02	6,98
GeoB17603-3-9, 880-881	880	90,00	0,00	100,00	0,00
GeoB17603-3-10, 890-891	890	0,00	0,00	0,00	0,00
GeoB17603-3-10, 900-901	900	80,00	0,00	80,00	20,00
GeoB17603-3-10, 910-911	910	57,14	0,00	57,14	42,86
GeoB17603-3-10, 920-921	920	85,71	0,00	85,71	14,29
GeoB17603-3-10, 930-931	930	65,38	0,00	69,23	30,77
GeoB17603-3-10, 940-941	940	50,00	50,00	100,00	0,00
GeoB17603-3-10, 950-951	950	80,77	0,00	84,62	15,38
GeoB17603-3-10, 960-961	960	88,89	3,70	96,30	3,70
GeoB17603-3-10, 970-971	970	91,75	1,03	97,94	2,06

Sample	Depth (cm)	H/P ratio	Dominance index	Shannon diversity index	CEX *C. pel.*(modif. Dittert et al., 1999)
GeoB17603-3-1, 0-1	0	-0,07	0,32	1,20	0,46
GeoB17603-3-1, 10-11	10	-0,14	0,33	1,18	0,42
GeoB17603-3-1, 20-21	20	-0,12	0,32	1,24	0,43
GeoB17603-3-1, 30-31	30	-0,06	0,31	1,27	0,46
GeoB17603-3-1, 40-41	40	0,09	0,32	1,23	0,55
GeoB17603-3-1, 50-51	50	0,35	0,36	1,21	0,69
GeoB17603-3-1, 60-61	60	0,08	0,31	1,29	0,54
GeoB17603-3-1, 70-71	70	0,07	0,31	1,25	0,54
GeoB17603-3-1, 80-81	80	0,23	0,31	1,35	0,63
GeoB17603-3-2, 90-91	90	0,00	0,31	1,28	0,50
GeoB17603-3-2, 100-101	100	0,03	0,30	1,32	0,52

GeoB17603-3-2, 110-111	110	-0,03	0,31	1,26	0,48
GeoB17603-3-2, 120-121	120	0,12	0,32	1,25	0,57
GeoB17603-3-2, 130-131	130	0,29	0,35	1,18	0,66
GeoB17603-3-2, 140-141	140	0,44	0,38	1,20	0,73
GeoB17603-3-2, 150-151	150	0,05	0,31	1,25	0,53
GeoB17603-3-2, 160-161	160	-0,16	0,32	1,22	0,41
GeoB17603-3-2, 170-171	170	0,02	0,31	1,26	0,51
GeoB17603-3-2, 180-181	180	0,34	0,34	1,28	0,69
GeoB17603-3-3, 190-191	190	0,43	0,34	1,33	0,73
GeoB17603-3-3, 200-201	200	0,29	0,31	1,37	0,66
GeoB17603-3-3, 210-211	210	0,17	0,29	1,38	0,60
GeoB17603-3-3, 220-221	220	0,30	0,28	1,47	0,66
GeoB17603-3-3, 230-231	230	0,35	0,29	1,44	0,69
GeoB17603-3-3, 240-241	240	0,29	0,26	1,56	0,66
GeoB17603-3-3, 250-251	250	0,35	0,31	1,40	0,69
GeoB17603-3-3, 260-261	260	0,32	0,29	1,43	0,68
GeoB17603-3-3, 270-271	270	0,35	0,31	1,38	0,69
GeoB17603-3-3, 280-281	280	0,42	0,32	1,41	0,72
GeoB17603-3-4, 290-291	290	0,68	0,43	1,24	0,83
GeoB17603-3-4, 300-301	300	0,39	0,32	1,41	0,71
GeoB17603-3-4, 310-311	310	0,63	0,43	1,20	0,81
GeoB17603-3-4, 320-321	320	0,41	0,33	1,37	0,72

GeoB17603-3-4, 330-331	330	0,82	0,46	1,23	0,87
GeoB17603-3-4, 340-341	340	0,76	0,48	1,14	0,85
GeoB17603-3-4, 350-351	350	1,02	0,56	1,01	0,91
GeoB17603-3-4, 360-361	360	1,30	0,65	0,84	0,95
GeoB17603-3-4, 370-371	370	0,96	0,54	1,04	0,90
GeoB17603-3-4, 380-381	380	1,05	0,53	1,07	0,92
GeoB17603-3-5, 390-391	390	1,30	0,62	0,89	0,95
GeoB17603-3-5, 400-401	400	1,59	0,72	0,69	0,97
GeoB17603-3-5, 410-411	410	1,68	0,68	0,76	0,98
GeoB17603-3-5, 420-421	420	1,77	0,75	0,59	0,98
GeoB17603-3-5, 430-431	430		0,78	0,51	1,00
GeoB17603-3-5, 440-441	440		0,75	0,55	1,00
GeoB17603-3-5, 450-451	450	3,14	0,80	0,48	1,00
GeoB17603-3-5, 460-461	460	2,98	0,81	0,47	1,00
GeoB17603-3-5, 470-471	470	2,89	0,82	0,43	1,00
GeoB17603-3-5, 480-481	480	2,54	0,82	0,46	1,00
GeoB17603-3-6, 490-491	490	2,88	0,84	0,42	1,00
GeoB17603-3-6, 500-501	500	2,58	0,77	0,57	1,00
GeoB17603-3-6, 510-511	510	2,90	0,78	0,54	1,00
GeoB17603-3-6, 520-521	520	2,93	0,80	0,51	1,00
GeoB17603-3-6, 530-531	530	2,41	0,83	0,45	1,00
GeoB17603-3-6, 540-541	540	2,77	0,81	0,46	1,00

GeoB17603-3-6, 550-551	550	2,66	0,83	0,45	1,00
GeoB17603-3-6, 560-561	560	2,05	0,79	0,54	0,99
GeoB17603-3-6, 570-571	570	2,59	0,85	0,41	1,00
GeoB17603-3-6, 580-581	580	2,87	0,90	0,31	1,00
GeoB17603-3-7, 590-591	590	2,67	0,78	0,56	1,00
GeoB17603-3-7, 600-601	600	2,74	0,83	0,44	1,00
GeoB17603-3-7, 610-611	610		0,84	0,41	1,00
GeoB17603-3-7, 620-621	620	2,20	0,80	0,52	0,99
GeoB17603-3-7, 630-631	630	1,71	0,83	0,43	0,98
GeoB17603-3-7, 640-641	640		0,73	0,60	1,00
GeoB17603-3-7, 650-651	650		0,66	0,75	1,00
GeoB17603-3-7, 660-661	660		1,00	0,00	1,00
GeoB17603-3-7, 670-671	670	2,24	0,75	0,55	0,99
GeoB17603-3-7, 680-681	680	2,08	0,67	0,70	0,99
GeoB17603-3-8, 690-691	690	1,77	0,63	0,77	0,98
GeoB17603-3-8, 700-701	700		0,71	0,57	1,00
GeoB17603-3-8, 710-711	710		0,72	0,49	1,00
GeoB17603-3-8, 720-721	720		0,54	0,75	1,00
GeoB17603-3-8, 730-731	730		0,73	0,56	1,00
GeoB17603-3-8, 740-741	740	2,55	0,76	0,52	1,00
GeoB17603-3-8, 750-751	750		0,56	0,64	1,00
GeoB17603-3-8, 760-761	760		0,60	0,69	1,00

GeoB17603-3-8, 770-771	770		0,72	0,56	1,00
GeoB17603-3-8, 780-781	780	2,02	0,52	0,90	0,99
GeoB17603-3-9, 790-791	790		0,57	0,83	1,00
GeoB17603-3-9, 800-801	800		0,65	0,62	1,00
GeoB17603-3-9, 810-811	810		0,52	0,84	1,00
GeoB17603-3-9, 820-821	820		0,47	0,91	1,00
GeoB17603-3-9, 830-831	830		0,61	0,71	1,00
GeoB17603-3-9, 840-841	840		0,46	0,86	1,00
GeoB17603-3-9, 850-851	850		0,58	0,61	1,00
GeoB17603-3-9, 860-861	860		0,64	0,55	1,00
GeoB17603-3-9, 870-871	870		0,55	0,78	1,00
GeoB17603-3-9, 880-881	880		0,45	1,01	1,00
GeoB17603-3-10, 890-891	890		0,63	0,56	
GeoB17603-3-10, 900-901	900		0,50	0,69	1,00
GeoB17603-3-10, 910-911	910		0,50	0,69	1,00
GeoB17603-3-10, 920-921	920		0,45	0,87	1,00
GeoB17603-3-10, 930-931	930		0,33	1,10	1,00
GeoB17603-3-10, 940-941	940	0,00	0,46	0,85	0,50
GeoB17603-3-10, 950-951	950		0,44	1,04	1,00
GeoB17603-3-10, 960-961	960	1,38	0,52	0,86	0,96
GeoB17603-3-10, 970-971	970	1,95			0,99

Planktonic foraminifera

Sample	Depth (cm)	% *Neogloboquadrina pachyderma* (s)	% *Neogloboquadrina incompta*	% *Turborotalita quinqueloba*	% Planktonic foraminifera fragments	Planktonic foraminifera total abundance (N ind/g)	*N. pachyderma* (s) flux	*N. incompta* flux	*T. quinqueloba* flux	Dominance index	Shannon diversity index	PFAR
GeoB17603-3-1, 0-1	0	74,6	12,0	12,0	18,677	98,039	2572	412	412	0,59	0,80	3445
GeoB17603-3-1, 10-11	10	61,3	15,7	21,2	25,326	285,765	2556	655	883	0,45	1,00	4167
GeoB17603-3-1, 20-21	20	69,0	15,3	14,2	51,095	408,136	12230	2710	2512	0,52	0,89	17716
GeoB17603-3-1, 30-31	30	51,9	17,6	29,6	38,636	67,462	899	305	514	0,39	1,05	1733
GeoB17603-3-1, 40-41	40	74,4	18,6	7,0	31,746	30,884	598	150	56	0,59	0,72	804
GeoB17603-3-1, 50-51	50	90,9	9,1	0,0	64,516	15,632	500	50	0	0,83	0,30	550
GeoB17603-3-1, 60-61	60	85,9	4,7	8,7	12,094	300,743	9061	496	920	0,75	0,53	10548
GeoB17603-3-1, 70-71	70	72,6	9,9	16,7	19,489	293,483	7575	1035	1738	0,57	0,80	10431
GeoB17603-3-1, 80-81	80	82,1	11,4	6,5	63,063	110,537	3970	550	314	0,69	0,59	4835
GeoB17603-3-2, 90-91	90	76,8	6,9	15,7	20,088	313,151	10692	962	2192	0,62	0,71	13923
GeoB17603-3-2, 100-101	100	73,5	11,8	14,7	25,275	79,532	2615	418	523	0,58	0,76	3557
GeoB17603-3-2, 110-111	110	67,7	13,2	17,2	16,986	375,566	11267	2199	2858	0,50	0,92	16654

GeoB17603-3-2, 120-121	120	57,6	11,4	26,5	20,242	155,836	3924	774	1807	0,42	1,10	6815
GeoB17603-3-2, 130-131	130	82,0	6,0	10,0	32,432	26,325	936	68	114	0,69	0,64	1141
GeoB17603-3-2, 140-141	140	83,7	7,6	7,0	27,426	168,195	12627	1140	1052	0,71	0,61	15082
GeoB17603-3-2, 150-151	150	58,7	7,0	30,4	10,945	414,308	21871	2604	11352	0,44	1,04	37285
GeoB17603-3-2, 160-161	160	57,7	5,7	30,4	9,562	518,156	28916	2870	15231	0,43	1,08	50107
GeoB17603-3-2, 170-171	170	66,8	6,7	22,4	12,387	170,651	11158	1116	3733	0,50	0,95	16693
GeoB17603-3-2, 180-181	180	49,4	7,5	36,1	13,851	165,971	8012	1208	5850	0,38	1,18	16214
GeoB17603-3-3, 190-191	190	48,4	11,8	33,0	13,333	67,978	3215	781	2194	0,36	1,23	6641
GeoB17603-3-3, 200-201	200	61,6	9,7	25,7	16,356	204,194	12247	1918	5115	0,46	1,01	19871
GeoB17603-3-3, 210-211	210											
GeoB17603-3-3, 220-221	220	86,1	4,2	8,3	20,000	29,012	2288	111	221	0,75	0,53	2657
GeoB17603-3-3, 230-231	230	33,6	7,6	55,6	8,545	269,219	8305	1873	13738	0,43	1,03	24728
GeoB17603-3-3, 240-241	240	43,3	3,9	48,8	13,386	162,264	12198	1109	13733	0,43	1,01	28148
GeoB17603-3-3, 250-251	250	40,2	10,2	48,1	11,628	145,729	10169	2566	12165	0,40	1,03	25280
GeoB17603-3-3, 260-261	260	58,0	8,0	24,0	15,254	25,321	2567	354	1062	0,41	1,14	4427
GeoB17603-3-3, 270-271	270	43,8	12,5	38,9	13,253	120,230	18447	5271	16397	0,36	1,18	42164
GeoB17603-3-3, 280-281	280	29,9	11,3	54,6	7,619	90,527	9374	3556	17133	0,40	1,09	31356
GeoB17603-3-4, 290-291	290	29,0	16,1	51,6	13,889	23,303	2376	1320	4224	0,38	1,11	8185
GeoB17603-3-4, 300-301	300	20,4	9,9	61,7	7,429	71,004	5049	2448	15300	0,44	1,12	24786
GeoB17603-3-4, 310-311	310	30,4	21,7	39,1	9,804	28,563	3066	2190	3942	0,30	1,27	10073
GeoB17603-3-4, 320-321	320	27,5	8,2	46,2	6,186	84,204	8109	2433	13623	0,31	1,41	29515
GeoB17603-3-4, 330-331	330	17,2	14,2	56,5	7,364	139,603	8371	6942	27562	0,38	1,26	48795

GeoB17603-3-4, 340-341	340	28,8	5,8	51,9	8,772	52,471	5274	1055	9494	0,36	1,25	18284
GeoB17603-3-4, 350-351	350	10,7	11,9	66,7	15,714	139,750	5236	5787	32520	0,47	1,14	48780
GeoB17603-3-4, 360-361	360	19,5	2,3	73,8	3,396	83,756	2690	323	1291	0,38	1,24	4895
GeoB17603-3-4, 370-371	370	23,4	6,4	55,3	9,615	37,957	1460	398	3450	0,38	1,23	6237
GeoB17603-3-4, 380-381	380											
GeoB17603-3-5, 390-391	390	18,6	5,7	51,4	11,392	52,083	1605	494	4444	0,34	1,33	8641
GeoB17603-3-5, 400-401	400											
GeoB17603-3-5, 410-411	410	3,3	4,7	81,3	9,639	121,222	666	932	16240	0,67	0,80	19967
GeoB17603-3-5, 420-421	420											
GeoB17603-3-5, 430-431	430	4,0	24,0	52,0	10,714	12,906	84	507	1098	0,35	1,32	2111
GeoB17603-3-5, 440-441	440											
GeoB17603-3-5, 450-451	450	15,8	7,9	60,5	11,628	21,018	538	269	2064	0,41	1,25	3410
GeoB17603-3-5, 460-461	460											
GeoB17603-3-5, 470-471	470											
GeoB17603-3-5, 480-481	480											
GeoB17603-3-6, 490-491	490											
GeoB17603-3-6, 500-501	500											
GeoB17603-3-6, 510-511	510	27,8	25,0	36,1	5,263	21,911	1010	909	1314	0,28	1,38	3638
GeoB17603-3-6, 520-521	520											
GeoB17603-3-6, 530-531	530	55,6	22,2	22,2	5,263	13,527	1249	499	499	0,41	1,00	2248
GeoB17603-3-6, 540-541	540											
GeoB17603-3-6, 550-551	550											

GeoB17603-3-6, 560-561	560											
GeoB17603-3-6, 570-571	570	41,2	17,6	41,2	0,000	13,914	969	415	969	0,37	1,04	2354
GeoB17603-3-6, 580-581	580											
GeoB17603-3-7, 590-591	590	40,0	20,0	40,0	6,250	4,553	320	160	320	0,36	1,06	799
GeoB17603-3-7, 600-601	600											
GeoB17603-3-7, 610-611	610	76,0	4,0	0,0	0,000	6,244	836	44	0	0,60	0,79	1099
GeoB17603-3-7, 620-621	620											
GeoB17603-3-7, 630-631	630	94,6	1,8	0,0	5,085	21,579	3749	71	0	0,90	0,24	3961
GeoB17603-3-7, 640-641	640											
GeoB17603-3-7, 650-651	650	95,7	2,2	0,0	35,088	49,727	8765	198	0	0,92	0,21	9161
GeoB17603-3-7, 660-661	660											
GeoB17603-3-7, 670-671	670											
GeoB17603-3-7, 680-681	680											
GeoB17603-3-8, 690-691	690											
GeoB17603-3-8, 700-701	700											
GeoB17603-3-8, 710-711	710											
GeoB17603-3-8, 720-721	720											
GeoB17603-3-8, 730-731	730	93,0	4,2	2,8	7,792	16,435	5123	233	155	0,87	0,30	5511
GeoB17603-3-8, 740-741	740											
GeoB17603-3-8, 750-751	750											
GeoB17603-3-8, 760-761	760											
GeoB17603-3-8, 770-771	770	95,8	4,2	0,0	2,041	10,959	3593	156	0	0,92	0,17	3749

GeoB17603-3-8, 780-781	780											
GeoB17603-3-9, 790-791	790											
GeoB17603-3-9, 800-801	800											
GeoB17603-3-9, 810-811	810	96,4	1,8	1,8	5,172	10,913	7184	136	136	0,93	0,18	7455

Diatoms

Sample	Depth (cm)	Fields	*Azpetia* spp.	*Actinoptychus* sp.	*Hyalodiscus* sp.	*Biddulphia* sp.	*Coscinodiscus* spp.	CRS	*Chaetoceros* veg. spp.	*Fossula arctica*	*Fragilariopsis cylindrus*	*Fragilariopsis* sp.	*Paralia sulcata*	*Porosira glacialis*	*Proboscia* spp.	*Rhizosolenia* cf. *borealis*	*Stellarima microtrias*	*Stephanopyxis* sp.
GeoB17603-3-1, 0-1	0	1000	1,57	0,00	0,00	0,78	3,14	55,69	3,53	0,00	0,00	0,00	16,86	0,39	1,96	1,18	0,00	0,00
GeoB17603-3-1, 10-11	10																	
GeoB17603-3-1, 20-21	20	1000	0,00	0,00	0,00	0,00	3,85	67,31	5,77	1,92	0,00	0,00	3,85	0,00	0,00	0,00	0,00	0,00
GeoB17603-3-1, 30-31	30																	
GeoB17603-3-1, 40-41	40	1000	0,00	0,00	0,00	0,00	6,90	65,52	3,45	0,00	0,00	0,00	0,00	0,00	0,00	0,00	0,00	0,00
GeoB17603-3-1, 50-51	50																	
GeoB17603-3-1, 60-61	60	1000	0,65	0,00	0,00	0,00	2,58	87,10	3,23	1,94	0,00	0,00	1,29	0,00	0,00	0,00	0,00	0,00
GeoB17603-3-1, 70-71	70																	
GeoB17603-3-1, 80-81	80	1000	0,00	0,00	0,00	0,00	0,00	0,00	0,00	0,00	0,00	0,00	0,00	0,00	0,00	0,00	0,00	0,00
GeoB17603-3-2, 90-91	90																	
GeoB17603-3-2, 100-101	100	1000	0,00	0,00	0,00	0,00	0,00	66,67	0,00	0,00	0,00	0,00	33,33	0,00	0,00	0,00	0,00	0,00
GeoB17603-3-2, 110-111	110																	
GeoB17603-3-2, 120-121	120																	

GeoB17603-3-2, 130-131	130																	
GeoB17603-3-2, 140-141	140	1000	0,00	6,25	0,00	0,00	6,25	31,25	0,00	0,00	0,00	0,00	31,25	0,00	0,00	0,00	0,00	6,25
GeoB17603-3-2, 150-151	150																	
GeoB17603-3-2, 160-161	160	1000	2,94	2,94	0,00	0,00	5,88	55,88	1,47	0,00	0,00	0,00	14,71	0,00	0,00	1,47	0,00	0,00
GeoB17603-3-2, 170-171	170																	
GeoB17603-3-2, 180-181	180	1000	5,26	2,63	0,00	0,00	5,26	13,16	0,00	0,00	0,00	0,00	52,63	0,00	0,00	0,00	0,00	0,00
GeoB17603-3-3, 190-191	190																	
GeoB17603-3-3, 200-201	200	1000	0,00	0,00	0,00	0,00	8,70	4,35	0,00	0,00	0,00	0,00	47,83	0,00	0,00	0,00	0,00	0,00
GeoB17603-3-3, 210-211	210																	
GeoB17603-3-3, 220-221	220	1000	0,00	0,00	0,00	0,00	9,38	9,38	0,00	0,00	0,00	0,00	43,75	0,00	0,00	3,13	0,00	0,00
GeoB17603-3-3, 230-231	230																	
GeoB17603-3-3, 240-241	240	1000	0,00	0,00	0,00	0,00	11,11	11,11	0,00	0,00	0,00	0,00	22,22	0,00	1,85	3,70	3,70	0,00
GeoB17603-3-3, 250-251	250																	
GeoB17603-3-3, 260-261	260	1000	8,11	0,00	2,70	0,00	32,43	8,11	0,00	0,00	0,00	0,00	13,51	0,00	0,00	5,41	0,00	0,00
GeoB17603-3-3, 270-271	270																	
GeoB17603-3-3, 280-281	280	1000	0,00	0,00	3,39	0,00	42,37	1,69	1,69	0,00	0,00	3,39	25,42	0,00	0,00	1,69	0,00	0,00
GeoB17603-3-4, 290-291	290																	
GeoB17603-3-4, 300-301	300	1000	0,00	0,00	0,00	0,00	36,90	4,76	1,19	0,00	0,00	2,38	25,00	0,00	0,00	1,19	0,00	0,00
GeoB17603-3-4, 310-311	310																	
GeoB17603-3-4, 320-321	320	1000	0,00	0,00	0,00	0,00	45,38	10,08	0,00	0,00	0,00	3,36	16,81	0,00	0,00	2,52	0,00	0,00
GeoB17603-3-4, 330-331	330																	
GeoB17603-3-4, 340-341	340	1000	0,00	1,35	0,00	0,00	44,59	2,70	0,00	0,00	0,00	0,00	5,41	0,00	0,00	10,81	0,00	0,00

GeoB17603-3-4, 350-351	350																	
GeoB17603-3-4, 360-361	360	1000	1,18	0,00	0,00	0,00	43,53	0,00	0,00	0,00	0,00	0,00	8,24	0,00	0,00	15,29	0,00	0,00
GeoB17603-3-4, 370-371	370																	
GeoB17603-3-4, 380-381	380	1000	1,23	1,23	0,00	0,00	34,57	4,94	0,00	0,00	1,23	0,00	37,04	0,00	0,00	3,70	1,23	0,00
GeoB17603-3-5, 390-391	390																	
GeoB17603-3-5, 400-401	400	1000	0,00	0,00	0,00	0,00	50,57	0,00	0,00	0,00	0,00	0,00	25,29	0,00	0,00	9,20	0,00	0,00
GeoB17603-3-5, 410-411	410																	
GeoB17603-3-5, 420-421	420	1000	0,99	0,00	0,00	0,00	54,46	3,96	0,00	0,00	0,00	0,00	11,88	0,00	0,00	8,91	0,00	0,00
GeoB17603-3-5, 430-431	430																	
GeoB17603-3-5, 440-441	440	1000	0,00	0,00	0,00	0,00	39,25	9,35	0,93	0,00	0,00	0,00	19,63	0,00	0,00	6,54	0,00	0,00
GeoB17603-3-5, 450-451	450																	
GeoB17603-3-5, 460-461	460	1000	0,86	0,00	0,00	0,00	25,00	11,21	0,00	0,00	1,72	0,00	20,69	2,59	0,00	10,34	0,00	0,00
GeoB17603-3-5, 470-471	470																	
GeoB17603-3-5, 480-481	480	1000	0,00	0,81	0,00	0,00	43,55	9,68	0,00	0,81	0,81	0,00	11,29	0,00	0,81	8,06	0,00	0,00
GeoB17603-3-6, 490-491	490																	
GeoB17603-3-6, 500-501	500	1000	1,47	0,00	0,00	0,00	63,24	10,29	0,00	2,94	0,00	0,00	13,24	0,00	0,00	1,47	0,00	0,00
GeoB17603-3-6, 510-511	510																	
GeoB17603-3-6, 520-521	520	1000	0,00	0,00	0,00	0,00	54,05	9,46	0,00	0,00	0,00	0,00	24,32	2,70	0,00	0,00	0,00	0,00
GeoB17603-3-6, 530-531	530																	
GeoB17603-3-6, 540-541	540	1000	2,27	0,00	0,00	0,00	43,18	2,27	0,00	2,27	0,00	0,00	25,00	0,00	0,00	4,55	0,00	0,00
GeoB17603-3-6, 550-551	550																	
GeoB17603-3-6, 560-561	560	1000	1,25	1,25	0,00	0,00	58,75	6,25	0,00	0,00	0,00	0,00	17,50	0,00	0,00	5,00	1,25	0,00

GeoB17603-3-6, 570-571	570																	
GeoB17603-3-6, 580-581	580	1000	0,00	0,00	0,00	0,00	41,67	28,57	0,00	0,00	0,00	0,00	8,33	0,00	0,00	5,95	0,00	0,00
GeoB17603-3-7, 590-591	590																	
GeoB17603-3-7, 600-601	600	1000	0,00	0,00	0,00	0,00	75,34	5,48	0,00	0,00	0,00	0,00	12,33	0,00	0,00	0,00	1,37	0,00
GeoB17603-3-7, 610-611	610																	
GeoB17603-3-7, 620-621	620	1000	4,41	0,00	0,00	0,00	52,94	16,18	0,00	1,47	0,00	0,00	16,18	0,00	0,00	1,47	0,00	0,00
GeoB17603-3-7, 630-631	630																	
GeoB17603-3-7, 640-641	640	1000	1,82	5,45	1,82	0,00	9,09	32,73	0,00	3,64	0,00	3,64	32,73	0,00	0,00	0,00	0,00	0,00
GeoB17603-3-7, 650-651	650																	
GeoB17603-3-7, 660-661	660	1000	0,00	0,00	0,00	0,00	0,00	0,00	0,00	0,00	0,00	0,00	0,00	0,00	0,00	0,00	0,00	0,00
GeoB17603-3-7, 670-671	670																	
GeoB17603-3-7, 680-681	680	1000	0,00	0,00	0,00	0,00	4,55	13,64	0,00	0,00	0,00	0,00	68,18	0,00	0,00	0,00	0,00	0,00
GeoB17603-3-8, 690-691	690																	
GeoB17603-3-8, 700-701	700	1000	0,00	0,00	0,00	0,00	0,00	42,86	0,00	0,00	0,00	0,00	42,86	0,00	0,00	0,00	0,00	0,00
GeoB17603-3-8, 710-711	710																	
GeoB17603-3-8, 720-721	720	1000	0,00	0,00	0,00	0,00	0,00	0,00	0,00	0,00	0,00	0,00	100,00	0,00	0,00	0,00	0,00	0,00
GeoB17603-3-8, 730-731	730																	
GeoB17603-3-8, 740-741	740	1000	0,00	0,00	0,00	0,00	4,55	36,36	0,00	0,00	0,00	4,55	36,36	0,00	0,00	0,00	0,00	4,55
GeoB17603-3-8, 750-751	750																	
GeoB17603-3-8, 760-761	760	1000	0,00	0,00	6,67	0,00	6,67	40,00	0,00	0,00	0,00	0,00	20,00	0,00	0,00	0,00	0,00	0,00
GeoB17603-3-8, 770-771	770																	
GeoB17603-3-8, 780-781	780	1000	3,45	0,00	0,00	0,00	13,79	27,59	0,00	0,00	3,45	0,00	20,69	0,00	0,00	0,00	0,00	0,00

GeoB17603-3-9, 790-791	790																	
GeoB17603-3-9, 800-801	800	1000	3,45	0,00	0,00	0,00	10,34	27,59	0,00	6,90	0,00	0,00	10,34	0,00	0,00	0,00	0,00	0,00
GeoB17603-3-9, 810-811	810																	
GeoB17603-3-9, 820-821	820	1000	2,22	0,00	0,00	0,00	4,44	26,67	0,00	0,00	0,00	0,00	28,89	0,00	0,00	0,00	0,00	0,00
GeoB17603-3-9, 830-831	830																	
GeoB17603-3-9, 840-841	840	1000	35,71	0,00	0,00	0,00	7,14	0,00	0,00	0,00	0,00	0,00	28,57	0,00	0,00	0,00	0,00	0,00
GeoB17603-3-9, 850-851	850																	
GeoB17603-3-9, 860-861	860	1000	0,00	0,00	0,00	0,00	0,00	0,00	0,00	0,00	0,00	0,00	0,00	0,00	0,00	0,00	0,00	0,00
GeoB17603-3-9, 870-871	870																	
GeoB17603-3-9, 880-881	880	1000	0,00	0,00	0,00	0,00	0,00	0,00	0,00	0,00	0,00	0,00	0,00	0,00	0,00	0,00	0,00	0,00
GeoB17603-3-10, 890-891	890																	
GeoB17603-3-10, 900-901	900	1000	0,00	0,00	0,00	0,00	0,00	0,00	0,00	0,00	0,00	0,00	0,00	0,00	0,00	0,00	0,00	0,00
GeoB17603-3-10, 910-911	910																	
GeoB17603-3-10, 920-921	920	1000	0,00	0,00	0,00	0,00	0,00	0,00	0,00	0,00	0,00	0,00	0,00	0,00	0,00	0,00	0,00	0,00
GeoB17603-3-10, 930-931	930																	
GeoB17603-3-10, 940-941	940	1000	0,00	0,00	0,00	0,00	0,00	0,00	0,00	0,00	0,00	0,00	0,00	0,00	0,00	0,00	0,00	0,00
GeoB17603-3-10, 950-951	950																	
GeoB17603-3-10, 960-961	960	1000	0,00	0,00	0,00	0,00	0,00	0,00	0,00	0,00	0,00	0,00	0,00	0,00	0,00	0,00	0,00	0,00

Sample	**Depth (cm)**	**Fields**	***Thalassiosira antarctica***	***Thalassiosira eccentrica***	***T. gravida***	***T. nordenskeioldii***	***T. oestrupii***	***T. poroseriata***	***Thalassiosira* sp.**	***Thalassiosira* cf. *tumida***	***Thalassionema* spp.**	***Thalassiotrix* sp.**	**Absolute Diatom Abundance (ADA) ($x10^6$ v/gdw)**	**Dominance index**	**Shannon diversity index**
GeoB17603-3-1, 0-1	0	1000	6,27	0,00	0,39	0,39	0,00	0,00	0,00	1,96	5,88	0,00	23,25	0,35	1,57
GeoB17603-3-1, 10-11	10														
GeoB17603-3-1, 20-21	20	1000	5,77	0,00	0,00	0,00	1,92	0,00	0,00	0,00	1,92	0,00	5,42	0,54	1,08
GeoB17603-3-1, 30-31	30														
GeoB17603-3-1, 40-41	40	1000	3,45	0,00	0,00	3,45	0,00	0,00	0,00	3,45	13,79	0,00	2,55	0,46	1,20
GeoB17603-3-1, 50-51	50														
GeoB17603-3-1, 60-61	60	1000	0,00	0,00	0,00	0,00	0,00	0,00	0,00	0,65	1,94	0,00	14,02	0,77	0,60
GeoB17603-3-1, 70-71	70														
GeoB17603-3-1, 80-81	80	1000	0,00	0,00	0,00	0,00	0,00	0,00	0,00	0,00	0,00	0,00	0,18		
GeoB17603-3-2, 90-91	90														
GeoB17603-3-2, 100-101	100	1000	0,00	0,00	0,00	0,00	0,00	0,00	0,00	0,00	0,00	0,00	0,23	0,56	0,64
GeoB17603-3-2, 110-111	110														
GeoB17603-3-2, 120-121	120														
GeoB17603-3-2, 130-131	130														

GeoB17603-3-2, 140-141	140	1000	0,00	0,00	0,00	0,00	6,25	0,00	0,00	0,00	12,50	0,00	1,51	0,23	1,68
GeoB17603-3-2, 150-151	150														
GeoB17603-3-2, 160-161	160	1000	1,47	0,00	1,47	0,00	1,47	0,00	0,00	0,00	8,82	0,00	3,01	0,36	1,51
GeoB17603-3-2, 170-171	170														
GeoB17603-3-2, 180-181	180	1000	5,26	0,00	0,00	0,00	13,16	0,00	0,00	0,00	2,63	0,00	3,62	0,32	1,53
GeoB17603-3-3, 190-191	190														
GeoB17603-3-3, 200-201	200	1000	0,00	0,00	0,00	0,00	26,09	4,35	0,00	8,70	0,00	0,00	1,88	0,32	1,40
GeoB17603-3-3, 210-211	210														
GeoB17603-3-3, 220-221	220	1000	0,00	0,00	0,00	0,00	18,75	0,00	0,00	3,13	9,38	3,13	3,10	0,26	1,67
GeoB17603-3-3, 230-231	230														
GeoB17603-3-3, 240-241	240	1000	1,85	0,00	1,85	0,00	27,78	0,00	0,00	3,70	9,26	0,00	5,46	0,17	2,01
GeoB17603-3-3, 250-251	250														
GeoB17603-3-3, 260-261	260	1000	5,41	0,00	0,00	0,00	24,32	0,00	0,00	0,00	0,00	0,00	3,70	0,20	1,80
GeoB17603-3-3, 270-271	270														
GeoB17603-3-3, 280-281	280	1000	0,00	0,00	1,69	0,00	10,17	0,00	0,00	3,39	3,39	0,00	5,91	0,27	1,69
GeoB17603-3-4, 290-291	290														
GeoB17603-3-4, 300-301	300	1000	3,57	0,00	0,00	0,00	21,43	0,00	0,00	1,19	1,19	1,19	6,82	0,25	1,66
GeoB17603-3-4, 310-311	310														
GeoB17603-3-4, 320-321	320	1000	2,52	0,00	1,68	0,84	9,24	0,00	1,68	3,36	1,68	0,00	11,90	0,26	1,78
GeoB17603-3-4, 330-331	330														
GeoB17603-3-4, 340-341	340	1000	1,35	0,00	1,35	0,00	22,97	1,35	0,00	0,00	5,41	0,00	7,18	0,29	1,60
GeoB17603-3-4, 350-351	350														

GeoB17603-3-4, 360-361	360	1000	3,53	0,00	0,00	0,00	18,82	3,53	0,00	1,18	3,53	1,18	8,75	0,26	1,68
GeoB17603-3-4, 370-371	370														
GeoB17603-3-4, 380-381	380	1000	0,00	0,00	0,00	0,00	1,23	1,23	0,00	1,23	9,88	0,00	7,98	0,28	1,62
GeoB17603-3-5, 390-391	390														
GeoB17603-3-5, 400-401	400	1000	0,00	0,00	2,30	0,00	8,05	1,15	0,00	1,15	1,15	0,00	7,83	0,34	1,36
GeoB17603-3-5, 410-411	410														
GeoB17603-3-5, 420-421	420	1000	2,97	0,00	0,99	0,00	2,97	0,00	0,00	4,95	6,93	0,00	10,11	0,34	1,57
GeoB17603-3-5, 430-431	430														
GeoB17603-3-5, 440-441	440	1000	0,00	0,00	4,67	0,00	9,35	0,00	0,00	1,87	3,74	0,00	10,82	0,24	1,73
GeoB17603-3-5, 450-451	450														
GeoB17603-3-5, 460-461	460	1000	0,00	0,00	0,86	0,00	15,52	0,00	0,86	1,72	6,90	0,00	11,73	0,16	2,00
GeoB17603-3-5, 470-471	470														
GeoB17603-3-5, 480-481	480	1000	0,81	0,00	0,81	0,00	12,90	0,00	0,00	0,00	7,26	0,81	12,36	0,25	1,78
GeoB17603-3-6, 490-491	490														
GeoB17603-3-6, 500-501	500	1000	0,00	0,00	1,47	0,00	0,00	0,00	1,47	1,47	2,94	0,00	6,56	0,43	1,31
GeoB17603-3-6, 510-511	510														
GeoB17603-3-6, 520-521	520	1000	4,05	0,00	0,00	0,00	0,00	0,00	0,00	2,70	0,00	0,00	7,59	0,38	1,23
GeoB17603-3-6, 530-531	530														
GeoB17603-3-6, 540-541	540	1000	2,27	0,00	2,27	0,00	4,55	0,00	0,00	9,09	0,00	0,00	4,47	0,28	1,65
GeoB17603-3-6, 550-551	550														
GeoB17603-3-6, 560-561	560	1000	2,50	0,00	0,00	0,00	0,00	0,00	0,00	0,00	1,25	0,00	7,43	0,42	1,27
GeoB17603-3-6, 570-571	570														

GeoB17603-3-6, 580-581	580	1000	1,19	0,00	0,00	0,00	11,90	0,00	0,00	1,19	0,00	0,00	7,28	0,29	1,46
GeoB17603-3-7, 590-591	590														
GeoB17603-3-7, 600-601	600	1000	0,00	0,00	0,00	0,00	0,00	0,00	0,00	2,74	0,00	0,00	7,41	0,62	0,78
GeoB17603-3-7, 610-611	610														
GeoB17603-3-7, 620-621	620	1000	2,94	0,00	0,00	0,00	0,00	0,00	0,00	0,00	2,94	0,00	6,16	0,35	1,40
GeoB17603-3-7, 630-631	630														
GeoB17603-3-7, 640-641	640	1000	0,00	0,00	0,00	0,00	1,82	0,00	0,00	1,82	0,00	0,00	5,52	0,26	1,68
GeoB17603-3-7, 650-651	650														
GeoB17603-3-7, 660-661	660	1000	0,00	0,00	0,00	0,00	0,00	0,00	0,00	0,00	0,00	0,00	0,00		
GeoB17603-3-7, 670-671	670														
GeoB17603-3-7, 680-681	680	1000	4,55	0,00	0,00	0,00	0,00	0,00	0,00	4,55	0,00	0,00	2,04	0,54	0,95
GeoB17603-3-8, 690-691	690														
GeoB17603-3-8, 700-701	700	1000	0,00	0,00	0,00	0,00	14,29	0,00	0,00	0,00	0,00	0,00	0,65	0,39	1,00
GeoB17603-3-8, 710-711	710														
GeoB17603-3-8, 720-721	720	1000	0,00	0,00	0,00	0,00	0,00	0,00	0,00	0,00	0,00	0,00	0,10	1,00	0,00
GeoB17603-3-8, 730-731	730														
GeoB17603-3-8, 740-741	740	1000	0,00	4,55	0,00	0,00	0,00	0,00	0,00	0,00	0,00	0,00	1,97	0,33	1,33
GeoB17603-3-8, 750-751	750														
GeoB17603-3-8, 760-761	760	1000	6,67	6,67	0,00	0,00	6,67	6,67	0,00	0,00	0,00	0,00	1,43	0,23	1,77
GeoB17603-3-8, 770-771	770														
GeoB17603-3-8, 780-781	780	1000	3,45	3,45	0,00	0,00	3,45	10,34	0,00	6,90	0,00	0,00	2,77	0,17	1,99
GeoB17603-3-9, 790-791	790														

GeoB17603-3-9, 800-801	800	1000	10,34	17,24	0,00	3,45	3,45	0,00	0,00	3,45	0,00	0,00	2,88	0,16	2,05
GeoB17603-3-9, 810-811	810														
GeoB17603-3-9, 820-821	820	1000	2,22	13,33	0,00	0,00	2,22	2,22	0,00	6,67	0,00	0,00	4,18	0,23	1,72
GeoB17603-3-9, 830-831	830														
GeoB17603-3-9, 840-841	840	1000	14,29	0,00	0,00	0,00	0,00	7,14	0,00	7,14	0,00	0,00	1,31	0,24	1,57
GeoB17603-3-9, 850-851	850														
GeoB17603-3-9, 860-861	860	1000	0,00	0,00	0,00	0,00	0,00	0,00	0,00	0,00	0,00	0,00	0,00		
GeoB17603-3-9, 870-871	870														
GeoB17603-3-9, 880-881	880	1000	0,00	0,00	0,00	0,00	0,00	0,00	0,00	0,00	0,00	0,00	0,00		
GeoB17603-3-10, 890-891	890														
GeoB17603-3-10, 900-901	900	1000	0,00	0,00	0,00	0,00	0,00	0,00	0,00	0,00	0,00	0,00	0,00		
GeoB17603-3-10, 910-911	910														
GeoB17603-3-10, 920-921	920	1000	0,00	0,00	0,00	0,00	0,00	0,00	0,00	0,00	0,00	0,00	0,00		
GeoB17603-3-10, 930-931	930														
GeoB17603-3-10, 940-941	940	1000	0,00	0,00	0,00	0,00	0,00	0,00	0,00	0,00	0,00	0,00	0,00		
GeoB17603-3-10, 950-951	950														
GeoB17603-3-10, 960-961	960	1000	0,00	0,00	0,00	0,00	0,00	0,00	0,00	0,00	0,00	0,00	0,00		

Sample	Depth (cm)	Age (cal age BP)
GeoB17603-3-1, 0-1	0	302,00
GeoB17603-3-1, 10-11	10	736,00
GeoB17603-3-1, 20-21	20	1813,00
GeoB17603-3-1, 30-31	30	2183,00
GeoB17603-3-1, 40-41	40	2780,00
GeoB17603-3-1, 50-51	50	3377,00
GeoB17603-3-1, 60-61	60	3825,67
GeoB17603-3-1, 70-71	70	4274,33
GeoB17603-3-1, 80-81	80	4723,00
GeoB17603-3-2, 90-91	90	5093,50
GeoB17603-3-2, 100-101	100	5464,00
GeoB17603-3-2, 110-111	110	5834,50
GeoB17603-3-2, 120-121	120	6205,00

GeoB17603-3-2, 130-131	130	6575,50
GeoB17603-3-2, 140-141	140	6946,00
GeoB17603-3-2, 150-151	150	7124,50
GeoB17603-3-2, 160-161	160	7303,00
GeoB17603-3-2, 170-171	170	7471,00
GeoB17603-3-2, 180-181	180	7639,00
GeoB17603-3-3, 190-191	190	7807,00
GeoB17603-3-3, 200-201	200	7975,00
GeoB17603-3-3, 210-211	210	8143,00
GeoB17603-3-3, 220-221	220	8320,67
GeoB17603-3-3, 230-231	230	8498,33
GeoB17603-3-3, 240-241	240	8676,00
GeoB17603-3-3, 250-251	250	8768,67
GeoB17603-3-3, 260-261	260	8861,33
GeoB17603-3-3, 270-271	270	8954,00
GeoB17603-3-3, 280-281	280	9000,00
GeoB17603-3-4, 290-291	290	9046,00
GeoB17603-3-4, 300-301	300	9093,00
GeoB17603-3-4, 310-311	310	9138,89
GeoB17603-3-4, 320-321	320	9185,11
GeoB17603-3-4, 330-331	330	9231,33
GeoB17603-3-4, 340-341	340	9277,56

GeoB17603-3-4, 350-351	350	9323,78
GeoB17603-3-4, 360-361	360	9370,00
GeoB17603-3-4, 370-371	370	9468,83
GeoB17603-3-4, 380-381	380	9567,67
GeoB17603-3-5, 390-391	390	9666,50
GeoB17603-3-5, 400-401	400	9765,33
GeoB17603-3-5, 410-411	410	9864,17
GeoB17603-3-5, 420-421	420	9963,00
GeoB17603-3-5, 430-431	430	10061,83
GeoB17603-3-5, 440-441	440	10160,67
GeoB17603-3-5, 450-451	450	10259,50
GeoB17603-3-5, 460-461	460	10358,33
GeoB17603-3-5, 470-471	470	10457,17
GeoB17603-3-5, 480-481	480	10556,00
GeoB17603-3-6, 490-491	490	10654,83
GeoB17603-3-6, 500-501	500	10753,67
GeoB17603-3-6, 510-511	510	10852,50
GeoB17603-3-6, 520-521	520	10951,33
GeoB17603-3-6, 530-531	530	11050,17
GeoB17603-3-6, 540-541	540	11149,00
GeoB17603-3-6, 550-551	550	11247,83
GeoB17603-3-6, 560-561	560	11346,67

GeoB17603-3-6, 570-571	570	11445,50
GeoB17603-3-6, 580-581	580	11544,33
GeoB17603-3-7, 590-591	590	11643,17
GeoB17603-3-7, 600-601	600	11742,00
GeoB17603-3-7, 610-611	610	11840,83
GeoB17603-3-7, 620-621	620	11939,67
GeoB17603-3-7, 630-631	630	12038,50
GeoB17603-3-7, 640-641	640	12137,33
GeoB17603-3-7, 650-651	650	12236,17
GeoB17603-3-7, 660-661	660	12335,00
GeoB17603-3-7, 670-671	670	12697,00
GeoB17603-3-7, 680-681	680	13059,00
GeoB17603-3-8, 690-691	690	13111,93
GeoB17603-3-8, 700-701	700	13164,86
GeoB17603-3-8, 710-711	710	13217,79
GeoB17603-3-8, 720-721	720	13270,71
GeoB17603-3-8, 730-731	730	13323,64
GeoB17603-3-8, 740-741	740	13376,57
GeoB17603-3-8, 750-751	750	13429,50
GeoB17603-3-8, 760-761	760	13482,43
GeoB17603-3-8, 770-771	770	13535,36
GeoB17603-3-8, 780-781	780	13588,29

GeoB17603-3-9, 790-791	790	13641,21
GeoB17603-3-9, 800-801	800	13694,14
GeoB17603-3-9, 810-811	810	13747,07
GeoB17603-3-9, 820-821	820	13800,00
GeoB17603-3-9, 830-831	830	14027,30
GeoB17603-3-9, 840-841	840	14061,42
GeoB17603-3-9, 850-851	850	14095,54
GeoB17603-3-9, 860-861	860	14129,66
GeoB17603-3-9, 870-871	870	14163,78
GeoB17603-3-9, 880-881	880	14197,91
GeoB17603-3-10, 890-891	890	14232,03
GeoB17603-3-10, 900-901	900	14266,15
GeoB17603-3-10, 910-911	910	14300,27
GeoB17603-3-10, 920-921	920	14334,39
GeoB17603-3-10, 930-931	930	14368,51
GeoB17603-3-10, 940-941	940	14402,64
GeoB17603-3-10, 950-951	950	14436,76
GeoB17603-3-10, 960-961	960	14470,88
GeoB17603-3-10, 970-971	970	14505,00

SUPPLEMENTARY C- GeoB17605-3 nannofossil abundance

Sample	Depth (cm)	Fields	*Coccolithus pelagicus pelagicus*	*Emiliania huxleyi* < 4 µm	*Emiliania huxleyi* > 4µm	*Gephyrocapsa muellerae*	Reworked	*Thoracosphaera* spp.	Total *E. huxleyi*	Total abundance (with reworked)	Total abundance (NO reworked)
GeoB17605-3-1,0-1	0	200	0	10	1	1	8	0	11	20	12
GeoB17605-3-1,10-11	10	200	0	48	13	5	15	0	61	81	66
GeoB17605-3-1,20-21	20	200	0	39	17	1	12	0	56	69	57
GeoB17605-3-2,30-31	30	200	0	24	8	1	10	0	32	43	33
GeoB17605-3-2,40-41	40	200	1	19	8	1	9	1	27	39	30
GeoB17605-3-2,50-51	50	200	0	14	2	2	17	0	16	35	18
GeoB17605-3-2,60-61	60	200	0	45	5	6	6	0	50	62	56
GeoB17605-3-2,70-71	70	200	0	68	19	0	11	0	87	98	87
GeoB17605-3-2,80-81	80	200	0	22	3	6	33	0	25	64	31
GeoB17605-3-2,90-91	90	200	0	31	13	0	7	0	44	51	44

GeoB17605-3-2,100-101	100	200	0	30	12	2	6	0	42	50	44
GeoB17605-3-2,110-111	110	200	0	4	0	0	5	0	4	9	4
GeoB17605-3-2,120-121	120	200	0	34	2	1	13	0	36	50	37
GeoB17605-3-3,130-131	130	200	0	6	1	0	4	0	7	11	7
GeoB17605-3-3,140-141	140	200	0	27	3	0	9	0	30	39	30
GeoB17605-3-3,150-151	150	200	0	3	0	0	8	0	3	11	3
GeoB17605-3-3,160-161	160	200	0	7	0	2	11	0	7	20	9
GeoB17605-3-3,170-171	170	200	0	30	4	3	8	0	34	45	37
GeoB17605-3-3,180-181	180	200	0	16	5	4	26	0	21	51	25
GeoB17605-3-3,190-191	190	200	0	18	2	1	21	0	20	42	21
GeoB17605-3-3,200-201	200	200	0	6	1	0	25	0	7	32	7
GeoB17605-3-3,210-211	210	200	0	23	1	4	13	0	24	41	28
GeoB17605-3-3,220-221	220	200	0	8	1	2	14	0	9	25	11
GeoB17605-3-4,230-231	230	200	0	10	1	0	7	0	11	18	11
GeoB17605-3-4,240-241	240	200	0	10	0	0	18	0	10	28	10
GeoB17605-3-4,250-251	250	200	1	12	0	0	19	0	12	32	13
GeoB17605-3-4,260-261	260	200	1	18	1	0	24	0	19	44	20
GeoB17605-3-4,270-271	270	200	0	21	1	0	13	0	22	35	22
GeoB17605-3-4,280-281	280	200	0	25	4	1	21	0	29	51	30
GeoB17605-3-4,290-291	290	200	0	5	0	0	22	0	5	27	5
GeoB17605-3-4,300-301	300	200	0	20	5	3	20	0	25	48	28
GeoB17605-3-4,310-311	310	200	0	9	2	1	22	0	11	34	12

GeoB17605-3-4,320-321	320	200	1	64	8	1	17	0	72	91	74
GeoB17605-3-5, 330-331	330	200	1	3	1	2	14	0	4	21	7
GeoB17605-3-5, 340-341	340	200	0	13	4	3	19	0	17	39	20
GeoB17605-3-5, 350-351	350	200	0	24	4	4	15	0	28	47	32
GeoB17605-3-5, 360-361	360	200	2	8	1	2	17	0	9	30	13
GeoB17605-3-5, 370-371	370	200	1	15	0	0	24	0	15	40	16
GeoB17605-3-5, 380-381	380	200	0	14	2	0	9	0	16	25	16
GeoB17605-3-5, 390-391	390	200	1	15	3	1	7	0	18	27	20
GeoB17605-3-5, 400-401	400	200	0	58	20	2	9	1	78	90	81

Sample	Depth (cm)	Observed surface (mm^2)	*C. pel. pelagicus*/10 mm^2	*E. huxleyi* < 4 µm/10 mm^2	*E. huxleyi* > 4µm/10 mm^2	*G. muellerae*/10 mm^2	Reworked/10 mm^2	*Thoracosphaera* spp. /10 mm^2	Total *E. huxleyi* /10 mm^2	Total abundance (with reworked) /10 mm^2	Total abundance (NO reworked) /10 mm^2
GeoB17605-3-1,0-1	0	6,28	0,00	15,92	1,59	1,59	12,74	0,00	17,52	31,85	19,11
GeoB17605-3-1,10-11	10	6,28	0,00	76,43	20,70	7,96	23,89	0,00	97,13	128,98	105,10
GeoB17605-3-1,20-21	20	6,28	0,00	62,10	27,07	1,59	19,11	0,00	89,17	109,87	90,76
GeoB17605-3-2,30-31	30	6,28	0,00	38,22	12,74	1,59	15,92	0,00	50,96	68,47	52,55
GeoB17605-3-2,40-41	40	6,28	1,59	30,25	12,74	1,59	14,33	1,59	42,99	62,10	47,77
GeoB17605-3-2,50-51	50	6,28	0,00	22,29	3,18	3,18	27,07	0,00	25,48	55,73	28,66
GeoB17605-3-2,60-61	60	6,28	0,00	71,66	7,96	9,55	9,55	0,00	79,62	98,73	89,17
GeoB17605-3-2,70-71	70	6,28	0,00	108,28	30,25	0,00	17,52	0,00	138,54	156,05	138,54
GeoB17605-3-2,80-81	80	6,28	0,00	35,03	4,78	9,55	52,55	0,00	39,81	101,91	49,36
GeoB17605-3-2,90-91	90	6,28	0,00	49,36	20,70	0,00	11,15	0,00	70,06	81,21	70,06
GeoB17605-3-2,100-101	100	6,28	0,00	47,77	19,11	3,18	9,55	0,00	66,88	79,62	70,06
GeoB17605-3-2,110-111	110	6,28	0,00	6,37	0,00	0,00	7,96	0,00	6,37	14,33	6,37
GeoB17605-3-2,120-121	120	6,28	0,00	54,14	3,18	1,59	20,70	0,00	57,32	79,62	58,92

GeoB17605-3-3,130-131	130	6,28	0,00	9,55	1,59	0,00	6,37	0,00	11,15	17,52	11,15
GeoB17605-3-3,140-141	140	6,28	0,00	42,99	4,78	0,00	14,33	0,00	47,77	62,10	47,77
GeoB17605-3-3,150-151	150	6,28	0,00	4,78	0,00	0,00	12,74	0,00	4,78	17,52	4,78
GeoB17605-3-3,160-161	160	6,28	0,00	11,15	0,00	3,18	17,52	0,00	11,15	31,85	14,33
GeoB17605-3-3,170-171	170	6,28	0,00	47,77	6,37	4,78	12,74	0,00	54,14	71,66	58,92
GeoB17605-3-3,180-181	180	6,28	0,00	25,48	7,96	6,37	41,40	0,00	33,44	81,21	39,81
GeoB17605-3-3,190-191	190	6,28	0,00	28,66	3,18	1,59	33,44	0,00	31,85	66,88	33,44
GeoB17605-3-3,200-201	200	6,28	0,00	9,55	1,59	0,00	39,81	0,00	11,15	50,96	11,15
GeoB17605-3-3,210-211	210	6,28	0,00	36,62	1,59	6,37	20,70	0,00	38,22	65,29	44,59
GeoB17605-3-3,220-221	220	6,28	0,00	12,74	1,59	3,18	22,29	0,00	14,33	39,81	17,52
GeoB17605-3-4,230-231	230	6,28	0,00	15,92	1,59	0,00	11,15	0,00	17,52	28,66	17,52
GeoB17605-3-4,240-241	240	6,28	0,00	15,92	0,00	0,00	28,66	0,00	15,92	44,59	15,92
GeoB17605-3-4,250-251	250	6,28	1,59	19,11	0,00	0,00	30,25	0,00	19,11	50,96	20,70
GeoB17605-3-4,260-261	260	6,28	1,59	28,66	1,59	0,00	38,22	0,00	30,25	70,06	31,85
GeoB17605-3-4,270-271	270	6,28	0,00	33,44	1,59	0,00	20,70	0,00	35,03	55,73	35,03
GeoB17605-3-4,280-281	280	6,28	0,00	39,81	6,37	1,59	33,44	0,00	46,18	81,21	47,77
GeoB17605-3-4,290-291	290	6,28	0,00	7,96	0,00	0,00	35,03	0,00	7,96	42,99	7,96
GeoB17605-3-4,300-301	300	6,28	0,00	31,85	7,96	4,78	31,85	0,00	39,81	76,43	44,59
GeoB17605-3-4,310-311	310	6,28	0,00	14,33	3,18	1,59	35,03	0,00	17,52	54,14	19,11
GeoB17605-3-4,320-321	320	6,28	1,59	101,91	12,74	1,59	27,07	0,00	114,65	144,90	117,83
GeoB17605-3-5, 330-331	330	6,28	1,59	4,78	1,59	3,18	22,29	0,00	6,37	33,44	11,15
GeoB17605-3-5, 340-341	340	6,28	0,00	20,70	6,37	4,78	30,25	0,00	27,07	62,10	31,85

GeoB17605-3-5, 350-351	350	6,28	0,00	38,22	6,37	6,37	23,89	0,00	44,59	74,84	50,96
GeoB17605-3-5, 360-361	360	6,28	3,18	12,74	1,59	3,18	27,07	0,00	14,33	47,77	20,70
GeoB17605-3-5, 370-371	370	6,28	1,59	23,89	0,00	0,00	38,22	0,00	23,89	63,69	25,48
GeoB17605-3-5, 380-381	380	6,28	0,00	22,29	3,18	0,00	14,33	0,00	25,48	39,81	25,48
GeoB17605-3-5, 390-391	390	6,28	1,59	23,89	4,78	1,59	11,15	0,00	28,66	42,99	31,85
GeoB17605-3-5, 400-401	400	6,28	0,00	92,36	31,85	3,18	14,33	1,59	124,20	143,31	128,98

Sample	Depth (cm)	% *C. pel. pelagicus*	% *E. huxleyi* < 4 µm	% *E. huxleyi* > 4µm	% *G. muellerae*	% Reworked	% *Thoracosphaera* spp.	% Total *E. huxleyi*	% Total abundance (NO reworked)
GeoB17605-3-1,0-1	0	0,00	50,00	5,00	5,00	40,00	0,00	55,00	60,00
GeoB17605-3-1,10-11	10	0,00	59,26	16,05	6,17	18,52	0,00	75,31	81,48
GeoB17605-3-1,20-21	20	0,00	56,52	24,64	1,45	17,39	0,00	81,16	82,61
GeoB17605-3-2,30-31	30	0,00	55,81	18,60	2,33	23,26	0,00	74,42	76,74
GeoB17605-3-2,40-41	40	2,56	48,72	20,51	2,56	23,08	2,56	69,23	76,92
GeoB17605-3-2,50-51	50	0,00	40,00	5,71	5,71	48,57	0,00	45,71	51,43
GeoB17605-3-2,60-61	60	0,00	72,58	8,06	9,68	9,68	0,00	80,65	90,32
GeoB17605-3-2,70-71	70	0,00	69,39	19,39	0,00	11,22	0,00	88,78	88,78
GeoB17605-3-2,80-81	80	0,00	34,38	4,69	9,38	51,56	0,00	39,06	48,44
GeoB17605-3-2,90-91	90	0,00	60,78	25,49	0,00	13,73	0,00	86,27	86,27
GeoB17605-3-2,100-101	100	0,00	60,00	24,00	4,00	12,00	0,00	84,00	88,00
GeoB17605-3-2,110-111	110	0,00	44,44	0,00	0,00	55,56	0,00	44,44	44,44
GeoB17605-3-2,120-121	120	0,00	68,00	4,00	2,00	26,00	0,00	72,00	74,00

GeoB17605-3-3,130-131	130	0,00	54,55	9,09	0,00	36,36	0,00	63,64	63,64
GeoB17605-3-3,140-141	140	0,00	69,23	7,69	0,00	23,08	0,00	76,92	76,92
GeoB17605-3-3,150-151	150	0,00	27,27	0,00	0,00	72,73	0,00	27,27	27,27
GeoB17605-3-3,160-161	160	0,00	35,00	0,00	10,00	55,00	0,00	35,00	45,00
GeoB17605-3-3,170-171	170	0,00	66,67	8,89	6,67	17,78	0,00	75,56	82,22
GeoB17605-3-3,180-181	180	0,00	31,37	9,80	7,84	50,98	0,00	41,18	49,02
GeoB17605-3-3,190-191	190	0,00	42,86	4,76	2,38	50,00	0,00	47,62	50,00
GeoB17605-3-3,200-201	200	0,00	18,75	3,13	0,00	78,13	0,00	21,88	21,88
GeoB17605-3-3,210-211	210	0,00	56,10	2,44	9,76	31,71	0,00	58,54	68,29
GeoB17605-3-3,220-221	220	0,00	32,00	4,00	8,00	56,00	0,00	36,00	44,00
GeoB17605-3-4,230-231	230	0,00	55,56	5,56	0,00	38,89	0,00	61,11	61,11
GeoB17605-3-4,240-241	240	0,00	35,71	0,00	0,00	64,29	0,00	35,71	35,71
GeoB17605-3-4,250-251	250	3,13	37,50	0,00	0,00	59,38	0,00	37,50	40,63
GeoB17605-3-4,260-261	260	2,27	40,91	2,27	0,00	54,55	0,00	43,18	45,45
GeoB17605-3-4,270-271	270	0,00	60,00	2,86	0,00	37,14	0,00	62,86	62,86
GeoB17605-3-4,280-281	280	0,00	49,02	7,84	1,96	41,18	0,00	56,86	58,82
GeoB17605-3-4,290-291	290	0,00	18,52	0,00	0,00	81,48	0,00	18,52	18,52
GeoB17605-3-4,300-301	300	0,00	41,67	10,42	6,25	41,67	0,00	52,08	58,33
GeoB17605-3-4,310-311	310	0,00	26,47	5,88	2,94	64,71	0,00	32,35	35,29
GeoB17605-3-4,320-321	320	1,10	70,33	8,79	1,10	18,68	0,00	79,12	81,32
GeoB17605-3-5, 330-331	330	4,76	14,29	4,76	9,52	66,67	0,00	19,05	33,33
GeoB17605-3-5, 340-341	340	0,00	33,33	10,26	7,69	48,72	0,00	43,59	51,28

GeoB17605-3-5, 350-351	350	0,00	51,06	8,51	8,51	31,91	0,00	59,57	68,09
GeoB17605-3-5, 360-361	360	6,67	26,67	3,33	6,67	56,67	0,00	30,00	43,33
GeoB17605-3-5, 370-371	370	2,50	37,50	0,00	0,00	60,00	0,00	37,50	40,00
GeoB17605-3-5, 380-381	380	0,00	56,00	8,00	0,00	36,00	0,00	64,00	64,00
GeoB17605-3-5, 390-391	390	3,70	55,56	11,11	3,70	25,93	0,00	66,67	74,07
GeoB17605-3-5, 400-401	400	0,00	64,44	22,22	2,22	10,00	1,11	86,67	90,00

Sample	Depth (cm)	H/P ratio	Dominance index	Shannon diversity index	CEX *C. pel.*(modif. Dittert et al., 1999)
GeoB17605-3-1,0-1	0		0,83	0,40	1,00
GeoB17605-3-1,10-11	10		0,54	0,91	1,00
GeoB17605-3-1,20-21	20		0,58	0,83	1,00
GeoB17605-3-2,30-31	30		0,69	0,66	1,00
GeoB17605-3-2,40-41	40	1,43	0,71	0,66	0,96
GeoB17605-3-2,50-51	50		0,73	0,58	1,00
GeoB17605-3-2,60-61	60		0,61	0,76	1,00
GeoB17605-3-2,70-71	70		0,51	0,90	1,00
GeoB17605-3-2,80-81	80		0,60	0,81	1,00
GeoB17605-3-2,90-91	90		0,65	0,69	1,00
GeoB17605-3-2,100-101	100		0,66	0,71	1,00
GeoB17605-3-2,110-111	110		0,92	0,21	1,00
GeoB17605-3-2,120-121	120		0,66	0,66	1,00

GeoB17605-3-3,130-131	130		0,90	0,25	1,00
GeoB17605-3-3,140-141	140		0,71	0,57	1,00
GeoB17605-3-3,150-151	150		0,90	0,24	1,00
GeoB17605-3-3,160-161	160		0,83	0,39	1,00
GeoB17605-3-3,170-171	170		0,68	0,66	1,00
GeoB17605-3-3,180-181	180		0,65	0,74	1,00
GeoB17605-3-3,190-191	190		0,70	0,63	1,00
GeoB17605-3-3,200-201	200		0,76	0,49	1,00
GeoB17605-3-3,210-211	210		0,70	0,63	1,00
GeoB17605-3-3,220-221	220		0,80	0,46	1,00
GeoB17605-3-4,230-231	230		0,84	0,36	1,00
GeoB17605-3-4,240-241	240		0,78	0,45	1,00
GeoB17605-3-4,250-251	250	1,08	0,75	0,51	0,92
GeoB17605-3-4,260-261	260	1,28	0,69	0,63	0,95
GeoB17605-3-4,270-271	270		0,74	0,54	1,00
GeoB17605-3-4,280-281	280		0,65	0,71	1,00
GeoB17605-3-4,290-291	290		0,79	0,42	1,00
GeoB17605-3-4,300-301	300		0,66	0,71	1,00
GeoB17605-3-4,310-311	310		0,74	0,55	1,00
GeoB17605-3-4,320-321	320	1,86	0,52	0,89	0,99
GeoB17605-3-5, 330-331	330	0,60	0,82	0,41	0,80
GeoB17605-3-5, 340-341	340		0,71	0,63	1,00

GeoB17605-3-5, 350-351	350		0,67	0,70	1,00
GeoB17605-3-5, 360-361	360	0,65	0,76	0,54	0,82
GeoB17605-3-5, 370-371	370	1,18	0,71	0,58	0,94
GeoB17605-3-5, 380-381	380		0,80	0,45	1,00
GeoB17605-3-5, 390-391	390	1,26	0,78	0,50	0,95
GeoB17605-3-5, 400-401	400		0,52	0,92	1,00

SUPPLEMENTARY D- GeoB17623-2 nannofossil abundance

Sample	**Depth (cm)**	**Fields**	***Calcidiscus leptoporus***	***Coccolithus pelagicus pelagicus***	***Emiliania huxleyi* < 4 µm**	***Emiliania huxleyi* > 4µm**	***Gephyrocapsa muellerae***	***Gephyrocapsa oceanica***	**Reworked Cenozoic**	**Reworked Cretaceous**	**Small *Gephyrocapsa* spp. (<3)**	***Syracosphaera* spp.**	***Thoracosphaera* spp.**	**Total *E. huxleyi***	**Total abundance (with reworked)**	**Total abundance (NO reworked)**	**Total Reworked**
GeoB17623-2-1, 2-3	2	200	0	75	71	0	0	0	0	0	0	0	4	71	150	150	0
GeoB17623-2-1, 5-6	5	200	0	67	63	0	0	0	0	0	0	0	4	63	134	134	0
GeoB17623-2-1, 10-11	10	200	0	229	59	0	0	0	0	0	1	0	12	59	301	301	0
GeoB17623-2-1, 15-16	15	200	0	167	36	0	0	0	0	0	2	0	7	36	212	212	0
GeoB17623-2-1, 20-21	20	200	0	80	60	0	0	0	0	1	0	0	1	60	142	141	1
GeoB17623-2-1, 25-26	25	200	0	61	9	0	0	0	0	0	1	0	6	9	77	77	0
GeoB17623-2-1, 30-31	30	200	0	39	20	0	0	0	0	0	0	0	6	20	65	65	0
GeoB17623-2-1, 35-36	35	200	0	155	31	0	0	0	0	0	0	0	12	31	198	198	0
GeoB17623-2-1, 40-41	40	200	2	77	38	0	0	1	0	0	0	0	8	38	126	126	0
GeoB17623-2-1, 45-46	45	200	0	94	43	0	0	0	0	0	0	0	1	43	138	138	0

GeoB17623-2-1, 50-51	50	200	2	67	52	0	0	0	0	0	0	1	1	52	123	123	0
GeoB17623-2-2, 60-61	60	200	0	112	61	0	0	0	0	0	0	0	5	61	178	178	0
GeoB17623-2-2, 70-71	70	200	1	62	39	0	1	1	0	0	0	0	4	39	108	108	0
GeoB17623-2-2, 80-81	80	200	4	79	20	0	0	0	0	0	0	0	3	20	106	106	0
GeoB17623-2-2, 90-91	90	200	0	27	24	0	0	0	0	0	0	0	3	24	54	54	0
GeoB17623-2-2, 100-101	100	200	0	31	7	0	0	0	0	0	0	0	7	7	45	45	0
GeoB17623-2-2, 110-111	110	200	0	40	7	0	0	0	0	0	0	0	3	7	50	50	0
GeoB17623-2-2, 120-121	120	200	0	54	15	0	0	0	0	0	0	0	4	15	73	73	0
GeoB17623-2-2, 130-131	130	200	1	33	4	0	0	0	0	0	0	0	4	4	42	42	0
GeoB17623-2-2, 140-141	140	200	0	79	76	0	0	0	0	0	0	0	3	76	158	158	0
GeoB17623-2-2, 150-151	150	200	1	39	4	1	0	0	1	0	0	0	8	5	54	53	1

Sample	Depth (cm)	Observed surface (mm^2)	*C. leptoporus*/10 mm^2	*C. pel. pelagicus*/10 mm^2	*E. huxleyi* < 4 µm/10 mm^2	*E. huxleyi* > 4µm/10 mm^2	*G. muellerae*/10 mm^2	*G. oceanica*/10 mm^2	Reworked Cenozoic/10 mm^2	Reworked Cretaceous/10 mm^2	Small *Gephyrocapsa* spp. (<3)/10 mm^2	*Syracosphaera* spp./10 mm^2	*Thoracosphaera* spp. /10 mm^2	Total *E. huxleyi* /10 mm^2	Total abundance (with reworked) /10 mm^2	Total abundance (NO reworked) /10 mm^2	Total Reworked /10 mm^2
GeoB17623-2-1, 2-3	2	6,28	0,00	119,43	113,06	0,00	0,00	0,00	0,00	0,00	0,00	0,00	6,37	113,06	238,85	238,85	0,00
GeoB17623-2-1, 5-6	5	6,28	0,00	106,69	100,32	0,00	0,00	0,00	0,00	0,00	0,00	0,00	6,37	100,32	213,38	213,38	0,00
GeoB17623-2-1, 10-11	10	6,28	0,00	364,65	93,95	0,00	0,00	0,00	0,00	0,00	1,59	0,00	19,11	93,95	479,30	479,30	0,00
GeoB17623-2-1, 15-16	15	6,28	0,00	265,92	57,32	0,00	0,00	0,00	0,00	0,00	3,18	0,00	11,15	57,32	337,58	337,58	0,00
GeoB17623-2-1, 20-21	20	6,28	0,00	127,39	95,54	0,00	0,00	0,00	0,00	1,59	0,00	0,00	1,59	95,54	226,11	224,52	1,59
GeoB17623-2-1, 25-26	25	6,28	0,00	97,13	14,33	0,00	0,00	0,00	0,00	0,00	1,59	0,00	9,55	14,33	122,61	122,61	0,00
GeoB17623-2-1, 30-31	30	6,28	0,00	62,10	31,85	0,00	0,00	0,00	0,00	0,00	0,00	0,00	9,55	31,85	103,50	103,50	0,00
GeoB17623-2-1, 35-36	35	6,28	0,00	246,82	49,36	0,00	0,00	0,00	0,00	0,00	0,00	0,00	19,11	49,36	315,29	315,29	0,00
GeoB17623-2-1, 40-41	40	6,28	3,18	122,61	60,51	0,00	0,00	1,59	0,00	0,00	0,00	0,00	12,74	60,51	200,64	200,64	0,00
GeoB17623-2-1, 45-46	45	6,28	0,00	149,68	68,47	0,00	0,00	0,00	0,00	0,00	0,00	0,00	1,59	68,47	219,75	219,75	0,00
GeoB17623-2-1, 50-51	50	6,28	3,18	106,69	82,80	0,00	0,00	0,00	0,00	0,00	0,00	1,59	1,59	82,80	195,86	195,86	0,00
GeoB17623-2-2, 60-61	60	6,28	0,00	178,34	97,13	0,00	0,00	0,00	0,00	0,00	0,00	0,00	7,96	97,13	283,44	283,44	0,00
GeoB17623-2-2, 70-71	70	6,28	1,59	98,73	62,10	0,00	1,59	1,59	0,00	0,00	0,00	0,00	6,37	62,10	171,97	171,97	0,00

GeoB17623-2-2, 80-81	80	6,28	6,37	125,80	31,85	0,00	0,00	0,00	0,00	0,00	0,00	0,00	4,78	31,85	168,79	168,79	0,00
GeoB17623-2-2, 90-91	90	6,28	0,00	42,99	38,22	0,00	0,00	0,00	0,00	0,00	0,00	0,00	4,78	38,22	85,99	85,99	0,00
GeoB17623-2-2, 100-101	100	6,28	0,00	49,36	11,15	0,00	0,00	0,00	0,00	0,00	0,00	0,00	11,15	11,15	71,66	71,66	0,00
GeoB17623-2-2, 110-111	110	6,28	0,00	63,69	11,15	0,00	0,00	0,00	0,00	0,00	0,00	0,00	4,78	11,15	79,62	79,62	0,00
GeoB17623-2-2, 120-121	120	6,28	0,00	85,99	23,89	0,00	0,00	0,00	0,00	0,00	0,00	0,00	6,37	23,89	116,24	116,24	0,00
GeoB17623-2-2, 130-131	130	6,28	1,59	52,55	6,37	0,00	0,00	0,00	0,00	0,00	0,00	0,00	6,37	6,37	66,88	66,88	0,00
GeoB17623-2-2, 140-141	140	6,28	0,00	125,80	121,02	0,00	0,00	0,00	0,00	0,00	0,00	0,00	4,78	121,02	251,59	251,59	0,00
GeoB17623-2-2, 150-151	150	6,28	1,59	62,10	6,37	1,59	0,00	0,00	1,59	0,00	0,00	0,00	12,74	7,96	85,99	84,39	1,59

Sample	Depth (cm)	% *C. leptoporus*	% *C. pel. pelagicus*	% *E. huxleyi* < 4 µm	% *E. huxleyi* > 4µm	% *G. muellerae*	% *G. oceanica*	% Reworked Cenozoic	% Reworked Cretaceous	% Small *Gephyrocapsa* spp. (<3)	% *Syracosphaera* spp.	% *Thoracosphaera* spp.	% Total *E. huxleyi*	% Total abundance (NO reworked)	% Total Reworked
GeoB17623-2-1, 2-3	2	0,00	50,00	47,33	0,00	0,00	0,00	0,00	0,00	0,00	0,00	2,67	47,33	100,00	0,00
GeoB17623-2-1, 5-6	5	0,00	50,00	47,01	0,00	0,00	0,00	0,00	0,00	0,00	0,00	2,99	47,01	100,00	0,00
GeoB17623-2-1, 10-11	10	0,00	76,08	19,60	0,00	0,00	0,00	0,00	0,00	0,33	0,00	3,99	19,60	100,00	0,00
GeoB17623-2-1, 15-16	15	0,00	78,77	16,98	0,00	0,00	0,00	0,00	0,00	0,94	0,00	3,30	16,98	100,00	0,00
GeoB17623-2-1, 20-21	20	0,00	56,34	42,25	0,00	0,00	0,00	0,00	0,70	0,00	0,00	0,70	42,25	99,30	0,70
GeoB17623-2-1, 25-26	25	0,00	79,22	11,69	0,00	0,00	0,00	0,00	0,00	1,30	0,00	7,79	11,69	100,00	0,00
GeoB17623-2-1, 30-31	30	0,00	60,00	30,77	0,00	0,00	0,00	0,00	0,00	0,00	0,00	9,23	30,77	100,00	0,00
GeoB17623-2-1, 35-36	35	0,00	78,28	15,66	0,00	0,00	0,00	0,00	0,00	0,00	0,00	6,06	15,66	100,00	0,00
GeoB17623-2-1, 40-41	40	1,59	61,11	30,16	0,00	0,00	0,79	0,00	0,00	0,00	0,00	6,35	30,16	100,00	0,00
GeoB17623-2-1, 45-46	45	0,00	68,12	31,16	0,00	0,00	0,00	0,00	0,00	0,00	0,00	0,72	31,16	100,00	0,00
GeoB17623-2-1, 50-51	50	1,63	54,47	42,28	0,00	0,00	0,00	0,00	0,00	0,00	0,81	0,81	42,28	100,00	0,00
GeoB17623-2-2, 60-61	60	0,00	62,92	34,27	0,00	0,00	0,00	0,00	0,00	0,00	0,00	2,81	34,27	100,00	0,00
GeoB17623-2-2, 70-71	70	0,93	57,41	36,11	0,00	0,93	0,93	0,00	0,00	0,00	0,00	3,70	36,11	100,00	0,00

GeoB17623-2-2, 80-81	80	3,77	74,53	18,87	0,00	0,00	0,00	0,00	0,00	0,00	0,00	2,83	18,87	100,00	0,00
GeoB17623-2-2, 90-91	90	0,00	50,00	44,44	0,00	0,00	0,00	0,00	0,00	0,00	0,00	5,56	44,44	100,00	0,00
GeoB17623-2-2, 100-101	100	0,00	68,89	15,56	0,00	0,00	0,00	0,00	0,00	0,00	0,00	15,56	15,56	100,00	0,00
GeoB17623-2-2, 110-111	110	0,00	80,00	14,00	0,00	0,00	0,00	0,00	0,00	0,00	0,00	6,00	14,00	100,00	0,00
GeoB17623-2-2, 120-121	120	0,00	73,97	20,55	0,00	0,00	0,00	0,00	0,00	0,00	0,00	5,48	20,55	100,00	0,00
GeoB17623-2-2, 130-131	130	2,38	78,57	9,52	0,00	0,00	0,00	0,00	0,00	0,00	0,00	9,52	9,52	100,00	0,00
GeoB17623-2-2, 140-141	140	0,00	50,00	48,10	0,00	0,00	0,00	0,00	0,00	0,00	0,00	1,90	48,10	100,00	0,00
GeoB17623-2-2, 150-151	150	1,85	72,22	7,41	1,85	0,00	0,00	1,85	0,00	0,00	0,00	14,81	9,26	98,15	1,85

Sample	Depth (cm)	H/P ratio	Dominance index	Shannon diversity index	CEX *C. pel.*(modif. Dittert et al., 1999)
GeoB17623-2-1, 2-3	2	-0,02	0,47	0,80	0,49
GeoB17623-2-1, 5-6	5	-0,03	0,47	0,81	0,48
GeoB17623-2-1, 10-11	10	-0,59	0,62	0,67	0,20
GeoB17623-2-1, 15-16	15	-0,67	0,65	0,65	0,18
GeoB17623-2-1, 20-21	20	-0,12	0,50	0,76	0,43
GeoB17623-2-1, 25-26	25	-0,83	0,65	0,69	0,13
GeoB17623-2-1, 30-31	30	-0,29	0,46	0,89	0,34
GeoB17623-2-1, 35-36	35	-0,70	0,64	0,65	0,17
GeoB17623-2-1, 40-41	40	-0,31	0,47	0,94	0,33
GeoB17623-2-1, 45-46	45	-0,34	0,56	0,66	0,31
GeoB17623-2-1, 50-51	50	-0,11	0,48	0,84	0,44
GeoB17623-2-2, 60-61	60	-0,26	0,51	0,76	0,35
GeoB17623-2-2, 70-71	70	-0,20	0,46	0,94	0,39

GeoB17623-2-2, 80-81	80	-0,60	0,59	0,76	0,20
GeoB17623-2-2, 90-91	90	-0,05	0,45	0,87	0,47
GeoB17623-2-2, 100-101	100	-0,65	0,52	0,84	0,18
GeoB17623-2-2, 110-111	110	-0,76	0,66	0,62	0,15
GeoB17623-2-2, 120-121	120	-0,56	0,59	0,71	0,22
GeoB17623-2-2, 130-131	130	-0,92	0,64	0,73	0,11
GeoB17623-2-2, 140-141	140	-0,02	0,48	0,77	0,49
GeoB17623-2-2, 150-151	150	-0,89	0,55	0,93	0,11

SUPPLEMENTARY E - EG 01 microfossil abundances

		Planktonic foraminifera			Benthic foraminifera				Calcareous nannofossils	
Sample	**Depth (cm)**	***Neogloboquadrina pachyderma* (s)**	***Neogloboquadrina incompta***	***Turborotalita quinqueloba***	***Cassidulina neoteretis***	***Cassidulina reniforme***	***Melonis barleeanus***	***Islandiella* spp.**	***Coccolithus pelagicus***	***Emiliania huxleyi***
1 1 0	0	92,3	6,1	1,7	28,2	14,2	11,0	0,0	403	520
1 1 10	10	94,6	4,8	0,0	33,1	14,4	10,2	0,0	81	12
1 1 20	20	0,0	0,0	0,0	0,0	0,0	100,0	0,0	0	0
1 1 30	30	100,0	0,0	0,0	0,0	0,0	72,5	9,8	1	0
1 2 3	40,5	100,0	0,0	0,0	13,5	3,6	46,8	22,5	0	1
1 2 13	50,5	97,8	2,2	0,0	11,6	3,3	46,3	24,8	0	8
1 2 23	60,5	100,0	0,0	0,0	34,6	0,6	56,2	5,6	1	12
1 2 33	70,5	100,0	0,0	0,0	49,2	0,0	38,1	4,8	0	5

1 2 43	80,5	100,0	0,0	0,0	35,0	0,0	60,0	0,0	0	0
1 2 53	90,5	0,0	0,0	0,0	12,5	25,0	0,0	62,5	0	0
1 2 63	100,5	0,0	0,0	0,0	0,0	0,0	50,0	0,0	1	5
1 2 73	110,5	0,0	0,0	0,0	11,3	79,0	0,0	0,0	0	0
1 2 83	120,5	0,0	0,0	0,0	0,0	100,0	0,0	0,0	0	0
1 3 0	129,5	0,0	0,0	0,0	0,0	0,0	0,0	0,0	0	2
1 3 10	139,5	0,0	0,0	0,0	0,0	0,0	0,0	0,0	1	0
1 3 20	149,5	0,0	0,0	0,0	0,0	0,0	0,0	0,0	0	0
1 3 30	159,5	0,0	0,0	0,0	0,0	0,0	0,0	0,0	0	0
1 3 40	169,5	0,0	0,0	0,0	0,0	95,7	0,0	0,0	0	1
1 3 50	179,5	0,0	0,0	0,0	0,0	40,0	0,0	6,7	0	0
1 3 60	189,5	0,0	0,0	0,0	33,3	66,7	0,0	0,0	0	0
1 3 70	199,5	0,0	0,0	0,0	0,0	0,0	0,0	0,0	0	0
1 3 80	209,5	0,0	0,0	0,0	0,0	0,0	0,0	0,0	0	0
1 3 90	219,5	0,0	0,0	0,0	38,2	2,0	47,1	7,8	1	0

SUPPLEMENTARY F- EG-02 microfossil abundances

		Planktonic foraminifera			Benthic foraminifera						
Sample	**Depth (cm)**	**% *Neogloboquadrina pachyderma* (s)**	**% *Neogloboquadrina incompta***	**% *Turborotalita quinqueloba***	***Cibicidoides wuellerstorfi* (%)**	***Oridorsalis tener* (%)**	***Cassidulina teretis* (%)**	***Cassidulina reniforme* (%)**	***Stetsonia horvathi* (%)**	***Epistominella exigua***	**Agglutinated taxa**
2 1 0	0	93,23	1,82	4,69	12,41	5,11	2,19	5,49	0,36	11,68	42,34
2 1 10	10	87,36	2,30	9,20	9,27	14,24	1,66	3,97	0,00	19,54	27,15
2 1 20	20	98,03	1,69	0,28	3,03	11,21	1,82	5,76	0,00	21,52	17,88
2 1 30	30	99,11	0,89	0,00	0,91	39,09	0,00	10,00	0,00	12,73	0,00
2 1 40	40	98,31	1,06	0,63	6,39	26,52	0,00	9,27	23,32	2,24	0,32
2 1 50	50	98,17	1,83	0,00	2,86	20,63	0,00	4,13	40,63	0,00	0,00
2 1 60	60	93,03	3,35	3,35	49,71	21,10	0,58	2,31	10,12	0,87	0,00
2 1 70	70	87,76	5,06	6,75	3,08	22,37	0,00	1,54	53,47	0,00	0,00
2 1 80	80	51,74	8,99	37,43	26,47	15,88	0,59	2,35	34,12	1,18	0,00

2 1 90	90	19,35	5,16	72,26	7,22	59,79	0,00	0,00	23,71	0,00	0,00
2 1 100	100	74,73	4,40	17,58	24,71	49,41	0,00	4,71	11,76	0,00	0,00
2 1 110	110	92,59	2,47	4,94	45,40	39,88	0,00	3,07	3,07	0,00	0,00
2 1 120	120	64,17	2,50	32,50	51,02	34,69	0,00	6,12	2,04	1,02	0,00
2 2 10	131,5	95,62	1,09	2,92	52,43	23,30	0,00	1,94	0,97	0,00	0,00
2 2 20	141,5	97,98	2,02	0,00	0,00	65,52	3,45	0,00	6,90	0,00	0,00
2 2 30	151,5	100,00	0,00	0,00	0,00	66,67	0,00	16,67	0,00	0,00	0,00
2 2 40	161,5	100,00	0,00	0,00	0,00	18,18	18,18	27,27	0,00	0,00	0,00
2 2 50	171,5	99,50	0,50	0,00	0,00	0,00	16,67	33,33	0,00	0,00	0,00
2 2 60	181,5	99,44	0,56	0,00	0,00	0,00	28,57	0,00	0,00	0,00	0,00
2 2 70	191,5	97,93	1,55	0,00	0,00	0,00	38,46	23,08	0,00	0,00	0,00
2 2 80	201,5	100,00	0,00	0,00	0,00	0,00	0,00	60,00	0,00	0,00	0,00
2 3 0	212,5	99,42	0,58	0,00	0,00	3,33	8,33	23,33	3,33	0,00	11,67
2 3 10	222,5	100,00	0,00	0,00	0,00	0,00	100,00	0,00	0,00	0,00	0,00
2 3 20	232,5	0,00	0,00	0,00	0,00	0,00	0,00	0,00	0,00	0,00	0,00
2 3 30	242,5	100,00	0,00	0,00	0,00	0,00	50,00	16,67	0,00	0,00	0,00
2 3 40	252,5	100,00	0,00	0,00	0,00	0,00	20,34	20,34	55,93	0,00	0,00
2 3 50	262,5	0,00	0,00	0,00	0,00	0,00	10,00	60,00	0,00	0,00	10,00
2 3 60	272,5	0,00	0,00	0,00	0,00	0,00	33,33	66,67	0,00	0,00	0,00
2 3 70	282,5	100,00	0,00	0,00	0,00	12,50	12,50	75,00	0,00	0,00	0,00
2 3 80	292,5	100,00	0,00	0,00	0,00	0,00	25,00	25,00	0,00	25,00	0,00
2 3 90	302,5	98,59	1,41	0,00	0,00	0,00	18,75	18,75	0,00	0,00	0,00

		Calcareous nannofossils						Diatoms			
Sample	**Depth (cm)**	***Calcidiscus leptoporus***	***Coccolithus pelagicus pelagicus***	***Coccolithus pelagicus braarudi***	***Emiliania huxleyi***	***Gephyrocapsa muellerae***	**Reworked**	***Coscinodiscus* spp.%**	***Chaetoceros* RS %**	***Thalassiosira* spp. %**	***Paralia sulcata* %**
2 1 0	0	10,00	1195,00	40,00	280,00	5,00	5,00	5,33	47,93	25,44	5,92
2 1 10	10	20,00	215,00	0,00	105,00	0,00	0,00	3,87	72,38	11,05	3,87
2 1 20	20	35,00	845,00	85,00	490,00	10,00	5,00	25,81	32,26	9,68	16,13
2 1 30	30	45,00	840,00	55,00	885,00	5,00	5,00	0,00	0,00	0,00	0,00
2 1 40	40	25,00	175,00	5,00	55,00	0,00	0,00	0,00	0,00	0,00	0,00
2 1 50	50	10,00	1250,00	10,00	135,00	0,00	0,00	0,00	0,00	0,00	0,00
2 1 60	60	55,00	800,00	5,00	280,00	15,00	10,00	0,00	0,00	0,00	100,00
2 1 70	70	150,00	560,00	30,00	340,00	25,00	5,00	34,62	0,00	3,85	61,54
2 1 80	80	5,00	43,00	0,00	13,00	1,00	0,00	47,62	4,76	3,17	39,68
2 1 90	90	4,00	2,00	0,00	35,00	6,00	0,00	71,32	1,47	1,47	24,26
2 1 100	100	0,00	0,00	0,00	8,00	3,00	1,00	68,00	4,00	0,00	26,00
2 1 110	110	4,00	1,00	0,00	32,00	3,00	0,00	52,03	1,63	2,44	42,28

2 1 120	120	5,00	1,00	0,00	31,00	2,00	0,00	60,47	4,65	4,65	30,23
2 2 10	131,5	0,00	1,00	0,00	29,00	0,00	2,00	0,00	0,00	0,00	0,00
2 2 20	141,5	0,00	2,00	0,00	8,00	0,00	2,00	0,00	0,00	0,00	0,00
2 2 30	151,5	0,00	0,00	0,00	0,00	0,00	0,00	0,00	0,00	0,00	0,00
2 2 40	161,5	1,00	0,00	0,00	89,00	2,00	2,00	0,00	0,00	0,00	0,00
2 2 50	171,5	1,00	0,00	0,00	22,00	0,00	0,00	0,00	0,00	0,00	0,00
2 2 60	181,5	no nannofossil data						0,00	0,00	0,00	0,00
2 2 70	191,5	10,00	0,00	0,00	245,00	10,00	5,00	0,00	0,00	0,00	0,00
2 2 80	201,5	4,00	2,00	0,00	48,00	2,00	2,00	0,00	0,00	0,00	0,00
2 3 0	212,5	0,00	5,00	0,00	345,00	2,00	15,00	0,00	0,00	0,00	0,00
2 3 10	222,5	0,00	0,00	0,00	12,00	0,00	4,00	0,00	0,00	0,00	0,00
2 3 20	232,5	0,00	0,00	0,00	11,00	0,00	2,00	0,00	0,00	0,00	0,00
2 3 30	242,5	0,00	0,00	0,00	19,00	0,00	2,00	0,00	0,00	0,00	0,00
2 3 40	252,5	0,00	0,00	0,00	1,00	0,00	0,00	0,00	0,00	0,00	0,00
2 3 50	262,5	1,00	0,00	0,00	1,00	0,00	0,00	0,00	0,00	0,00	0,00
2 3 60	272,5	0,00	0,00	0,00	3,00	0,00	0,00	0,00	0,00	0,00	0,00
2 3 70	282,5	0,00	0,00	0,00	3,00	0,00	1,00	0,00	0,00	0,00	0,00
2 3 80	292,5	0,00	0,00	0,00	1,00	0,00	0,00	0,00	0,00	0,00	0,00
2 3 90	302,5	0,00	1,00	0,00	21,00	0,00	4,00	0,00	0,00	0,00	0,00

Sample	Depth (cm)	Age (cal age BP)
2 1 0	0	1606,00
2 1 10	10	2801,00
2 1 20	20	3644,00
2 1 30	30	4351,00
2 1 40	40	6774,00
2 1 50	50	7914,00
2 1 60	60	8431,00
2 1 70	70	8833,00
2 1 80	80	9236,00
2 1 90	90	9638,00
2 1 100	100	10041,94
2 1 110	110	10461,29
2 1 120	120	10880,65
2 2 10	131,5	11340,00
2 2 20	141,5	11740,00

2 2 30	151,5	12120,60
2 2 40	161,5	12522,60
2 2 50	171,5	12924,60
2 2 60	181,5	13326,60
2 2 70	191,5	13728,60
2 2 80	201,5	14042,70
2 3 0	212,5	14151,70
2 3 10	222,5	14271,60
2 3 20	232,5	14380,60
2 3 30	242,5	14489,60
2 3 40	252,5	14598,60
2 3 50	262,5	14707,60
2 3 60	272,5	14816,60
2 3 70	282,5	14925,60
2 3 80	292,5	15034,60
2 3 90	302,5	16233,33

SUPPLEMENTARY G- EG-03 microfossil abundances

		Planktonic foraminifera			Benthic foraminifera							
Sample	**Depth (cm)**	**% *Neogloboquadrina pachyderma* (s)**	**% *Neogloboquadrina incompta***	**% *Turborotalita quinqueloba***	***Cibicidoides wuellerstorfi* (%)**	***Melonis barleeanus* (%)**	***Oridorsalis tener* (%)**	***Cassidulina neoteretis***	***Cassidulina reniforme* (%)**	***Epistominella arctica* (%)**	***Stetsonia horvathi* (%)**	**Agglutinated taxa**
3 1 0	0	82,2	6,6	9,4	2,49	3,12	0,31	19,00	11,53	0,00	4,36	38,94
3 1 10	10	70,0	7,5	15,0	4,23	14,08	2,82	5,63	14,08	0,00	1,41	26,76
3 1 20	20	81,7	8,7	9,1	9,38	3,23	4,69	34,31	4,69	2,05	4,69	3,81
3 1 30	30	89,0	8,8	1,9	3,12	3,68	4,25	21,53	12,46	5,67	13,03	5,95
3 1 40	40	86,8	6,2	6,6	2,52	6,92	6,92	18,24	15,41	8,81	10,06	4,09
3 1 44	44											
3 1 46	46					no foraminiferal data						
3 1 48	48											
3 1 50	50	97,5	1,7	0,8	1,85	6,77	4,31	13,54	12,92	12,31	14,46	7,38

3 1 52	52											
3 1 54	54	no foraminiferal data										
3 1 60	60	100,0	0,0	0,0	2,68	9,06	0,67	9,40	12,42	16,78	13,09	1,34
3 1 70	70	94,8	5,2	0,0	0,87	2,31	1,16	3,47	13,29	23,70	15,32	4,34
3 1 80	80	85,1	4,1	10,5	10,63	3,75	4,06	13,75	11,88	13,75	14,06	1,56
3 1 90	90	95,4	3,4	0,0	3,35	5,79	9,45	16,16	15,55	7,93	20,12	0,30
3 1 100	100	81,9	5,5	11,0	2,26	4,52	12,43	9,04	16,95	6,21	23,16	2,26
3 2 6	110	77,5	6,4	13,8	9,57	3,19	2,32	7,83	17,39	11,30	21,16	2,03
3 2 16	120	86,3	3,9	8,2	6,71	3,96	7,01	5,79	21,65	10,06	19,82	3,66
3 2 26	130	81,2	4,5	14,3	9,52	4,23	7,94	2,65	21,69	3,17	24,87	3,70
3 2 36	140	87,8	6,5	5,4	1,97	2,53	11,80	3,65	23,60	1,69	26,40	3,93
3 2 142	142											
3 2 144	144											
3 2 146	146	no foraminiferal data										
3 2 148	148											
3 2 46	150	39,6	2,9	57,1	5,25	5,90	4,92	2,30	18,03	2,62	19,67	4,26
3 2 152	152	no foraminiferal data										
3 2 56	160	70,4	7,8	20,8	1,23	4,32	3,09	6,79	17,90	1,85	29,01	2,16
3 2 66	170	42,0	10,1	45,1	29,84	3,63	8,47	6,05	8,87	1,21	15,32	1,61
3 2 76	180	21,7	3,9	72,4	11,22	4,29	3,30	4,62	19,14	1,32	23,10	1,98
3 2 86	190	12,3	5,7	77,6	22,89	2,41	1,81	3,01	6,63	0,00	18,07	1,81
3 3 8	200	8,6	4,9	84,0	20,31	0,00	6,25	15,63	9,38	0,00	3,13	1,56

3 3 18	210	4,7	2,9	89,1	27,30	1,19	12,17	2,67	17,51	0,00	7,42	2,67
3 3 28	220	51,8	1,7	45,2	32,26	12,90	3,23	3,23	9,68	0,00	0,00	0,00
3 3 38	230	42,8	2,6	52,6	54,74	0,26	23,95	0,00	5,00	0,00	2,11	1,84
3 3 48	240	58,5	1,5	33,8	10,17	2,54	26,27	1,69	16,10	0,00	16,10	3,39
3 3 58	250	81,8	6,8	6,8	20,37	7,41	55,56	0,00	3,70	0,00	1,85	1,85
3 3 68	260	89,5	0,0	10,5	16,07	39,29	5,36	7,14	14,29	0,00	0,00	7,14
3 3 78	270	100,0	0,0	0,0	17,65	44,12	5,88	2,94	2,94	0,00	0,00	5,88
3 3 88	280	100,0	0,0	0,0	0,00	0,00	0,00	0,00	0,00	0,00	0,00	0,00

		Calcareous nannofossils											Diatoms			
Sample	**Depth (cm)**	***Calcidiscus leptoporus***	***Coccolithus pelagicus pelagicus***	***Coccolithus pelagicus braarudi***	***Emiliania huxleyi***	***Gephyrocapsa oceanica***	***Gephyrocapsa muellerae***	***Pseudoemiliania lacunosa***	***Reticulofenestra asanoi***	**Reworked**	**Small *Gephyrocapsa***	***Thoracosphaera* spp.**	***Coscinodiscus* spp. %**	***Chaetoceros* RS %**	***Paralia sulcata* %**	***Rhizosolenia* spp. %**
3 1 0	0	10,00	235,00	25,00	710,00	0,00	0,00	0,00	0,00	0,00	0,00	0,00	2,62	74,24	3,49	3,93
3 1 10	10	45,00	635,00	30,00	725,00	0,00	5,00	0,00	0,00	0,00	0,00	0,00	3,45	67,82	5,17	5,75
3 1 20	20	135,00	745,00	40,00	1480,00	0,00	10,00	0,00	0,00	0,00	0,00	0,00	2,56	81,20	0,85	3,42
3 1 30	30	185,00	1035,00	85,00	1615,00	0,00	30,00	0,00	0,00	0,00	0,00	0,00	9,09	36,36	9,09	0,00
3 1 40	40	30,00	240,00	0,00	460,00	0,00	0,00	0,00	0,00	0,00	0,00	0,00	60,00	40,00	0,00	0,00
3 1 44	44	25,00	180,00	20,00	950,00	0,00	335,00	0,00	10,00	30,00	0,00	0,00				
3 1 46	46	35,00	215,00	10,00	910,00	0,00	370,00	0,00	0,00	20,00	0,00	0,00		no diatom data		
3 1 48	48	35,00	290,00	30,00	1135,00	0,00	305,00	0,00	0,00	60,00	0,00	0,00				
3 1 50	50	25,00	270,00	20,00	965,00	0,00	285,00	0,00	0,00	35,00	0,00	0,00	9,09	54,55	0,00	18,18
3 1 52	52	25,00	215,00	15,00	1060,00	0,00	290,00	0,00	0,00	25,00	0,00	0,00				
3 1 54	54	10,00	295,00	5,00	535,00	0,00	345,00	0,00	0,00	15,00	0,00	5,00		no diatom data		
3 1 60	60	15,00	325,00	15,00	495,00	0,00	270,00	0,00	0,00	30,00	0,00	0,00	20,00	20,00	60,00	0,00

3 1 70	70	5,00	305,00	0,00	345,00	0,00	0,00	0,00	0,00	0,00	0,00	0,00	37,50	12,50	37,50	0,00
3 1 80	80	35,00	300,00	35,00	840,00	0,00	5,00	15,00	0,00	0,00	10,00	0,00	5,56	5,56	83,33	0,00
3 1 90	90	50,00	525,00	15,00	410,00	0,00	0,00	0,00	0,00	0,00	0,00	0,00	0,00	0,00	66,67	0,00
3 1 100	100	0,00	220,00	5,00	135,00	0,00	5,00	0,00	0,00	0,00	0,00	0,00	14,29	0,00	57,14	0,00
3 2 6	110	20,00	480,00	0,00	1130,00	0,00	5,00	0,00	0,00	0,00	0,00	0,00	0,00	20,00	50,00	0,00
3 2 16	120	5,00	705,00	0,00	1225,00	0,00	10,00	0,00	0,00	5,00	15,00	0,00	29,17	45,83	16,67	0,00
3 2 26	130	0,00	20,00	0,00	255,00	0,00	0,00	0,00	0,00	0,00	0,00	0,00	33,33	33,33	33,33	0,00
3 2 36	140	15,00	220,00	0,00	625,00	0,00	35,00	5,00	0,00	10,00	5,00	0,00	17,39	4,35	65,22	0,00
3 2 142	142	75,00	335,00	5,00	590,00	0,00	295,00	0,00	0,00	65,00	0,00	5,00				
3 2 144	144	45,00	395,00	10,00	615,00	0,00	325,00	0,00	0,00	65,00	0,00	0,00				
3 2 146	146	40,00	370,00	10,00	660,00	0,00	380,00	0,00	0,00	20,00	0,00	0,00	no diatom data			
3 2 148	148	45,00	360,00	5,00	670,00	0,00	315,00	0,00	0,00	25,00	0,00	0,00				
3 2 46	150	85,00	345,00	10,00	640,00	0,00	225,00	0,00	0,00	60,00	0,00	5,00	53,85	15,38	0,00	7,69
3 2 152	152	30,00	330,00	5,00	685,00	0,00	290,00	0,00	0,00	50,00	0,00	0,00	no diatom data			
3 2 56	160	50,00	260,00	5,00	700,00	0,00	85,00	0,00	0,00	10,00	0,00	0,00	60,98	9,76	14,63	0,00
3 2 66	170	5,00	151,00	0,00	385,00	0,00	11,00	0,00	0,00	3,00	0,00	0,00	56,00	10,00	22,00	0,00
3 2 76	180	25,00	225,00	10,00	595,00	0,00	55,00	0,00	0,00	5,00	0,00	0,00	51,91	16,03	19,08	0,76
3 2 86	190	20,00	120,00	0,00	585,00	0,00	30,00	0,00	0,00	0,00	0,00	0,00	42,77	12,58	15,72	5,03
3 3 8	200	11,00	43,00	0,00	465,00	0,00	21,00	0,00	0,00	0,00	0,00	3,00	49,50	11,88	17,82	6,93
3 3 18	210	31,00	0,00	0,00	481,00	0,00	42,00	0,00	0,00	0,00	0,00	0,00	61,40	10,53	8,77	6,14
3 3 28	220	0,00	3,00	0,00	54,00	0,00	15,00	0,00	0,00	0,00	0,00	0,00	64,66	3,01	17,29	3,01
3 3 38	230	18,00	0,00	0,00	258,00	0,00	14,00	2,00	0,00	0,00	0,00	0,00	52,63	5,26	25,26	4,21

3 3 48	240	34,00	0,00	0,00	49,00	0,00	12,00	0,00	0,00	0,00	0,00	0,00	65,96	2,13	25,53	0,00
3 3 58	250	16,00	0,00	0,00	75,00	0,00	6,00	0,00	1,00	2,00	0,00	0,00	60,44	6,59	18,68	1,10
3 3 68	260	0,00	2,00	0,00	34,00	0,00	0,00	0,00	0,00	0,00	0,00	0,00	32,81	0,00	51,56	0,00
3 3 78	270	0,00	0,00	0,00	5,00	0,00	0,00	0,00	0,00	1,00	0,00	0,00	43,86	3,51	43,86	0,00
3 3 88	280	0,00	0,00	0,00	0,00	0,00	0,00	0,00	0,00	0,00	0,00	0,00	0,00	0,00	0,00	0,00

Sample	Depth (cm)	Age (cal age BP)
3 1 0	0	50
3 1 10	10	688
3 1 20	20	964
3 1 30	30	1278
3 1 40	40	1708
3 1 44	44	
3 1 46	46	
3 1 48	48	
3 1 50	50	2390
3 1 52	52	
3 1 54	54	
3 1 60	60	3337
3 1 70	70	4232
3 1 80	80	4637
3 1 90	90	5000

3 1 100	100	5650
3 2 6	110	6300
3 2 16	120	6888,24
3 2 26	130	7438,46
3 2 36	140	7900
3 2 142	142	
3 2 144	144	
3 2 146	146	
3 2 148	148	
3 2 46	150	8304,35
3 2 152	152	
3 2 56	160	8652,17
3 2 66	170	9000
3 2 76	180	9175
3 2 86	190	9350
3 3 8	200	9525
3 3 18	210	9700
3 3 28	220	10025,49
3 3 38	230	10280,39
3 3 48	240	10535,29
3 3 58	250	10790,2
3 3 68	260	11045,1

3 3 78	270	11300
3 3 88	280	11980

SUPPLEMENTARY H- GS191-01PC nannofossil abundance

Sample	Depth (cm)	Fields	*Braarudosphaera bigelowii*	*Calcidiscus leptoporus*	*Coccolithus pelagicus braarudi*	*Coccolithus pelagicus pelagicus*	*Emiliania huxleyi* < 4 µm	*Emiliania huxleyi* > 4µm	*Gephyrocapsa caribbeanica*	*Gephyrocapsa muellerae*	*Gephyrocapsa oceanica*	*Helicosphaera carteri*	Reworked Cenozoic	Reworked Cretaceous	Small *Gephyrocapsa* spp. (<3)	*Syracosphaera* spp.	*Thoracosphaera* spp.	Total *E. huxleyi*	Total *C. pelagicus*	Total abundance (with reworked)	Total abundance (NO reworked)	Total Reworked
GS191-01PC-1, 0-1	0	200	0	48	5	1875	2299	1	0	1	6	0	8	5	8	5	3	2300	1880	4264	4251	13
GS191-01PC-1, 10-11	10	200	2	82	7	3447	2183	22	0	0	12	0	5	9	6	5	14	2205	3454	5794	5780	14
GS191-01PC-1, 20-21	20	200	0	37	2	1388	1683	1	0	0	3	0	3	9	2	7	8	1684	1390	3143	3131	12
GS191-01PC-1, 30-31	30	200	0	110	4	2536	3416	4	0	1	12	0	0	8	9	14	11	3420	2540	6125	6117	8
GS191-01PC-2, 6-7	40	200	0	111	2	1617	1859	4	0	1	11	0	2	6	0	4	7	1863	1619	3624	3616	8
GS191-01PC-2, 16-17	50	200	0	47	1	578	962	7	0	0	8	0	2	2	2	0	4	969	579	1613	1609	4
GS191-01PC-2, 26-27	60	200	1	200	11	2585	3425	10	0	0	23	0	1	6	3	22	2	3435	2596	6289	6282	7
GS191-01PC-2, 36-37	70	200	0	114	4	1182	1910	6	0	0	7	0	1	7	0	4	1	1916	1186	3236	3228	8
GS191-01PC-2, 46-47	80	200	0	58	2	1150	1598	3	0	0	4	0	1	2	3	5	2	1601	1152	2828	2825	3
GS191-01PC-2, 56-57	90	200	0	34	2	940	1433	2	0	0	6	0	0	6	5	2	3	1435	942	2433	2427	6

GS191-01PC-2, 66-67	100	200	0	57	3	1479	2087	18	0	0	19	1	4	9	3	8	5	2105	1482	3693	3680	13
GS191-01PC-2, 76-77	110	200	0	36	4	1185	1770	6	0	0	7	0	2	4	6	7	4	1776	1189	3031	3025	6
GS191-01PC-2, 86-87	120	200	1	50	10	1700	2224	9	0	0	14	1	0	5	9	7	8	2233	1710	4038	4033	5
GS191-01PC-2, 96-97	130	200	0	19	0	735	1505	2	0	0	5	1	0	3	4	8	5	1507	735	2287	2284	3
GS191-01PC-3, 6-7	140	200	0	40	4	1110	2438	20	0	0	12	0	1	2	1	3	1	2458	1114	3632	3629	3
GS191-01PC-3, 16-17	150	200	0	9	7	855	1877	16	0	0	11	0	0	4	0	9	3	1893	862	2791	2787	4
GS191-01PC-3, 26-27	160	200	0	26	0	1076	1196	2	0	0	6	0	0	7	1	7	2	1198	1076	2323	2316	7
GS191-01PC-3, 36-37	170	200	0	70	8	2168	1690	6	0	0	7	0	0	13	0	5	6	1696	2176	3973	3960	13
GS191-01PC-3, 46-47	180	200	0	32	0	959	1120	11	0	0	4	0	2	5	4	2	3	1131	959	2142	2135	7
GS191-01PC-3, 56-57	190	200	0	81	1	2481	2328	15	0	0	4	0	3	10	0	2	7	2343	2482	4932	4919	13
GS191-01PC-3, 66-67	200	200	0	38	0	727	976	4	0	0	4	0	2	2	0	1	3	980	727	1757	1753	4
GS191-01PC-3, 76-77	210	200	0	69	2	1178	2316	19	0	0	18	0	1	9	15	2	5	2335	1180	3634	3624	10
GS191-01PC-3, 86-87	220	200	0	56	0	740	1262	9	0	0	6	0	2	2	12	2	2	1271	740	2093	2089	4
GS191-01PC-3, 96-97	230	200	0	38	1	1074	1587	14	0	0	10	0	1	3	4	4	6	1601	1075	2742	2738	4
GS191-01PC-4, 6-7	240	200	0	22	1	374	784	6	0	0	2	0	0	1	3	2	4	790	375	1199	1198	1
GS191-01PC-4, 16-17	250	200	0	75	0	1115	1868	12	0	0	8	0	0	1	4	8	13	1880	1115	3104	3103	1
GS191-01PC-4, 26-27	260	200	0	43	13	1895	2189	43	0	0	37	0	4	12	9	3	13	2232	1908	4261	4245	16
GS191-01PC-4, 36-37	270	200	0	24	0	705	1427	6	0	0	28	0	0	2	0	5	1	1433	705	2198	2196	2
GS191-01PC-4, 46-47	280	200	0	68	9	3185	2978	12	0	0	92	0	3	11	0	10	12	2990	3194	6380	6366	14
GS191-01PC-4, 56-57	290	200	0	32	1	1165	1974	6	0	0	52	0	2	4	0	3	4	1980	1166	3243	3237	6
GS191-01PC-4, 66-67	300	200	0	56	9	1813	2668	5	0	0	156	0	2	8	1	3	3	2673	1822	4724	4714	10
GS191-01PC-4, 76-77	310	200	0	52	1	1172	2357	3	0	0	150	0	4	8	0	3	8	2360	1173	3758	3746	12

GS191-01PC-4, 86-87	320	200	0	16	0	296	542	1	0	0	58	0	1	5	0	1	1	543	296	921	915	6
GS191-01PC-5, 6-7	330	200	0	82	5	932	1721	10	0	0	150	0	0	13	0	2	2	1731	937	2917	2904	13
GS191-01PC-5, 16-17	340	200	0	114	18	1419	1723	3	0	0	241	0	3	4	0	4	11	1726	1437	3540	3533	7
GS191-01PC-5, 26-27	350	200	0	108	10	1700	2082	5	0	0	381	0	1	12	0	5	3	2087	1710	4307	4294	13
GS191-01PC-5, 36-37	360	200	0	66	8	958	1643	19	0	0	303	0	1	9	1	10	4	1662	966	3022	3012	10
GS191-01PC-5, 46-47	370	200	0	129	12	1844	2340	7	0	0	261	0	1	10	0	2	12	2347	1856	4618	4607	11
GS191-01PC-5, 56-57	380	200	0	81	5	659	1615	6	0	0	160	0	1	1	0	3	1	1621	664	2532	2530	2
GS191-01PC-5, 66-67	390	200	0	111	5	1160	2078	4	0	0	398	0	2	9	0	9	9	2082	1165	3785	3774	11
GS191-01PC-5, 76-77	400	200	0	64	2	1075	1827	9	0	0	343	0	0	7	0	2	2	1836	1077	3331	3324	7
GS191-01PC-5, 86-87	410	200	0	97	4	1553	2481	7	0	0	447	0	2	12	0	8	3	2488	1557	4614	4600	14
GS191-01PC-5, 96-97	420	200	0	90	5	1196	2433	6	0	0	365	2	0	6	0	3	5	2439	1201	4111	4105	6
GS191-01PC-6, 6-7	430	200	0	58	4	687	2409	1	0	0	455	0	1	14	0	14	3	2410	691	3646	3631	15
GS191-01PC-6, 16-17	440	200	0	26	2	399	1511	2	0	0	175	0	1	8	0	1	2	1513	401	2127	2118	9
GS191-01PC-6, 26-27	450	200	0	18	3	351	1405	0	0	0	211	0	1	6	0	1	6	1405	354	2002	1995	7
GS191-01PC-6, 36-37	460	200	0	29	0	130	1818	2	0	0	220	0	3	10	0	0	5	1820	130	2217	2204	13
GS191-01PC-6, 46-47	470	200	0	25	0	108	1601	1	0	0	211	0	1	6	1	4	1	1602	108	1959	1952	7
GS191-01PC-6, 56-57	480	200	0	10	0	8	412	0	0	0	22	0	1	3	0	0	2	412	8	458	454	4
GS191-01PC-6, 66-67	490	200	0	13	0	2	502	1	0	0	19	0	2	5	0	0	0	503	2	544	537	7
GS191-01PC-6, 76-77	500	200	0	28	0	3	879	0	0	0	35	0	1	4	0	0	2	879	3	952	947	5
GS191-01PC-6, 86-87	510	200	0	63	0	3	2102	0	0	0	168	0	0	9	0	4	2	2102	3	2351	2342	9
GS191-01PC-6, 96-97	520	200	0	33	0	4	962	0	0	0	84	0	0	7	0	0	2	962	4	1092	1085	7
GS191-01PC-7, 6-7	530	200	0	22	0	1	368	0	0	0	35	0	0	4	0	1	0	368	1	431	427	4

GS191-01PC-7, 16-17	540	200	0	30	0	0	771	0	0	0	55	0	0	7	0	0	2	771	0	865	858	7
GS191-01PC-7, 26-27	550	200	0	3	0	40	154	0	0	0	3	0	0	0	0	0	2	154	40	202	202	0
GS191-01PC-7, 36-37	560	200	0	0	0	0	4	0	0	0	0	0	0	0	0	0	1	4	0	5	5	0
GS191-01PC-7, 46-47	570	200	0	1	0	1	52	0	0	0	0	0	1	1	0	0	4	52	1	60	58	2
GS191-01PC-7, 56-57	580	200	0	0	0	0	54	0	0	0	1	0	0	0	0	0	2	54	0	57	57	0
GS191-01PC-7, 66-67	590	200	0	0	0	1	19	0	0	0	0	0	0	3	0	0	1	19	1	24	21	3
GS191-01PC-7, 76-77	600	200	0	1	0	18	16	0	0	0	0	0	0	1	0	1	0	16	18	37	36	1
GS191-01PC-8, 6-7	610	200	0	0	0	0	0	0	0	0	0	0	0	0	0	0	1	0	0	1	1	0
GS191-01PC-8, 16-17	620	200	0	5	0	0	210	2	0	0	8	0	1	5	0	0	0	212	0	231	225	6
GS191-01PC-8, 26-27	630	200	0	2	0	0	376	5	0	0	2	0	0	12	0	0	0	381	0	397	385	12
GS191-01PC-8, 36-37	640	200	0	8	0	1	626	0	0	2	36	0	0	5	0	0	0	626	1	678	673	5
GS191-01PC-8, 46-47	650	200	0	5	0	1	560	2	0	0	12	0	1	11	0	0	0	562	1	592	580	12
GS191-01PC-8, 56-57	660	200	0	0	0	0	54	0	0	0	0	0	0	0	0	0	0	54	0	54	54	0
GS191-01PC-8, 66-67	670	200	0	3	0	1	126	0	0	2	4	0	2	4	0	0	0	126	1	142	136	6
GS191-01PC-9, 0-1	680	200	0	0	0	6	133	1	0	0	2	0	2	8	0	0	0	134	6	152	142	10
GS191-01PC-9, 10-11	690	200	0	0	0	0	38	0	0	0	0	0	0	1	0	0	0	38	0	39	38	1
GS191-01PC-9, 20-21	700	200	0	3	2	45	450	36	0	0	8	0	0	18	0	1	2	486	47	565	547	18
GS191-01PC-9, 30-31	710	200	0	0	0	4	269	0	0	0	3	0	1	9	0	0	0	269	4	286	276	10
GS191-01PC-9, 40-41	720	200	0	0	0	0	197	0	0	0	2	0	1	6	0	1	0	197	0	207	200	7
GS191-01PC-9, 50-51	730	200	0	0	0	1	49	0	0	0	1	0	1	1	0	0	0	49	1	53	51	2
GS191-01PC-9, 60-61	740	200	0	0	0	0	36	0	0	0	0	0	1	3	0	0	0	36	0	40	36	4
GS191-01PC-9, 70-71	750	200	0	0	0	11	69	1	0	0	4	0	2	8	0	1	1	70	11	97	87	10

GS191-01PC-9, 80-81	760	200	0	0	0	0	0	0	0	0	0	0	0	1	0	0	0	0	0	1	0	1
GS191-01PC-9, 90-91	770	200	0	0	0	0	4	0	0	0	0	0	0	1	0	0	0	4	0	5	4	1
GS191-01PC-10, 0-1	780	200	0	0	0	0	1	0	0	0	0	0	0	1	0	0	0	1	0	2	1	1
GS191-01PC-10, 10-11	790	200	0	0	0	0	4	0	0	0	2	0	0	3	1	0	0	4	0	10	7	3
GS191-01PC-10, 20-21	800	200	0	0	0	1	2	0	0	0	0	0	0	2	0	0	1	2	1	6	4	2
GS191-01PC-10, 30-31	810	200	0	0	0	4	7	0	0	0	0	0	0	2	0	0	1	7	4	14	12	2
GS191-01PC-10, 40-41	820	200	0	0	0	23	29	0	0	0	0	0	0	2	0	1	0	29	23	55	53	2
GS191-01PC-10, 50-51	830	200	0	0	0	0	1	0	0	0	0	0	0	2	0	0	0	1	0	3	1	2
GS191-01PC-10, 60-61	840	200	0	0	0	0	1	0	0	0	1	0	0	4	0	0	0	1	0	6	2	4
GS191-01PC-10, 70-71	850	200	0	0	0	0	3	0	0	0	0	0	0	2	0	0	0	3	0	5	3	2
GS191-01PC-10, 80-81	860	200	0	0	0	0	0	0	0	0	0	0	0	1	0	0	0	0	0	1	0	1
GS191-01PC-11, 0-1	870	200	0	0	0	0	3	0	0	0	0	0	0	1	0	0	0	3	0	4	3	1
GS191-01PC-11, 10-11	880	200	0	0	0	0	65	0	0	0	1	0	0	8	0	1	0	65	0	75	67	8
GS191-01PC-11, 20-21	890	200	0	0	0	0	2	0	0	0	0	0	0	0	0	0	0	2	0	2	2	0
GS191-01PC-11, 30-31	900	200	0	0	0	0	101	0	0	0	1	0	1	14	0	1	0	101	0	118	103	15
GS191-01PC-11, 40-41	910	200	0	0	0	2	53	0	0	0	1	0	4	23	0	0	0	53	2	83	56	27
GS191-01PC-11, 50-51	920	200	0	0	0	0	4	0	0	0	0	0	1	4	0	0	0	4	0	9	4	5
GS191-01PC-11, 60-61	930	200	0	0	0	3	45	0	0	0	1	0	2	37	0	1	1	45	3	90	51	39
GS191-01PC-11, 70-71	940	200	0	0	0	0	29	0	0	0	2	0	0	12	0	0	0	29	0	43	31	12
GS191-01PC-11, 80-81	950	200	0	0	0	4	186	0	0	0	5	0	4	49	0	3	0	186	4	251	198	53
GS191-01PC-11, 90-91	960	200	0	0	0	5	305	6	0	0	7	0	4	70	0	1	0	311	5	398	324	74
GS191-01PC-12, 0-1	970	200	0	0	0	7	56	0	0	0	3	0	2	34	0	0	0	56	7	102	66	36

GS191-01PC-12, 10-11	980	200	0	0	1	3	81	0	0	0	13	0	4	104	0	0	0	81	4	206	98	108
GS191-01PC-12, 20-21	990	200	0	0	0	0	24	0	0	0	3	0	0	13	0	0	0	24	0	40	27	13
GS191-01PC-12, 30-31	1000	200	0	0	1	5	69	0	0	0	5	0	3	56	0	0	1	69	6	140	81	59
GS191-01PC-12, 40-41	1010	200	0	0	0	0	22	0	0	0	2	0	4	18	0	0	0	22	0	46	24	22
GS191-01PC-12, 50-51	1020	200	0	0	0	0	37	2	0	0	0	0	1	23	0	0	0	39	0	63	39	24
GS191-01PC-12, 60-61	1030	200	0	0	0	1	13	0	0	0	2	0	3	29	0	0	1	13	1	49	17	32
GS191-01PC-12, 70-71	1040	200	0	0	0	0	267	9	0	0	10	0	0	40	0	2	1	276	0	329	289	40
GS191-01PC-12, 80-81	1050	200	0	0	0	2	17	0	0	0	5	0	1	19	0	0	0	17	2	44	24	20
GS191-01PC-12, 90-91	1060	200	0	0	0	0	0	0	0	0	0	0	0	1	0	0	0	0	0	1	0	1
GS191-01PC-13, 0-1	1070	200	0	0	0	1	1	0	0	0	0	0	0	0	0	0	0	1	1	2	2	0
GS191-01PC-13, 10-11	1080	200	0	0	0	0	0	0	0	0	0	0	0	1	0	0	0	0	0	1	0	1
GS191-01PC-13, 20-21	1090	200	0	0	0	1	0	0	0	0	0	0	0	0	0	0	0	0	1	1	1	0
GS191-01PC-13, 30-31	1100	200	0	0	0	0	1	0	0	0	0	0	0	3	0	0	0	1	0	4	1	3
GS191-01PC-13, 40-41	1110	200	0	0	0	0	4	0	0	0	0	0	1	2	0	0	0	4	0	7	4	3
GS191-01PC-13, 52-53	1122	200	0	2	0	1	343	4	0	0	6	0	4	37	0	2	0	347	1	399	358	41
GS191-01PC-13, 60-61	1130	200	0	0	0	4	68	0	0	0	8	0	2	87	1	0	2	68	4	172	83	89
GS191-01PC-13, 70-71	1140	200	0	0	0	0	48	1	0	0	6	0	3	58	1	0	0	49	0	117	56	61
GS191-01PC-13, 80-81	1150	200	0	1	0	2	43	0	0	0	2	0	1	38	0	0	0	43	2	87	48	39
GS191-01PC-13, 90-91	1160	200	0	0	0	2	96	0	0	0	3	0	1	30	0	1	0	96	2	133	102	31
GS191-01PC-14, 0-1	1170	200	0	0	0	0	146	4	0	0	0	0	2	43	0	0	1	150	0	196	151	45
GS191-01PC-14, 10-11	1180	200	0	0	0	0	298	0	0	0	1	0	0	31	0	0	0	298	0	330	299	31
GS191-01PC-14, 20-21	1190	200	0	0	0	0	420	3	0	0	0	0	2	26	1	1	0	423	0	453	425	28

GS191-01PC-14, 30-31	1200	200	0	0	0	0	9	0	0	0	2	0	1	10	0	0	0	9	0	22	11	11
GS191-01PC-14, 40-41	1210	200	0	0	0	0	8	0	0	0	0	0	0	3	0	0	0	8	0	11	8	3
GS191-01PC-14, 50-51	1220	200	0	0	0	0	0	0	0	0	0	0	0	0	0	0	0	0	0	0	0	0
GS191-01PC-14, 60-61	1230	200	0	1	0	0	98	1	0	0	1	0	0	9	0	0	0	99	0	110	101	9
GS191-01PC-14, 70-71	1240	200	0	0	0	0	3	0	0	0	0	0	0	2	0	0	0	3	0	5	3	2
GS191-01PC-14, 80-81	1250	200	0	2	0	0	21	0	0	0	3	0	0	8	0	0	0	21	0	34	26	8
GS191-01PC-14, 90-91	1260	200	0	0	0	0	65	1	0	0	1	0	0	7	0	0	0	66	0	74	67	7
GS191-01PC-15, 0-1	1270	200	0	1	0	1	99	1	0	0	0	0	1	7	0	0	0	100	1	110	102	8
GS191-01PC-15, 10-11	1280	200	0	2	0	1	402	0	0	0	2	0	0	10	0	0	1	402	1	418	408	10
GS191-01PC-15, 20-21	1290	200	0	0	0	0	28	0	0	0	0	0	0	1	0	0	1	28	0	30	29	1
GS191-01PC-15, 30-31	1300	200	0	0	0	0	0	0	0	0	0	0	0	0	0	0	0	0	0	0	0	0
GS191-01PC-15, 40-41	1310	200	0	0	0	0	1	0	0	0	0	0	0	1	0	0	0	1	0	2	1	1
GS191-01PC-15, 50-51	1320	200	0	0	0	0	11	0	0	0	0	0	0	0	0	0	0	11	0	11	11	0
GS191-01PC-15, 60-61	1330	200	0	0	0	0	6	0	0	0	0	0	0	8	0	0	1	6	0	15	7	8
GS191-01PC-15, 70-71	1340	200	0	0	0	0	50	0	0	0	0	0	0	4	0	0	0	50	0	54	50	4
GS191-01PC-15, 80-81	1350	200	0	0	0	0	8	0	0	0	1	0	0	1	0	0	0	8	0	10	9	1
GS191-01PC-15, 90-91	1360	200	0	1	0	0	88	0	0	0	0	0	0	4	0	0	1	88	0	94	90	4
GS191-01PC-16, 0-1	1370	200	0	0	0	0	0	0	0	0	0	0	1	0	0	0	0	0	0	1	0	1
GS191-01PC-16, 10-11	1380	200	0	0	0	0	2	0	0	0	0	0	0	3	0	0	0	2	0	5	2	3
GS191-01PC-16, 20-21	1390	200	0	0	0	0	19	0	0	0	3	0	1	7	0	0	0	19	0	30	22	8
GS191-01PC-16, 30-31	1400	200	0	0	0	0	225	1	0	0	10	0	0	26	0	0	0	226	0	262	236	26
GS191-01PC-16, 40-41	1410	200	0	0	0	0	5	0	0	0	0	0	0	2	0	0	0	5	0	7	5	2

GS191-01PC-16, 50-51	1420	200	0	0	0	0	40	0	0	0	0	0	1	11	0	0	0	40	0	52	40	12
GS191-01PC-16, 60-61	1430	200	0	1	0	0	24	0	0	0	0	0	0	6	0	0	0	24	0	31	25	6
GS191-01PC-16, 70-71	1440	200	0	0	1	0	98	0	0	0	13	0	0	8	1	0	0	98	1	121	113	8
GS191-01PC-16, 80-81	1450	200	0	0	0	0	49	0	0	0	4	0	2	11	1	0	0	49	0	67	54	13
GS191-01PC-17, 0-1	1460	200	0	0	0	0	1	0	0	0	0	0	0	1	0	0	0	1	0	2	1	1
GS191-01PC-17, 10-11	1470	200	0	0	0	0	27	1	0	0	1	0	0	3	0	0	0	28	0	32	29	3
GS191-01PC-17, 20-21	1480	200	0	0	0	0	45	0	0	0	0	0	0	1	0	0	0	45	0	46	45	1
GS191-01PC-17, 30-31	1490	200	0	0	0	0	51	2	0	0	1	0	0	9	0	0	0	53	0	63	54	9
GS191-01PC-17, 40-41	1500	200	0	1	1	3	190	1	0	0	17	0	0	15	0	0	0	191	4	228	213	15
GS191-01PC-17, 50-51	1510	200	0	0	0	0	0	0	0	0	0	0	0	0	0	0	0	0	0	0	0	0
GS191-01PC-17, 60-61	1520	200	0	0	0	0	43	0	0	0	0	0	0	5	0	0	0	43	0	48	43	5
GS191-01PC-17, 70-71	1530	200	0	1	0	1	81	0	0	0	3	0	0	7	0	0	0	81	1	93	86	7
GS191-01PC-17, 80-81	1540	200	0	0	0	3	137	3	0	0	8	0	0	9	0	0	0	140	3	160	151	9
GS191-01PC-17, 90-91	1550	200	0	0	2	0	774	9	0	1	32	0	0	22	0	0	3	783	2	843	821	22
GS191-01PC-18, 0-1	1560	200	0	0	0	0	2	0	0	0	0	0	0	7	0	0	0	2	0	9	2	7
GS191-01PC-18, 10-11	1570	200	0	0	0	0	43	1	0	0	2	0	0	10	0	0	0	44	0	56	46	10
GS191-01PC-18, 20-21	1580	200	0	0	0	0	123	1	0	0	2	0	1	25	0	1	0	124	0	153	127	26
GS191-01PC-18, 30-31	1590	200	0	0	0	0	4	0	0	0	0	0	0	0	0	0	0	4	0	4	4	0
GS191-01PC-18, 40-41	1600	200	0	0	0	0	2	0	0	0	0	0	0	0	0	0	0	2	0	2	2	0
GS191-01PC-18, 50-51	1610	200	0	0	0	0	3	0	0	0	0	0	0	0	0	0	0	3	0	3	3	0
GS191-01PC-18, 60-61	1620	200	0	0	0	1	19	0	0	0	0	0	1	1	0	0	0	19	1	22	20	2
GS191-01PC-18, 70-71	1630	200	0	0	0	0	0	0	0	0	0	0	0	0	0	0	0	0	0	0	0	0

GS191-01PC-18, 80-81	1640	200	0	0	0	0	50	0	0	0	4	0	3	2	0	0	0	50	0	59	54	5
GS191-01PC-18, 90-91	1650	200	0	0	0	0	1	0	0	0	0	0	0	0	0	0	0	1	0	1	1	0
GS191-01PC-19, 0-1	1660	200	0	0	0	0	6	0	0	0	0	0	1	1	0	0	0	6	0	8	6	2
GS191-01PC-19, 10-11	1670	200	0	0	0	0	800	2	0	0	7	0	2	12	0	0	1	802	0	824	810	14
GS191-01PC-19, 20-21	1680	200	0	1	2	1	71	0	1	0	10	0	1	8	0	0	0	71	3	95	86	9
GS191-01PC-19, 30-31	1690	200	0	1	0	0	259	1	1	0	22	0	0	10	0	0	0	260	0	294	284	10
GS191-01PC-19, 40-41	1700	200	0	0	0	0	0	0	0	0	0	0	0	0	0	0	0	0	0	0	0	0
GS191-01PC-19, 50-51	1710	200	0	0	0	0	0	0	0	0	0	0	0	0	0	0	0	0	0	0	0	0
GS191-01PC-19, 60-61	1720	200	0	1	0	3	507	1	0	0	7	0	2	8	0	1	0	508	3	530	520	10
GS191-01PC-19, 70-71	1730	200	0	0	0	0	0	0	0	0	0	0	0	0	0	0	0	0	0	0	0	0
GS191-01PC-19, 80-81	1740	200	0	0	1	0	308	2	0	0	3	0	0	4	0	0	3	310	1	321	317	4
GS191-01PC-19, 90-91	1750	200	0	0	0	6	152	0	0	0	14	0	1	0	0	0	1	152	6	174	173	1
GS191-01PC-20, 0-1	1760	200	0	0	0	0	3	0	0	0	0	0	0	0	0	0	0	3	0	3	3	0
GS191-01PC-20, 10-11	1770	200	0	0	0	0	45	0	0	0	2	0	1	2	0	0	0	45	0	50	47	3
GS191-01PC-20, 20-21	1780	200	0	0	0	0	43	2	0	0	5	0	0	3	0	0	0	45	0	53	50	3
GS191-01PC-20, 30-31	1790	200	0	0	0	0	7	0	0	0	0	0	0	1	0	0	0	7	0	8	7	1
GS191-01PC-20, 40-41	1800	200	0	0	1	0	17	0	0	0	3	0	0	0	0	0	0	17	1	21	21	0
GS191-01PC-20, 50-51	1810	200	0	0	0	0	11	0	0	0	0	0	0	4	0	0	0	11	0	15	11	4
GS191-01PC-20, 60-61	1820	200	0	0	0	0	52	1	0	0	4	0	0	1	0	0	0	53	0	58	57	1
GS191-01PC-20, 70-71	1830	200	0	0	0	0	8	0	0	0	0	0	0	1	0	0	0	8	0	9	8	1
GS191-01PC-20, 80-81	1840	200	0	0	0	0	0	0	0	0	0	0	0	1	0	0	0	0	0	1	0	1
GS191-01PC-20, 90-91	1850	200	0	0	0	0	1	0	0	0	0	0	0	4	0	0	0	1	0	5	1	4

GS191-01PC-21, 0-1	1860	200	0	0	0	0	0	0	0	0	0	0	0	0	0	0	0	0	0	0	0
GS191-01PC-21, 10-11	1870	200	0	0	0	0	0	0	0	0	0	0	0	0	0	0	0	0	0	0	0
GS191-01PC-21, 20-21	1880	200	0	0	0	0	25	2	0	0	5	0	1	4	0	0	0	27	0	37	32	5
GS191-01PC-21, 30-31	1890	200	0	0	0	0	171	1	0	0	8	0	0	6	0	0	1	172	0	187	181	6
GS191-01PC-21, 40-41	1900	200	0	0	0	0	0	0	0	0	0	0	0	0	0	0	0	0	0	0	0	0
GS191-01PC-21, 50-51	1910	200	0	0	0	0	0	0	0	0	0	0	0	1	0	0	0	0	0	1	0	1
GS191-01PC-21, 60-61	1920	200	0	0	0	0	0	0	0	0	0	0	0	1	0	0	0	0	0	1	0	1
GS191-01PC-21, 70-71	1930	200	0	0	0	0	0	0	0	0	0	0	0	0	0	0	0	0	0	0	0	0
GS191-01PC-21, 80-81	1940	200	0	0	0	0	24	0	0	0	10	0	4	20	0	0	0	24	0	58	34	24
GS191-01PC-21, 90-91	1950	200	0	0	0	1	63	0	1	0	20	0	0	3	0	0	0	63	1	88	85	3
GS191-01PC-21, 99-100	1960	200	0	0	6	18	350	0	0	0	310	0	2	6	0	0	0	350	24	692	684	8

Sample	Depth (cm)	Observed surface (mm^2)	*B. bigelowii*/10 mm^2	*C. leptoporus*/10 mm^2	*C. pel. braarudi*/10 mm^2	*C. pel. pelagicus*/10 mm^2	*E. huxleyi* < 4 µm/10 mm^2	*E. huxleyi* > 4µm/10 mm^2	*G. caribbeanica*/10 mm^2	*G. muellerae*/10 mm^2	*G. oceanica*/10 mm^2	*H. carteri*/10 mm^2	Reworked Cenozoic/10 mm^2	Reworked Cretaceous/10 mm^2	Small *Gephyrocapsa* spp. (<3µm)/10 mm^2	*Syracosphaera* spp./10 mm^2	*Thoracosphaera* spp. /10 mm^2
GS191-01PC-1, 0-1	0	6,28	0,00	76,43	7,96	2985,67	3660,83	1,59	0,00	1,59	9,55	0,00	12,74	7,96	12,74	7,96	4,78
GS191-01PC-1, 10-11	10	6,28	3,18	130,57	11,15	5488,85	3476,11	35,03	0,00	0,00	19,11	0,00	7,96	14,33	9,55	7,96	22,29
GS191-01PC-1, 20-21	20	6,28	0,00	58,92	3,18	2210,19	2679,94	1,59	0,00	0,00	4,78	0,00	4,78	14,33	3,18	11,15	12,74
GS191-01PC-1, 30-31	30	6,28	0,00	175,16	6,37	4038,22	5439,49	6,37	0,00	1,59	19,11	0,00	0,00	12,74	14,33	22,29	17,52
GS191-01PC-2, 6-7	40	6,28	0,00	176,75	3,18	2574,84	2960,19	6,37	0,00	1,59	17,52	0,00	3,18	9,55	0,00	6,37	11,15
GS191-01PC-2, 16-17	50	6,28	0,00	74,84	1,59	920,38	1531,85	11,15	0,00	0,00	12,74	0,00	3,18	3,18	3,18	0,00	6,37
GS191-01PC-2, 26-27	60	6,28	1,59	318,47	17,52	4116,24	5453,82	15,92	0,00	0,00	36,62	0,00	1,59	9,55	4,78	35,03	3,18
GS191-01PC-2, 36-37	70	6,28	0,00	181,53	6,37	1882,17	3041,40	9,55	0,00	0,00	11,15	0,00	1,59	11,15	0,00	6,37	1,59
GS191-01PC-2, 46-47	80	6,28	0,00	92,36	3,18	1831,21	2544,59	4,78	0,00	0,00	6,37	0,00	1,59	3,18	4,78	7,96	3,18
GS191-01PC-2, 56-57	90	6,28	0,00	54,14	3,18	1496,82	2281,85	3,18	0,00	0,00	9,55	0,00	0,00	9,55	7,96	3,18	4,78
GS191-01PC-2, 66-67	100	6,28	0,00	90,76	4,78	2355,10	3323,25	28,66	0,00	0,00	30,25	1,59	6,37	14,33	4,78	12,74	7,96
GS191-01PC-2, 76-77	110	6,28	0,00	57,32	6,37	1886,94	2818,47	9,55	0,00	0,00	11,15	0,00	3,18	6,37	9,55	11,15	6,37
GS191-01PC-2, 86-87	120	6,28	1,59	79,62	15,92	2707,01	3541,40	14,33	0,00	0,00	22,29	1,59	0,00	7,96	14,33	11,15	12,74

GS191-01PC-2, 96-97	130	6,28	0,00	30,25	0,00	1170,38	2396,50	3,18	0,00	0,00	7,96	1,59	0,00	4,78	6,37	12,74	7,96
GS191-01PC-3, 6-7	140	6,28	0,00	63,69	6,37	1767,52	3882,17	31,85	0,00	0,00	19,11	0,00	1,59	3,18	1,59	4,78	1,59
GS191-01PC-3, 16-17	150	6,28	0,00	14,33	11,15	1361,46	2988,85	25,48	0,00	0,00	17,52	0,00	0,00	6,37	0,00	14,33	4,78
GS191-01PC-3, 26-27	160	6,28	0,00	41,40	0,00	1713,38	1904,46	3,18	0,00	0,00	9,55	0,00	0,00	11,15	1,59	11,15	3,18
GS191-01PC-3, 36-37	170	6,28	0,00	111,46	12,74	3452,23	2691,08	9,55	0,00	0,00	11,15	0,00	0,00	20,70	0,00	7,96	9,55
GS191-01PC-3, 46-47	180	6,28	0,00	50,96	0,00	1527,07	1783,44	17,52	0,00	0,00	6,37	0,00	3,18	7,96	6,37	3,18	4,78
GS191-01PC-3, 56-57	190	6,28	0,00	128,98	1,59	3950,64	3707,01	23,89	0,00	0,00	6,37	0,00	4,78	15,92	0,00	3,18	11,15
GS191-01PC-3, 66-67	200	6,28	0,00	60,51	0,00	1157,64	1554,14	6,37	0,00	0,00	6,37	0,00	3,18	3,18	0,00	1,59	4,78
GS191-01PC-3, 76-77	210	6,28	0,00	109,87	3,18	1875,80	3687,90	30,25	0,00	0,00	28,66	0,00	1,59	14,33	23,89	3,18	7,96
GS191-01PC-3, 86-87	220	6,28	0,00	89,17	0,00	1178,34	2009,55	14,33	0,00	0,00	9,55	0,00	3,18	3,18	19,11	3,18	3,18
GS191-01PC-3, 96-97	230	6,28	0,00	60,51	1,59	1710,19	2527,07	22,29	0,00	0,00	15,92	0,00	1,59	4,78	6,37	6,37	9,55
GS191-01PC-4, 6-7	240	6,28	0,00	35,03	1,59	595,54	1248,41	9,55	0,00	0,00	3,18	0,00	0,00	1,59	4,78	3,18	6,37
GS191-01PC-4, 16-17	250	6,28	0,00	119,43	0,00	1775,48	2974,52	19,11	0,00	0,00	12,74	0,00	0,00	1,59	6,37	12,74	20,70
GS191-01PC-4, 26-27	260	6,28	0,00	68,47	20,70	3017,52	3485,67	68,47	0,00	0,00	58,92	0,00	6,37	19,11	14,33	4,78	20,70
GS191-01PC-4, 36-37	270	6,28	0,00	38,22	0,00	1122,61	2272,29	9,55	0,00	0,00	44,59	0,00	0,00	3,18	0,00	7,96	1,59
GS191-01PC-4, 46-47	280	6,28	0,00	108,28	14,33	5071,66	4742,04	19,11	0,00	0,00	146,50	0,00	4,78	17,52	0,00	15,92	19,11
GS191-01PC-4, 56-57	290	6,28	0,00	50,96	1,59	1855,10	3143,31	9,55	0,00	0,00	82,80	0,00	3,18	6,37	0,00	4,78	6,37
GS191-01PC-4, 66-67	300	6,28	0,00	89,17	14,33	2886,94	4248,41	7,96	0,00	0,00	248,41	0,00	3,18	12,74	1,59	4,78	4,78
GS191-01PC-4, 76-77	310	6,28	0,00	82,80	1,59	1866,24	3753,18	4,78	0,00	0,00	238,85	0,00	6,37	12,74	0,00	4,78	12,74
GS191-01PC-4, 86-87	320	6,28	0,00	25,48	0,00	471,34	863,06	1,59	0,00	0,00	92,36	0,00	1,59	7,96	0,00	1,59	1,59
GS191-01PC-5, 6-7	330	6,28	0,00	130,57	7,96	1484,08	2740,45	15,92	0,00	0,00	238,85	0,00	0,00	20,70	0,00	3,18	3,18
GS191-01PC-5, 16-17	340	6,28	0,00	181,53	28,66	2259,55	2743,63	4,78	0,00	0,00	383,76	0,00	4,78	6,37	0,00	6,37	17,52

GS191-01PC-5, 26-27	350	6,28	0,00	171,97	15,92	2707,01	3315,29	7,96	0,00	0,00	606,69	0,00	1,59	19,11	0,00	7,96	4,78
GS191-01PC-5, 36-37	360	6,28	0,00	105,10	12,74	1525,48	2616,24	30,25	0,00	0,00	482,48	0,00	1,59	14,33	1,59	15,92	6,37
GS191-01PC-5, 46-47	370	6,28	0,00	205,41	19,11	2936,31	3726,11	11,15	0,00	0,00	415,61	0,00	1,59	15,92	0,00	3,18	19,11
GS191-01PC-5, 56-57	380	6,28	0,00	128,98	7,96	1049,36	2571,66	9,55	0,00	0,00	254,78	0,00	1,59	1,59	0,00	4,78	1,59
GS191-01PC-5, 66-67	390	6,28	0,00	176,75	7,96	1847,13	3308,92	6,37	0,00	0,00	633,76	0,00	3,18	14,33	0,00	14,33	14,33
GS191-01PC-5, 76-77	400	6,28	0,00	101,91	3,18	1711,78	2909,24	14,33	0,00	0,00	546,18	0,00	0,00	11,15	0,00	3,18	3,18
GS191-01PC-5, 86-87	410	6,28	0,00	154,46	6,37	2472,93	3950,64	11,15	0,00	0,00	711,78	0,00	3,18	19,11	0,00	12,74	4,78
GS191-01PC-5, 96-97	420	6,28	0,00	143,31	7,96	1904,46	3874,20	9,55	0,00	0,00	581,21	3,18	0,00	9,55	0,00	4,78	7,96
GS191-01PC-6, 6-7	430	6,28	0,00	92,36	6,37	1093,95	3835,99	1,59	0,00	0,00	724,52	0,00	1,59	22,29	0,00	22,29	4,78
GS191-01PC-6, 16-17	440	6,28	0,00	41,40	3,18	635,35	2406,05	3,18	0,00	0,00	278,66	0,00	1,59	12,74	0,00	1,59	3,18
GS191-01PC-6, 26-27	450	6,28	0,00	28,66	4,78	558,92	2237,26	0,00	0,00	0,00	335,99	0,00	1,59	9,55	0,00	1,59	9,55
GS191-01PC-6, 36-37	460	6,28	0,00	46,18	0,00	207,01	2894,90	3,18	0,00	0,00	350,32	0,00	4,78	15,92	0,00	0,00	7,96
GS191-01PC-6, 46-47	470	6,28	0,00	39,81	0,00	171,97	2549,36	1,59	0,00	0,00	335,99	0,00	1,59	9,55	1,59	6,37	1,59
GS191-01PC-6, 56-57	480	6,28	0,00	15,92	0,00	12,74	656,05	0,00	0,00	0,00	35,03	0,00	1,59	4,78	0,00	0,00	3,18
GS191-01PC-6, 66-67	490	6,28	0,00	20,70	0,00	3,18	799,36	1,59	0,00	0,00	30,25	0,00	3,18	7,96	0,00	0,00	0,00
GS191-01PC-6, 76-77	500	6,28	0,00	44,59	0,00	4,78	1399,68	0,00	0,00	0,00	55,73	0,00	1,59	6,37	0,00	0,00	3,18
GS191-01PC-6, 86-87	510	6,28	0,00	100,32	0,00	4,78	3347,13	0,00	0,00	0,00	267,52	0,00	0,00	14,33	0,00	6,37	3,18
GS191-01PC-6, 96-97	520	6,28	0,00	52,55	0,00	6,37	1531,85	0,00	0,00	0,00	133,76	0,00	0,00	11,15	0,00	0,00	3,18
GS191-01PC-7, 6-7	530	6,28	0,00	35,03	0,00	1,59	585,99	0,00	0,00	0,00	55,73	0,00	0,00	6,37	0,00	1,59	0,00
GS191-01PC-7, 16-17	540	6,28	0,00	47,77	0,00	0,00	1227,71	0,00	0,00	0,00	87,58	0,00	0,00	11,15	0,00	0,00	3,18
GS191-01PC-7, 26-27	550	6,28	0,00	4,78	0,00	63,69	245,22	0,00	0,00	0,00	4,78	0,00	0,00	0,00	0,00	0,00	3,18
GS191-01PC-7, 36-37	560	6,28	0,00	0,00	0,00	0,00	6,37	0,00	0,00	0,00	0,00	0,00	0,00	0,00	0,00	0,00	1,59

GS191-01PC-7, 46-47	570	6,28	0,00	1,59	0,00	1,59	82,80	0,00	0,00	0,00	0,00	0,00	1,59	1,59	0,00	0,00	6,37
GS191-01PC-7, 56-57	580	6,28	0,00	0,00	0,00	0,00	85,99	0,00	0,00	0,00	1,59	0,00	0,00	0,00	0,00	0,00	3,18
GS191-01PC-7, 66-67	590	6,28	0,00	0,00	0,00	1,59	30,25	0,00	0,00	0,00	0,00	0,00	0,00	4,78	0,00	0,00	1,59
GS191-01PC-7, 76-77	600	6,28	0,00	1,59	0,00	28,66	25,48	0,00	0,00	0,00	0,00	0,00	0,00	1,59	0,00	1,59	0,00
GS191-01PC-8, 6-7	610	6,28	0,00	0,00	0,00	0,00	0,00	0,00	0,00	0,00	0,00	0,00	0,00	0,00	0,00	0,00	1,59
GS191-01PC-8, 16-17	620	6,28	0,00	7,96	0,00	0,00	334,39	3,18	0,00	0,00	12,74	0,00	1,59	7,96	0,00	0,00	0,00
GS191-01PC-8, 26-27	630	6,28	0,00	3,18	0,00	0,00	598,73	7,96	0,00	0,00	3,18	0,00	0,00	19,11	0,00	0,00	0,00
GS191-01PC-8, 36-37	640	6,28	0,00	12,74	0,00	1,59	996,82	0,00	0,00	3,18	57,32	0,00	0,00	7,96	0,00	0,00	0,00
GS191-01PC-8, 46-47	650	6,28	0,00	7,96	0,00	1,59	891,72	3,18	0,00	0,00	19,11	0,00	1,59	17,52	0,00	0,00	0,00
GS191-01PC-8, 56-57	660	6,28	0,00	0,00	0,00	0,00	85,99	0,00	0,00	0,00	0,00	0,00	0,00	0,00	0,00	0,00	0,00
GS191-01PC-8, 66-67	670	6,28	0,00	4,78	0,00	1,59	200,64	0,00	0,00	3,18	6,37	0,00	3,18	6,37	0,00	0,00	0,00
GS191-01PC-9, 0-1	680	6,28	0,00	0,00	0,00	9,55	211,78	1,59	0,00	0,00	3,18	0,00	3,18	12,74	0,00	0,00	0,00
GS191-01PC-9, 10-11	690	6,28	0,00	0,00	0,00	0,00	60,51	0,00	0,00	0,00	0,00	0,00	0,00	1,59	0,00	0,00	0,00
GS191-01PC-9, 20-21	700	6,28	0,00	4,78	3,18	71,66	716,56	57,32	0,00	0,00	12,74	0,00	0,00	28,66	0,00	1,59	3,18
GS191-01PC-9, 30-31	710	6,28	0,00	0,00	0,00	6,37	428,34	0,00	0,00	0,00	4,78	0,00	1,59	14,33	0,00	0,00	0,00
GS191-01PC-9, 40-41	720	6,28	0,00	0,00	0,00	0,00	313,69	0,00	0,00	0,00	3,18	0,00	1,59	9,55	0,00	1,59	0,00
GS191-01PC-9, 50-51	730	6,28	0,00	0,00	0,00	1,59	78,03	0,00	0,00	0,00	1,59	0,00	1,59	1,59	0,00	0,00	0,00
GS191-01PC-9, 60-61	740	6,28	0,00	0,00	0,00	0,00	57,32	0,00	0,00	0,00	0,00	0,00	1,59	4,78	0,00	0,00	0,00
GS191-01PC-9, 70-71	750	6,28	0,00	0,00	0,00	17,52	109,87	1,59	0,00	0,00	6,37	0,00	3,18	12,74	0,00	1,59	1,59
GS191-01PC-9, 80-81	760	6,28	0,00	0,00	0,00	0,00	0,00	0,00	0,00	0,00	0,00	0,00	0,00	1,59	0,00	0,00	0,00
GS191-01PC-9, 90-91	770	6,28	0,00	0,00	0,00	0,00	6,37	0,00	0,00	0,00	0,00	0,00	0,00	1,59	0,00	0,00	0,00
GS191-01PC-10, 0-1	780	6,28	0,00	0,00	0,00	0,00	1,59	0,00	0,00	0,00	0,00	0,00	0,00	1,59	0,00	0,00	0,00

GS191-01PC-10, 10-11	790	6,28	0,00	0,00	0,00	0,00	6,37	0,00	0,00	0,00	3,18	0,00	0,00	4,78	1,59	0,00	0,00
GS191-01PC-10, 20-21	800	6,28	0,00	0,00	0,00	1,59	3,18	0,00	0,00	0,00	0,00	0,00	0,00	3,18	0,00	0,00	1,59
GS191-01PC-10, 30-31	810	6,28	0,00	0,00	0,00	6,37	11,15	0,00	0,00	0,00	0,00	0,00	0,00	3,18	0,00	0,00	1,59
GS191-01PC-10, 40-41	820	6,28	0,00	0,00	0,00	36,62	46,18	0,00	0,00	0,00	0,00	0,00	0,00	3,18	0,00	1,59	0,00
GS191-01PC-10, 50-51	830	6,28	0,00	0,00	0,00	0,00	1,59	0,00	0,00	0,00	0,00	0,00	0,00	3,18	0,00	0,00	0,00
GS191-01PC-10, 60-61	840	6,28	0,00	0,00	0,00	0,00	1,59	0,00	0,00	0,00	1,59	0,00	0,00	6,37	0,00	0,00	0,00
GS191-01PC-10, 70-71	850	6,28	0,00	0,00	0,00	0,00	4,78	0,00	0,00	0,00	0,00	0,00	0,00	3,18	0,00	0,00	0,00
GS191-01PC-10, 80-81	860	6,28	0,00	0,00	0,00	0,00	0,00	0,00	0,00	0,00	0,00	0,00	0,00	1,59	0,00	0,00	0,00
GS191-01PC-11, 0-1	870	6,28	0,00	0,00	0,00	0,00	4,78	0,00	0,00	0,00	0,00	0,00	0,00	1,59	0,00	0,00	0,00
GS191-01PC-11, 10-11	880	6,28	0,00	0,00	0,00	0,00	103,50	0,00	0,00	0,00	1,59	0,00	0,00	12,74	0,00	1,59	0,00
GS191-01PC-11, 20-21	890	6,28	0,00	0,00	0,00	0,00	3,18	0,00	0,00	0,00	0,00	0,00	0,00	0,00	0,00	0,00	0,00
GS191-01PC-11, 30-31	900	6,28	0,00	0,00	0,00	0,00	160,83	0,00	0,00	0,00	1,59	0,00	1,59	22,29	0,00	1,59	0,00
GS191-01PC-11, 40-41	910	6,28	0,00	0,00	0,00	3,18	84,39	0,00	0,00	0,00	1,59	0,00	6,37	36,62	0,00	0,00	0,00
GS191-01PC-11, 50-51	920	6,28	0,00	0,00	0,00	0,00	6,37	0,00	0,00	0,00	0,00	0,00	1,59	6,37	0,00	0,00	0,00
GS191-01PC-11, 60-61	930	6,28	0,00	0,00	0,00	4,78	71,66	0,00	0,00	0,00	1,59	0,00	3,18	58,92	0,00	1,59	1,59
GS191-01PC-11, 70-71	940	6,28	0,00	0,00	0,00	0,00	46,18	0,00	0,00	0,00	3,18	0,00	0,00	19,11	0,00	0,00	0,00
GS191-01PC-11, 80-81	950	6,28	0,00	0,00	0,00	6,37	296,18	0,00	0,00	0,00	7,96	0,00	6,37	78,03	0,00	4,78	0,00
GS191-01PC-11, 90-91	960	6,28	0,00	0,00	0,00	7,96	485,67	9,55	0,00	0,00	11,15	0,00	6,37	111,46	0,00	1,59	0,00
GS191-01PC-12, 0-1	970	6,28	0,00	0,00	0,00	11,15	89,17	0,00	0,00	0,00	4,78	0,00	3,18	54,14	0,00	0,00	0,00
GS191-01PC-12, 10-11	980	6,28	0,00	0,00	1,59	4,78	128,98	0,00	0,00	0,00	20,70	0,00	6,37	165,61	0,00	0,00	0,00
GS191-01PC-12, 20-21	990	6,28	0,00	0,00	0,00	0,00	38,22	0,00	0,00	0,00	4,78	0,00	0,00	20,70	0,00	0,00	0,00
GS191-01PC-12, 30-31	1000	6,28	0,00	0,00	1,59	7,96	109,87	0,00	0,00	0,00	7,96	0,00	4,78	89,17	0,00	0,00	1,59

GS191-01PC-12, 40-41	1010	6,28	0,00	0,00	0,00	0,00	35,03	0,00	0,00	0,00	3,18	0,00	6,37	28,66	0,00	0,00	0,00
GS191-01PC-12, 50-51	1020	6,28	0,00	0,00	0,00	0,00	58,92	3,18	0,00	0,00	0,00	0,00	1,59	36,62	0,00	0,00	0,00
GS191-01PC-12, 60-61	1030	6,28	0,00	0,00	0,00	1,59	20,70	0,00	0,00	0,00	3,18	0,00	4,78	46,18	0,00	0,00	1,59
GS191-01PC-12, 70-71	1040	6,28	0,00	0,00	0,00	0,00	425,16	14,33	0,00	0,00	15,92	0,00	0,00	63,69	0,00	3,18	1,59
GS191-01PC-12, 80-81	1050	6,28	0,00	0,00	0,00	3,18	27,07	0,00	0,00	0,00	7,96	0,00	1,59	30,25	0,00	0,00	0,00
GS191-01PC-12, 90-91	1060	6,28	0,00	0,00	0,00	0,00	0,00	0,00	0,00	0,00	0,00	0,00	0,00	1,59	0,00	0,00	0,00
GS191-01PC-13, 0-1	1070	6,28	0,00	0,00	0,00	1,59	1,59	0,00	0,00	0,00	0,00	0,00	0,00	0,00	0,00	0,00	0,00
GS191-01PC-13, 10-11	1080	6,28	0,00	0,00	0,00	0,00	0,00	0,00	0,00	0,00	0,00	0,00	0,00	1,59	0,00	0,00	0,00
GS191-01PC-13, 20-21	1090	6,28	0,00	0,00	0,00	1,59	0,00	0,00	0,00	0,00	0,00	0,00	0,00	0,00	0,00	0,00	0,00
GS191-01PC-13, 30-31	1100	6,28	0,00	0,00	0,00	0,00	1,59	0,00	0,00	0,00	0,00	0,00	0,00	4,78	0,00	0,00	0,00
GS191-01PC-13, 40-41	1110	6,28	0,00	0,00	0,00	0,00	6,37	0,00	0,00	0,00	0,00	0,00	1,59	3,18	0,00	0,00	0,00
GS191-01PC-13, 52-53	1122	6,28	0,00	3,18	0,00	1,59	546,18	6,37	0,00	0,00	9,55	0,00	6,37	58,92	0,00	3,18	0,00
GS191-01PC-13, 60-61	1130	6,28	0,00	0,00	0,00	6,37	108,28	0,00	0,00	0,00	12,74	0,00	3,18	138,54	1,59	0,00	3,18
GS191-01PC-13, 70-71	1140	6,28	0,00	0,00	0,00	0,00	76,43	1,59	0,00	0,00	9,55	0,00	4,78	92,36	1,59	0,00	0,00
GS191-01PC-13, 80-81	1150	6,28	0,00	1,59	0,00	3,18	68,47	0,00	0,00	0,00	3,18	0,00	1,59	60,51	0,00	0,00	0,00
GS191-01PC-13, 90-91	1160	6,28	0,00	0,00	0,00	3,18	152,87	0,00	0,00	0,00	4,78	0,00	1,59	47,77	0,00	1,59	0,00
GS191-01PC-14, 0-1	1170	6,28	0,00	0,00	0,00	0,00	232,48	6,37	0,00	0,00	0,00	0,00	3,18	68,47	0,00	0,00	1,59
GS191-01PC-14, 10-11	1180	6,28	0,00	0,00	0,00	0,00	474,52	0,00	0,00	0,00	1,59	0,00	0,00	49,36	0,00	0,00	0,00
GS191-01PC-14, 20-21	1190	6,28	0,00	0,00	0,00	0,00	668,79	4,78	0,00	0,00	0,00	0,00	3,18	41,40	1,59	1,59	0,00
GS191-01PC-14, 30-31	1200	6,28	0,00	0,00	0,00	0,00	14,33	0,00	0,00	0,00	3,18	0,00	1,59	15,92	0,00	0,00	0,00
GS191-01PC-14, 40-41	1210	6,28	0,00	0,00	0,00	0,00	12,74	0,00	0,00	0,00	0,00	0,00	0,00	4,78	0,00	0,00	0,00
GS191-01PC-14, 50-51	1220	6,28	0,00	0,00	0,00	0,00	0,00	0,00	0,00	0,00	0,00	0,00	0,00	0,00	0,00	0,00	0,00

GS191-01PC-14, 60-61	1230	6,28	0,00	1,59	0,00	0,00	156,05	1,59	0,00	0,00	1,59	0,00	0,00	14,33	0,00	0,00	0,00
GS191-01PC-14, 70-71	1240	6,28	0,00	0,00	0,00	0,00	4,78	0,00	0,00	0,00	0,00	0,00	0,00	3,18	0,00	0,00	0,00
GS191-01PC-14, 80-81	1250	6,28	0,00	3,18	0,00	0,00	33,44	0,00	0,00	0,00	4,78	0,00	0,00	12,74	0,00	0,00	0,00
GS191-01PC-14, 90-91	1260	6,28	0,00	0,00	0,00	0,00	103,50	1,59	0,00	0,00	1,59	0,00	0,00	11,15	0,00	0,00	0,00
GS191-01PC-15, 0-1	1270	6,28	0,00	1,59	0,00	1,59	157,64	1,59	0,00	0,00	0,00	0,00	1,59	11,15	0,00	0,00	0,00
GS191-01PC-15, 10-11	1280	6,28	0,00	3,18	0,00	1,59	640,13	0,00	0,00	0,00	3,18	0,00	0,00	15,92	0,00	0,00	1,59
GS191-01PC-15, 20-21	1290	6,28	0,00	0,00	0,00	0,00	44,59	0,00	0,00	0,00	0,00	0,00	0,00	1,59	0,00	0,00	1,59
GS191-01PC-15, 30-31	1300	6,28	0,00	0,00	0,00	0,00	0,00	0,00	0,00	0,00	0,00	0,00	0,00	0,00	0,00	0,00	0,00
GS191-01PC-15, 40-41	1310	6,28	0,00	0,00	0,00	0,00	1,59	0,00	0,00	0,00	0,00	0,00	0,00	1,59	0,00	0,00	0,00
GS191-01PC-15, 50-51	1320	6,28	0,00	0,00	0,00	0,00	17,52	0,00	0,00	0,00	0,00	0,00	0,00	0,00	0,00	0,00	0,00
GS191-01PC-15, 60-61	1330	6,28	0,00	0,00	0,00	0,00	9,55	0,00	0,00	0,00	0,00	0,00	0,00	12,74	0,00	0,00	1,59
GS191-01PC-15, 70-71	1340	6,28	0,00	0,00	0,00	0,00	79,62	0,00	0,00	0,00	0,00	0,00	0,00	6,37	0,00	0,00	0,00
GS191-01PC-15, 80-81	1350	6,28	0,00	0,00	0,00	0,00	12,74	0,00	0,00	0,00	1,59	0,00	0,00	1,59	0,00	0,00	0,00
GS191-01PC-15, 90-91	1360	6,28	0,00	1,59	0,00	0,00	140,13	0,00	0,00	0,00	0,00	0,00	0,00	6,37	0,00	0,00	1,59
GS191-01PC-16, 0-1	1370	6,28	0,00	0,00	0,00	0,00	0,00	0,00	0,00	0,00	0,00	0,00	1,59	0,00	0,00	0,00	0,00
GS191-01PC-16, 10-11	1380	6,28	0,00	0,00	0,00	0,00	3,18	0,00	0,00	0,00	0,00	0,00	0,00	4,78	0,00	0,00	0,00
GS191-01PC-16, 20-21	1390	6,28	0,00	0,00	0,00	0,00	30,25	0,00	0,00	0,00	4,78	0,00	1,59	11,15	0,00	0,00	0,00
GS191-01PC-16, 30-31	1400	6,28	0,00	0,00	0,00	0,00	358,28	1,59	0,00	0,00	15,92	0,00	0,00	41,40	0,00	0,00	0,00
GS191-01PC-16, 40-41	1410	6,28	0,00	0,00	0,00	0,00	7,96	0,00	0,00	0,00	0,00	0,00	0,00	3,18	0,00	0,00	0,00
GS191-01PC-16, 50-51	1420	6,28	0,00	0,00	0,00	0,00	63,69	0,00	0,00	0,00	0,00	0,00	1,59	17,52	0,00	0,00	0,00
GS191-01PC-16, 60-61	1430	6,28	0,00	1,59	0,00	0,00	38,22	0,00	0,00	0,00	0,00	0,00	0,00	9,55	0,00	0,00	0,00
GS191-01PC-16, 70-71	1440	6,28	0,00	0,00	1,59	0,00	156,05	0,00	0,00	0,00	20,70	0,00	0,00	12,74	1,59	0,00	0,00

GS191-01PC-16, 80-81	1450	6,28	0,00	0,00	0,00	0,00	78,03	0,00	0,00	0,00	6,37	0,00	3,18	17,52	1,59	0,00	0,00
GS191-01PC-17, 0-1	1460	6,28	0,00	0,00	0,00	0,00	1,59	0,00	0,00	0,00	0,00	0,00	0,00	1,59	0,00	0,00	0,00
GS191-01PC-17, 10-11	1470	6,28	0,00	0,00	0,00	0,00	42,99	1,59	0,00	0,00	1,59	0,00	0,00	4,78	0,00	0,00	0,00
GS191-01PC-17, 20-21	1480	6,28	0,00	0,00	0,00	0,00	71,66	0,00	0,00	0,00	0,00	0,00	0,00	1,59	0,00	0,00	0,00
GS191-01PC-17, 30-31	1490	6,28	0,00	0,00	0,00	0,00	81,21	3,18	0,00	0,00	1,59	0,00	0,00	14,33	0,00	0,00	0,00
GS191-01PC-17, 40-41	1500	6,28	0,00	1,59	1,59	4,78	302,55	1,59	0,00	0,00	27,07	0,00	0,00	23,89	0,00	0,00	0,00
GS191-01PC-17, 50-51	1510	6,28	0,00	0,00	0,00	0,00	0,00	0,00	0,00	0,00	0,00	0,00	0,00	0,00	0,00	0,00	0,00
GS191-01PC-17, 60-61	1520	6,28	0,00	0,00	0,00	0,00	68,47	0,00	0,00	0,00	0,00	0,00	0,00	7,96	0,00	0,00	0,00
GS191-01PC-17, 70-71	1530	6,28	0,00	1,59	0,00	1,59	128,98	0,00	0,00	0,00	4,78	0,00	0,00	11,15	0,00	0,00	0,00
GS191-01PC-17, 80-81	1540	6,28	0,00	0,00	0,00	4,78	218,15	4,78	0,00	0,00	12,74	0,00	0,00	14,33	0,00	0,00	0,00
GS191-01PC-17, 90-91	1550	6,28	0,00	0,00	3,18	0,00	1232,48	14,33	0,00	1,59	50,96	0,00	0,00	35,03	0,00	0,00	4,78
GS191-01PC-18, 0-1	1560	6,28	0,00	0,00	0,00	0,00	3,18	0,00	0,00	0,00	0,00	0,00	0,00	11,15	0,00	0,00	0,00
GS191-01PC-18, 10-11	1570	6,28	0,00	0,00	0,00	0,00	68,47	1,59	0,00	0,00	3,18	0,00	0,00	15,92	0,00	0,00	0,00
GS191-01PC-18, 20-21	1580	6,28	0,00	0,00	0,00	0,00	195,86	1,59	0,00	0,00	3,18	0,00	1,59	39,81	0,00	1,59	0,00
GS191-01PC-18, 30-31	1590	6,28	0,00	0,00	0,00	0,00	6,37	0,00	0,00	0,00	0,00	0,00	0,00	0,00	0,00	0,00	0,00
GS191-01PC-18, 40-41	1600	6,28	0,00	0,00	0,00	0,00	3,18	0,00	0,00	0,00	0,00	0,00	0,00	0,00	0,00	0,00	0,00
GS191-01PC-18, 50-51	1610	6,28	0,00	0,00	0,00	0,00	4,78	0,00	0,00	0,00	0,00	0,00	0,00	0,00	0,00	0,00	0,00
GS191-01PC-18, 60-61	1620	6,28	0,00	0,00	0,00	1,59	30,25	0,00	0,00	0,00	0,00	0,00	1,59	1,59	0,00	0,00	0,00
GS191-01PC-18, 70-71	1630	6,28	0,00	0,00	0,00	0,00	0,00	0,00	0,00	0,00	0,00	0,00	0,00	0,00	0,00	0,00	0,00
GS191-01PC-18, 80-81	1640	6,28	0,00	0,00	0,00	0,00	79,62	0,00	0,00	0,00	6,37	0,00	4,78	3,18	0,00	0,00	0,00
GS191-01PC-18, 90-91	1650	6,28	0,00	0,00	0,00	0,00	1,59	0,00	0,00	0,00	0,00	0,00	0,00	0,00	0,00	0,00	0,00
GS191-01PC-19, 0-1	1660	6,28	0,00	0,00	0,00	0,00	9,55	0,00	0,00	0,00	0,00	0,00	1,59	1,59	0,00	0,00	0,00

GS191-01PC-19, 10-11	1670	6,28	0,00	0,00	0,00	0,00	1273,89	3,18	0,00	0,00	11,15	0,00	3,18	19,11	0,00	0,00	1,59
GS191-01PC-19, 20-21	1680	6,28	0,00	1,59	3,18	1,59	113,06	0,00	1,59	0,00	15,92	0,00	1,59	12,74	0,00	0,00	0,00
GS191-01PC-19, 30-31	1690	6,28	0,00	1,59	0,00	0,00	412,42	1,59	1,59	0,00	35,03	0,00	0,00	15,92	0,00	0,00	0,00
GS191-01PC-19, 40-41	1700	6,28	0,00	0,00	0,00	0,00	0,00	0,00	0,00	0,00	0,00	0,00	0,00	0,00	0,00	0,00	0,00
GS191-01PC-19, 50-51	1710	6,28	0,00	0,00	0,00	0,00	0,00	0,00	0,00	0,00	0,00	0,00	0,00	0,00	0,00	0,00	0,00
GS191-01PC-19, 60-61	1720	6,28	0,00	1,59	0,00	4,78	807,32	1,59	0,00	0,00	11,15	0,00	3,18	12,74	0,00	1,59	0,00
GS191-01PC-19, 70-71	1730	6,28	0,00	0,00	0,00	0,00	0,00	0,00	0,00	0,00	0,00	0,00	0,00	0,00	0,00	0,00	0,00
GS191-01PC-19, 80-81	1740	6,28	0,00	0,00	1,59	0,00	490,45	3,18	0,00	0,00	4,78	0,00	0,00	6,37	0,00	0,00	4,78
GS191-01PC-19, 90-91	1750	6,28	0,00	0,00	0,00	9,55	242,04	0,00	0,00	0,00	22,29	0,00	1,59	0,00	0,00	0,00	1,59
GS191-01PC-20, 0-1	1760	6,28	0,00	0,00	0,00	0,00	4,78	0,00	0,00	0,00	0,00	0,00	0,00	0,00	0,00	0,00	0,00
GS191-01PC-20, 10-11	1770	6,28	0,00	0,00	0,00	0,00	71,66	0,00	0,00	0,00	3,18	0,00	1,59	3,18	0,00	0,00	0,00
GS191-01PC-20, 20-21	1780	6,28	0,00	0,00	0,00	0,00	68,47	3,18	0,00	0,00	7,96	0,00	0,00	4,78	0,00	0,00	0,00
GS191-01PC-20, 30-31	1790	6,28	0,00	0,00	0,00	0,00	11,15	0,00	0,00	0,00	0,00	0,00	0,00	1,59	0,00	0,00	0,00
GS191-01PC-20, 40-41	1800	6,28	0,00	0,00	1,59	0,00	27,07	0,00	0,00	0,00	4,78	0,00	0,00	0,00	0,00	0,00	0,00
GS191-01PC-20, 50-51	1810	6,28	0,00	0,00	0,00	0,00	17,52	0,00	0,00	0,00	0,00	0,00	0,00	6,37	0,00	0,00	0,00
GS191-01PC-20, 60-61	1820	6,28	0,00	0,00	0,00	0,00	82,80	1,59	0,00	0,00	6,37	0,00	0,00	1,59	0,00	0,00	0,00
GS191-01PC-20, 70-71	1830	6,28	0,00	0,00	0,00	0,00	12,74	0,00	0,00	0,00	0,00	0,00	0,00	1,59	0,00	0,00	0,00
GS191-01PC-20, 80-81	1840	6,28	0,00	0,00	0,00	0,00	0,00	0,00	0,00	0,00	0,00	0,00	0,00	1,59	0,00	0,00	0,00
GS191-01PC-20, 90-91	1850	6,28	0,00	0,00	0,00	0,00	1,59	0,00	0,00	0,00	0,00	0,00	0,00	6,37	0,00	0,00	0,00
GS191-01PC-21, 0-1	1860	6,28	0,00	0,00	0,00	0,00	0,00	0,00	0,00	0,00	0,00	0,00	0,00	0,00	0,00	0,00	0,00
GS191-01PC-21, 10-11	1870	6,28	0,00	0,00	0,00	0,00	0,00	0,00	0,00	0,00	0,00	0,00	0,00	0,00	0,00	0,00	0,00
GS191-01PC-21, 20-21	1880	6,28	0,00	0,00	0,00	0,00	39,81	3,18	0,00	0,00	7,96	0,00	1,59	6,37	0,00	0,00	0,00

GS191-01PC-21, 30-31	1890	6,28	0,00	0,00	0,00	0,00	272,29	1,59	0,00	0,00	12,74	0,00	0,00	9,55	0,00	0,00	1,59
GS191-01PC-21, 40-41	1900	6,28	0,00	0,00	0,00	0,00	0,00	0,00	0,00	0,00	0,00	0,00	0,00	0,00	0,00	0,00	0,00
GS191-01PC-21, 50-51	1910	6,28	0,00	0,00	0,00	0,00	0,00	0,00	0,00	0,00	0,00	0,00	0,00	1,59	0,00	0,00	0,00
GS191-01PC-21, 60-61	1920	6,28	0,00	0,00	0,00	0,00	0,00	0,00	0,00	0,00	0,00	0,00	0,00	1,59	0,00	0,00	0,00
GS191-01PC-21, 70-71	1930	6,28	0,00	0,00	0,00	0,00	0,00	0,00	0,00	0,00	0,00	0,00	0,00	0,00	0,00	0,00	0,00
GS191-01PC-21, 80-81	1940	6,28	0,00	0,00	0,00	0,00	38,22	0,00	0,00	0,00	15,92	0,00	6,37	31,85	0,00	0,00	0,00
GS191-01PC-21, 90-91	1950	6,28	0,00	0,00	0,00	1,59	100,32	0,00	1,59	0,00	31,85	0,00	0,00	4,78	0,00	0,00	0,00
GS191-01PC-21, 99-100	1960	6,28	0,00	0,00	9,55	28,66	557,32	0,00	0,00	0,00	493,63	0,00	3,18	9,55	0,00	0,00	0,00

Sample	Depth (cm)	Observed surface (mm^2)	Total *E. huxleyi* /10 mm^2	Total *C. pelagicus* /10 mm^2	Total abundance (with reworked) /10 mm^2	Total abundance (NO reworked) /10 mm^2	Total Reworked /10 mm^2
GS191-01PC-1, 0-1	0	6,28	3662,42	2993,63	6789,81	6769,11	20,70
GS191-01PC-1, 10-11	10	6,28	3511,15	5500,00	9226,11	9203,82	22,29
GS191-01PC-1, 20-21	20	6,28	2681,53	2213,38	5004,78	4985,67	19,11
GS191-01PC-1, 30-31	30	6,28	5445,86	4044,59	9753,18	9740,45	12,74
GS191-01PC-2, 6-7	40	6,28	2966,56	2578,03	5770,70	5757,96	12,74
GS191-01PC-2, 16-17	50	6,28	1542,99	921,97	2568,47	2562,10	6,37
GS191-01PC-2, 26-27	60	6,28	5469,75	4133,76	10014,33	10003,18	11,15
GS191-01PC-2, 36-37	70	6,28	3050,96	1888,54	5152,87	5140,13	12,74
GS191-01PC-2, 46-47	80	6,28	2549,36	1834,39	4503,18	4498,41	4,78
GS191-01PC-2, 56-57	90	6,28	2285,03	1500,00	3874,20	3864,65	9,55
GS191-01PC-2, 66-67	100	6,28	3351,91	2359,87	5880,57	5859,87	20,70
GS191-01PC-2, 76-77	110	6,28	2828,03	1893,31	4826,43	4816,88	9,55
GS191-01PC-2, 86-87	120	6,28	3555,73	2722,93	6429,94	6421,97	7,96

GS191-01PC-2, 96-97	130	6,28	2399,68	1170,38	3641,72	3636,94	4,78
GS191-01PC-3, 6-7	140	6,28	3914,01	1773,89	5783,44	5778,66	4,78
GS191-01PC-3, 16-17	150	6,28	3014,33	1372,61	4444,27	4437,90	6,37
GS191-01PC-3, 26-27	160	6,28	1907,64	1713,38	3699,04	3687,90	11,15
GS191-01PC-3, 36-37	170	6,28	2700,64	3464,97	6326,43	6305,73	20,70
GS191-01PC-3, 46-47	180	6,28	1800,96	1527,07	3410,83	3399,68	11,15
GS191-01PC-3, 56-57	190	6,28	3730,89	3952,23	7853,50	7832,80	20,70
GS191-01PC-3, 66-67	200	6,28	1560,51	1157,64	2797,77	2791,40	6,37
GS191-01PC-3, 76-77	210	6,28	3718,15	1878,98	5786,62	5770,70	15,92
GS191-01PC-3, 86-87	220	6,28	2023,89	1178,34	3332,80	3326,43	6,37
GS191-01PC-3, 96-97	230	6,28	2549,36	1711,78	4366,24	4359,87	6,37
GS191-01PC-4, 6-7	240	6,28	1257,96	597,13	1909,24	1907,64	1,59
GS191-01PC-4, 16-17	250	6,28	2993,63	1775,48	4942,68	4941,08	1,59
GS191-01PC-4, 26-27	260	6,28	3554,14	3038,22	6785,03	6759,55	25,48
GS191-01PC-4, 36-37	270	6,28	2281,85	1122,61	3500,00	3496,82	3,18
GS191-01PC-4, 46-47	280	6,28	4761,15	5085,99	10159,24	10136,94	22,29
GS191-01PC-4, 56-57	290	6,28	3152,87	1856,69	5164,01	5154,46	9,55
GS191-01PC-4, 66-67	300	6,28	4256,37	2901,27	7522,29	7506,37	15,92
GS191-01PC-4, 76-77	310	6,28	3757,96	1867,83	5984,08	5964,97	19,11
GS191-01PC-4, 86-87	320	6,28	864,65	471,34	1466,56	1457,01	9,55
GS191-01PC-5, 6-7	330	6,28	2756,37	1492,04	4644,90	4624,20	20,70
GS191-01PC-5, 16-17	340	6,28	2748,41	2288,22	5636,94	5625,80	11,15

GS191-01PC-5, 26-27	350	6,28	3323,25	2722,93	6858,28	6837,58	20,70
GS191-01PC-5, 36-37	360	6,28	2646,50	1538,22	4812,10	4796,18	15,92
GS191-01PC-5, 46-47	370	6,28	3737,26	2955,41	7353,50	7335,99	17,52
GS191-01PC-5, 56-57	380	6,28	2581,21	1057,32	4031,85	4028,66	3,18
GS191-01PC-5, 66-67	390	6,28	3315,29	1855,10	6027,07	6009,55	17,52
GS191-01PC-5, 76-77	400	6,28	2923,57	1714,97	5304,14	5292,99	11,15
GS191-01PC-5, 86-87	410	6,28	3961,78	2479,30	7347,13	7324,84	22,29
GS191-01PC-5, 96-97	420	6,28	3883,76	1912,42	6546,18	6536,62	9,55
GS191-01PC-6, 6-7	430	6,28	3837,58	1100,32	5805,73	5781,85	23,89
GS191-01PC-6, 16-17	440	6,28	2409,24	638,54	3386,94	3372,61	14,33
GS191-01PC-6, 26-27	450	6,28	2237,26	563,69	3187,90	3176,75	11,15
GS191-01PC-6, 36-37	460	6,28	2898,09	207,01	3530,25	3509,55	20,70
GS191-01PC-6, 46-47	470	6,28	2550,96	171,97	3119,43	3108,28	11,15
GS191-01PC-6, 56-57	480	6,28	656,05	12,74	729,30	722,93	6,37
GS191-01PC-6, 66-67	490	6,28	800,96	3,18	866,24	855,10	11,15
GS191-01PC-6, 76-77	500	6,28	1399,68	4,78	1515,92	1507,96	7,96
GS191-01PC-6, 86-87	510	6,28	3347,13	4,78	3743,63	3729,30	14,33
GS191-01PC-6, 96-97	520	6,28	1531,85	6,37	1738,85	1727,71	11,15
GS191-01PC-7, 6-7	530	6,28	585,99	1,59	686,31	679,94	6,37
GS191-01PC-7, 16-17	540	6,28	1227,71	0,00	1377,39	1366,24	11,15
GS191-01PC-7, 26-27	550	6,28	245,22	63,69	321,66	321,66	0,00
GS191-01PC-7, 36-37	560	6,28	6,37	0,00	7,96	7,96	0,00

GS191-01PC-7, 46-47	570	6,28	82,80	1,59	95,54	92,36	3,18
GS191-01PC-7, 56-57	580	6,28	85,99	0,00	90,76	90,76	0,00
GS191-01PC-7, 66-67	590	6,28	30,25	1,59	38,22	33,44	4,78
GS191-01PC-7, 76-77	600	6,28	25,48	28,66	58,92	57,32	1,59
GS191-01PC-8, 6-7	610	6,28	0,00	0,00	1,59	1,59	0,00
GS191-01PC-8, 16-17	620	6,28	337,58	0,00	367,83	358,28	9,55
GS191-01PC-8, 26-27	630	6,28	606,69	0,00	632,17	613,06	19,11
GS191-01PC-8, 36-37	640	6,28	996,82	1,59	1079,62	1071,66	7,96
GS191-01PC-8, 46-47	650	6,28	894,90	1,59	942,68	923,57	19,11
GS191-01PC-8, 56-57	660	6,28	85,99	0,00	85,99	85,99	0,00
GS191-01PC-8, 66-67	670	6,28	200,64	1,59	226,11	216,56	9,55
GS191-01PC-9, 0-1	680	6,28	213,38	9,55	242,04	226,11	15,92
GS191-01PC-9, 10-11	690	6,28	60,51	0,00	62,10	60,51	1,59
GS191-01PC-9, 20-21	700	6,28	773,89	74,84	899,68	871,02	28,66
GS191-01PC-9, 30-31	710	6,28	428,34	6,37	455,41	439,49	15,92
GS191-01PC-9, 40-41	720	6,28	313,69	0,00	329,62	318,47	11,15
GS191-01PC-9, 50-51	730	6,28	78,03	1,59	84,39	81,21	3,18
GS191-01PC-9, 60-61	740	6,28	57,32	0,00	63,69	57,32	6,37
GS191-01PC-9, 70-71	750	6,28	111,46	17,52	154,46	138,54	15,92
GS191-01PC-9, 80-81	760	6,28	0,00	0,00	1,59	0,00	1,59
GS191-01PC-9, 90-91	770	6,28	6,37	0,00	7,96	6,37	1,59
GS191-01PC-10, 0-1	780	6,28	1,59	0,00	3,18	1,59	1,59

GS191-01PC-10, 10-11	790	6,28	6,37	0,00	15,92	11,15	4,78
GS191-01PC-10, 20-21	800	6,28	3,18	1,59	9,55	6,37	3,18
GS191-01PC-10, 30-31	810	6,28	11,15	6,37	22,29	19,11	3,18
GS191-01PC-10, 40-41	820	6,28	46,18	36,62	87,58	84,39	3,18
GS191-01PC-10, 50-51	830	6,28	1,59	0,00	4,78	1,59	3,18
GS191-01PC-10, 60-61	840	6,28	1,59	0,00	9,55	3,18	6,37
GS191-01PC-10, 70-71	850	6,28	4,78	0,00	7,96	4,78	3,18
GS191-01PC-10, 80-81	860	6,28	0,00	0,00	1,59	0,00	1,59
GS191-01PC-11, 0-1	870	6,28	4,78	0,00	6,37	4,78	1,59
GS191-01PC-11, 10-11	880	6,28	103,50	0,00	119,43	106,69	12,74
GS191-01PC-11, 20-21	890	6,28	3,18	0,00	3,18	3,18	0,00
GS191-01PC-11, 30-31	900	6,28	160,83	0,00	187,90	164,01	23,89
GS191-01PC-11, 40-41	910	6,28	84,39	3,18	132,17	89,17	42,99
GS191-01PC-11, 50-51	920	6,28	6,37	0,00	14,33	6,37	7,96
GS191-01PC-11, 60-61	930	6,28	71,66	4,78	143,31	81,21	62,10
GS191-01PC-11, 70-71	940	6,28	46,18	0,00	68,47	49,36	19,11
GS191-01PC-11, 80-81	950	6,28	296,18	6,37	399,68	315,29	84,39
GS191-01PC-11, 90-91	960	6,28	495,22	7,96	633,76	515,92	117,83
GS191-01PC-12, 0-1	970	6,28	89,17	11,15	162,42	105,10	57,32
GS191-01PC-12, 10-11	980	6,28	128,98	6,37	328,03	156,05	171,97
GS191-01PC-12, 20-21	990	6,28	38,22	0,00	63,69	42,99	20,70
GS191-01PC-12, 30-31	1000	6,28	109,87	9,55	222,93	128,98	93,95

GS191-01PC-12, 40-41	1010	6,28	35,03	0,00	73,25	38,22	35,03
GS191-01PC-12, 50-51	1020	6,28	62,10	0,00	100,32	62,10	38,22
GS191-01PC-12, 60-61	1030	6,28	20,70	1,59	78,03	27,07	50,96
GS191-01PC-12, 70-71	1040	6,28	439,49	0,00	523,89	460,19	63,69
GS191-01PC-12, 80-81	1050	6,28	27,07	3,18	70,06	38,22	31,85
GS191-01PC-12, 90-91	1060	6,28	0,00	0,00	1,59	0,00	1,59
GS191-01PC-13, 0-1	1070	6,28	1,59	1,59	3,18	3,18	0,00
GS191-01PC-13, 10-11	1080	6,28	0,00	0,00	1,59	0,00	1,59
GS191-01PC-13, 20-21	1090	6,28	0,00	1,59	1,59	1,59	0,00
GS191-01PC-13, 30-31	1100	6,28	1,59	0,00	6,37	1,59	4,78
GS191-01PC-13, 40-41	1110	6,28	6,37	0,00	11,15	6,37	4,78
GS191-01PC-13, 52-53	1122	6,28	552,55	1,59	635,35	570,06	65,29
GS191-01PC-13, 60-61	1130	6,28	108,28	6,37	273,89	132,17	141,72
GS191-01PC-13, 70-71	1140	6,28	78,03	0,00	186,31	89,17	97,13
GS191-01PC-13, 80-81	1150	6,28	68,47	3,18	138,54	76,43	62,10
GS191-01PC-13, 90-91	1160	6,28	152,87	3,18	211,78	162,42	49,36
GS191-01PC-14, 0-1	1170	6,28	238,85	0,00	312,10	240,45	71,66
GS191-01PC-14, 10-11	1180	6,28	474,52	0,00	525,48	476,11	49,36
GS191-01PC-14, 20-21	1190	6,28	673,57	0,00	721,34	676,75	44,59
GS191-01PC-14, 30-31	1200	6,28	14,33	0,00	35,03	17,52	17,52
GS191-01PC-14, 40-41	1210	6,28	12,74	0,00	17,52	12,74	4,78
GS191-01PC-14, 50-51	1220	6,28	0,00	0,00	0,00	0,00	0,00

GS191-01PC-14, 60-61	1230	6,28	157,64	0,00	175,16	160,83	14,33
GS191-01PC-14, 70-71	1240	6,28	4,78	0,00	7,96	4,78	3,18
GS191-01PC-14, 80-81	1250	6,28	33,44	0,00	54,14	41,40	12,74
GS191-01PC-14, 90-91	1260	6,28	105,10	0,00	117,83	106,69	11,15
GS191-01PC-15, 0-1	1270	6,28	159,24	1,59	175,16	162,42	12,74
GS191-01PC-15, 10-11	1280	6,28	640,13	1,59	665,61	649,68	15,92
GS191-01PC-15, 20-21	1290	6,28	44,59	0,00	47,77	46,18	1,59
GS191-01PC-15, 30-31	1300	6,28	0,00	0,00	0,00	0,00	0,00
GS191-01PC-15, 40-41	1310	6,28	1,59	0,00	3,18	1,59	1,59
GS191-01PC-15, 50-51	1320	6,28	17,52	0,00	17,52	17,52	0,00
GS191-01PC-15, 60-61	1330	6,28	9,55	0,00	23,89	11,15	12,74
GS191-01PC-15, 70-71	1340	6,28	79,62	0,00	85,99	79,62	6,37
GS191-01PC-15, 80-81	1350	6,28	12,74	0,00	15,92	14,33	1,59
GS191-01PC-15, 90-91	1360	6,28	140,13	0,00	149,68	143,31	6,37
GS191-01PC-16, 0-1	1370	6,28	0,00	0,00	1,59	0,00	1,59
GS191-01PC-16, 10-11	1380	6,28	3,18	0,00	7,96	3,18	4,78
GS191-01PC-16, 20-21	1390	6,28	30,25	0,00	47,77	35,03	12,74
GS191-01PC-16, 30-31	1400	6,28	359,87	0,00	417,20	375,80	41,40
GS191-01PC-16, 40-41	1410	6,28	7,96	0,00	11,15	7,96	3,18
GS191-01PC-16, 50-51	1420	6,28	63,69	0,00	82,80	63,69	19,11
GS191-01PC-16, 60-61	1430	6,28	38,22	0,00	49,36	39,81	9,55
GS191-01PC-16, 70-71	1440	6,28	156,05	1,59	192,68	179,94	12,74

GS191-01PC-16, 80-81	1450	6,28	78,03	0,00	106,69	85,99	20,70
GS191-01PC-17, 0-1	1460	6,28	1,59	0,00	3,18	1,59	1,59
GS191-01PC-17, 10-11	1470	6,28	44,59	0,00	50,96	46,18	4,78
GS191-01PC-17, 20-21	1480	6,28	71,66	0,00	73,25	71,66	1,59
GS191-01PC-17, 30-31	1490	6,28	84,39	0,00	100,32	85,99	14,33
GS191-01PC-17, 40-41	1500	6,28	304,14	6,37	363,06	339,17	23,89
GS191-01PC-17, 50-51	1510	6,28	0,00	0,00	0,00	0,00	0,00
GS191-01PC-17, 60-61	1520	6,28	68,47	0,00	76,43	68,47	7,96
GS191-01PC-17, 70-71	1530	6,28	128,98	1,59	148,09	136,94	11,15
GS191-01PC-17, 80-81	1540	6,28	222,93	4,78	254,78	240,45	14,33
GS191-01PC-17, 90-91	1550	6,28	1246,82	3,18	1342,36	1307,32	35,03
GS191-01PC-18, 0-1	1560	6,28	3,18	0,00	14,33	3,18	11,15
GS191-01PC-18, 10-11	1570	6,28	70,06	0,00	89,17	73,25	15,92
GS191-01PC-18, 20-21	1580	6,28	197,45	0,00	243,63	202,23	41,40
GS191-01PC-18, 30-31	1590	6,28	6,37	0,00	6,37	6,37	0,00
GS191-01PC-18, 40-41	1600	6,28	3,18	0,00	3,18	3,18	0,00
GS191-01PC-18, 50-51	1610	6,28	4,78	0,00	4,78	4,78	0,00
GS191-01PC-18, 60-61	1620	6,28	30,25	1,59	35,03	31,85	3,18
GS191-01PC-18, 70-71	1630	6,28	0,00	0,00	0,00	0,00	0,00
GS191-01PC-18, 80-81	1640	6,28	79,62	0,00	93,95	85,99	7,96
GS191-01PC-18, 90-91	1650	6,28	1,59	0,00	1,59	1,59	0,00
GS191-01PC-19, 0-1	1660	6,28	9,55	0,00	12,74	9,55	3,18

GS191-01PC-19, 10-11	1670	6,28	1277,07	0,00	1312,10	1289,81	22,29
GS191-01PC-19, 20-21	1680	6,28	113,06	4,78	151,27	136,94	14,33
GS191-01PC-19, 30-31	1690	6,28	414,01	0,00	468,15	452,23	15,92
GS191-01PC-19, 40-41	1700	6,28	0,00	0,00	0,00	0,00	0,00
GS191-01PC-19, 50-51	1710	6,28	0,00	0,00	0,00	0,00	0,00
GS191-01PC-19, 60-61	1720	6,28	808,92	4,78	843,95	828,03	15,92
GS191-01PC-19, 70-71	1730	6,28	0,00	0,00	0,00	0,00	0,00
GS191-01PC-19, 80-81	1740	6,28	493,63	1,59	511,15	504,78	6,37
GS191-01PC-19, 90-91	1750	6,28	242,04	9,55	277,07	275,48	1,59
GS191-01PC-20, 0-1	1760	6,28	4,78	0,00	4,78	4,78	0,00
GS191-01PC-20, 10-11	1770	6,28	71,66	0,00	79,62	74,84	4,78
GS191-01PC-20, 20-21	1780	6,28	71,66	0,00	84,39	79,62	4,78
GS191-01PC-20, 30-31	1790	6,28	11,15	0,00	12,74	11,15	1,59
GS191-01PC-20, 40-41	1800	6,28	27,07	1,59	33,44	33,44	0,00
GS191-01PC-20, 50-51	1810	6,28	17,52	0,00	23,89	17,52	6,37
GS191-01PC-20, 60-61	1820	6,28	84,39	0,00	92,36	90,76	1,59
GS191-01PC-20, 70-71	1830	6,28	12,74	0,00	14,33	12,74	1,59
GS191-01PC-20, 80-81	1840	6,28	0,00	0,00	1,59	0,00	1,59
GS191-01PC-20, 90-91	1850	6,28	1,59	0,00	7,96	1,59	6,37
GS191-01PC-21, 0-1	1860	6,28	0,00	0,00	0,00	0,00	0,00
GS191-01PC-21, 10-11	1870	6,28	0,00	0,00	0,00	0,00	0,00
GS191-01PC-21, 20-21	1880	6,28	42,99	0,00	58,92	50,96	7,96

GS191-01PC-21, 30-31	1890	6,28	273,89	0,00	297,77	288,22	9,55
GS191-01PC-21, 40-41	1900	6,28	0,00	0,00	0,00	0,00	0,00
GS191-01PC-21, 50-51	1910	6,28	0,00	0,00	1,59	0,00	1,59
GS191-01PC-21, 60-61	1920	6,28	0,00	0,00	1,59	0,00	1,59
GS191-01PC-21, 70-71	1930	6,28	0,00	0,00	0,00	0,00	0,00
GS191-01PC-21, 80-81	1940	6,28	38,22	0,00	92,36	54,14	38,22
GS191-01PC-21, 90-91	1950	6,28	100,32	1,59	140,13	135,35	4,78
GS191-01PC-21, 99-100	1960	6,28	557,32	38,22	1101,91	1089,17	12,74

Sample	Depth (cm)	% *B. bigelowii*	% *C. leptoporus*	% *C. pel. braarudi*	% *C. pel. pelagicus*	% *E. huxleyi* < 4 µm	% *E. huxleyi* > 4µm	% *G. caribbeanica*	% *G. muellerae*	% *G. oceanica*	% *H. carteri*	% Reworked Cenozoic	% Reworked Cretaceous	% Small *Gephyrocapsa* spp. (<3 µm)	% *Syracosphaera* spp.	% *Thoracosphaera* spp.
GS191-01PC-1, 0-1	0	0,00	1,13	0,12	43,97	53,92	0,02	0,00	0,02	0,14	0,00	0,19	0,12	0,19	0,12	0,07
GS191-01PC-1, 10-11	10	0,03	1,42	0,12	59,49	37,68	0,38	0,00	0,00	0,21	0,00	0,09	0,16	0,10	0,09	0,24
GS191-01PC-1, 20-21	20	0,00	1,18	0,06	44,16	53,55	0,03	0,00	0,00	0,10	0,00	0,10	0,29	0,06	0,22	0,25
GS191-01PC-1, 30-31	30	0,00	1,80	0,07	41,40	55,77	0,07	0,00	0,02	0,20	0,00	0,00	0,13	0,15	0,23	0,18
GS191-01PC-2, 6-7	40	0,00	3,06	0,06	44,62	51,30	0,11	0,00	0,03	0,30	0,00	0,06	0,17	0,00	0,11	0,19
GS191-01PC-2, 16-17	50	0,00	2,91	0,06	35,83	59,64	0,43	0,00	0,00	0,50	0,00	0,12	0,12	0,12	0,00	0,25
GS191-01PC-2, 26-27	60	0,02	3,18	0,17	41,10	54,46	0,16	0,00	0,00	0,37	0,00	0,02	0,10	0,05	0,35	0,03
GS191-01PC-2, 36-37	70	0,00	3,52	0,12	36,53	59,02	0,19	0,00	0,00	0,22	0,00	0,03	0,22	0,00	0,12	0,03
GS191-01PC-2, 46-47	80	0,00	2,05	0,07	40,66	56,51	0,11	0,00	0,00	0,14	0,00	0,04	0,07	0,11	0,18	0,07
GS191-01PC-2, 56-57	90	0,00	1,40	0,08	38,64	58,90	0,08	0,00	0,00	0,25	0,00	0,00	0,25	0,21	0,08	0,12
GS191-01PC-2, 66-67	100	0,00	1,54	0,08	40,05	56,51	0,49	0,00	0,00	0,51	0,03	0,11	0,24	0,08	0,22	0,14
GS191-01PC-2, 76-77	110	0,00	1,19	0,13	39,10	58,40	0,20	0,00	0,00	0,23	0,00	0,07	0,13	0,20	0,23	0,13
GS191-01PC-2, 86-87	120	0,02	1,24	0,25	42,10	55,08	0,22	0,00	0,00	0,35	0,02	0,00	0,12	0,22	0,17	0,20

GS191-01PC-2, 96-97	130	0,00	0,83	0,00	32,14	65,81	0,09	0,00	0,00	0,22	0,04	0,00	0,13	0,17	0,35	0,22
GS191-01PC-3, 6-7	140	0,00	1,10	0,11	30,56	67,13	0,55	0,00	0,00	0,33	0,00	0,03	0,06	0,03	0,08	0,03
GS191-01PC-3, 16-17	150	0,00	0,32	0,25	30,63	67,25	0,57	0,00	0,00	0,39	0,00	0,00	0,14	0,00	0,32	0,11
GS191-01PC-3, 26-27	160	0,00	1,12	0,00	46,32	51,49	0,09	0,00	0,00	0,26	0,00	0,00	0,30	0,04	0,30	0,09
GS191-01PC-3, 36-37	170	0,00	1,76	0,20	54,57	42,54	0,15	0,00	0,00	0,18	0,00	0,00	0,33	0,00	0,13	0,15
GS191-01PC-3, 46-47	180	0,00	1,49	0,00	44,77	52,29	0,51	0,00	0,00	0,19	0,00	0,09	0,23	0,19	0,09	0,14
GS191-01PC-3, 56-57	190	0,00	1,64	0,02	50,30	47,20	0,30	0,00	0,00	0,08	0,00	0,06	0,20	0,00	0,04	0,14
GS191-01PC-3, 66-67	200	0,00	2,16	0,00	41,38	55,55	0,23	0,00	0,00	0,23	0,00	0,11	0,11	0,00	0,06	0,17
GS191-01PC-3, 76-77	210	0,00	1,90	0,06	32,42	63,73	0,52	0,00	0,00	0,50	0,00	0,03	0,25	0,41	0,06	0,14
GS191-01PC-3, 86-87	220	0,00	2,68	0,00	35,36	60,30	0,43	0,00	0,00	0,29	0,00	0,10	0,10	0,57	0,10	0,10
GS191-01PC-3, 96-97	230	0,00	1,39	0,04	39,17	57,88	0,51	0,00	0,00	0,36	0,00	0,04	0,11	0,15	0,15	0,22
GS191-01PC-4, 6-7	240	0,00	1,83	0,08	31,19	65,39	0,50	0,00	0,00	0,17	0,00	0,00	0,08	0,25	0,17	0,33
GS191-01PC-4, 16-17	250	0,00	2,42	0,00	35,92	60,18	0,39	0,00	0,00	0,26	0,00	0,00	0,03	0,13	0,26	0,42
GS191-01PC-4, 26-27	260	0,00	1,01	0,31	44,47	51,37	1,01	0,00	0,00	0,87	0,00	0,09	0,28	0,21	0,07	0,31
GS191-01PC-4, 36-37	270	0,00	1,09	0,00	32,07	64,92	0,27	0,00	0,00	1,27	0,00	0,00	0,09	0,00	0,23	0,05
GS191-01PC-4, 46-47	280	0,00	1,07	0,14	49,92	46,68	0,19	0,00	0,00	1,44	0,00	0,05	0,17	0,00	0,16	0,19
GS191-01PC-4, 56-57	290	0,00	0,99	0,03	35,92	60,87	0,19	0,00	0,00	1,60	0,00	0,06	0,12	0,00	0,09	0,12
GS191-01PC-4, 66-67	300	0,00	1,19	0,19	38,38	56,48	0,11	0,00	0,00	3,30	0,00	0,04	0,17	0,02	0,06	0,06
GS191-01PC-4, 76-77	310	0,00	1,38	0,03	31,19	62,72	0,08	0,00	0,00	3,99	0,00	0,11	0,21	0,00	0,08	0,21
GS191-01PC-4, 86-87	320	0,00	1,74	0,00	32,14	58,85	0,11	0,00	0,00	6,30	0,00	0,11	0,54	0,00	0,11	0,11
GS191-01PC-5, 6-7	330	0,00	2,81	0,17	31,95	59,00	0,34	0,00	0,00	5,14	0,00	0,00	0,45	0,00	0,07	0,07
GS191-01PC-5, 16-17	340	0,00	3,22	0,51	40,08	48,67	0,08	0,00	0,00	6,81	0,00	0,08	0,11	0,00	0,11	0,31

GS191-01PC-5, 26-27	350	0,00	2,51	0,23	39,47	48,34	0,12	0,00	0,00	8,85	0,00	0,02	0,28	0,00	0,12	0,07
GS191-01PC-5, 36-37	360	0,00	2,18	0,26	31,70	54,37	0,63	0,00	0,00	10,03	0,00	0,03	0,30	0,03	0,33	0,13
GS191-01PC-5, 46-47	370	0,00	2,79	0,26	39,93	50,67	0,15	0,00	0,00	5,65	0,00	0,02	0,22	0,00	0,04	0,26
GS191-01PC-5, 56-57	380	0,00	3,20	0,20	26,03	63,78	0,24	0,00	0,00	6,32	0,00	0,04	0,04	0,00	0,12	0,04
GS191-01PC-5, 66-67	390	0,00	2,93	0,13	30,65	54,90	0,11	0,00	0,00	10,52	0,00	0,05	0,24	0,00	0,24	0,24
GS191-01PC-5, 76-77	400	0,00	1,92	0,06	32,27	54,85	0,27	0,00	0,00	10,30	0,00	0,00	0,21	0,00	0,06	0,06
GS191-01PC-5, 86-87	410	0,00	2,10	0,09	33,66	53,77	0,15	0,00	0,00	9,69	0,00	0,04	0,26	0,00	0,17	0,07
GS191-01PC-5, 96-97	420	0,00	2,19	0,12	29,09	59,18	0,15	0,00	0,00	8,88	0,05	0,00	0,15	0,00	0,07	0,12
GS191-01PC-6, 6-7	430	0,00	1,59	0,11	18,84	66,07	0,03	0,00	0,00	12,48	0,00	0,03	0,38	0,00	0,38	0,08
GS191-01PC-6, 16-17	440	0,00	1,22	0,09	18,76	71,04	0,09	0,00	0,00	8,23	0,00	0,05	0,38	0,00	0,05	0,09
GS191-01PC-6, 26-27	450	0,00	0,90	0,15	17,53	70,18	0,00	0,00	0,00	10,54	0,00	0,05	0,30	0,00	0,05	0,30
GS191-01PC-6, 36-37	460	0,00	1,31	0,00	5,86	82,00	0,09	0,00	0,00	9,92	0,00	0,14	0,45	0,00	0,00	0,23
GS191-01PC-6, 46-47	470	0,00	1,28	0,00	5,51	81,73	0,05	0,00	0,00	10,77	0,00	0,05	0,31	0,05	0,20	0,05
GS191-01PC-6, 56-57	480	0,00	2,18	0,00	1,75	89,96	0,00	0,00	0,00	4,80	0,00	0,22	0,66	0,00	0,00	0,44
GS191-01PC-6, 66-67	490	0,00	2,39	0,00	0,37	92,28	0,18	0,00	0,00	3,49	0,00	0,37	0,92	0,00	0,00	0,00
GS191-01PC-6, 76-77	500	0,00	2,94	0,00	0,32	92,33	0,00	0,00	0,00	3,68	0,00	0,11	0,42	0,00	0,00	0,21
GS191-01PC-6, 86-87	510	0,00	2,68	0,00	0,13	89,41	0,00	0,00	0,00	7,15	0,00	0,00	0,38	0,00	0,17	0,09
GS191-01PC-6, 96-97	520	0,00	3,02	0,00	0,37	88,10	0,00	0,00	0,00	7,69	0,00	0,00	0,64	0,00	0,00	0,18
GS191-01PC-7, 6-7	530	0,00	5,10	0,00	0,23	85,38	0,00	0,00	0,00	8,12	0,00	0,00	0,93	0,00	0,23	0,00
GS191-01PC-7, 16-17	540	0,00	3,47	0,00	0,00	89,13	0,00	0,00	0,00	6,36	0,00	0,00	0,81	0,00	0,00	0,23
GS191-01PC-7, 26-27	550	0,00	1,49	0,00	19,80	76,24	0,00	0,00	0,00	1,49	0,00	0,00	0,00	0,00	0,00	0,99
GS191-01PC-7, 36-37	560	0,00	0,00	0,00	0,00	80,00	0,00	0,00	0,00	0,00	0,00	0,00	0,00	0,00	0,00	20,00

GS191-01PC-7, 46-47	570	0,00	1,67	0,00	1,67	86,67	0,00	0,00	0,00	0,00	0,00	1,67	1,67	0,00	0,00	6,67
GS191-01PC-7, 56-57	580	0,00	0,00	0,00	0,00	94,74	0,00	0,00	0,00	1,75	0,00	0,00	0,00	0,00	0,00	3,51
GS191-01PC-7, 66-67	590	0,00	0,00	0,00	4,17	79,17	0,00	0,00	0,00	0,00	0,00	0,00	12,50	0,00	0,00	4,17
GS191-01PC-7, 76-77	600	0,00	2,70	0,00	48,65	43,24	0,00	0,00	0,00	0,00	0,00	0,00	2,70	0,00	2,70	0,00
GS191-01PC-8, 6-7	610	0,00	0,00	0,00	0,00	0,00	0,00	0,00	0,00	0,00	0,00	0,00	0,00	0,00	0,00	100,00
GS191-01PC-8, 16-17	620	0,00	2,16	0,00	0,00	90,91	0,87	0,00	0,00	3,46	0,00	0,43	2,16	0,00	0,00	0,00
GS191-01PC-8, 26-27	630	0,00	0,50	0,00	0,00	94,71	1,26	0,00	0,00	0,50	0,00	0,00	3,02	0,00	0,00	0,00
GS191-01PC-8, 36-37	640	0,00	1,18	0,00	0,15	92,33	0,00	0,00	0,29	5,31	0,00	0,00	0,74	0,00	0,00	0,00
GS191-01PC-8, 46-47	650	0,00	0,84	0,00	0,17	94,59	0,34	0,00	0,00	2,03	0,00	0,17	1,86	0,00	0,00	0,00
GS191-01PC-8, 56-57	660	0,00	0,00	0,00	0,00	100,00	0,00	0,00	0,00	0,00	0,00	0,00	0,00	0,00	0,00	0,00
GS191-01PC-8, 66-67	670	0,00	2,11	0,00	0,70	88,73	0,00	0,00	1,41	2,82	0,00	1,41	2,82	0,00	0,00	0,00
GS191-01PC-9, 0-1	680	0,00	0,00	0,00	3,95	87,50	0,66	0,00	0,00	1,32	0,00	1,32	5,26	0,00	0,00	0,00
GS191-01PC-9, 10-11	690	0,00	0,00	0,00	0,00	97,44	0,00	0,00	0,00	0,00	0,00	0,00	2,56	0,00	0,00	0,00
GS191-01PC-9, 20-21	700	0,00	0,53	0,35	7,96	79,65	6,37	0,00	0,00	1,42	0,00	0,00	3,19	0,00	0,18	0,35
GS191-01PC-9, 30-31	710	0,00	0,00	0,00	1,40	94,06	0,00	0,00	0,00	1,05	0,00	0,35	3,15	0,00	0,00	0,00
GS191-01PC-9, 40-41	720	0,00	0,00	0,00	0,00	95,17	0,00	0,00	0,00	0,97	0,00	0,48	2,90	0,00	0,48	0,00
GS191-01PC-9, 50-51	730	0,00	0,00	0,00	1,89	92,45	0,00	0,00	0,00	1,89	0,00	1,89	1,89	0,00	0,00	0,00
GS191-01PC-9, 60-61	740	0,00	0,00	0,00	0,00	90,00	0,00	0,00	0,00	0,00	0,00	2,50	7,50	0,00	0,00	0,00
GS191-01PC-9, 70-71	750	0,00	0,00	0,00	11,34	71,13	1,03	0,00	0,00	4,12	0,00	2,06	8,25	0,00	1,03	1,03
GS191-01PC-9, 80-81	760	0,00	0,00	0,00	0,00	0,00	0,00	0,00	0,00	0,00	0,00	0,00	100,00	0,00	0,00	0,00
GS191-01PC-9, 90-91	770	0,00	0,00	0,00	0,00	80,00	0,00	0,00	0,00	0,00	0,00	0,00	20,00	0,00	0,00	0,00
GS191-01PC-10, 0-1	780	0,00	0,00	0,00	0,00	50,00	0,00	0,00	0,00	0,00	0,00	0,00	50,00	0,00	0,00	0,00

GS191-01PC-10, 10-11	790	0,00	0,00	0,00	0,00	40,00	0,00	0,00	0,00	20,00	0,00	0,00	30,00	10,00	0,00	0,00
GS191-01PC-10, 20-21	800	0,00	0,00	0,00	16,67	33,33	0,00	0,00	0,00	0,00	0,00	0,00	33,33	0,00	0,00	16,67
GS191-01PC-10, 30-31	810	0,00	0,00	0,00	28,57	50,00	0,00	0,00	0,00	0,00	0,00	0,00	14,29	0,00	0,00	7,14
GS191-01PC-10, 40-41	820	0,00	0,00	0,00	41,82	52,73	0,00	0,00	0,00	0,00	0,00	0,00	3,64	0,00	1,82	0,00
GS191-01PC-10, 50-51	830	0,00	0,00	0,00	0,00	33,33	0,00	0,00	0,00	0,00	0,00	0,00	66,67	0,00	0,00	0,00
GS191-01PC-10, 60-61	840	0,00	0,00	0,00	0,00	16,67	0,00	0,00	0,00	16,67	0,00	0,00	66,67	0,00	0,00	0,00
GS191-01PC-10, 70-71	850	0,00	0,00	0,00	0,00	60,00	0,00	0,00	0,00	0,00	0,00	0,00	40,00	0,00	0,00	0,00
GS191-01PC-10, 80-81	860	0,00	0,00	0,00	0,00	0,00	0,00	0,00	0,00	0,00	0,00	0,00	100,00	0,00	0,00	0,00
GS191-01PC-11, 0-1	870	0,00	0,00	0,00	0,00	75,00	0,00	0,00	0,00	0,00	0,00	0,00	25,00	0,00	0,00	0,00
GS191-01PC-11, 10-11	880	0,00	0,00	0,00	0,00	86,67	0,00	0,00	0,00	1,33	0,00	0,00	10,67	0,00	1,33	0,00
GS191-01PC-11, 20-21	890	0,00	0,00	0,00	0,00	100,00	0,00	0,00	0,00	0,00	0,00	0,00	0,00	0,00	0,00	0,00
GS191-01PC-11, 30-31	900	0,00	0,00	0,00	0,00	85,59	0,00	0,00	0,00	0,85	0,00	0,85	11,86	0,00	0,85	0,00
GS191-01PC-11, 40-41	910	0,00	0,00	0,00	2,41	63,86	0,00	0,00	0,00	1,20	0,00	4,82	27,71	0,00	0,00	0,00
GS191-01PC-11, 50-51	920	0,00	0,00	0,00	0,00	44,44	0,00	0,00	0,00	0,00	0,00	11,11	44,44	0,00	0,00	0,00
GS191-01PC-11, 60-61	930	0,00	0,00	0,00	3,33	50,00	0,00	0,00	0,00	1,11	0,00	2,22	41,11	0,00	1,11	1,11
GS191-01PC-11, 70-71	940	0,00	0,00	0,00	0,00	67,44	0,00	0,00	0,00	4,65	0,00	0,00	27,91	0,00	0,00	0,00
GS191-01PC-11, 80-81	950	0,00	0,00	0,00	1,59	74,10	0,00	0,00	0,00	1,99	0,00	1,59	19,52	0,00	1,20	0,00
GS191-01PC-11, 90-91	960	0,00	0,00	0,00	1,26	76,63	1,51	0,00	0,00	1,76	0,00	1,01	17,59	0,00	0,25	0,00
GS191-01PC-12, 0-1	970	0,00	0,00	0,00	6,86	54,90	0,00	0,00	0,00	2,94	0,00	1,96	33,33	0,00	0,00	0,00
GS191-01PC-12, 10-11	980	0,00	0,00	0,49	1,46	39,32	0,00	0,00	0,00	6,31	0,00	1,94	50,49	0,00	0,00	0,00
GS191-01PC-12, 20-21	990	0,00	0,00	0,00	0,00	60,00	0,00	0,00	0,00	7,50	0,00	0,00	32,50	0,00	0,00	0,00
GS191-01PC-12, 30-31	1000	0,00	0,00	0,71	3,57	49,29	0,00	0,00	0,00	3,57	0,00	2,14	40,00	0,00	0,00	0,71

GS191-01PC-12, 40-41	1010	0,00	0,00	0,00	0,00	47,83	0,00	0,00	0,00	4,35	0,00	8,70	39,13	0,00	0,00	0,00
GS191-01PC-12, 50-51	1020	0,00	0,00	0,00	0,00	58,73	3,17	0,00	0,00	0,00	0,00	1,59	36,51	0,00	0,00	0,00
GS191-01PC-12, 60-61	1030	0,00	0,00	0,00	2,04	26,53	0,00	0,00	0,00	4,08	0,00	6,12	59,18	0,00	0,00	2,04
GS191-01PC-12, 70-71	1040	0,00	0,00	0,00	0,00	81,16	2,74	0,00	0,00	3,04	0,00	0,00	12,16	0,00	0,61	0,30
GS191-01PC-12, 80-81	1050	0,00	0,00	0,00	4,55	38,64	0,00	0,00	0,00	11,36	0,00	2,27	43,18	0,00	0,00	0,00
GS191-01PC-12, 90-91	1060	0,00	0,00	0,00	0,00	0,00	0,00	0,00	0,00	0,00	0,00	0,00	100,00	0,00	0,00	0,00
GS191-01PC-13, 0-1	1070	0,00	0,00	0,00	50,00	50,00	0,00	0,00	0,00	0,00	0,00	0,00	0,00	0,00	0,00	0,00
GS191-01PC-13, 10-11	1080	0,00	0,00	0,00	0,00	0,00	0,00	0,00	0,00	0,00	0,00	0,00	100,00	0,00	0,00	0,00
GS191-01PC-13, 20-21	1090	0,00	0,00	0,00	100,00	0,00	0,00	0,00	0,00	0,00	0,00	0,00	0,00	0,00	0,00	0,00
GS191-01PC-13, 30-31	1100	0,00	0,00	0,00	0,00	25,00	0,00	0,00	0,00	0,00	0,00	0,00	75,00	0,00	0,00	0,00
GS191-01PC-13, 40-41	1110	0,00	0,00	0,00	0,00	57,14	0,00	0,00	0,00	0,00	0,00	14,29	28,57	0,00	0,00	0,00
GS191-01PC-13, 52-53	1122	0,00	0,50	0,00	0,25	85,96	1,00	0,00	0,00	1,50	0,00	1,00	9,27	0,00	0,50	0,00
GS191-01PC-13, 60-61	1130	0,00	0,00	0,00	2,33	39,53	0,00	0,00	0,00	4,65	0,00	1,16	50,58	0,58	0,00	1,16
GS191-01PC-13, 70-71	1140	0,00	0,00	0,00	0,00	41,03	0,85	0,00	0,00	5,13	0,00	2,56	49,57	0,85	0,00	0,00
GS191-01PC-13, 80-81	1150	0,00	1,15	0,00	2,30	49,43	0,00	0,00	0,00	2,30	0,00	1,15	43,68	0,00	0,00	0,00
GS191-01PC-13, 90-91	1160	0,00	0,00	0,00	1,50	72,18	0,00	0,00	0,00	2,26	0,00	0,75	22,56	0,00	0,75	0,00
GS191-01PC-14, 0-1	1170	0,00	0,00	0,00	0,00	74,49	2,04	0,00	0,00	0,00	0,00	1,02	21,94	0,00	0,00	0,51
GS191-01PC-14, 10-11	1180	0,00	0,00	0,00	0,00	90,30	0,00	0,00	0,00	0,30	0,00	0,00	9,39	0,00	0,00	0,00
GS191-01PC-14, 20-21	1190	0,00	0,00	0,00	0,00	92,72	0,66	0,00	0,00	0,00	0,00	0,44	5,74	0,22	0,22	0,00
GS191-01PC-14, 30-31	1200	0,00	0,00	0,00	0,00	40,91	0,00	0,00	0,00	9,09	0,00	4,55	45,45	0,00	0,00	0,00
GS191-01PC-14, 40-41	1210	0,00	0,00	0,00	0,00	72,73	0,00	0,00	0,00	0,00	0,00	0,00	27,27	0,00	0,00	0,00
GS191-01PC-14, 50-51	1220	0,00	0,00	0,00	0,00	0,00	0,00	0,00	0,00	0,00	0,00	0,00	0,00	0,00	0,00	0,00

GS191-01PC-14, 60-61	1230	0,00	0,91	0,00	0,00	89,09	0,91	0,00	0,00	0,91	0,00	0,00	8,18	0,00	0,00	0,00
GS191-01PC-14, 70-71	1240	0,00	0,00	0,00	0,00	60,00	0,00	0,00	0,00	0,00	0,00	0,00	40,00	0,00	0,00	0,00
GS191-01PC-14, 80-81	1250	0,00	5,88	0,00	0,00	61,76	0,00	0,00	0,00	8,82	0,00	0,00	23,53	0,00	0,00	0,00
GS191-01PC-14, 90-91	1260	0,00	0,00	0,00	0,00	87,84	1,35	0,00	0,00	1,35	0,00	0,00	9,46	0,00	0,00	0,00
GS191-01PC-15, 0-1	1270	0,00	0,91	0,00	0,91	90,00	0,91	0,00	0,00	0,00	0,00	0,91	6,36	0,00	0,00	0,00
GS191-01PC-15, 10-11	1280	0,00	0,48	0,00	0,24	96,17	0,00	0,00	0,00	0,48	0,00	0,00	2,39	0,00	0,00	0,24
GS191-01PC-15, 20-21	1290	0,00	0,00	0,00	0,00	93,33	0,00	0,00	0,00	0,00	0,00	0,00	3,33	0,00	0,00	3,33
GS191-01PC-15, 30-31	1300	0,00	0,00	0,00	0,00	0,00	0,00	0,00	0,00	0,00	0,00	0,00	0,00	0,00	0,00	0,00
GS191-01PC-15, 40-41	1310	0,00	0,00	0,00	0,00	50,00	0,00	0,00	0,00	0,00	0,00	0,00	50,00	0,00	0,00	0,00
GS191-01PC-15, 50-51	1320	0,00	0,00	0,00	0,00	100,00	0,00	0,00	0,00	0,00	0,00	0,00	0,00	0,00	0,00	0,00
GS191-01PC-15, 60-61	1330	0,00	0,00	0,00	0,00	40,00	0,00	0,00	0,00	0,00	0,00	0,00	53,33	0,00	0,00	6,67
GS191-01PC-15, 70-71	1340	0,00	0,00	0,00	0,00	92,59	0,00	0,00	0,00	0,00	0,00	0,00	7,41	0,00	0,00	0,00
GS191-01PC-15, 80-81	1350	0,00	0,00	0,00	0,00	80,00	0,00	0,00	0,00	10,00	0,00	0,00	10,00	0,00	0,00	0,00
GS191-01PC-15, 90-91	1360	0,00	1,06	0,00	0,00	93,62	0,00	0,00	0,00	0,00	0,00	0,00	4,26	0,00	0,00	1,06
GS191-01PC-16, 0-1	1370	0,00	0,00	0,00	0,00	0,00	0,00	0,00	0,00	0,00	0,00	100,00	0,00	0,00	0,00	0,00
GS191-01PC-16, 10-11	1380	0,00	0,00	0,00	0,00	40,00	0,00	0,00	0,00	0,00	0,00	0,00	60,00	0,00	0,00	0,00
GS191-01PC-16, 20-21	1390	0,00	0,00	0,00	0,00	63,33	0,00	0,00	0,00	10,00	0,00	3,33	23,33	0,00	0,00	0,00
GS191-01PC-16, 30-31	1400	0,00	0,00	0,00	0,00	85,88	0,38	0,00	0,00	3,82	0,00	0,00	9,92	0,00	0,00	0,00
GS191-01PC-16, 40-41	1410	0,00	0,00	0,00	0,00	71,43	0,00	0,00	0,00	0,00	0,00	0,00	28,57	0,00	0,00	0,00
GS191-01PC-16, 50-51	1420	0,00	0,00	0,00	0,00	76,92	0,00	0,00	0,00	0,00	0,00	1,92	21,15	0,00	0,00	0,00
GS191-01PC-16, 60-61	1430	0,00	3,23	0,00	0,00	77,42	0,00	0,00	0,00	0,00	0,00	0,00	19,35	0,00	0,00	0,00
GS191-01PC-16, 70-71	1440	0,00	0,00	0,83	0,00	80,99	0,00	0,00	0,00	10,74	0,00	0,00	6,61	0,83	0,00	0,00

GS191-01PC-16, 80-81	1450	0,00	0,00	0,00	0,00	73,13	0,00	0,00	0,00	5,97	0,00	2,99	16,42	1,49	0,00	0,00
GS191-01PC-17, 0-1	1460	0,00	0,00	0,00	0,00	50,00	0,00	0,00	0,00	0,00	0,00	0,00	50,00	0,00	0,00	0,00
GS191-01PC-17, 10-11	1470	0,00	0,00	0,00	0,00	84,38	3,13	0,00	0,00	3,13	0,00	0,00	9,38	0,00	0,00	0,00
GS191-01PC-17, 20-21	1480	0,00	0,00	0,00	0,00	97,83	0,00	0,00	0,00	0,00	0,00	0,00	2,17	0,00	0,00	0,00
GS191-01PC-17, 30-31	1490	0,00	0,00	0,00	0,00	80,95	3,17	0,00	0,00	1,59	0,00	0,00	14,29	0,00	0,00	0,00
GS191-01PC-17, 40-41	1500	0,00	0,44	0,44	1,32	83,33	0,44	0,00	0,00	7,46	0,00	0,00	6,58	0,00	0,00	0,00
GS191-01PC-17, 50-51	1510	0,00	0,00	0,00	0,00	0,00	0,00	0,00	0,00	0,00	0,00	0,00	0,00	0,00	0,00	0,00
GS191-01PC-17, 60-61	1520	0,00	0,00	0,00	0,00	89,58	0,00	0,00	0,00	0,00	0,00	0,00	10,42	0,00	0,00	0,00
GS191-01PC-17, 70-71	1530	0,00	1,08	0,00	1,08	87,10	0,00	0,00	0,00	3,23	0,00	0,00	7,53	0,00	0,00	0,00
GS191-01PC-17, 80-81	1540	0,00	0,00	0,00	1,88	85,63	1,88	0,00	0,00	5,00	0,00	0,00	5,63	0,00	0,00	0,00
GS191-01PC-17, 90-91	1550	0,00	0,00	0,24	0,00	91,81	1,07	0,00	0,12	3,80	0,00	0,00	2,61	0,00	0,00	0,36
GS191-01PC-18, 0-1	1560	0,00	0,00	0,00	0,00	22,22	0,00	0,00	0,00	0,00	0,00	0,00	77,78	0,00	0,00	0,00
GS191-01PC-18, 10-11	1570	0,00	0,00	0,00	0,00	76,79	1,79	0,00	0,00	3,57	0,00	0,00	17,86	0,00	0,00	0,00
GS191-01PC-18, 20-21	1580	0,00	0,00	0,00	0,00	80,39	0,65	0,00	0,00	1,31	0,00	0,65	16,34	0,00	0,65	0,00
GS191-01PC-18, 30-31	1590	0,00	0,00	0,00	0,00	100,00	0,00	0,00	0,00	0,00	0,00	0,00	0,00	0,00	0,00	0,00
GS191-01PC-18, 40-41	1600	0,00	0,00	0,00	0,00	100,00	0,00	0,00	0,00	0,00	0,00	0,00	0,00	0,00	0,00	0,00
GS191-01PC-18, 50-51	1610	0,00	0,00	0,00	0,00	100,00	0,00	0,00	0,00	0,00	0,00	0,00	0,00	0,00	0,00	0,00
GS191-01PC-18, 60-61	1620	0,00	0,00	0,00	4,55	86,36	0,00	0,00	0,00	0,00	0,00	4,55	4,55	0,00	0,00	0,00
GS191-01PC-18, 70-71	1630	0,00	0,00	0,00	0,00	0,00	0,00	0,00	0,00	0,00	0,00	0,00	0,00	0,00	0,00	0,00
GS191-01PC-18, 80-81	1640	0,00	0,00	0,00	0,00	84,75	0,00	0,00	0,00	6,78	0,00	5,08	3,39	0,00	0,00	0,00
GS191-01PC-18, 90-91	1650	0,00	0,00	0,00	0,00	100,00	0,00	0,00	0,00	0,00	0,00	0,00	0,00	0,00	0,00	0,00
GS191-01PC-19, 0-1	1660	0,00	0,00	0,00	0,00	75,00	0,00	0,00	0,00	0,00	0,00	12,50	12,50	0,00	0,00	0,00

GS191-01PC-19, 10-11	1670	0,00	0,00	0,00	0,00	97,09	0,24	0,00	0,00	0,85	0,00	0,24	1,46	0,00	0,00	0,12
GS191-01PC-19, 20-21	1680	0,00	1,05	2,11	1,05	74,74	0,00	1,05	0,00	10,53	0,00	1,05	8,42	0,00	0,00	0,00
GS191-01PC-19, 30-31	1690	0,00	0,34	0,00	0,00	88,10	0,34	0,34	0,00	7,48	0,00	0,00	3,40	0,00	0,00	0,00
GS191-01PC-19, 40-41	1700	0,00	0,00	0,00	0,00	0,00	0,00	0,00	0,00	0,00	0,00	0,00	0,00	0,00	0,00	0,00
GS191-01PC-19, 50-51	1710	0,00	0,00	0,00	0,00	0,00	0,00	0,00	0,00	0,00	0,00	0,00	0,00	0,00	0,00	0,00
GS191-01PC-19, 60-61	1720	0,00	0,19	0,00	0,57	95,66	0,19	0,00	0,00	1,32	0,00	0,38	1,51	0,00	0,19	0,00
GS191-01PC-19, 70-71	1730	0,00	0,00	0,00	0,00	0,00	0,00	0,00	0,00	0,00	0,00	0,00	0,00	0,00	0,00	0,00
GS191-01PC-19, 80-81	1740	0,00	0,00	0,31	0,00	95,95	0,62	0,00	0,00	0,93	0,00	0,00	1,25	0,00	0,00	0,93
GS191-01PC-19, 90-91	1750	0,00	0,00	0,00	3,45	87,36	0,00	0,00	0,00	8,05	0,00	0,57	0,00	0,00	0,00	0,57
GS191-01PC-20, 0-1	1760	0,00	0,00	0,00	0,00	100,00	0,00	0,00	0,00	0,00	0,00	0,00	0,00	0,00	0,00	0,00
GS191-01PC-20, 10-11	1770	0,00	0,00	0,00	0,00	90,00	0,00	0,00	0,00	4,00	0,00	2,00	4,00	0,00	0,00	0,00
GS191-01PC-20, 20-21	1780	0,00	0,00	0,00	0,00	81,13	3,77	0,00	0,00	9,43	0,00	0,00	5,66	0,00	0,00	0,00
GS191-01PC-20, 30-31	1790	0,00	0,00	0,00	0,00	87,50	0,00	0,00	0,00	0,00	0,00	0,00	12,50	0,00	0,00	0,00
GS191-01PC-20, 40-41	1800	0,00	0,00	4,76	0,00	80,95	0,00	0,00	0,00	14,29	0,00	0,00	0,00	0,00	0,00	0,00
GS191-01PC-20, 50-51	1810	0,00	0,00	0,00	0,00	73,33	0,00	0,00	0,00	0,00	0,00	0,00	26,67	0,00	0,00	0,00
GS191-01PC-20, 60-61	1820	0,00	0,00	0,00	0,00	89,66	1,72	0,00	0,00	6,90	0,00	0,00	1,72	0,00	0,00	0,00
GS191-01PC-20, 70-71	1830	0,00	0,00	0,00	0,00	88,89	0,00	0,00	0,00	0,00	0,00	0,00	11,11	0,00	0,00	0,00
GS191-01PC-20, 80-81	1840	0,00	0,00	0,00	0,00	0,00	0,00	0,00	0,00	0,00	0,00	0,00	100,00	0,00	0,00	0,00
GS191-01PC-20, 90-91	1850	0,00	0,00	0,00	0,00	20,00	0,00	0,00	0,00	0,00	0,00	0,00	80,00	0,00	0,00	0,00
GS191-01PC-21, 0-1	1860	0,00	0,00	0,00	0,00	0,00	0,00	0,00	0,00	0,00	0,00	0,00	0,00	0,00	0,00	0,00
GS191-01PC-21, 10-11	1870	0,00	0,00	0,00	0,00	0,00	0,00	0,00	0,00	0,00	0,00	0,00	0,00	0,00	0,00	0,00
GS191-01PC-21, 20-21	1880	0,00	0,00	0,00	0,00	67,57	5,41	0,00	0,00	13,51	0,00	2,70	10,81	0,00	0,00	0,00

GS191-01PC-21, 30-31	1890	0,00	0,00	0,00	0,00	91,44	0,53	0,00	0,00	4,28	0,00	0,00	3,21	0,00	0,00	0,53
GS191-01PC-21, 40-41	1900	0,00	0,00	0,00	0,00	0,00	0,00	0,00	0,00	0,00	0,00	0,00	0,00	0,00	0,00	0,00
GS191-01PC-21, 50-51	1910	0,00	0,00	0,00	0,00	0,00	0,00	0,00	0,00	0,00	0,00	0,00	100,00	0,00	0,00	0,00
GS191-01PC-21, 60-61	1920	0,00	0,00	0,00	0,00	0,00	0,00	0,00	0,00	0,00	0,00	0,00	100,00	0,00	0,00	0,00
GS191-01PC-21, 70-71	1930	0,00	0,00	0,00	0,00	0,00	0,00	0,00	0,00	0,00	0,00	0,00	0,00	0,00	0,00	0,00
GS191-01PC-21, 80-81	1940	0,00	0,00	0,00	0,00	41,38	0,00	0,00	0,00	17,24	0,00	6,90	34,48	0,00	0,00	0,00
GS191-01PC-21, 90-91	1950	0,00	0,00	0,00	1,14	71,59	0,00	1,14	0,00	22,73	0,00	0,00	3,41	0,00	0,00	0,00
GS191-01PC-21, 99-100	1960	0,00	0,00	0,87	2,60	50,58	0,00	0,00	0,00	44,80	0,00	0,29	0,87	0,00	0,00	0,00

Sample	Depth (cm)	% Total *E. huxleyi*	% Total *C. pelagicus*	% Total abundance (NO reworked)	% Total Reworked
GS191-01PC-1, 0-1	0	53,94	44,09	99,70	0,30
GS191-01PC-1, 10-11	10	38,06	59,61	99,76	0,24
GS191-01PC-1, 20-21	20	53,58	44,23	99,62	0,38
GS191-01PC-1, 30-31	30	55,84	41,47	99,87	0,13
GS191-01PC-2, 6-7	40	51,41	44,67	99,78	0,22
GS191-01PC-2, 16-17	50	60,07	35,90	99,75	0,25
GS191-01PC-2, 26-27	60	54,62	41,28	99,89	0,11
GS191-01PC-2, 36-37	70	59,21	36,65	99,75	0,25
GS191-01PC-2, 46-47	80	56,61	40,74	99,89	0,11
GS191-01PC-2, 56-57	90	58,98	38,72	99,75	0,25
GS191-01PC-2, 66-67	100	57,00	40,13	99,65	0,35
GS191-01PC-2, 76-77	110	58,59	39,23	99,80	0,20
GS191-01PC-2, 86-87	120	55,30	42,35	99,88	0,12

GS191-01PC-2, 96-97	130	65,89	32,14	99,87	0,13
GS191-01PC-3, 6-7	140	67,68	30,67	99,92	0,08
GS191-01PC-3, 16-17	150	67,83	30,88	99,86	0,14
GS191-01PC-3, 26-27	160	51,57	46,32	99,70	0,30
GS191-01PC-3, 36-37	170	42,69	54,77	99,67	0,33
GS191-01PC-3, 46-47	180	52,80	44,77	99,67	0,33
GS191-01PC-3, 56-57	190	47,51	50,32	99,74	0,26
GS191-01PC-3, 66-67	200	55,78	41,38	99,77	0,23
GS191-01PC-3, 76-77	210	64,25	32,47	99,72	0,28
GS191-01PC-3, 86-87	220	60,73	35,36	99,81	0,19
GS191-01PC-3, 96-97	230	58,39	39,20	99,85	0,15
GS191-01PC-4, 6-7	240	65,89	31,28	99,92	0,08
GS191-01PC-4, 16-17	250	60,57	35,92	99,97	0,03
GS191-01PC-4, 26-27	260	52,38	44,78	99,62	0,38
GS191-01PC-4, 36-37	270	65,20	32,07	99,91	0,09
GS191-01PC-4, 46-47	280	46,87	50,06	99,78	0,22
GS191-01PC-4, 56-57	290	61,05	35,95	99,81	0,19
GS191-01PC-4, 66-67	300	56,58	38,57	99,79	0,21
GS191-01PC-4, 76-77	310	62,80	31,21	99,68	0,32
GS191-01PC-4, 86-87	320	58,96	32,14	99,35	0,65
GS191-01PC-5, 6-7	330	59,34	32,12	99,55	0,45
GS191-01PC-5, 16-17	340	48,76	40,59	99,80	0,20

GS191-01PC-5, 26-27	350	48,46	39,70	99,70	0,30
GS191-01PC-5, 36-37	360	55,00	31,97	99,67	0,33
GS191-01PC-5, 46-47	370	50,82	40,19	99,76	0,24
GS191-01PC-5, 56-57	380	64,02	26,22	99,92	0,08
GS191-01PC-5, 66-67	390	55,01	30,78	99,71	0,29
GS191-01PC-5, 76-77	400	55,12	32,33	99,79	0,21
GS191-01PC-5, 86-87	410	53,92	33,75	99,70	0,30
GS191-01PC-5, 96-97	420	59,33	29,21	99,85	0,15
GS191-01PC-6, 6-7	430	66,10	18,95	99,59	0,41
GS191-01PC-6, 16-17	440	71,13	18,85	99,58	0,42
GS191-01PC-6, 26-27	450	70,18	17,68	99,65	0,35
GS191-01PC-6, 36-37	460	82,09	5,86	99,41	0,59
GS191-01PC-6, 46-47	470	81,78	5,51	99,64	0,36
GS191-01PC-6, 56-57	480	89,96	1,75	99,13	0,87
GS191-01PC-6, 66-67	490	92,46	0,37	98,71	1,29
GS191-01PC-6, 76-77	500	92,33	0,32	99,47	0,53
GS191-01PC-6, 86-87	510	89,41	0,13	99,62	0,38
GS191-01PC-6, 96-97	520	88,10	0,37	99,36	0,64
GS191-01PC-7, 6-7	530	85,38	0,23	99,07	0,93
GS191-01PC-7, 16-17	540	89,13	0,00	99,19	0,81
GS191-01PC-7, 26-27	550	76,24	19,80	100,00	0,00
GS191-01PC-7, 36-37	560	80,00	0,00	100,00	0,00

GS191-01PC-7, 46-47	570	86,67	1,67	96,67	3,33
GS191-01PC-7, 56-57	580	94,74	0,00	100,00	0,00
GS191-01PC-7, 66-67	590	79,17	4,17	87,50	12,50
GS191-01PC-7, 76-77	600	43,24	48,65	97,30	2,70
GS191-01PC-8, 6-7	610	0,00	0,00	100,00	0,00
GS191-01PC-8, 16-17	620	91,77	0,00	97,40	2,60
GS191-01PC-8, 26-27	630	95,97	0,00	96,98	3,02
GS191-01PC-8, 36-37	640	92,33	0,15	99,26	0,74
GS191-01PC-8, 46-47	650	94,93	0,17	97,97	2,03
GS191-01PC-8, 56-57	660	100,00	0,00	100,00	0,00
GS191-01PC-8, 66-67	670	88,73	0,70	95,77	4,23
GS191-01PC-9, 0-1	680	88,16	3,95	93,42	6,58
GS191-01PC-9, 10-11	690	97,44	0,00	97,44	2,56
GS191-01PC-9, 20-21	700	86,02	8,32	96,81	3,19
GS191-01PC-9, 30-31	710	94,06	1,40	96,50	3,50
GS191-01PC-9, 40-41	720	95,17	0,00	96,62	3,38
GS191-01PC-9, 50-51	730	92,45	1,89	96,23	3,77
GS191-01PC-9, 60-61	740	90,00	0,00	90,00	10,00
GS191-01PC-9, 70-71	750	72,16	11,34	89,69	10,31
GS191-01PC-9, 80-81	760	0,00	0,00	0,00	100,00
GS191-01PC-9, 90-91	770	80,00	0,00	80,00	20,00
GS191-01PC-10, 0-1	780	50,00	0,00	50,00	50,00

GS191-01PC-10, 10-11	790	40,00	0,00	70,00	30,00
GS191-01PC-10, 20-21	800	33,33	16,67	66,67	33,33
GS191-01PC-10, 30-31	810	50,00	28,57	85,71	14,29
GS191-01PC-10, 40-41	820	52,73	41,82	96,36	3,64
GS191-01PC-10, 50-51	830	33,33	0,00	33,33	66,67
GS191-01PC-10, 60-61	840	16,67	0,00	33,33	66,67
GS191-01PC-10, 70-71	850	60,00	0,00	60,00	40,00
GS191-01PC-10, 80-81	860	0,00	0,00	0,00	100,00
GS191-01PC-11, 0-1	870	75,00	0,00	75,00	25,00
GS191-01PC-11, 10-11	880	86,67	0,00	89,33	10,67
GS191-01PC-11, 20-21	890	100,00	0,00	100,00	0,00
GS191-01PC-11, 30-31	900	85,59	0,00	87,29	12,71
GS191-01PC-11, 40-41	910	63,86	2,41	67,47	32,53
GS191-01PC-11, 50-51	920	44,44	0,00	44,44	55,56
GS191-01PC-11, 60-61	930	50,00	3,33	56,67	43,33
GS191-01PC-11, 70-71	940	67,44	0,00	72,09	27,91
GS191-01PC-11, 80-81	950	74,10	1,59	78,88	21,12
GS191-01PC-11, 90-91	960	78,14	1,26	81,41	18,59
GS191-01PC-12, 0-1	970	54,90	6,86	64,71	35,29
GS191-01PC-12, 10-11	980	39,32	1,94	47,57	52,43
GS191-01PC-12, 20-21	990	60,00	0,00	67,50	32,50
GS191-01PC-12, 30-31	1000	49,29	4,29	57,86	42,14

GS191-01PC-12, 40-41	1010	47,83	0,00	52,17	47,83
GS191-01PC-12, 50-51	1020	61,90	0,00	61,90	38,10
GS191-01PC-12, 60-61	1030	26,53	2,04	34,69	65,31
GS191-01PC-12, 70-71	1040	83,89	0,00	87,84	12,16
GS191-01PC-12, 80-81	1050	38,64	4,55	54,55	45,45
GS191-01PC-12, 90-91	1060	0,00	0,00	0,00	100,00
GS191-01PC-13, 0-1	1070	50,00	50,00	100,00	0,00
GS191-01PC-13, 10-11	1080	0,00	0,00	0,00	100,00
GS191-01PC-13, 20-21	1090	0,00	100,00	100,00	0,00
GS191-01PC-13, 30-31	1100	25,00	0,00	25,00	75,00
GS191-01PC-13, 40-41	1110	57,14	0,00	57,14	42,86
GS191-01PC-13, 52-53	1122	86,97	0,25	89,72	10,28
GS191-01PC-13, 60-61	1130	39,53	2,33	48,26	51,74
GS191-01PC-13, 70-71	1140	41,88	0,00	47,86	52,14
GS191-01PC-13, 80-81	1150	49,43	2,30	55,17	44,83
GS191-01PC-13, 90-91	1160	72,18	1,50	76,69	23,31
GS191-01PC-14, 0-1	1170	76,53	0,00	77,04	22,96
GS191-01PC-14, 10-11	1180	90,30	0,00	90,61	9,39
GS191-01PC-14, 20-21	1190	93,38	0,00	93,82	6,18
GS191-01PC-14, 30-31	1200	40,91	0,00	50,00	50,00
GS191-01PC-14, 40-41	1210	72,73	0,00	72,73	27,27
GS191-01PC-14, 50-51	1220	0,00	0,00	0,00	0,00

GS191-01PC-14, 60-61	1230	90,00	0,00	91,82	8,18
GS191-01PC-14, 70-71	1240	60,00	0,00	60,00	40,00
GS191-01PC-14, 80-81	1250	61,76	0,00	76,47	23,53
GS191-01PC-14, 90-91	1260	89,19	0,00	90,54	9,46
GS191-01PC-15, 0-1	1270	90,91	0,91	92,73	7,27
GS191-01PC-15, 10-11	1280	96,17	0,24	97,61	2,39
GS191-01PC-15, 20-21	1290	93,33	0,00	96,67	3,33
GS191-01PC-15, 30-31	1300	0,00	0,00	0,00	0,00
GS191-01PC-15, 40-41	1310	50,00	0,00	50,00	50,00
GS191-01PC-15, 50-51	1320	100,00	0,00	100,00	0,00
GS191-01PC-15, 60-61	1330	40,00	0,00	46,67	53,33
GS191-01PC-15, 70-71	1340	92,59	0,00	92,59	7,41
GS191-01PC-15, 80-81	1350	80,00	0,00	90,00	10,00
GS191-01PC-15, 90-91	1360	93,62	0,00	95,74	4,26
GS191-01PC-16, 0-1	1370	0,00	0,00	0,00	100,00
GS191-01PC-16, 10-11	1380	40,00	0,00	40,00	60,00
GS191-01PC-16, 20-21	1390	63,33	0,00	73,33	26,67
GS191-01PC-16, 30-31	1400	86,26	0,00	90,08	9,92
GS191-01PC-16, 40-41	1410	71,43	0,00	71,43	28,57
GS191-01PC-16, 50-51	1420	76,92	0,00	76,92	23,08
GS191-01PC-16, 60-61	1430	77,42	0,00	80,65	19,35
GS191-01PC-16, 70-71	1440	80,99	0,83	93,39	6,61

GS191-01PC-16, 80-81	1450	73,13	0,00	80,60	19,40
GS191-01PC-17, 0-1	1460	50,00	0,00	50,00	50,00
GS191-01PC-17, 10-11	1470	87,50	0,00	90,63	9,38
GS191-01PC-17, 20-21	1480	97,83	0,00	97,83	2,17
GS191-01PC-17, 30-31	1490	84,13	0,00	85,71	14,29
GS191-01PC-17, 40-41	1500	83,77	1,75	93,42	6,58
GS191-01PC-17, 50-51	1510	0,00	0,00	0,00	0,00
GS191-01PC-17, 60-61	1520	89,58	0,00	89,58	10,42
GS191-01PC-17, 70-71	1530	87,10	1,08	92,47	7,53
GS191-01PC-17, 80-81	1540	87,50	1,88	94,38	5,63
GS191-01PC-17, 90-91	1550	92,88	0,24	97,39	2,61
GS191-01PC-18, 0-1	1560	22,22	0,00	22,22	77,78
GS191-01PC-18, 10-11	1570	78,57	0,00	82,14	17,86
GS191-01PC-18, 20-21	1580	81,05	0,00	83,01	16,99
GS191-01PC-18, 30-31	1590	100,00	0,00	100,00	0,00
GS191-01PC-18, 40-41	1600	100,00	0,00	100,00	0,00
GS191-01PC-18, 50-51	1610	100,00	0,00	100,00	0,00
GS191-01PC-18, 60-61	1620	86,36	4,55	90,91	9,09
GS191-01PC-18, 70-71	1630	0,00	0,00	0,00	0,00
GS191-01PC-18, 80-81	1640	84,75	0,00	91,53	8,47
GS191-01PC-18, 90-91	1650	100,00	0,00	100,00	0,00
GS191-01PC-19, 0-1	1660	75,00	0,00	75,00	25,00

GS191-01PC-19, 10-11	1670	97,33	0,00	98,30	1,70
GS191-01PC-19, 20-21	1680	74,74	3,16	90,53	9,47
GS191-01PC-19, 30-31	1690	88,44	0,00	96,60	3,40
GS191-01PC-19, 40-41	1700	0,00	0,00	0,00	0,00
GS191-01PC-19, 50-51	1710	0,00	0,00	0,00	0,00
GS191-01PC-19, 60-61	1720	95,85	0,57	98,11	1,89
GS191-01PC-19, 70-71	1730	0,00	0,00	0,00	0,00
GS191-01PC-19, 80-81	1740	96,57	0,31	98,75	1,25
GS191-01PC-19, 90-91	1750	87,36	3,45	99,43	0,57
GS191-01PC-20, 0-1	1760	100,00	0,00	100,00	0,00
GS191-01PC-20, 10-11	1770	90,00	0,00	94,00	6,00
GS191-01PC-20, 20-21	1780	84,91	0,00	94,34	5,66
GS191-01PC-20, 30-31	1790	87,50	0,00	87,50	12,50
GS191-01PC-20, 40-41	1800	80,95	4,76	100,00	0,00
GS191-01PC-20, 50-51	1810	73,33	0,00	73,33	26,67
GS191-01PC-20, 60-61	1820	91,38	0,00	98,28	1,72
GS191-01PC-20, 70-71	1830	88,89	0,00	88,89	11,11
GS191-01PC-20, 80-81	1840	0,00	0,00	0,00	100,00
GS191-01PC-20, 90-91	1850	20,00	0,00	20,00	80,00
GS191-01PC-21, 0-1	1860	0,00	0,00	0,00	0,00
GS191-01PC-21, 10-11	1870	0,00	0,00	0,00	0,00
GS191-01PC-21, 20-21	1880	72,97	0,00	86,49	13,51

GS191-01PC-21, 30-31	1890	91,98	0,00	96,79	3,21
GS191-01PC-21, 40-41	1900	0,00	0,00	0,00	0,00
GS191-01PC-21, 50-51	1910	0,00	0,00	0,00	100,00
GS191-01PC-21, 60-61	1920	0,00	0,00	0,00	100,00
GS191-01PC-21, 70-71	1930	0,00	0,00	0,00	0,00
GS191-01PC-21, 80-81	1940	41,38	0,00	58,62	41,38
GS191-01PC-21, 90-91	1950	71,59	1,14	96,59	3,41
GS191-01PC-21, 99-100	1960	50,58	3,47	98,84	1,16

Sample	Depth (cm)	H/P ratio log	Dominance index	Shannon diversity index	CEX *C. pel.*(modif. Dittert et al., 1999)
GS191-01PC-1, 0-1	0	0,09	0,4872	0,7901	0,55
GS191-01PC-1, 10-11	10	-0,19	0,4985	0,8091	0,39
GS191-01PC-1, 20-21	20	0,08	0,4856	0,7943	0,55
GS191-01PC-1, 30-31	30	0,13	0,4841	0,8208	0,57
GS191-01PC-2, 6-7	40	0,06	0,4652	0,8601	0,54
GS191-01PC-2, 16-17	50	0,22	0,4874	0,8564	0,63
GS191-01PC-2, 26-27	60	0,12	0,4676	0,8752	0,57
GS191-01PC-2, 36-37	70	0,21	0,4854	0,8405	0,62
GS191-01PC-2, 46-47	80	0,14	0,4861	0,8132	0,58
GS191-01PC-2, 56-57	90	0,18	0,4988	0,7917	0,60
GS191-01PC-2, 66-67	100	0,15	0,4834	0,8419	0,59
GS191-01PC-2, 76-77	110	0,17	0,496	0,8037	0,60
GS191-01PC-2, 86-87	120	0,12	0,482	0,8361	0,57

GS191-01PC-2, 96-97	130	0,31	0,5378	0,7469	0,67
GS191-01PC-3, 6-7	140	0,34	0,5451	0,7447	0,69
GS191-01PC-3, 16-17	150	0,34	0,5478	0,7396	0,69
GS191-01PC-3, 26-27	160	0,05	0,4827	0,7963	0,53
GS191-01PC-3, 36-37	170	-0,11	0,4822	0,8164	0,44
GS191-01PC-3, 46-47	180	0,07	0,4772	0,8273	0,54
GS191-01PC-3, 56-57	190	-0,03	0,4787	0,8046	0,49
GS191-01PC-3, 66-67	200	0,13	0,4825	0,817	0,57
GS191-01PC-3, 76-77	210	0,30	0,5145	0,8208	0,66
GS191-01PC-3, 86-87	220	0,23	0,4912	0,8523	0,63
GS191-01PC-3, 96-97	230	0,17	0,4901	0,8254	0,60
GS191-01PC-4, 6-7	240	0,32	0,5261	0,8022	0,68
GS191-01PC-4, 16-17	250	0,23	0,4922	0,847	0,63
GS191-01PC-4, 26-27	260	0,07	0,4655	0,8896	0,54
GS191-01PC-4, 36-37	270	0,31	0,5256	0,7833	0,67
GS191-01PC-4, 46-47	280	-0,03	0,4695	0,8547	0,48
GS191-01PC-4, 56-57	290	0,23	0,5018	0,8103	0,63
GS191-01PC-4, 66-67	300	0,17	0,4695	0,8855	0,59
GS191-01PC-4, 76-77	310	0,30	0,4956	0,87	0,67
GS191-01PC-4, 86-87	320	0,26	0,4599	0,9432	0,65
GS191-01PC-5, 6-7	330	0,27	0,4577	0,9691	0,65
GS191-01PC-5, 16-17	340	0,08	0,4049	1,069	0,55

GS191-01PC-5, 26-27	350	0,09	0,4003	1,06	0,55
GS191-01PC-5, 36-37	360	0,24	0,4094	1,088	0,63
GS191-01PC-5, 46-47	370	0,10	0,4222	1,018	0,56
GS191-01PC-5, 56-57	380	0,39	0,4804	0,9594	0,71
GS191-01PC-5, 66-67	390	0,25	0,4096	1,077	0,64
GS191-01PC-5, 76-77	400	0,23	0,4177	1,034	0,63
GS191-01PC-5, 86-87	410	0,20	0,4148	1,039	0,62
GS191-01PC-5, 96-97	420	0,31	0,4446	1,003	0,67
GS191-01PC-6, 6-7	430	0,54	0,4919	0,9506	0,78
GS191-01PC-6, 16-17	440	0,58	0,5514	0,8388	0,79
GS191-01PC-6, 26-27	450	0,60	0,5382	0,8638	0,80
GS191-01PC-6, 36-37	460	1,15	0,694	0,6329	0,93
GS191-01PC-6, 46-47	470	1,17	0,6876	0,6434	0,94
GS191-01PC-6, 56-57	480	1,71	0,8267	0,4139	0,98
GS191-01PC-6, 66-67	490	2,40	0,8757	0,3039	1,00
GS191-01PC-6, 76-77	500	2,47	0,8638	0,3264	1,00
GS191-01PC-6, 86-87	510	2,85	0,8114	0,4087	1,00
GS191-01PC-6, 96-97	520	2,38	0,7931	0,4433	1,00
GS191-01PC-7, 6-7	530	2,57	0,7521	0,5144	1,00
GS191-01PC-7, 16-17	540		0,8128	0,4036	1,00
GS191-01PC-7, 26-27	550	0,59	0,621	0,6982	0,79
GS191-01PC-7, 36-37	560		0,68	0,5004	1,00

GS191-01PC-7, 46-47	570	1,72	0,8092	0,4223	0,98
GS191-01PC-7, 56-57	580		0,899	0,2397	1,00
GS191-01PC-7, 66-67	590	1,28	0,8231	0,3805	0,95
GS191-01PC-7, 76-77	600	-0,05	0,4491	0,9061	0,47
GS191-01PC-8, 6-7	610		1	0	
GS191-01PC-8, 16-17	620		0,8729	0,3096	1,00
GS191-01PC-8, 26-27	630		0,954	0,1342	1,00
GS191-01PC-8, 36-37	640	2,80	0,8682	0,3036	1,00
GS191-01PC-8, 46-47	650	2,75	0,9327	0,1856	1,00
GS191-01PC-8, 56-57	660		1	0	1,00
GS191-01PC-8, 66-67	670	2,10	0,86	0,3568	0,99
GS191-01PC-9, 0-1	680	1,35	0,8793	0,29	0,96
GS191-01PC-9, 10-11	690		1	0	1,00
GS191-01PC-9, 20-21	700	1,01	0,6882	0,688	0,91
GS191-01PC-9, 30-31	710	1,83	0,9502	0,1356	0,99
GS191-01PC-9, 40-41	720		0,9704	0,08743	1,00
GS191-01PC-9, 50-51	730	1,69	0,9239	0,1926	0,98
GS191-01PC-9, 60-61	740		1	0	1,00
GS191-01PC-9, 70-71	750	0,80	0,6475	0,7409	0,86
GS191-01PC-9, 80-81	760		1	0	
GS191-01PC-9, 90-91	770		1	0	1,00
GS191-01PC-10, 0-1	780		0,4286	0,9557	1,00

GS191-01PC-10, 10-11	790		0,375	1,04	1,00
GS191-01PC-10, 20-21	800	0,30	0,4583	0,8877	0,67
GS191-01PC-10, 30-31	810	0,24	0,4881	0,7671	0,64
GS191-01PC-10, 40-41	820	0,10	1	0	0,56
GS191-01PC-10, 50-51	830		0,5	0,6931	1,00
GS191-01PC-10, 60-61	840		1	0	1,00
GS191-01PC-10, 70-71	850		1	0	1,00
GS191-01PC-10, 80-81	860		0,9416	0,1549	
GS191-01PC-11, 0-1	870		1	0	1,00
GS191-01PC-11, 10-11	880		0,9617	0,1092	1,00
GS191-01PC-11, 20-21	890		0,8973	0,243	1,00
GS191-01PC-11, 30-31	900		1	0	1,00
GS191-01PC-11, 40-41	910	1,42	0,7832	0,5084	0,96
GS191-01PC-11, 50-51	920		0,8793	0,2392	1,00
GS191-01PC-11, 60-61	930	1,18	0,8837	0,2939	0,94
GS191-01PC-11, 70-71	940		0,8872	0,2958	1,00
GS191-01PC-11, 80-81	950	1,67	0,7332	0,5179	0,98
GS191-01PC-11, 90-91	960	1,79	0,7018	0,5789	0,98
GS191-01PC-12, 0-1	970	0,90	0,8025	0,3488	0,89
GS191-01PC-12, 10-11	980	1,31	0,7336	0,5889	0,95
GS191-01PC-12, 20-21	990		0,8472	0,2868	1,00
GS191-01PC-12, 30-31	1000	1,06	0,9027	0,2023	0,92

GS191-01PC-12, 40-41	1010		0,6055	0,7902	1,00
GS191-01PC-12, 50-51	1020		0,8558	0,3516	1,00
GS191-01PC-12, 60-61	1030	1,11	0,5521	0,7781	0,93
GS191-01PC-12, 70-71	1040		0,5	0,6931	1,00
GS191-01PC-12, 80-81	1050	0,93	1	0	0,89
GS191-01PC-12, 90-91	1060		1	0	
GS191-01PC-13, 0-1	1070	0,00	1	0	0,50
GS191-01PC-13, 10-11	1080		0,9184	0,2341	
GS191-01PC-13, 20-21	1090		0,6836	0,678	0,00
GS191-01PC-13, 30-31	1100		0,7468	0,5152	1,00
GS191-01PC-13, 40-41	1110		0,8064	0,444	1,00
GS191-01PC-13, 52-53	1122	2,54	0,8872	0,2832	1,00
GS191-01PC-13, 60-61	1130	1,23	0,9356	0,162	0,94
GS191-01PC-13, 70-71	1140		0,9933	0,0224	1,00
GS191-01PC-13, 80-81	1150	1,33	0,9767	0,07514	0,96
GS191-01PC-13, 90-91	1160	1,68	0,7025	0,4741	0,98
GS191-01PC-14, 0-1	1170		1	0	1,00
GS191-01PC-14, 10-11	1180		0,9418	0,1663	1,00
GS191-01PC-14, 20-21	1190		1	0	1,00
GS191-01PC-14, 30-31	1200		0,6716	0,619	1,00
GS191-01PC-14, 40-41	1210		0,9416	0,1549	1,00
GS191-01PC-14, 50-51	1220		0,9423	0,165	

GS191-01PC-14, 60-61	1230		0,9709	0,0962	1,00
GS191-01PC-14, 70-71	1240		0,9334	0,15	1,00
GS191-01PC-14, 80-81	1250		1	0	1,00
GS191-01PC-14, 90-91	1260		1	0	1,00
GS191-01PC-15, 0-1	1270	2,00	0,7551	0,4101	0,99
GS191-01PC-15, 10-11	1280	2,60	1	0	1,00
GS191-01PC-15, 20-21	1290		0,8025	0,3488	1,00
GS191-01PC-15, 30-31	1300		0,9563	0,122	
GS191-01PC-15, 40-41	1310		1	0	1,00
GS191-01PC-15, 50-51	1320		0,7645	0,3983	1,00
GS191-01PC-15, 60-61	1330		0,9108	0,2026	1,00
GS191-01PC-15, 70-71	1340		1	0	1,00
GS191-01PC-15, 80-81	1350		1	0	1,00
GS191-01PC-15, 90-91	1360		0,9232	0,1679	1,00
GS191-01PC-16, 0-1	1370		0,7655	0,456	
GS191-01PC-16, 10-11	1380		0,8292	0,3548	1,00
GS191-01PC-16, 20-21	1390		1	0	1,00
GS191-01PC-16, 30-31	1400		0,8692	0,2988	1,00
GS191-01PC-16, 40-41	1410		1	0	1,00
GS191-01PC-16, 50-51	1420		0,8937	0,2499	1,00
GS191-01PC-16, 60-61	1430		0,8023	0,4392	1,00
GS191-01PC-16, 70-71	1440	1,99	1	0	0,99

GS191-01PC-16, 80-81	1450		0,8886	0,2771	1,00
GS191-01PC-17, 0-1	1460		0,8268	0,3996	1,00
GS191-01PC-17, 10-11	1470		0,8904	0,2749	1,00
GS191-01PC-17, 20-21	1480		1	0	1,00
GS191-01PC-17, 30-31	1490		0,8762	0,2826	1,00
GS191-01PC-17, 40-41	1500	1,68	0,9384	0,1727	0,98
GS191-01PC-17, 50-51	1510		1	0	#DIV/0!
GS191-01PC-17, 60-61	1520		1	0	1,00
GS191-01PC-17, 70-71	1530	1,91	1	0	0,99
GS191-01PC-17, 80-81	1540	1,67	0,905	0,1985	0,98
GS191-01PC-17, 90-91	1550	2,59	0,8628	0,2641	1,00
GS191-01PC-18, 0-1	1560		1	0	1,00
GS191-01PC-18, 10-11	1570		1	0	1,00
GS191-01PC-18, 20-21	1580		0,9755	0,07642	1,00
GS191-01PC-18, 30-31	1590		0,6961	0,6513	1,00
GS191-01PC-18, 40-41	1600		0,8377	0,3419	1,00
GS191-01PC-18, 50-51	1610		0,9509	0,1485	1,00
GS191-01PC-18, 60-61	1620	1,28	0,9443	0,1663	0,95
GS191-01PC-18, 70-71	1630		0,7797	0,4635	
GS191-01PC-18, 80-81	1640		1	0	1,00
GS191-01PC-18, 90-91	1650		0,9185	0,176	1,00
GS191-01PC-19, 0-1	1660		0,7512	0,4887	1,00

GS191-01PC-19, 10-11	1670		1	0	1,00
GS191-01PC-19, 20-21	1680	1,37	0,678	0,594	0,96
GS191-01PC-19, 30-31	1690		1	0	1,00
GS191-01PC-19, 40-41	1700		0,8375	0,3411	
GS191-01PC-19, 50-51	1710		1	0	
GS191-01PC-19, 60-61	1720	2,23	1	0	0,99
GS191-01PC-19, 70-71	1730		0,6387	0,6562	
GS191-01PC-19, 80-81	1740	2,49	0,8946	0,249	1,00
GS191-01PC-19, 90-91	1750	1,40	0,5848	0,6058	0,96
GS191-01PC-20, 0-1	1760		0,605	0,667	1,00
GS191-01PC-20, 10-11	1770		0,468	0,8388	1,00
GS191-01PC-20, 20-21	1780				1,00
GS191-01PC-20, 30-31	1790				1,00
GS191-01PC-20, 40-41	1800	1,23			0,94
GS191-01PC-20, 50-51	1810				1,00
GS191-01PC-20, 60-61	1820				1,00
GS191-01PC-20, 70-71	1830				1,00
GS191-01PC-20, 80-81	1840				
GS191-01PC-20, 90-91	1850				1,00
GS191-01PC-21, 0-1	1860				
GS191-01PC-21, 10-11	1870				
GS191-01PC-21, 20-21	1880				1,00

GS191-01PC-21, 30-31	1890		1,00
GS191-01PC-21, 40-41	1900		
GS191-01PC-21, 50-51	1910		
GS191-01PC-21, 60-61	1920		
GS191-01PC-21, 70-71	1930		
GS191-01PC-21, 80-81	1940		1,00
GS191-01PC-21, 90-91	1950	1,80	0,98
GS191-01PC-21, 99-100	1960	1,16	0,94

SUPPLEMENTARY I- Lithological core logs

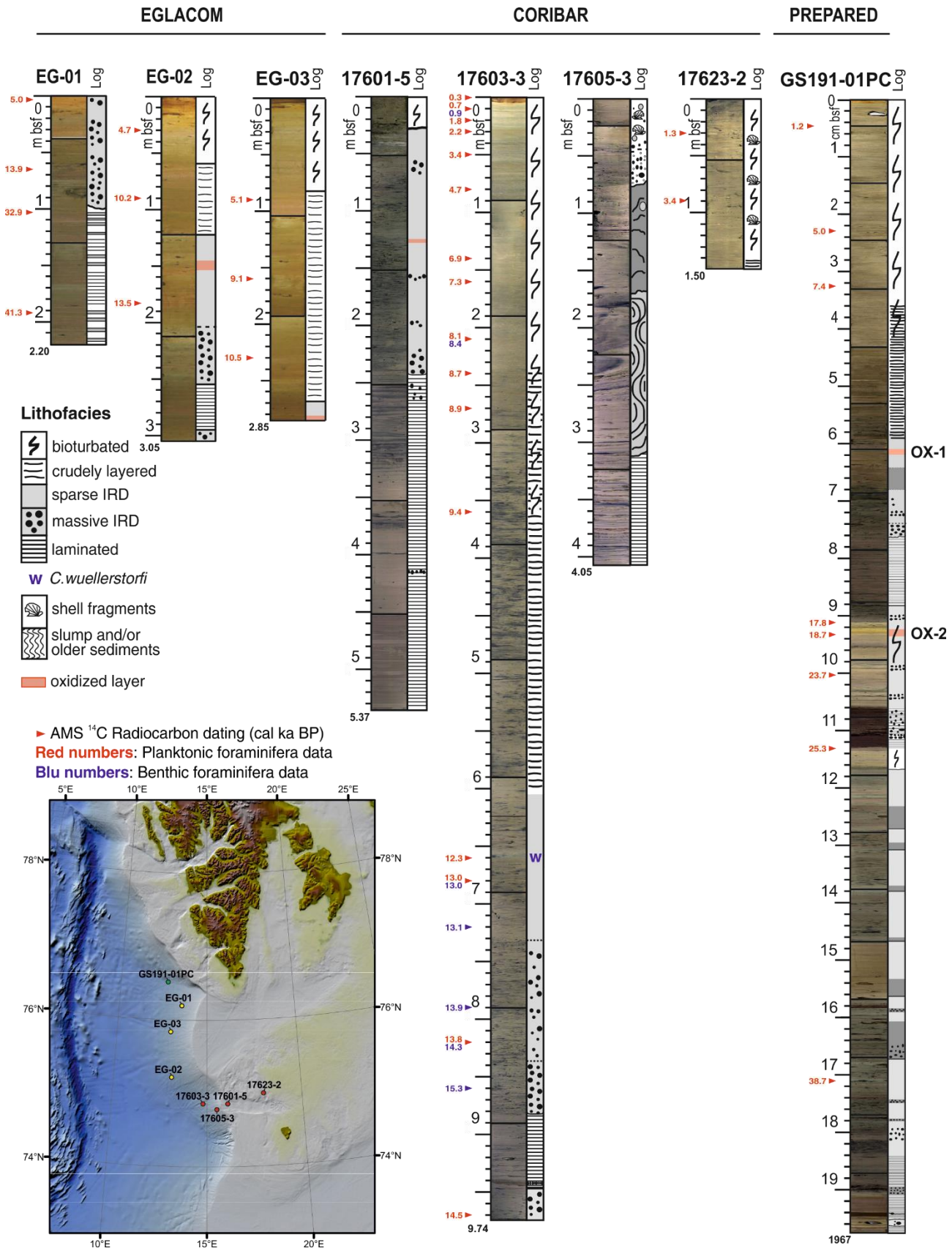

SUPPLEMENTARY L- GeoB17603-3 age model

Depth (cm)	Age (cal age BP)
0	**302**
1	345
2	389
3	432
4	476
5	519
6	562
7	606
8	649
9	693
10	**736**
11	844
12	951
13	1059
14	1167
15	1275
16	1382
17	1490
18	1598
19	1705
20	**1813**
21	1850
22	1887
23	1924
24	1961
25	1998
26	2035
27	2072
28	2109
29	2146
30	**2183**
31	2243

32	2302
33	2362
34	2422
35	2482
36	2541
37	2601
38	2661
39	2720
40	2780
41	2840
42	2899
43	2959
44	3019
45	3079
46	3138
47	3198
48	3258
49	3317
50	**3377**
51	3422
52	3467
53	3512
54	3556
55	3601
56	3646
57	3691
58	3736
59	3781
60	3826
61	3871
62	3915
63	3960
64	4005
65	4050
66	4095

67	4140
68	4185
69	4229
70	4274
71	4319
72	4364
73	4409
74	4454
75	4499
76	4544
77	4588
78	4633
79	4678
80	**4723**
81	4760
82	4797
83	4834
84	4871
85	4908
86	4945
87	4982
88	5019
89	5056
90	5094
91	5131
92	5168
93	5205
94	5242
95	5279
96	5316
97	5353
98	5390
99	5427
100	5464
101	5501

102	5538
103	5575
104	5612
105	5649
106	5686
107	5723
108	5760
109	5797
110	5835
111	5872
112	5909
113	5946
114	5983
115	6020
116	6057
117	6094
118	6131
119	6168
120	6205
121	6242
122	6279
123	6316
124	6353
125	6390
126	6427
127	6464
128	6501
129	6538
130	6576
131	6613
132	6650
133	6687
134	6724
135	6761
136	6798

137	6835
138	6872
139	6909
140	**6946**
141	6964
142	6982
143	7000
144	7017
145	7035
146	7053
147	7071
148	7089
149	7107
150	7125
151	7142
152	7160
153	7178
154	7196
155	7214
156	7232
157	7249
158	7267
159	7285
160	**7303**
161	7320
162	7337
163	7354
164	7372
165	7389
166	7406
167	7423
168	7440
169	7457
170	7475
171	7492

172	7509
173	7526
174	7543
175	7560
176	7578
177	7595
178	7612
179	7629
180	7646
181	7663
182	7681
183	7698
184	7715
185	7732
186	7749
187	7766
188	7784
189	7801
190	7818
191	7835
192	7852
193	7869
194	7887
195	7904
196	7921
197	7938
198	7955
199	7972
200	7990
201	8007
202	8024
203	8041
204	8058
205	8075
206	8092

207	8110
208	8127
209	8144
210	8161
211	8178
212	8195
213	8213
214	8230
215	8247
216	8264
217	8281
218	8298
219	8316
220	8333
221	8350
222	8367
223	8384
224	8401
225	8419
226	8436
227	8453
228	8470
229	8487
230	8504
231	8522
232	8539
233	8556
234	8573
235	8590
236	8607
237	8625
238	8642
239	8659
240	**8676**
241	8685

242	8695
243	8704
244	8713
245	8722
246	8732
247	8741
248	8750
249	8759
250	8769
251	8778
252	8787
253	8796
254	8806
255	8815
256	8824
257	8834
258	8843
259	8852
260	8861
261	8871
262	8880
263	8889
264	8898
265	8908
266	8917
267	8926
268	8935
269	8945
270	**8954**
271	8960
272	8967
273	8973
274	8980
275	8986
276	8993

277	8999
278	9006
279	9012
280	9019
281	9025
282	9031
283	9038
284	9044
285	9051
286	9057
287	9064
288	9070
289	9077
290	9083
291	9090
292	9096
293	9102
294	9109
295	9115
296	9122
297	9128
298	9135
299	9141
300	9148
301	9154
302	9161
303	9167
304	9173
305	9180
306	9186
307	9193
308	9199
309	9206
310	9212
311	9219

312	9225
313	9232
314	9238
315	9245
316	9251
317	9257
318	9264
319	9270
320	9277
321	9283
322	9290
323	9296
324	9303
325	9309
326	9316
327	9322
328	9328
329	9335
330	9341
331	9348
332	9354
333	9361
334	9367
335	9374
336	9380
337	9387
338	9393
339	9399
340	9406
341	9412
342	9419
343	9425
344	9432
345	9438
346	9445

347	9451
348	9458
349	9464
350	9470
351	9477
352	9483
353	9490
354	9496
355	9503
356	9509
357	9516
358	9522
359	9529
360	**9535**
361	9540
362	9544
363	9548
364	9553
365	9557
366	9562
367	9566
368	9570
369	9575
370	9579
371	9584
372	9588
373	9592
374	9597
375	9601
376	9605
377	9610
378	9614
379	9619
380	9623
381	9627

382	9632
383	9636
384	9641
385	9645
386	9649
387	9654
388	9658
389	9662
390	9667
391	9671
392	9676
393	9680
394	9684
395	9689
396	9693
397	9698
398	9702
399	9706
400	9711
401	9715
402	9720
403	9724
404	9728
405	9733
406	9737
407	9741
408	9746
409	9750
410	9755
411	9759
412	9763
413	9768
414	9772
415	9777
416	9781

417	9785
418	9790
419	9794
420	9798
421	9803
422	9807
423	9812
424	9816
425	9820
426	9825
427	9829
428	9834
429	9838
430	9842
431	9847
432	9851
433	9855
434	9860
435	9864
436	9869
437	9873
438	9877
439	9882
440	9886
441	9891
442	9895
443	9899
444	9904
445	9908
446	9913
447	9917
448	9921
449	9926
450	9930
451	9934

452	9939
453	9943
454	9948
455	9952
456	9956
457	9961
458	9965
459	9970
460	9974
461	9978
462	9983
463	9987
464	9991
465	9996
466	10000
467	10005
468	10009
469	10013
470	10018
471	10022
472	10027
473	10031
474	10035
475	10040
476	10044
477	10048
478	10053
479	10057
480	10062
481	10066
482	10070
483	10075
484	10079
485	10084
486	10088

487	10092
488	10097
489	10101
490	10106
491	10110
492	10114
493	10119
494	10123
495	10127
496	10132
497	10136
498	10141
499	10145
500	10149
501	10154
502	10158
503	10163
504	10167
505	10171
506	10176
507	10180
508	10184
509	10189
510	10193
511	10198
512	10202
513	10206
514	10211
515	10215
516	10220
517	10224
518	10228
519	10233
520	10237
521	10241

522	10246
523	10250
524	10255
525	10259
526	10263
527	10268
528	10272
529	10277
530	10281
531	10285
532	10290
533	10294
534	10299
535	10303
536	10307
537	10312
538	10316
539	10320
540	**10500**
541	10515
542	10531
543	10546
544	10561
545	10576
546	10592
547	10607
548	10622
549	10638
550	10653
551	10668
552	10684
553	10699
554	10714
555	10729
556	10745

557	10760
558	10775
559	10791
560	10806
561	10821
562	10836
563	10852
564	10867
565	10882
566	10898
567	10913
568	10928
569	10943
570	10959
571	10974
572	10989
573	11005
574	11020
575	11035
576	11051
577	11066
578	11081
579	11096
580	11112
581	11127
582	11142
583	11158
584	11173
585	11188
586	11203
587	11219
588	11234
589	11249
590	11265
591	11280

592	11295
593	11310
594	11326
595	11341
596	11356
597	11372
598	11387
599	11402
600	11418
601	11433
602	11448
603	11463
604	11479
605	11494
606	11509
607	11525
608	11540
609	11555
610	11570
611	11586
612	11601
613	11616
614	11632
615	11647
616	11662
617	11677
618	11693
619	11708
620	11723
621	11739
622	11754
623	11769
624	11784
625	11800
626	11815

627	11830
628	11846
629	11861
630	11876
631	11892
632	11907
633	11922
634	11937
635	11953
636	11968
637	11983
638	11999
639	12014
640	12029
641	12044
642	12060
643	12075
644	12090
645	12106
646	12121
647	12136
648	12151
649	12167
650	12182
651	12197
652	12213
653	12228
654	12243
655	12259
656	12274
657	12289
658	12304
659	12320
660	**12335**
661	12371

662	12407
663	12444
664	12480
665	12516
666	12552
667	12588
668	12625
669	12661
670	12697
671	12733
672	12769
673	12806
674	12842
675	12878
676	12914
677	12950
678	12987
679	13023
680	**13059**
681	13064
682	13070
683	13075
684	13080
685	13085
686	13091
687	13096
688	13101
689	13107
690	13112
691	13117
692	13123
693	13128
694	13133
695	13138
696	13144

697	13149
698	13154
699	13160
700	13165
701	13170
702	13175
703	13181
704	13186
705	13191
706	13197
707	13202
708	13207
709	13212
710	13218
711	13223
712	13228
713	13234
714	13239
715	13244
716	13250
717	13255
718	13260
719	13265
720	13271
721	13276
722	13281
723	13287
724	13292
725	13297
726	13302
727	13308
728	13313
729	13318
730	13324
731	13329

732	13334
733	13340
734	13345
735	13350
736	13355
737	13361
738	13366
739	13371
740	13377
741	13382
742	13387
743	13392
744	13398
745	13403
746	13408
747	13414
748	13419
749	13424
750	13430
751	13435
752	13440
753	13445
754	13451
755	13456
756	13461
757	13467
758	13472
759	13477
760	13482
761	13488
762	13493
763	13498
764	13504
765	13509
766	13514

767	13519
768	13525
769	13530
770	13535
771	13541
772	13546
773	13551
774	13557
775	13562
776	13567
777	13572
778	13578
779	13583
780	13588
781	13594
782	13599
783	13604
784	13609
785	13615
786	13620
787	13625
788	13631
789	13636
790	13641
791	13647
792	13652
793	13657
794	13662
795	13668
796	13673
797	13678
798	13684
799	13689
800	13694
801	13699

802	13705
803	13710
804	13715
805	13721
806	13726
807	13731
808	13736
809	13742
810	13747
811	13752
812	13758
813	13763
814	13768
815	13774
816	13779
817	13784
818	13789
819	13795
820	**13800**
821	13900
822	**14000**
823	14003
824	14007
825	14010
826	14014
827	14017
828	14020
829	14024
830	14027
831	14031
832	14034
833	14038
834	14041
835	14044
836	14048

837	14051
838	14055
839	14058
840	14061
841	14065
842	14068
843	14072
844	14075
845	14078
846	14082
847	14085
848	14089
849	14092
850	14096
851	14099
852	14102
853	14106
854	14109
855	14113
856	14116
857	14119
858	14123
859	14126
860	14130
861	14133
862	14136
863	14140
864	14143
865	14147
866	14150
867	14154
868	14157
869	14160
870	14164
871	14167

872	14171
873	14174
874	14177
875	14181
876	14184
877	14188
878	14191
879	14194
880	14198
881	14201
882	14205
883	14208
884	14212
885	14215
886	14218
887	14222
888	14225
889	14229
890	14232
891	14235
892	14239
893	14242
894	14246
895	14249
896	14253
897	14256
898	14259
899	14263
900	14266
901	14270
902	14273
903	14276
904	14280
905	14283
906	14287

907	14290
908	14293
909	14297
910	14300
911	14304
912	14307
913	14311
914	14314
915	14317
916	14321
917	14324
918	14328
919	14331
920	14334
921	14338
922	14341
923	14345
924	14348
925	14351
926	14355
927	14358
928	14362
929	14365
930	14369
931	14372
932	14375
933	14379
934	14382
935	14386
936	14389
937	14392
938	14396
939	14399
940	14403
941	14406

942	14409
943	14413
944	14416
945	14420
946	14423
947	14427
948	14430
949	14433
950	14437
951	14440
952	14444
953	14447
954	14450
955	14454
956	14457
957	14461
958	14464
959	14467
960	14471
961	14474
962	14478
963	14481
964	14485
965	14488
966	14491
967	14495
968	14498
969	14502
970	**14505**
971	14508
972	14512
973	14515
974	14519

SUPPLEMENTARY M- Presented posters at conferences and workshops

88° Congresso della Società Geologica Italiana

Naples (Italy) 7-9/09/2016

Integrated sedimentology and micropaleontology for the study of the deglaciation post LGM in the south- western Svalbard slope (Arctic Ocean)

Carbonara K.[1], Lucchi R.G.,[2] Melis R.,[3] Mezgec K., Morigi C.,[4] Musco M.E.[2,4], Varagona G.,[3] Villa G.[1]

[1]Department of Physics and Earth Sciences - University of Parma (Italy);
[2]National Institute of Oceanography and Experimental Geophysics (OGS) - Trieste (Italy);
[3]Department of Mathematics and Geosciences - University of Trieste (Italy);
[4]Department of Physical sciences, Earth and environment - University of Siena (Italy);
[5]Department of Earth Sciences - University of Pisa (Italy).

INTRODUCTION

The north-western continental margin of the Barents Sea represents the only gateway for deep-water masses moving between the North Atlantic and the Arctic Oceans. On this respect, the western Svalbard margin, located on the eastern side of the Fram Strait, represents a key area to study the paleoceanographic variation of the West and East Spitsbergen currents.

Contour currents along the south-western continental margin of the Svalbard area, generated expanded sedimentary sequences suitable for high-resolution paleoceanographic and paleoenvironmental reconstructions. The Storfjorden-Kveithola glacial sedimentary system (south of Svalbard) was investigated during the EGLACOM and CORIBAR projects (Fig. 1) with the aim of reconstructing the deep-water paleoceanographic/paleoenvironmental evolution after Last Glacial Maximum.

Integrated sedimentological and micropaleontological analyses on calcareous nannofossils, diatoms, planktonic and benthonic foraminifera and clay mineral assemblages have been performed on three sediment cores, collected during the EGLACOM (cores EG-02 and EG-03) and CORIBAR (core GeoB17603-3) projects from the Storfjorden-Kveithola depositional system (NW Barents Sea) (Fig. 1), to reconstruct the paleoceanographic and paleoenvironmental evolution after the Last Glacial Maximum. The CORIBAR core shows expanded Holocene sequence (about 6 m) if compared with the other two cores collected from the middle slope off Storfjorden glacial system (cores EG-02, Holocene sequence: about 1.2 m and EG-03, Holocene sequence: about 2.7 m) (Fig. 2).

A preliminary age model has been built on the basis of several ^{14}C AMS dates and magnetic susceptibility correlations between core GeoB17603-3and the previously studied cores (EG-02 and EG-03) (Sagnotti *et al.*, 2011; Carbonara et al., submitted).

STUDY AREA

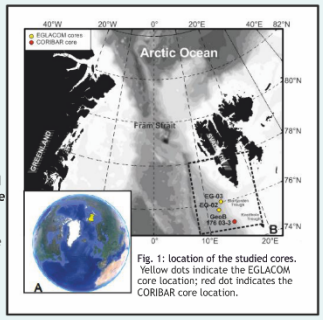

Fig. 1: location of the studied cores. Yellow dots indicate the EGLACOM core location; red dot indicates the CORIBAR core location.

Core ID	Water depth (m)	Location	Total recovery (cm)
EG-02	1722	Middle-slope of Storfjorden TMF	305
EG-03	1432	Middle-slope of Storfjorden TMF	291
GeoB 17603-3	1430	Middle slope of Kveithola TMF	990

EG = EGLACOM
GeoB = CORIBAR

This study was supported by the Italian Progetto Nazionale Ricerche in Antartide «CORIBAR-IT» (coord. R.G. Lucchi)

RESULTS

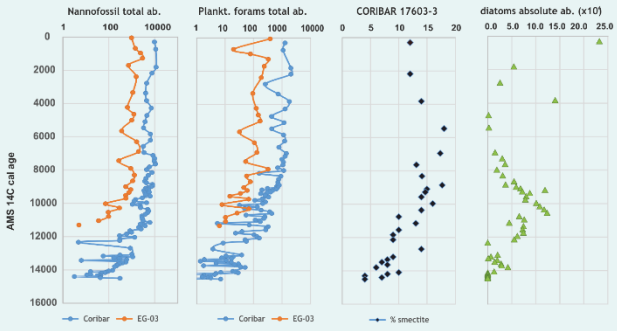

The microfossils are scarce in the lithological units representing the deglaciation after the LGM, and become more abundant in the Holocene sequences that record a clear upswing of the North Atlantic Current (NAC) strength. Nevertheless, the benthic assemblage is indicative of non-permanently ice-covered conditions since about 15 cal ka BP.

The planktonic microfossil distribution patterns are coherent with the trend of smectite content in the clay mineral assemblage that is mainly transported by the NAC, therefore high contents are associated to a vigorous current (Junttila et al., 2010).

Starting from about 12 cal ka BP, a significant occurrence of diatoms is recorded in all the stuidied cores.

The high abundance of diatoms, deposited in a sediment thickness of 40, 100 and about 250 cm in EG-02, EG-03 and GeoB17603-3, respectively, is responsible for high sedimentation rate during the early Holocene.

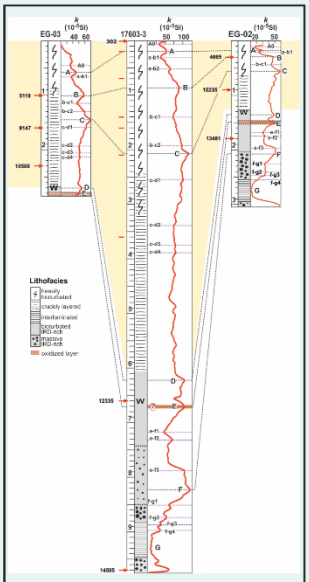

Fig. 2 Correlations among the cores were evidenced by magnetic susceptibility (red line) and lithological characters. CORIBAR core shows expanded Holocene sequence. Calibrated ages in years BP. W = first occurrence of *C. wuellerstorfi*.

The nannofossil assemblages during the Holocene, are dominated by *Emiliania huxleyi* (< 4 µm), confirming the climatic amelioration.

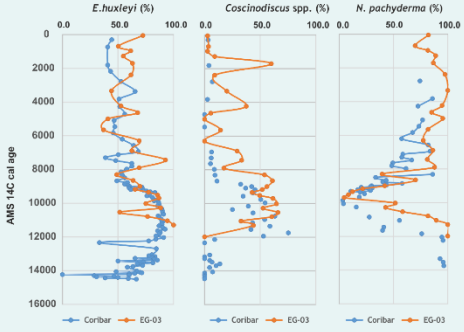

The diatom assemblages are dominated by *Chaetoceros* resting spores, related to stratified waters in association with ice melting at the beginning of Holocene. The presence of the diatom *Coscinodiscus* spp. and a more diversified planktonic foraminiferal assemblage, with *Neogloboquadrina pachyderma* (s), *N. incompta* and *Globigerina bulloides*, indicating subpolar conditions, confirms the onset of warm environmental period that were associated to the Holocene Thermal Maximum (HTM).

In the glaciomarine sediments the benthic foraminifera assemblage mainly contains *Cassidulina reniforme*, *Cassidulina neoteretis*, *Islandiella helenae/norcrossi* and *Cibicides lobatulus*. The first occurrence of *Cibicidoides wuellerstorfi* is located at about 12.3 cal ka BP (Melis et al., in prep).

The significant occurrence of small taxa, such as *Stetsonia horvati*, during the middle-late Holocene suggests a condition of low productivity and limited flux of organic matter to the sea floor during the medium-late Holocene.

In the late Holocene, an increasing occurrence of *Epistominella arctica*, *E. exigua* and *Eilohedra nipponica*, considered phytodetritus feeders, characterizes the uppermost sediments. Here the nannoplankton abundance reaches the highest concentration.

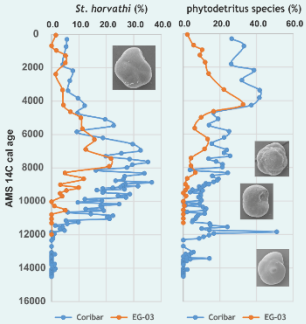

The abundance of agglutinated species, corresponding to high percentage of benthic foraminifera fragmentation, indicate aggressive bottom waters and, could suggest the influence of cold, salty and dense waters, coming from the shelf area.

References:

Junttila J., Aagaard-Sørensen S., Husum K. & Hald M., 2010. Late Glacial-Holocene clay minerals elucidating glacial history in the SW Barren Sea. *Mar. Geol.* 276, 71-85.

Sagnotti L., Macri P., Lucchi R.G., Rebesco M., Camerlenghi A., 2011. A Holocene paleosecular variation record from the northwestern Barents Sea continental margin. *Geochem. Geophys. Geosyst.* 12 (11), Q11Z33.

Carbonara K., Mezgec K., Varagona G., Musco M.E., Lucchi R.G., Villa G., Morigi C., Melis R., Caffau M. (under review). Palaeoclimatic changes in Kveithola, Svalbard, during the Late Pleistocene deglaciation and Holocene: evidences from microfossil and sedimentology records. *Palaeogeography, Palaeoclimatology, Palaeoecology.*

Melis R., Carbonara K., Villa G., Morigi C., Lucchi R.G., Barcena, M.A., Giorgetti G., Caburlotto A, Rebesco M. (under submission). - Late Quaternary integrated micropalaeontology for the palaeoenvironmental study of the southern Svalbard continental margin (north-western Barents Sea). *Palaeogeography, Palaeoclimatology, Palaeoecology.*

12th International Conference on Paleoceanography (ICP12)

Utrecht (Netherlands) 29-2/09/2016

MIDDLE EOCENE TO LOWER OLIGOCENE BIO-MAGNETOSTRATIGRAPHY FROM ODP SITE 709 (MADINGLEY RISE, EQUATORIAL INDIAN OCEAN) AND CALCAREOUS NANNOFOSSIL RESPONSE TO CLIMATE VARIABILITY

Giuliana Villa[1], Chiara Fioroni[2], Fabio Florindo[3], Katia Carbonara[1], Pontus Lurcock[3]

1)Dipartimento di Fisica e Scienze della Terra "Macedonio Melloni", Università di Parma, Parma, Italy; 2) Dipartimento di Scienze Chimiche e Geologiche, Università degli Studi di Modena e Reggio Emilia, Modena, Italy; 3) Istituto Nazionale di Geofisica e Vulcanologia, Rome, Italy

Leg 115 was drilled in the Indian Ocean (Duncan and Backman, 1990) to achieve a south - north bathymetric transect and to investigate the Réunion volcanic system and the Paleogene to Quaternary stratigraphy. Site 709 is situated at 3°55'S, 60°33'E on the Madingley Rise (water depth 3038 m) a local topographic high between the Mascarene Plateau and the Carlsberg Ridge. Three holes were drilled at this site, recovering a particularly homogeneous section of nannofossil ooze and chalk, ranging in age from Eocene to Holocene.

New quantitative calcareous nannofossil analyses, new paleomagnetic data, and correlation with a recent detailed biomagnetostratigraphic study of Site 711 (Fioroni et al., 2015), allow us to define a correlation at regional and global scale. High-resolution sampling and new biostratigraphic and taxonomic updates (Fornaciari et al., 2010, Bown and Dunkley Jones, 2012, Toffanin et al., 2013, Agnini et al., 2014) gave us the opportunity to produce a middle Eocene-early Oligocene biochronology. Analyses of the nannofossil assemblage variation suggest paleoceanographic changes before the onset of the Eocene-Oligocene Transition (EOT), foreshadowing the more dramatic shift of the early Oligocene.

GOALS

1) Using quantitative calcareous nannofossil analyses, to increase the number of useful bioevents and accordingly to improve the biostratigraphic resolution, andcompare the results with those from previous studies in this region (Site 711) and at global scale;
2) to investigate the magnetobiostratigraphy of this site by conducting new high-resolution paleomagnetic analyses;
3) using the abundance variations of calcareous nannofossil and magnetostratigraphy, to recognize global paleoceanographic events.

METHODS

•Smear slides were prepared, and quantitative analyses were conducted in the light microscope with 1250X counting at least 300 specimens per sample. Two additional long traverses were scanned in order to identify rare taxa. For each taxon the abundance was obtained by converting its number normalized to an area of 1 mm^2 plotted versus depth.

• All magnetic analyses were performed at the Istituto Nazionale di Geofisica e Vulcanologia (INGV) in Rome. Natural and artificial magnetizations were measured using a narrow-access pass-through 2-G Enterprises cryogenic magnetometer, housed in a magnetically shielded room. Samples were demagnetized at successive peak AFs of 5, 10, 15, 20, 25, 30, 40, 45, 50, 60, 80, and 100 mT. The stability of the natural remanent magnetization (NRM) was assessed using vector component diagrams. Characteristic remanent magnetization (ChRM) directions were determined using principal component analysis (PCA) with linear best fits calculated from 3 or more demagnetization steps.

The quantitative study of calcareous nannofossils of Hole 709C identified **31** bioevents in about **12** Myr. Biostratigraphic events are indicated with arrows as B (Base), Bc (Base common), T (top), Tc (top common).

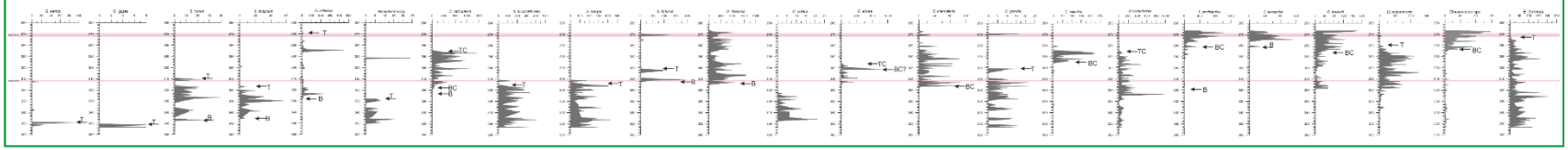

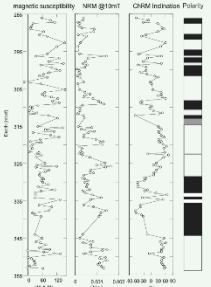

Stratigraphic variation of the low-field magnetic susceptibility, NRM intensity after demagnetization @ 10 mT, ChRM inclination and magnetic polarity zonation (black= normal polarity; white= reverse)

Magnetostratigraphy

Hole 709C is today at a latitude of 3°55'S. Based on a reconstructed position, its paleolatitude during Eocene was about 10°S. At this paleolatitude the geocentric axial dipole (GAD) field has an inclination of +/- 19.4°. Although it is not steep, ChRM inclinations are sufficient to determine polarity despite the fact that the cores lack azimuthal orientation. As reported by Savian et al. (2013) at the nearby Site 711, ChRM inclinations are steeper than the GAD inclination; this could be due to some unresolved combination of unaccounted-for motion of the plate, long-term non-dipole fields, and effects of hotspot motion on the plate circuit models.

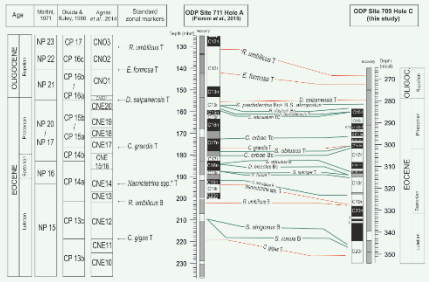

Biostratigraphic correlations for the middle Eocene–early Oligocene between the ODP Site 711 and Site 709.

Paleoecological remarks

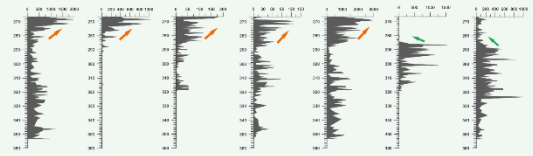

A turnover of the nannofossil assemblage is evidenced by an increase in eutrophic taxa and a decrease in oligotrophic/warm taxa from about 34.4 Ma. The same turnover occurs at Site 711 at about 34.5-34.1 Ma (Fioroni et al., 2015), before the EOT, highlighting a significant response of nannofossils to increased nutrient availability at the surface waters of the equatorial Indian Ocean.

This assemblage variation could be linked to the formation at high latitudes of nutrient-rich waters: in particular the Subantarctic Mode Water (SAMW) is a water mass created in the SO by deep mixing, that sinks below the ocean surface and moves northward, reaching most of the upper ocean.At the Southern Ocean sites a sudden turnover from oligotrophic to eutrophic conditions was highlighted by both nannofossil and magnetotactic bacteria assembalges at 36.2 Ma, in response to changing sea surface nutrient supply that is recorded both at Kerguelen Plateau and Maud Rise (Villa et la., 2014).

The turnover recorded at sites 711 and 709, though less evident, could represent a later response to oceanographic changes occurring in the SO, as a result of the cooling trend preceding the EOT.

PAST Gateways 4th International Conference

Trondheim (Norway) 23-27/05/2016

PAST GATEWAYS 2016 TRONDHEIM (NORWAY) 23-27 MAY 2016

LATE QUATERNARY DEGLACIATION IN THE ARCTIC OCEAN: EVIDENCES FROM MICROFOSSILS

CARBONARA K.[1], MEZGEC K.[2], VARAGONA G.[3], MUSCO M. E.[4], LUCCHI R. G.[4], MELIS R.[3], MORIGI C.[5], VILLA G.[1]

1Department of Physics and Earth Sciences University of Parma (Italy)

2 Department of Physical sciences, Earth and environment University of Siena (Italy)

3 Department of Mathematics and Geosciences University of Trieste (Italy)

4 National Institute of Oceanography and Experimental Geophysics (OGS) Trieste (Italy)

5 Department of Earth Sciences University of Pisa (Italy)

INTRODUCTION

Integrated micropaleontological and sedimentological analyses on calcareous nannofossils, diatoms, planktonic foraminifera and clay mineral assemblages have been performed on three sediment cores (Tab. 1), collected during the EGLACOM and CORIBAR projects from the Storfjorden-Kveithola depositional system (NW Barents Sea, Fig. 1).

Core ID	Water depth (m)	Location	Total recovery (cm)
EG-02	1722	Middle slope of Storfjorden TMF	305
EG-03	1432	Middle slope of Storfjorden TMF	291
GeoB 17603-3	1430	Middle slope of Kveithola TMF	990

Tab.1 Core locations, water depth, total sediment recovery and number of samples for the studied cores. EG= EGLACOM Gravity cores; GeoB= CORIBAR Gravity core; TMF= Trough Mouth Fan.

RESULTS

The recovered cores contain a thick sedimentary sequence that includes well preserved Holocene interglacial sediments.
The lithological sequence and the magnetic susceptibility are consistent between the EGLACOM and CORIBAR cores, allowing the construction of a preliminary age model.
The upper part of the CORIBAR core was directly related to the Holocene sequence contained in core EG-03, whereas the lower part was correlated to the post LGM sequence contained in core EG-02 (Fig. 2).

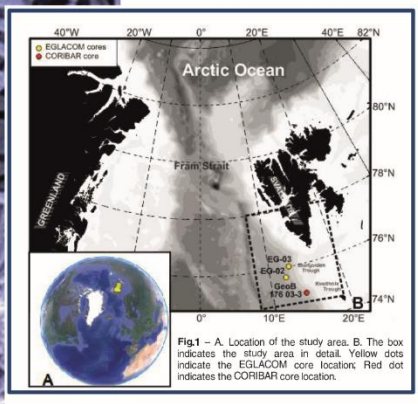

Fig.1 – A. Location of the study area. B. The box indicates the study area in detail. Yellow dots indicate the EGLACOM core location; Red dot indicates the CORIBAR core location.

The total abundances of all the fossil groups are characterized by similar patterns (Fig. 3).
The planktonic microfossil patterns of distribution are coherent with the trend of smectite content in the clay mineral assemblage that is mainly transported by the North Atlantic Current, therefore high contents are associated to a vigorous current (Junttila et al., 2010). The presence of nannofossils in the sediments is a clear indication of open-water/seasonal sea ice conditions as the nannofossils, unlike some diatom species, were photosynthetic algae that can not live under permanent sea-ice coverage.

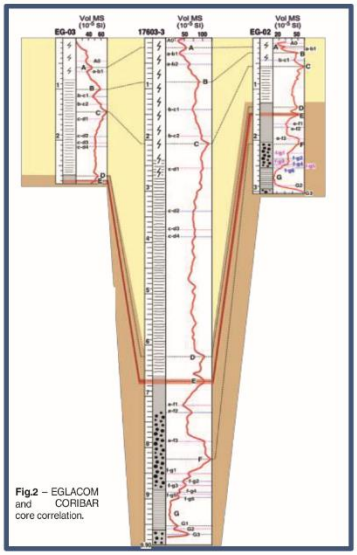

Fig.2 – EGLACOM and CORIBAR core correlation.

The diatom assemblages are dominated by *Chaetoceros* resting spores, related to stratified waters in association with ice melting at the beginning of Holocene.

The presence of the diatom *Coscinodiscus* spp. and a more diversified planktonic foraminiferal assemblage, with *Neogloboquadrina pachyderma* (s), *N. incompta* and *Globigerina bulloides*, indicating subpolar conditions, confirm the onset of warm environmental period that were associated to the Holocene Thermal Maximum.

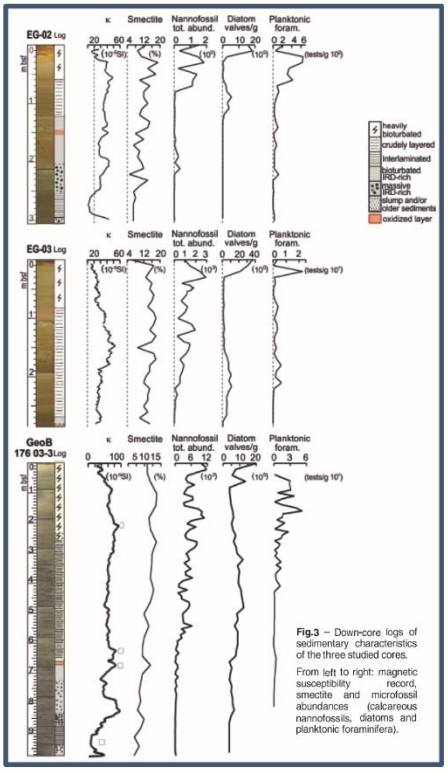

Fig.3 – Down-core logs of sedimentary characteristics of the three studied cores. From left to right: magnetic susceptibility record, smectite and microfossil abundances (calcareous nannofossils, diatoms and planktonic foraminifera).

Minor climatic fluctuations with inversed trends within the Holocene are well depicted by the microfossils assemblages and distribution of the smectite clay mineral.

Past Climate Reconstruction and Modelling Techniques (USSP)

Urbino (Italy) 15-31/07/2015

LATE QUATERNARY DEGLACIATION IN THE ARCTIC OCEAN: EVIDENCES FROM CALCAREOUS NANNOFOSSILS

Carbonara K.*

Introduction

Paleoceanographic interpretations can be accomplished by the study of microfossils.

Nannoflora association variations through time may indicate a biotic response to environmental changes.

Calcareous nannoplankton thrives in marine waters influenced by light, temperature and nutrients.

At very high latitudes these conditions are not always met as water temperatures are low, light is scarce for part of the year, and in particular the presence of sea-ice may additionally reduce the favourable condition for their growth.

The potential of microfossils as paleoenvironmental proxies in the Arctic seas has been outlined in several paleoceanographic studies (e.g. Gard and Backman, 1990; Baumann and Matthiessen, 1992; Samtleben et al., 1995; Baumann et al., 1997; Rasmussen et al., 2007; Ślubowska-Woldengen et al., 2007; Jessen et al., 2010; Rasmussen and Thomsen, 2015), but they mainly concern the continental shelf area of the northern and western sector of the Svalbard Island. On the contrary, the southern sector of the slope, in front of the Storfjorden-Kveithola Trough, is less investigated, especially from a micropaleontological point of view.

The study of contourite drifts is useful for the reconstruction of the oceanographic and climate history of continental margins since these sedimentary deposits typically form along the pathways of major bottom currents (Laberg et al., 2005; Rebesco et al., 2008).

The aims of these investigations are the evaluation of the main paleoceanographic- paleoclimatic conditions of the Arctic Ocean during the late Quaternary and the definition of a detailed age model for stratigraphic cross correlation, still lacking in this area, throughout a multidisciplinary approach in order to consider the interaction between various components of the Arctic system .

Methods

Three preparation techniques of calcareous nannofossil slides- the conventional smear slides, the settling techniques by de Kaenel & Villa (1996) and by Flores & Sierro (1997)- were compared in order to investigate which method is more suitable in studies for paleoceanographic reconstructions in the Arctic.

Finally, smear slides from unprocessed material have been preferred.

Counting of specimens was performed on a fixed area of the slide, using a polarised-light microscope at a magnification of 1250x.

References

Baumann, K.-H., Wolfteteson, J., 1992. Variations in surface water mass conditions in the Norwegian Sea: Evidence from Holocene coccolithoval and dinoflagellate cyst assemblages. Mar. Micropaleontol. 20 (3), 179–196.

Baumann, K.-H., Andruleit, H., Samtleben-Monna, A., Samtleben, C., 1997. Spatial and temporal dynamics of coccolithophore communities during marginal-ice phases in the Norwegian-Greenland Sea. In: Hass, H.C., Samtleben, W.-A. (Eds.), Contributions to the Micropaleontology and Paleoceanography of the Northern North Atlantic. Continental Shelf Sedim. Publ. 8, pp. 225–238.

Gard, G., Backman, J., 1990. Synthesis of Arctic and Sub-Arctic Coccolith Biostratigraphy and History of North Atlantic Drift Water influx during the Last 600 000 Years. In: Bleil, U., Thiede, J. (Eds.), Geological History of the Polar Oceans: Arctic versus Antarctic. NATO ASI Series 308, pp. 417–436.

Jessen, S.P., Rasmussen, T.L., Nielsen, T., Solheim, A., 2010. A new late Weichselian and Holocene marine chronology for the western Svalbard slope 30 000–Kyear model. Quaternary Sci. Rev. 29, 1301–1312.

Laberg, J.S., Dahlgren, K.I.T., Kuvaas, B., Haflidason, H., Hjelstuen, B.O., Nielsen, T., Shannon, P.M., Vorren, T.O., Knutsen, S.-M., Noormets, R., 2005. Contourite stratigraphy processes and sedimentary architecture of the Hill Bjørnøya–Atlantic margin. Mar. Pet. Geol. 22, 1069–1088.

Rebesco, M., Camerlenghi, A., Van Loon, A.J., 2008. Contourite research: A field in full development. In: Rebesco, M., Camerlenghi, A. (Eds.), Contourites. Developments in Sedimentology 60, pp. 1–10.

Rasmussen, T.L., Thomsen, E., 2015. Palaeoceanographic development in Storfjordrenna, Svalbard, during the deglacial/Holocene: evidence from benthic foraminiferal records. Boreas. 44, 24–44.

Rasmussen, T.L., Thomsen, E., Ślubowska-Woldengen, M., Koç, N., Klitgaard-Kristensen, D., Nilsen, F., Jennings, A., 2007. Paleoceanography of the northern Fram Strait/Yermak Plateau region during the last 30 000 cal yr B.P. Quaternary Sci. Rev. 26, 756–778.

Ślubowska-Woldengen, M., Rasmussen, T.L., Koç, N., Klitgaard-Kristensen, D., Nilsen, F., Solheim, A., 2007. Advanced retreat of the Late Weichselian ice-sheet in the central Fram Strait and timing of subsequent inflow of Atlantic water to the Nordic Seas. Quaternary Sci. Rev. 26, 463–478.

Study area

Effects caused by climatic changes at different scale can be seen very clearly in the Arctic Ocean since they are amplified, compared with low latitude environments.

The Arctic and its surroundings are characterized by strong regional variability.

The Storfjorden-Kveithola depositional system (Fig. 1), investigated during EGLACOM* and CORIBAR* cruises, was selected as target area because of the presence of a thick sedimentary sequence that includes well preserved late Quaternary sediments.

This area is expected to have sensitively responded to changes in regional climate and sea level.

The Eurofleets-2 PREPARED* cruise investigated the present and past oceanographic patterns around contourite drifts, located on the eastern side of the Fram Strait (Bellsund Drift- Fig. 1), thought to contain an expanded stratigraphic sequence necessary for high-resolution palaeoclimatic and palaeoenvironmental reconstructions.

The last 20 ky have witnessed the most recent global climatic changes, including the Last Glacial Maximum (LGM) followed by a deglaciation trend culminating after the Younger Dryas (YD) in the Holocene (oxidized layer- Fig. 2; Melis et al., 2015 submitted).

Quantitative analyses of PREPARED samples are now in progress.

Core ID	Water depth (m)	Location	Total recovery (cm)	N. samples
EG-01	1069	Gully upper slope	220	23
EG-02	1722	Middle-slope	305	30
EG-03	1432	Middle-slope	291	39
GeoB 17601-5	369,1	Grounding Zone Wedge	537	51
GeoB 17603-2 BC	1425	Of landscar	49	5
GeoB 17603-3	1430	Of landscar	990	98
GeoB 17605-3	768,1	Active gully	405	41
GeoB 17623-2	150,2	N channel/fault	442	21
GS191-01 PC	1647	Crest Bellsund Drift	1967	196

Tab.1 Core locations, water depth, total sediment recovery and number of samples for the studied cores. EG= EGLACOM Gravity cores; GeoB= CORIBAR Gravity cores; GS= PREPARED Calypso core.

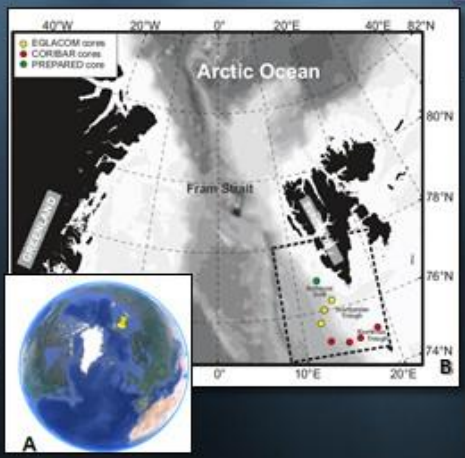

Fig.1 – A. Location of the study area. B. The box indicates the study area in detail. Yellow dots indicate the EGLACOM core location; Red dots indicate the CORIBAR core location; Green dot indicates PREPARED core location. (From EUROFLEETS-2 Cruise Summary Report, modified). See Tab. 1 for core location details.

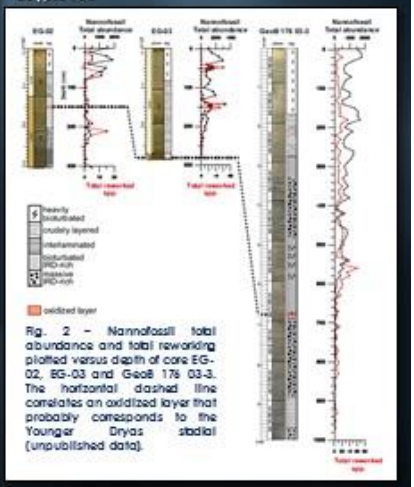

Fig. 2 – Nannofossil total abundance and total reworking plotted versus depth of core EG-02, EG-03 and GeoB 176 03-3. The horizontal dashed line correlates an oxidized layer that probably corresponds to the Younger Dryas stadial (unpublished data).

Results

Nannofossil total abundance and species diversity is generally low (Fig. 2), as expected in the Arctic setting (Baumann et al., 2000). The low species diversity could be due to the cool-water conditions that are not favourable to the nannoplankton flourishing. The assemblages are dominated by *Emiliania huxleyi* and cold-water adapted taxa, as *Coccolithus pelagicus* and *Gephyrocapsa muellerae*.

Though rare, other species may be indicative of different water mass influences. Intervals of absence of calcareous nannofossils could correspond to cooler climatic phases, or interval of more intense carbonate dissolution.

Outlook

Further investigations, scheduled for the next year of PhD, will be crucial to better refine the features of the Holocene climatic changes in the Arctic. The results will allow to improve the sedimentary models of polar areas and to evaluate the oceanographic changes that could derive from a potential ice melting increase in response to the present global warming.

In a collaborative sense, the different results from sedimentological, geochemical, geotechnical and palaeoceanographic investigations will be integreted. Ship-based field training is planned for June 2016, during the Eurofleets2- BURSTER* cruise.

* Carbonara Katia- PhD Student

Department of Physics and Earth Sciences - University of Parma (Italy)

katia.carbonara@studenti.unipr.it

Acknowledgments

First and foremost I want to thank my supervisor Prof. Giuliana Villa. It has been an honor to be her Ph.D. student. I appreciate all her contributions of time and funding to make my Ph.D. experience productive and stimulating.

I am also thankful to my co-supervisor Dr. Renata G. Lucchi. The joy and enthusiasm she has for her research was contagious and motivational for me. Thank you for the opportunity to participate in the Arctic oceanographic cruise BURSTER.

I am especially grateful to Proff. Romana Melis and Caterina Morigi and to my colleagues Karin Mezgec, Maria Elena Musco and Gabriella Varagona. Thank you for sharing your data with me.

I would like to acknowledge our technician Giovanna Gianelli for helping with sample preparations.

Other CAGE 14-5 and PS99-1 expedition members that I have had the pleasure to work with are colleagues from all over the world. Thank you to the USSP 2015 group for sharing Urbino summer school experience.

Thank you to Dr. Gonçalo Prista for being available for nannofossil data discussions.

The members of the “Rancio” group have contributed to my personal growth. The group has been a source of friendships as well as good advice and collaboration. To mention everybody’s name would increase the length of this thesis significantly. To each and every one, a big thank you.

To all the people I met during the past three years, to Gianluca, to my very big family, to my “Coinqui”, to everyone, I offer my sincere gratitude and thanks.